Microbial Ecology of Phytoplankton Blooms of the Arabian Sea and their Implications

A Thesis submitted to Goa University for the Award of the Degree of

DOCTOR OF PHILOSOPHY
IN
MICROBIOLOGY

By
Subhajit Basu (M.Sc.)

Research Guide
Prof Irene Furtado

Corrections, Suggestions are incorporated by the Candidate Mr. S. Basu in the final thesis.
Indeevari Kanagaraj
(External Examiner)

Goa University
Taleigao, Goa
AUGUST 2013

Furtado
(Internal Examiner)

T-631

...With Dedication to Memories...

Of Guruji and Baba,

Who always inspired to pursue research...

Declaration

As required by the Goa University ordinance OB-9.9, I state that the present thesis entitled "**MICROBIAL ECOLOGY OF PHYTOPLANKTON BLOOMS OF THE ARABIAN SEA AND THEIR IMPLICATIONS**" is my original contribution, and the same has not been submitted on any previous occasion. To the best of my knowledge the present study is the first comprehensive work of its kind from the study area. The literature related to the problem investigated has been cited. Due acknowledgements have been made wherever facilities and suggestions have been availed of.

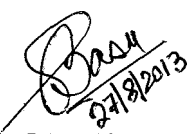

Subhajit Basu
Department of Microbiology
Goa University
August 2013

Certificate

This is to certify that this thesis entitled "***Microbial Ecology of Phytoplankton Blooms of the Arabian Sea and their implications***", submitted by **Subhajit Basu** for the award of the degree of ***Doctor of Philosophy in Microbiology*** is based on his original studies carried out under my guidance and supervision. The thesis or any part thereof has not been previously submitted for any other degree or diploma in any Universities or Institutions.

Furtado 27/8/13

Prof. Irene Furtado
Research Guide and Supervisor
Department of Microbiology
Goa University
Taleigao Plateau
Goa-403206
August 2013

Viva Voce Examiner: External Examiner.

Acknowledgements

I remain indebted to my mentor and guide Prof Irene Furtado for supervising me throughout the course of this PhD work. Training under my guide shaped orientation of thoughts to pursue research. My sincere acknowledgements of the unfailing patient supervision which helped to finally sail through in presenting this thesis, a journey which began during the 'Advanced post-graduate diploma in Marine Microbiology and Technology' (*An UGC sponsored 1 year course in innovative teaching and research*), conducted for a year during 2006-2007 at the Goa University, Department of Microbiology. I also sincerely acknowledge Dr M Sudhakar (Advisor; Ministry of Earth Sciences) in facilitating shipboard experience during this course; and to Dr SG Prabhu Matondkar (Former Senior Principal Scientist; National Institute of Oceanography-CSIR, Goa) for extending the rare opportunity to participate in *FORV Sagar Sampada 253* cruise of March-2007 in the Northern Arabian Sea. Preliminary observations of bloom during this cruise led to the further proposal of this research work.

I express my profound gratitude to my internal-guide Dr SG Prabhu Matondkar, and my sincere acknowledgments of his immense contribution in this thesis for all the assistance, discussions, and invaluable advice from his rich oceanographic experience, opportunities to participate in several cruises, extending laboratory facilities with prompt help and support whenever required throughout the course of this work.

I acknowledge the critical assessment of this work provided by VC's nominee Dr Savita Kerkar and by Prof GN Nayak, former Dean of Life Sciences and Environment.

I am grateful to Prof. Satish R Shetye, Vice-Chancellor, Goa University and former Director, National Institute of Oceanography (CSIR), for allowing laboratory facilities and opportunity to carry out this research work.

I convey my gratitude to Prof SK Dubey (Head of the Department), Dr S Nazareth, Dr S Garg of the department of Microbiology, Goa University and to Prof S Bhosle, Dean of Life Sciences and Environment, for all the support and help whenever required.

I gratefully acknowledge the Space Application Centre (ISRO), Ahmedabad fellowships received during the period 2007-2010.

Special thanks to Prof. Joaquim I Goes (Lamont Doherthy Earth Observatory, New York) for all the discussions. I was lucky enough to be working with him onboard three cruises and learnt oceanographic techniques hands-on, immensely benefiting from his expertise.

I am also thankful to Dr AK Shukla and Dr KN Babu for training to process OCM-II images at the Space Application centre (ISRO) Ahmedabad, Goa and also the help provided by Dr. RM Dwivedi in providing some of the OCM images.

My sincere acknowledgments to Dr S Shivaji (Director, LaCONES-CCMB) and Dr. Pavan Kumar Pindi of CCMB (CSIR) laboratories, Hyderabad for extending facilities and the brief hands-on experience received to carry out

16SrDNA sequencing and PCR techniques which helped later during this work. I also sincerely thank Prof Deepti D Deobagkar (Director, Bioinformatics centre, Pune-University) for all the discussions on phylogenetic analysis.

My sincere thanks also to S Sreepada and Dr NC Thakur at the National Institute of Oceanography, Goa for extending laboratory facilities at critical junctures; to Dr Helga-doR Gomes (Lamont Doherthy Earth Observatory, New York) for all your help and discussion during the cruises; and to Prof Colin R Roesler, Bowdein, USA for the brief discussion on analysis of C-DOM absorbtion spectra.

I am also thankful to Dr RM Dwivedi, Mini Raman (Space Application Centre, ISRO, Ahmedabad), and Dr KB Padmakumar (CMLRE, Kochi) for help and co-operation during the cruises. Thanks also to all the cruise participants, to M/s Norinco staff, officers and crews of FORV *Sagar Sampada*, ORV *Sagar Kanya* and CRV *Sagar Manjusha* who have been always helpful and cooperative.

To my colleagues Suraksha and Dr Sushma at NIO, Goa, thanks for the unstinted help, support and encouragements you have provided me and to my lab-mates Sherryanne, Sanika and Sushma in AF-36, Department of Microbiology, I thank you all for being there and providing help whenever it mattered most. It was my pleasure to be working with you all.

To my family and friends, thanks for all your support, love and help as always to move ahead.....

Subhajit Basu

Contents

Chapter I

Marine Phytoplankton Blooms and Associated Bacteria

1.1 Introduction

'Phytoplankton', the miscroscopic photosynthetic algae are known to form blooms in the ocean as they can quickly proliferate under ambient conditions of Sun-light, nutrients, temperature, grazing and water-column stability. Of the ~5000 documented species of phytoplankton around 300 species are known to form blooms, and they belong to different groups (Smayda 1990, Hallegraeff 1993), such as the diatoms, silicoflagellates, dinoflagellates, haptophytes, raphidophytes, prymnesiophytes, and the cyanobacteria (Plate 1.1).

The state of 'bloom' can be considered as an outburst of phytoplankton growth and hence, an increase in biomass indicated from chlorophyll *a* (Chl *a*) from the charactersitic base-line levels of the oceanic (<0.3 $\mu g\ L^{-1}$ Chl *a*) to coastal (>1$\mu g\ L^{-1}$ Chl *a*) ecosystems. A uniform criterion based on cell concentrations / Chl *a* have been untenable (Smayda 1997). The International Council for the Exploration of the Seas (ICES 1984) has referred to phytoplankton blooms as the "spring and autumn outburst of growth which are a normal feature of most sea areas"; whereas, 'exceptional' blooms were defined as: "those, which are noticeable, particularly to general public, directly or indirectly through their effects such as visible discolouration of the waters (Plate 1.2), foam production, and fish or invertebrate mortality or toxicity to humans". Such blooms which have toxic effects on the biota (Anderson et al. 2012) are referred to as the Harmful algal Blooms (HAB's).

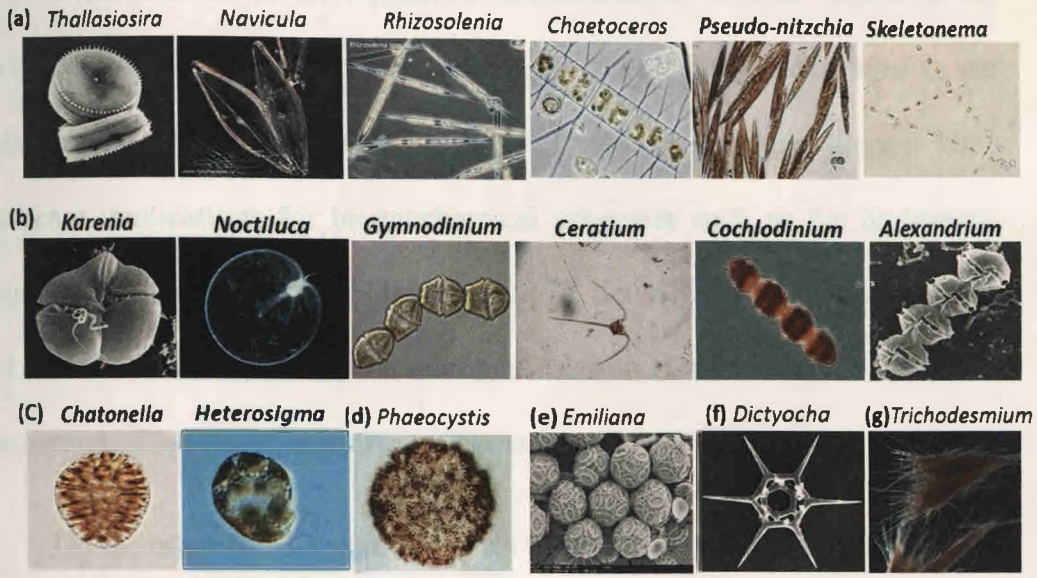

Plate 1.1 Photomicrographs of important bloom forming genera from different groups of phytoplankton: (a) Diatoms; (b) Dinoflagellates; (c) Raphidophytes; (d) Prymnesiophyte; (e) Haptophytes (Coccolithophores); (f) Silicoflagellates and (g) Cyanobacteria. Genera marked in bold include Harmful/toxic bloom forming species. *(Sources of photomicrographs: www. phytoplankton.org; C-MORE; marinespecies.org; GEOHAB; Wikipedia).*

Plate 1.2 Bloom (red-tide) of *Noctiluca miliaris* in New Zealand *(Source: Woods hole Oceanographic Institute www.whoi.edu, 2007).*

While blooms of phytoplankton accumulate as organic matter in the upper-ocean, they exhaust inorganic nutrients and are finally degraded in the water column. Due to the high turnover of organic biomass, blooms have significant implications for biogeochemical processes such as the biological-pump (Ducklow et al. 2001[b], Falkowski 1998), denitrification/annamox (Ward et al. 2009, Jensen et al. 2011), nitrogen-fixation (Capone et al. 1997) and dimethylsulphide (DMS) emissions (Charlson et al. 1987).

On the other hand, marine bacteria plays the key role of remineralizing bloom organic matter, bringing inorganic nutrients back to the system at deeper depths (Azam et al. 2007, Falkowski 2008). Wind-driven circulation and physical mixing processes (upwelling, convective mixing, mesoscale eddies) makes such regenerated nutrients available to phytoplankton again seasonally (Wiggert et al. 2005).

1.2 Factors regulating phytoplankton bloom formation

The principle factors regulating phytoplankton bloom formations can be broadly grouped into: (a) Bottom-up (Physico-chemical) and (b) Top-down (grazing, viral mortality) controls. The important bottom-up controls affecting formation of phytoplankton blooms are Sunlight, temperature, inorganic and trace nutrients availability, and water-column stability (Valiela 1995).

(a) Bottom-up (Abiotic) regulations

Sun-light: The availability of optimum photosynthetic available radiation (PAR) to phytoplankton in the visible electromagnetic spectrum ~400-700 nm

within the ocean euphotic zone (depth of 1% light; Fig. 1.1b) is essential to carry out photosynthetic fixation of carbon-dioxide. The factors affecting availability of Sun light to phytoplankton are: atmospheric cloud-cover and aerosol optical thickness which restricts incoming PAR into the ocean, water-column turbidity which leads to increased back-scattering of sunlight, and the variations in diurnal photo-periods of the tropical, temperate and polar oceanic gyres (Parsons et al. 1984)

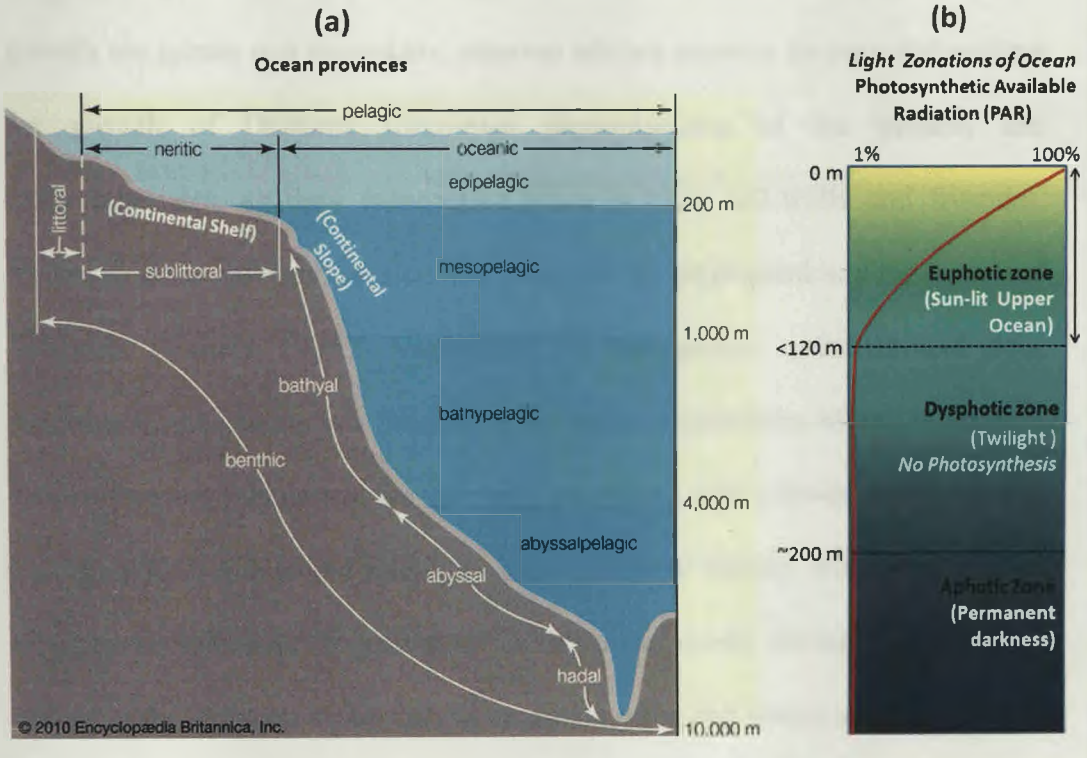

Fig 1.1 (a) Ocean provinces (*Adapted from Encyclopedia Britannica 2010*); and (b) light-based zonations of the Ocean.

Temperature: Temperature exerts fundamental control on the metbolic and growth rates of phytoplankton bloom forming species (Parsons et al. 1984). Temperature optima varies among bloom forming species of the colder polar

oceans to the temperate and warmer tropical oceans. Some bloom forming species are eurythermal and can grow over a wider temperature range e.g. the diatom *Rhizosolenia setigera* from -2 to 30°C (Guillard and Kilham 1977).

Salinity: Salinity affects osmotolerance of cells and is an important factor in selection of phytoplankton species in ecosystems with fluctuating salinity gradients, such as in the estuarine ecosystems (Pednekar et al. 2012).

Nutrients: The major macro inorganic nutrients required for phytoplankton growth are nitrate and phosphate, whereas silicate remains an essential nutrient for growth of Diatoms (dominant phytoplankton of the oceans) and Silicoflagellates, as they incorporate silica in their cell-walls and frustules. Essential trace nutrients which are required by phytoplankton are Iron and Vitamins (Valiela 1995). Availability of nitrogenous nutrients and trace nutrients in the oceans is a limiting factor for phytoplankton bloom formation. Bloom forming population are normally associated with a lower N: P ratio <10 (Arrigo 2005), due to the relatively high uptake of Nitrate. Reduced forms of nitrogenous nutrients 'regenerated' in the upper-ocean during the course of bloom in the euphotic zone such as ammonia, urea and amino acids are mostly preferred by certain bloom forming communities in succession to diatoms. They mainly include the flagellates and harmful algal bloom forming species (Davis 1982).

Mechanisms of Nutrient supply to euphotic zone: As temperature decreases with depth, the density of sea-water increases. From the upper ~100 m, the

temperature starts decreasing rapidly and leads to thermal stratification (thermocline) with the colder nutrient-rich denser bottom waters. This prevents mixing or nutrient availability to the upper mixed-layer of uniform density, essential for formation of phytoplankton blooms under ambient conditions of sun-light, temperature and stable water-column. The important mechanisms which seasonally govern the supply/replenishment of nutrients to the euphotic zone are wind-driven physical mixing processes such as coastal upwelling, convective mixing and the mesoscale eddies (Parsons et al. 1984, Falkowski 1994).

Upwelling occurs when winds blowing across the ocean surface push water away, leading to replenishments from beneath the surface to substitute the displaced water. Upwelling initiates along coastlines and can spread to the open ocean. Water parcels that rises to the surface as a result of upwelling are typically colder and rich in nutrients, supporting wide-spread blooms (Fig. 1.2a). On the other hand cooling of surface waters due to winter-winds leads to sinking of denser colder waters. This initiates buoyancy driven convective overturning, entraining nutrient rich waters from the base of the thermocline into the surface ocean and supporting blooms of phytoplankton (Fig. 1.2b). These wind-driven processes can typically bring-up nutrients to the surface from ~150 m depths of the ocean (Wiggert et al. 2005).

Water-column stability: An optimally stable water-column is essential to allow phytoplankton cells to grow and accumulate as bloom. Turbulent mixing/wave-

action is non-coducive for bloom formations. However, following violent storm events, growth of phytoplanktons can be favored due to the availability of nutrients from mixing due to wind-forcings (Babin et al. 2004).

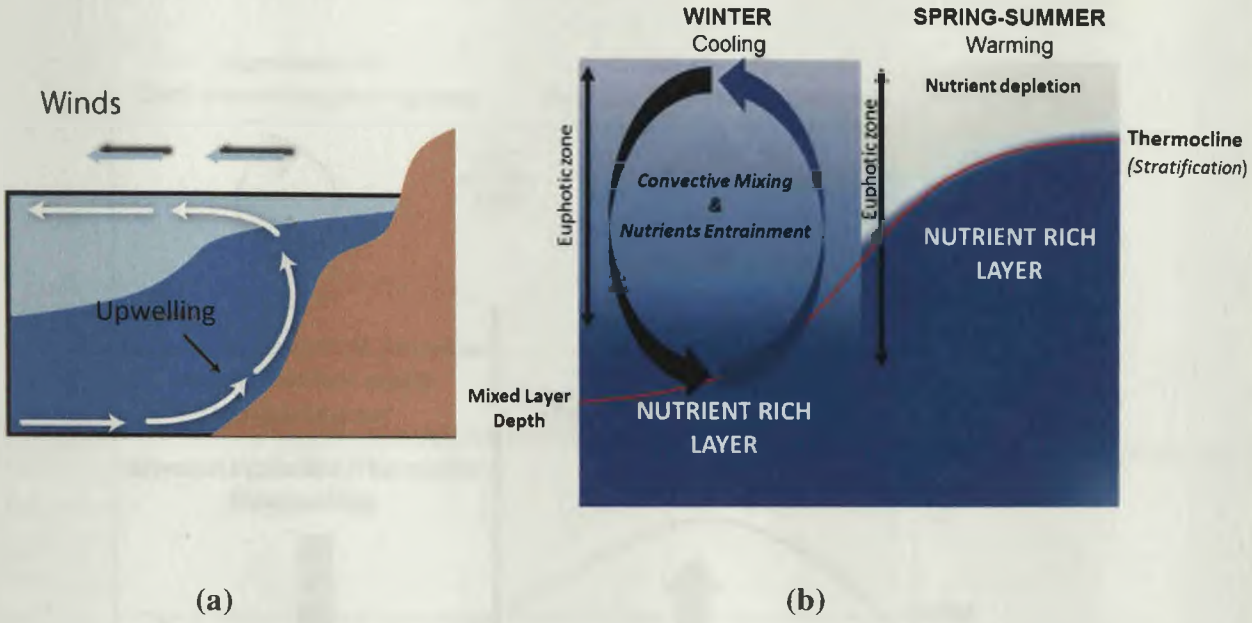

Fig 1.2 Replenishment of nutrients to euphotic zone during: (a) Upwelling and (b) Convective mixing.

Oceanic eddies on the other hand are rotating bodies of water (~10-500 km, mesoscale range) (Fig 1.3), and forms due to differences in gradients of pressure and density, a feature called as '*Baroclinic instability*' (McGillicudy and Robinson 1997). Cyclonic eddies which are anti-clock wise rotating in the Northern Hemisphere, are associated with a colder core temperature causing a depression in sea-surface height (~10 – 30 cm's) with respect to the surrounding and can pump nutrient rich waters into euphotic zone and thereby promote bloom formation. In contrast, anti-cyclonic eddies are associated with

a warmer core temperature leading to elevation of sea-surface height (by few cm's) and are unfavorable for bloom formation as they push down surface water, depressing the thermocline / pycnocline (depths of highest density gradient) and restricts nutrient supply to euphotic zone.

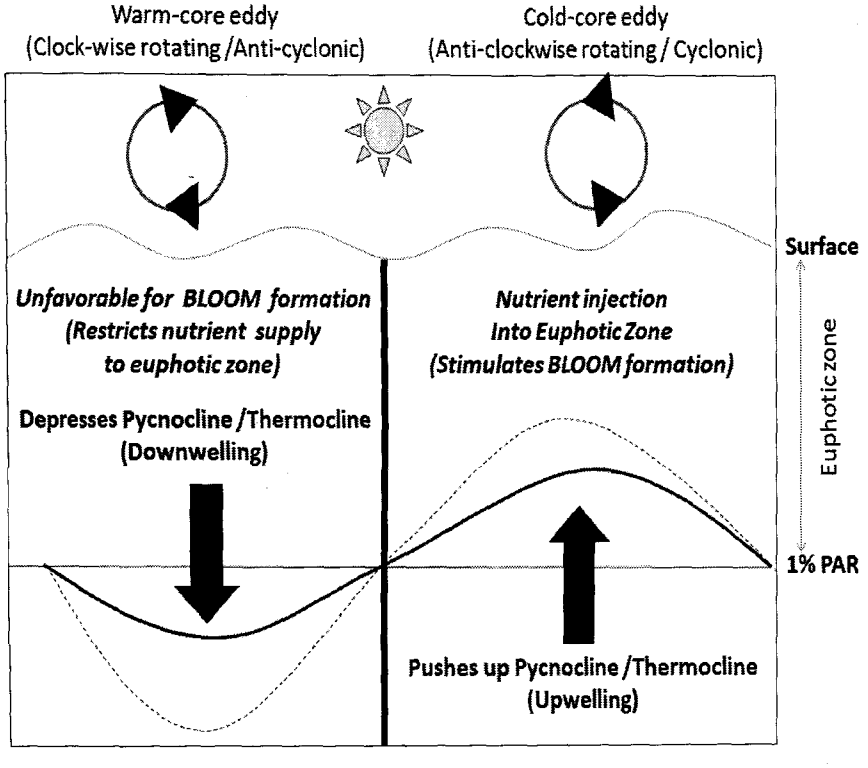

Fig. 1.3 Eddy mediated meachansims of nutrient supply to euphotic zone (*Modified from McGillicudy and Robinson 1997*).

In addition, world-wide escalations of fertilizer use of urea and their pollution of coastal-waters from run-offs has been identified as an important reason for occurrence of several harmful dinoflagellate blooms which prefers reduced nitrogenous nutrients such as Ammonia and Urea (Heisler et al. 2008).

(b) Top-down (Biotic) regulations

Grazing: The occurrence of seasonal annual spring / autumn phytoplankton growth (mostly of the chain forming diatoms) in the colder nitrate rich waters following upwelling and winter-time mixing (Valiela 1995), fuels life in the ocean through a complex 'network of food chains' or feeding relationships, as biomass is passed on from one species of living organisms to another: from phytoplankton at the base of the food-web to the zooplanktons to fishes to the biggest of mammals – the blue whales (Fig. 1.4). High zooplankton grazing pressure during such active periods of phytoplankton growth helps to quickly pass the phytoplankton biomass into the food-chain which ultimately supports the world-wide pelagic and demersal fisheries. Grazing pressure in the food-chain keeps the phytoplankton biomass under check from attaining bloom proportions. Estimates have shown that the grazing by herbivorous zooplanktons (dominated by Copepods,) represents about 59–75% of the photosynthetic carbon fixed by phytoplankton across the marine environments-from estuarine to oceanic (Calbet and Landry 2004).

Viral attack: The blooms of phytoplanktons can also come under viral attack leading to their quick termination (Bratbak et al. 1993), and is now well-known in the case of wide-spread blooms of the coccolithophore *Emiliana huxleyi* (Bratbak et al. 1993).

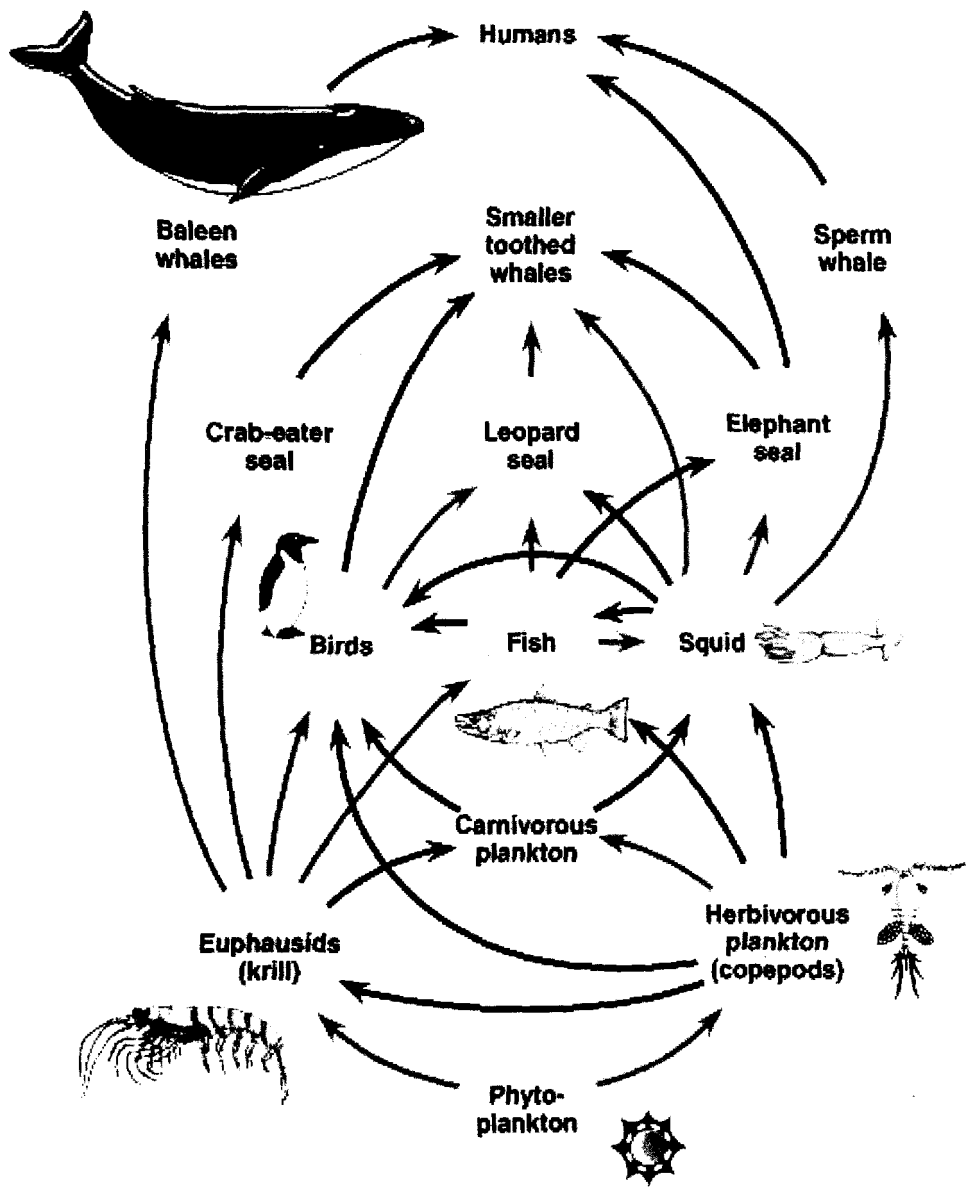

Fig 1.4 Grazing interactions supporting the marine food-web (*Adapted from Pearsons, Benjamin Cummings*).

1.3 Marine bacteria associated with Phytoplankton

With an abundnace of ~10^{8-9} cells L^{-1} in the sea-water, marine bacteria and archaea dominates the diversity and metabolic activity of the ocean (Azam and Malfatti 2007, DeLong and Karl 2005). The relationship of this micro-flora associating with bloom forming phytoplankton can be envisaged in light of their evolutionary insights, trophic-level significance and potential species-specific interactions (Cole 1982, Doucette 1998, Amin et al. 2012, Mayali and Azam 2004).

(a) Evolutionary insights

Molecular evolutionary studies predict that the first life forms were the chemosynthetic Archeae in the pre-cambrian earth, ~3.4 billion years old (Gribaldo and Brochier 2006). An early divergence of the domain Prokaryotes from the ancestral progenitor (Woese et al. 1990) subsequently led to the evolution of purple and green-sulfur bacteria (Falkowski and Raven 2007). They produced oxygen first using the abundance of sulphide and Iron, and were the first to develop the mechanism of capturing light, prior to the emergence of the oxygenic phototrophic cynaobacteria. Anoxygenic photosynthesis is presumed to largely precipitate the dissolved Iron out from the anoxic Oceans as Iron-sulphide (Falkowski and Raven 2007). As the ocean started getting oxygenated, cyanobacteria emerged from a fusion of the photosynthetic systems of these early anoxygenic phototrophs. **'Endosymbiosis and horizontal gene transfers'** spread across with

photosynthetic eukaryotes appearing somewhere in the Proterozoic oceans (~1.5 billion years ago). Much later in the Mesozoic (~251 – 65 million years ago), the three major phytoplankton lineages dominating the modern ocean evolved in succession as the Dinoflagellates, Coccolithophores and the Diatoms, all deriving their plastids (photosynthetic organelle) from an ancestral red-algae (Falkowski et al. 2004). Present day molecular evidences suggest occurrence of bacterial genes in the genomes of certain diatoms and also the presence of intracellular bacteria in certain diatoms and dinoflagellates (Amin et al. 2012). Hence, the relationship between prokaryotic microbes and phytoplankton has been probably age-old and had co-evolved over long periods of geological timescales of the earth.

(b) Trophic role of bacteria

Phytoplanktons release a highly variable fraction (~5-60%) of the total carbon fixed during photosynthesis, as dissolved organic matter (DOM) (Fogg 1983, Kirchman et al. 1991, Mague et al. 1980, Bidanda and Benner 1997). Extracellular release of DOM by phytoplankton further increases during senescent phases of blooms, sloppy grazing by protozoans and copepods, viral lysis (Brussaard 2004) and under high N:P stoichiometry (Penna et al. 1999, Myklestad 1977). The chemical nature of these phytoplankton exudates are species specific and vary with growth conditions. Several studies have shown that extracellular compounds released by phytoplankton contains: (i) **simple and complex carbohydrates** like glucose, galactose, mannose, arabinose,

ribose, glycerol, mannitol, **transparent exopolymeric particles** consisting of mainly acidic polysaccharides, **proteoglycans**; (ii) dissolved **free amino acids (DFAA)** like aspartic acid, glutamic acid, lysine, proline, alanine, histidine, valine, leucine, iso-leucine, low molecular organic acids like **glycolic acid**; (iii) proteins, lipids, nucleic acids etc. (Hellebust 1965, Brockmann et al. 1979, Sarmento et al. 2013, Penna et al. 1999, Myklestad 1989, Passow 2002). DOM released by phytoplankton is a source of nutrition for the marine heterotrophic bacteria (Azam and Malfatti 2007). Enzymatic potentials and nutritional diversity plays an important role in selection of the micro-flora with upcoming / declining blooms of phytoplankton (Chrost 1991, Cole 1982). The biomass of bacteria thriving primarily on phytoplankton based DOM in the euphotic zone averages 0.5 – 2 g C m^{-2} across major oceanic ecosystems (Table 1.1), with the ratio of bacterial production to primary production varying between 0.15 – 0.2 (Ducklow 2000). Bacterial biomass production from utilization of DOM and subsequent grazing by the nanoflagellates and ciliates, can bring back upto ~ 50% of the carbon fixed by phytoplankton into the food-chain through the '**Microbial Loop**' (Azam et al. 1983). The microbial-loop (Fig. 1.5) is particularly important for sustaining the food-chain of the oligotrophic oceans and dominates following the aftermath of bloom events due to release of the dissolved organic matter (Kirchman 2008). As dissolved organics are actively utilized back into the food-chain, the 'retention' of the organic matter is increased in the upper-ocean which can constrain the efficiency of the biological pump (Wassmann 2000).

Table 1.1 Average bacterial biomass and production rate data-sets from the open-ocean provinces during the Joint Global Ocean Flux expedition of major Oceanic provinces (modified from Ducklow 2000).

	Bacterial Biomass ($mgC\ m^{-2}$)	Bacterial Production ($mgC\ m^{-2}\ day^{-1}$)	Growth Rate (day^{-1})	Generation-time (days)
North-Atlantic	1000	275	0.3	55
Equatorial Pacific (spring)	1200	285	0.13	128
Equatorial Pacific (Fall)	1467	175	0.12	139
Hawaii	1500	Nd	Nd	Nd
Bermuda	1317	70	0.05	333
Ross-Sea	217	55	0.25	67
Arabian Sea	1448	257	0.18	92

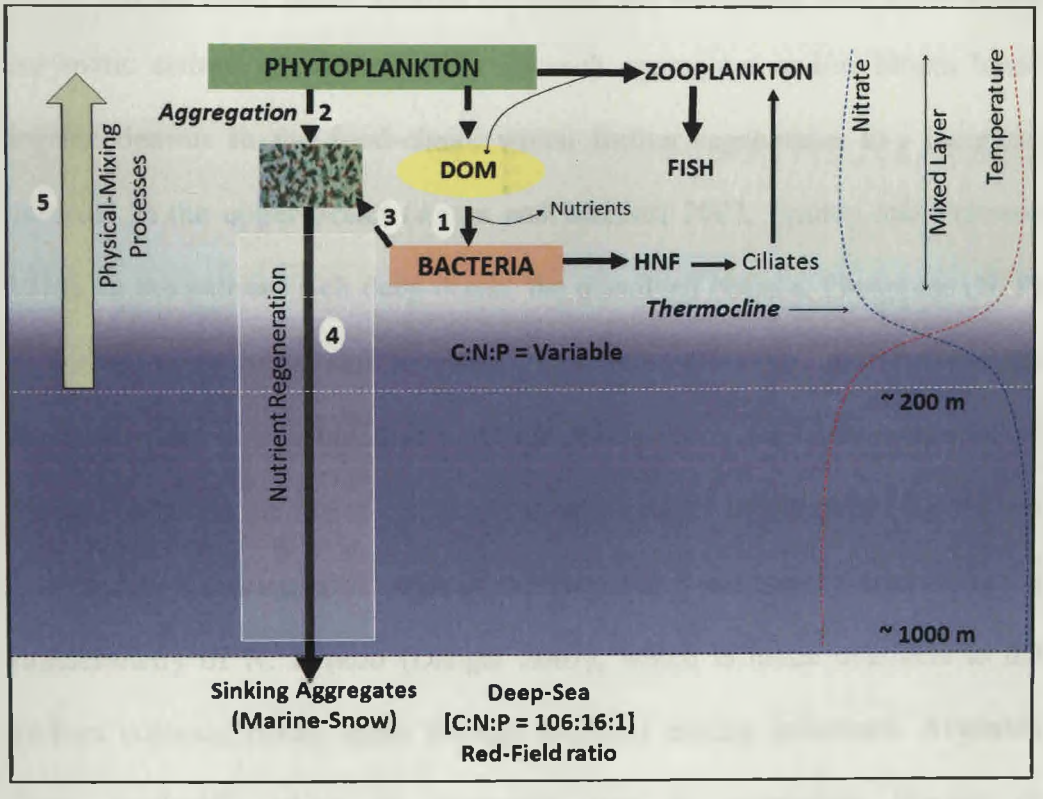

Fig. 1.5 A simplified view of the trophic role of Marine bacteria and nutrient regeneration in the ocean showing: (1) Bacterial utilization of dissolved organic-matter and transfer to higher trophic-levels via Microbial-loop. (2) Aggregation of phytoplankton on termination of bloom; (3) bacterial attachment to particles and formation of aggregates (marine-snow) sinking out from the euphotic zone. (4) Nutrient regeneration below the euphotic zone in the bottom epipelagic/mesopelagic depths; and (5) availability of nutrients to upper ocean through physical-mixing.

During the senescent phases of the bloom, phytoplankton cells forms aggregates with associated bacterial flora playing an important role in producing 'sticky' Exopolysaccharides (EPS) (Alldredge 1989). These particles ('marine-snow') can quickly sink out fast from the euphotic zone into the deeper ocean (Fig. 1.5), contributing immensely to the carbon-export and biological-pump (Smetacek 1985). Blooms of diatoms, coccolithophores etc. are particularly well known for such episodic sinking events (Smetacek 1985).

On the other hand, sinking processes are associated with extracellular enzymatic actions of bacteria cells on such aggregates and/or bloom based organic detritus in the food-chain, which further regenerates key inorganic nutrients in the upper-ocean (Azam and Malfatti 2007, Eppley and Peterson 1979). In the nutrient rich deep ocean, the dissolved Nitrate: Phosphate (N: P) is known to be in a stoichiometric 16:1 red-field ratio, and reflects the elemental ratio of phytoplankton (Arrigo 2005). Bacterial remineralization of organic matter in the lower epipelagic to upper mesopelagic zone (Fig 1.5 and 1.1a) makes it nutrient-rich (zone of the nutracline) and largely determines the stoichiometry of N: P ratio (Danger 2007), which is made available to the surface euphotic ocean again through physical mixing processes. Available "new nutrients", plays an important role in supporting blooms of phytoplankton (Eppley and Peterson 1979) and primarily the diatoms in the colder nitrate rich waters with bioavailable Iron (Lomas and Gilbert 1999). Bacterial regeneration of reduced nitrogenous nutrients (urea, ammonia,

amino-acids) during the course of the bloom mostly gives rise to a succession to flagellates including the Harmful algal bloom forming species (Davis 1982).

(c) Bacteria associated with algal blooms

The immediate region surrounding the phytoplankton cell has been termed as the 'phycosphere'(Bell and Mitchell 1972). Studies have shown that bacteria growing with phytoplankton can be species specific in the phycospheric region or may remain epibiotic as satellite bacteria (Sapp et al. 2007, Goecke et al. 2013, Schafer et al. 2002). Since, blooms of algae represent high organic environments and a sudden transition from the oligotrophic to eutrophic conditions in the oceans, the bacterial flora associating with algal blooms will have to adjust to such fluctuating osmolar conditions. Culturable and molecular analysis of bacterial community of bloom forming dinoflagellate species(s) *Gymnodinium catenatum*, *Alexandrium tamarense*, *Karenia brevis*, *Scripsiella trachoidea*, the diatom *Pseudo-nitzchia* spp., green-algae *Enteromorpha prolifera* bloom off Qingdao in Yellow Sea have shown that members of *alpha-proteobacteria* appears to be the dominant community with a high frequency of retreivable aerobic-anoxygenic phototrophic (AAP) bacteria, commonly referred to as the *Roseobacter* clade (Fandino et al. 2001, Gonzalez et al. 2000, Green et al. 2004, Guo et al. 2011, Jones et al. 2010, Tada et al. 2011). Further, the importance of bacteria associated with algal blooms have been investigated/hypothesized with respect to their potential

interactions – in formation of marine snow, dimethyl-sulfide production, stimulating or inhibiting the growth of algae based on Iron requirements, Vitamins, algicidal bacteria, relief from oxidative stress and promoting/inhibiting dinoflagellate cyst formations.

Marine Snow: Bacterial associates of the diatom *Thalassiosira weissflogii* have been demonstrated *in vitro* to produce 'transparent exopolymeric particles' which aids in the aggregation and formation of 'marine snow' following the demise of the bloom (Gardes et al. 2011), which can enhance the efficiency of the biological-pump.

DMS production: Several bloom forming algae are known to produce high concentrations of the osmolyte dimethylsulfoniopropionate (DMSP) e.g. the prymnesiophyte *Phaeocystis,* the coccolithophore *Emiliana*, the dinoflagellate *Alexandrium* etc. Bacteria associating with these algae, predominantly belonging to the α-proteobacterial phylum of *Roseobacter* spp. utilize DMSP and convert to the volatile Dimethyl-sulfide (DMS), which is oxidized to sulphate-aerosols and contributes to the planetary albedo (Charlson et al. 1987, Yoch 2002).

Iron acquistion: Bioavialability of Iron remains a limiting factor in the oceans as it is an essential trace nutrient (Hopkinson and Morel 2009). Phytoplanktons are known to mostly uptake Iron using a 'reductive uptake pathway' wherein membrane bound receptors can chelate both siderophore bound Iron produced by bacteria / other ligands (Fig. 1.6). A possible mutualism has also been

indicated based on availability of Iron to Phytoplankton through photolysis of siderophore complex Vibrioferrin in exchange of labile dissolved organic matter from phytoplankton (Amin et al. 2009).

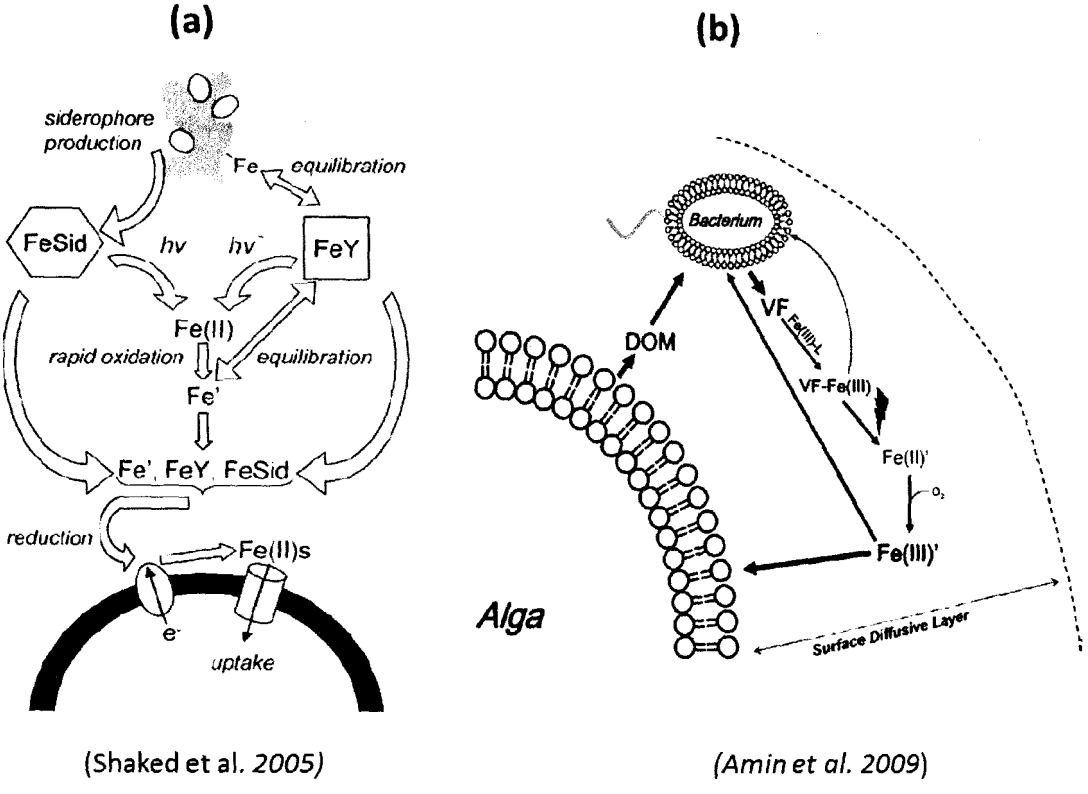

(Shaked et al. *2005)* *(Amin et al. 2009)*

Fig. 1.6 Siderophore mediated mechanism of Iron uptake from siderophores by phytoplankton adapted from: (a) Shaked et al. (2005) showing reductive uptake pathway of phytoplankton (FeSid- Siderophore bound Iron, hv – photo-oxidation of siderophores, FeY – possible other natural organic ligands, F' – all inorganic forms of Iron) (adapted from Hopkinson and Morel 2009); and (b) Amin et al. (2009) showing mutualistic sharing of Iron via photo-labile bacterial siderophores mutualistic for fixed carbon from phytoplankton.

Requirement of Vitamins: Several marine phytoplanktons are known to have an absolute requirement for Vitamin B_{12}. A recent examination of vitamin (B_{12},

B_7 and B_1) production from 40 strains of 27 different harmful bloom forming species (Tang et al. 2010) have shown that ~96% strains were auxotrophic for the vitamin B_{12} (cobalamin), ~74% for B_1 (thiamine) and ~37% for B_7 (biotin). Importantly, the majority of 40 strains surveyed belonged to the harmful species of dinoflagellates (28 strains from 18 species). Exogenous requirement for B_{12} was also indicated earlier from a review of 326 phytoplankton species showing 52% as auxotrophs (Croft et al. 2005). Present molecular evidence suggests that these B_{12} auxotrophic phytoplanktons lack the 'cobalamin independent methionine synthase' gene unlike their terrestrial counterparts (plants). Instead, they possess the enzymes methylmalonyl-CoA mutase and methionine synthase which absolutely requires cobalt-containing B_{12} as a cofactor just as higher animals/mammals and we humans do (Helliwell et al. 2011). Cobalamin is therefore, an essential requirement for B_{12}- auxotrophic phytoplanktons to carry out vital biosynthetic processes of nucleotide and amino-acid metabolism (Nelson et al. 2013). Hence, limiting concentrations can inhibit their proliferation in the high-seas (Bertrand et al. 2011[a]). On the other hand, the biosynthesis of cobalamin has been the exclusive domain of several bacteria (aerobic /anaerobic) and archaea. Hailed as a remarkable feat of organic-synthesis, the pathway requires 30 different enzymes (with several containing Iron-Sulfur active centres) and the trace metal Cobalt (Bertrand et al. 2011[b], Moore et al. 2013, Raux et al. 2000, Rodinov et al. 2003). Few laboratory evidences have further shown stimulation of diatoms growth by bacteria in absence of vitamin B_{12} (Haines et al. 1974). Induction of B_{12}

production in bacteria by the algal-extract fucoidin and occurrence of several phytoplankton as auxotrophs has led to a hypothesis of symbiosis: wherein bacteria supply B_{12} to phytoplankton in exchange for labile dissolved organic carbon (Croft et al. 2005). However, this blanket hypothesis also attracts strong criticism (Droop 2007) as possibility of other exogenous sources (benthic, run-offs, grazing, remineralizations etc) from where phytoplankton can scavenge trace quantities of B_{12} instead of direct symbiosis. As more molecular evidence keeps pouring in, it must be reiterated that the source for all phytoplanktons requiring cobalamin should be bacteria/archaea (direct mutualism in phycosphere / or through indirect regeneration processes of scavenging such as via bacteriophage lysis, grazing, bacterial phagocyctosis by mixotrophic phytoplanktons etc.). With further evidence from field and laboratory, this can have important implications for the role of bacteria during harmful phytoplankton blooms and ocean-productivity.

Relief from Oxidative Stress: Epiphytic/phycospheric bacteria may provide anti-oxidative defense to phytoplankton during periods of photosynthesis, a process which results in formation of damaging reactive oxygen species. Such a scenario is recently indicated as three epiphytic bacterial strains isolated from the Antarctic sea ice diatom *Amphiprora kufferathii* have been demonstrated to break down hydrogen-peroxide, a strong oxidant produced during photosynthesis (Hunken et al. 2008). Although the diatom expressed antioxidant enzymes superoxide dismutase and glutathione reductase, it lacked

catalase required to split hydrogen-peroxide. This was demonstrated as growth of the diatom was favored in presence of these bacterial strains belonging to the genera *Sulfitobacter (phylum α-proteobacteria)*, *Colwellia (phylum γ-proteobacteria)*, and *Pibocella* (phylum *Bacteriodetes),* in comparison to the axenic cultures. A similar stimulation of photosynthetic growth of *Scenedesmus cellularis* and *Chlorella* sp. was seen during co-culturing with phycopsheric bacterial strains *Pseudomonas diminuta* and *Pseudomonas vesicularis* (Mouget et al. 1995). The authors implicated role of bacterial respiration indirectly as photosynthesis was favored while maintaining low-oxygen concentrations in culture-flasks, probably minimizing oxidative stress.

***Algicidal Bacteria*:** An increasing world-wide frequency of Harmful Algal Blooms due to eutrophication/pollution of coastal-waters (Heisler et al. 2008) has provoked research on bacterial strains able to lyse or inhibit the growth of such toxin producing phytoplankton (Mayali and Azam 2004). These bacteria are termed as 'algicidal'. While growth of phytoplankton in cultures can be stimulated by addition of bacteria, inhibition of growth/cell lysis of phytoplankton due to bacteria can also occur (Fukami et al. 1997, Yoshinaga 1998, Lovejoy et al. 1998, Doucette et al. 1999, Keawtawee et al. 2012, Yoshinaga 1997). This raises the posiibility that they may perform similar actions during natural phytoplankton blooms. The methods used to selectively screen such bacteria are: (i) Cell-free supernatant of bacterial culture added to phytoplankton cultures, (ii) Filtrate from a lysed phytoplankton culture in

presence of algicidal bacteria is added to healthy culture, and by (iii) co-culturing phytoplankton and bacteria under physical separation using a dialysis-membrane/<0.22μm filter to allow free diffusion of dissolved molecules (Mayali and Azam 2004). Algicidal bacteria screened by such methods have been identified from several toxic bloom forming phytoplanktons and they to belong diverse genera (Table 1.2). The mechanism has been demonstrated as either through attachment or through release of dissolved metabolites.

However, despite the mounting laboratory evidence that these bacterial cultures are capable of killing phytoplankton cells at various phases of phytoplankton growth (mid-log to stationary), field demonstrations of actual bloom termination are lacking (Mayali and Azam 2004). Further, it raises questions whether bacterial attack of phytoplankton through attachment or release of extracellular compounds during their mid/late growth phases are due to the senescent nature of the phytoplankton cultures/aging under laboratory conditions. Nevertheless, potentials for field trials are beginning as in a successful co-culture experiment, the algicidal bacteria *Marinobacter salsuginis* strain BS2 has been shown to effectively kill the dinoflagellate *Noctiluca scintillans* causing mass mortality of shrimps (*Penaeus monodon* and *Litopenaeus vannamei)* in an aquaculture facility, Thailand. The bacterial strain killed all *Noctiluca* cells within 48 hours without harming the shrimps and increased their survival rates (Keawtawee et al. 2012).

Table 1.2 Major algicidal bacterial species reported from harmful bloom forming and other phytoplanktons.

Phytoplankton species	Algicidal bacterial species	Algicidal compound	Reference
Diatoms			
*Skeletonema costatum**	*Pseudoalteromonas* sp., A28	Serine-protease	Lee et al. 2000
	Kordia algicida, OT-1	Protease	Paul et al. 2011
Thalassiosira weissflogii	*Kordia algicida*, OT-1	Protease	Paul et al. 2011
Phaeodactylum tricornutum	*Kordia algicida*, OT-1	Protease	Paul et al. 2011
Chaetoceros ceratosporum	*Pseudomonas C55a-2*	2,3-indolinedione	Sakata et al. 2011
	Saprospira sp. SS98-5		Furusawa et al. 2003
Chaetoceros didymum	*Alteromonas* spp., S; K; D; R;		Imai et al. 1995
Ditylum brightwellii	*Alteromonas* spp., S; D; R;		Imai et al. 1995
Dinoflagellates			
*Gymnodinium catenatum**	*Pseudoalteromonas* sp., ACEM 4		Skerrat et al. 2002
	Zobellia sp., ACEM 20		
	Cellulophaga lytica, ACEM 21		
	Planomicrobium sp., ACEM 22		
	Bacillus cereus, ACEM 32		
	Pseudoalteromonas sp., Y		Lovejoy et al. 1998
*Gymnodinium mikimotoi**	*Flavobacterium* sp., 5N3		Fukami et al. 1991
	Alteromonas spp., S; K; D; R;		Imai et al. 1995
	Vibrio spp., A47; B42; C4		Yoshinaga et al. 1997
	Pseudomonas sp., G42		
	Vibrio sp., G62		
*Karenia brevis**	*Cytophaga* strain 41-DBG2		Mayali et al. 2002
*Cochlodinium polykrikoides**	*Hahella chejuensis*	Prodigiosin	Jeong et al. 2005
	Micrococcus sp. LG-1		Park et al. 1998
Noctiluca scintillans (red)*	*Marinobacter salsuginis*, BS2		Keawtawee et al. 2012
Raphidophytes			
*Heterosigma akashiwo**	*Flavobacterium* sp. C49		Yoshinaga et al. 1998
	Alteromonas sp. MC27; GY21		
	Cytophaga sp. MC8		
	Pseudoalteromonas sp., Y		Lovejoy et al. 1998
	Pseudomonas aeruginosa	Rhamnolipid	Wang et al. 2005
	Alteromonas spp., S; R;		Imai et al. 1995
*Chattonella marina**	*Pseudoalteromonas* sp., Y		Lovejoy et al. 1998
	Alteromonas spp., S; R;		Imai et al. 1995
*Chattonella antiqua**	Cytophaga sp., J18/M01		Imai et al. 2001
	Alteromonas spp., S; K; D; R		Imai et al. 1995

*Harmful bloom forming species

Algicidal compounds: As few studies throw more light on the nature of these algicidal compounds, the mechanistic strategies are just beginning to unravel. An extracellular serine-protease (50kDa) produced by the *Pseudoalteromonas* sp., A28 was identified as algicidal agent against *Skeletonema costatum* (Lee et al. 2000). Similarly, a >30kDa protease from the flavobacteriaceae member *Kordia algicida* strain OT-1(T), exhibited high algicidal effect against the diatoms *Skeletonema costatum* and to a lesser extent against *Thalassiosira weissflogii and Phaeodactylum tricornutum* (Paul et al. 2011). Rhamnolipid biosurfactants of a *Pseudomonas aeruginosa* strain has been shown to kill the raphidophyte *Heterosigma akashiwo* (Wang et al. 2005). Using a combination of culture and whole genome sequence analysis of *Hahella chejuensis* strain KCTC 2396^T (*γ-proteobacteria*), Jeong et al. (2005) confirmed that its red-pigmentation due to 'prodigiosin' was strongly algicidal against the toxic dinoflagellate *Cochlodinium polykrikoides*. Recently, an anti-proliferative (suspected anti-cancer) compound 2, 3-indolinedione (isatin) produced by a *Pseudomonas* sp. *C55a-2* against the diatom *Chaetoceros* sp. have been reported to be highly algicidal (Sakata et al. 2011).

Cyst formation: In continuity of such parasitic influence on phytoplankton, certain bacterial strains associating with bloom forming toxic dinoflagellates can also induce cyst formations, although their mechanistic principle remains unknown. *Similar studies have also shown encystment of the harmful dinoflagellates: Lingulodinium polyedrum by* epibiotic bacterial strains of phylum *Bacteroidetes* (Mayali et al. 2007), *Prorocentrum mexicanum by*

algicidal bacterial strains of *Pseudoalteromonas* spp. (Lovejoy et al. 1998), *and Heterocapsa circularisquama* by *unclassified novel bacterial strains* (Kitaguchi et al. 2001). Using MPN based screening methods, Adachi et al. (2002 and 2003) showed occurences of both cyst-promoting and cyst-inhibiting bacteria associated with dinoflagellate blooms of *Alexandrium catenella* and *Alexandrium tamarense* in the Hiroshima Bay, Japan. While cyst-inhibiting bacteria belonged to the genera *Alteromonas* and *Vibrio,* those promoting encystment belonged to *α-Proteobacterial members of Rhodobacter, Roseobacter,* a novel bacterial strain *Jannaschia cystaugens* (Adachi et al. 2004), and *γ-proteobacterial* forms belonging to *Marinobacter-Neptunomonas-Pseudomonas group.*

Toxin production: Bacterial has also been known to produce toxins, such as saxitoxins in association with harmful phytoplankton blooms (Doucette et al. 1998). The increasing frequency of toxic dinoflagellate blooms in coastal waters world-wide (Heisler et al. 2008) calls for further investigation into their mechanistic principles, population assessment of such species using targeted molecular probes and detection of suspected molecules during progression of these blooms.

(c) Retrieval of marine bacteria

While study of total bacterial distribution, biomass production and respiration rates underscores their trophic importance in marine ecosystems, study of their taxonomy and metabolic diversity have been subject to a far

greater degree of challenges. Traditional plating methods to culture bacteria from open-oceans results in hardly ~ 10 -100 cfu's per ml, whereas direct estimates based on epifluorescent microscopy have shown that bacteria are present ~10^8 cells L^{-1} in the ocean with 10-100 fold variations. The high percentage (~99%) of bacteria which remains uncultured has been one of the greatest challenges of studying microbial ecology. The high diversity of bacteria is also being reflected from recent advances in molecular techniques such as the metagenomics analysis, denaturation gradient gel electrophoresis (DGGE), transcriptomic and proteomic analysis, etc (Delong and Karl 2005, De Long 2009). However, in order to gain insights into bacterial physiology and to study their metabolic potentials techniques which have been proving to be useful for increasing retreivability of bacteria are as below:

(i) *Plating on diluted media*: Dilution of the all-purpose bacteriological media such as the Zobell's marine 2216E agar have shown that frequency of colony forming bacteria can increase considerably (~10 times). This is probably because the diluted media more suitably represents nutrient depleted conditions of the ocean and does not only favour the growth of the fast-growing forms.

(ii) MPN based enrichments: Modified MPN based enrichment methods helps to selectively target a wide-range of physiological groups – from marine halophiles, Nitrogen fixers, denitrifiers, sulphate reducers, nitrifiers and assess their importance in the ecosystem.

(iii) Extinction-dilution culturing: This method have resulted in culturing members of true oligotrophs (Giovannoni and Steingl 2007), such as the

Pelagibacter ubique and other members of the SAR-11 clusters which have been unculturable so far. The method includes the dilution of the inoculum to 1-5 cells in microtiter well plates. Positive growth is screened using epifluorescent microscopy. Pure culture is established later using sea-water agar medium / maintained as diluted liquid cultures (Connon and Giovannoni 2002). Phylogenetic probes further developed from retreived bacterial cultures are also helping to track their populations in the field and relationship to ecosystem components (Kirchman 2008). Important techniques developed for this purposes includes the epifluorescent microscopy based technique of Fluorescent *insitu* hybridization (FISH), which can enable counting of specific genera/groups and their relative entry to the ecosystem.

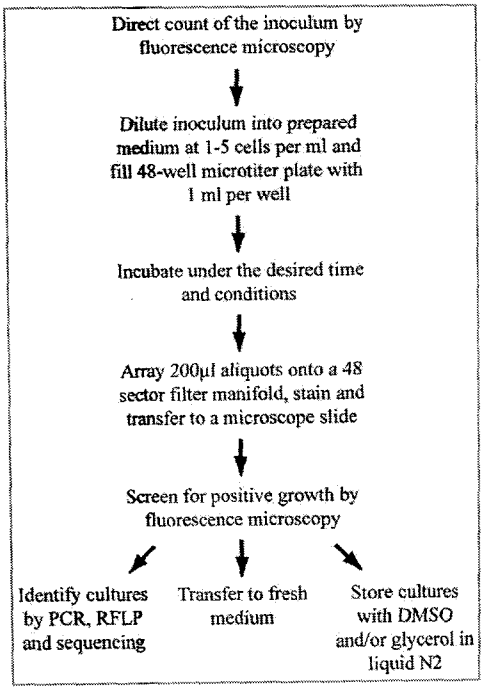

Fig. 1.6 Flow chart for dilution-extinction culturing (*adapted from Connon et al. 2002*).

1.3 Phytoplankton blooms of the Arabian Sea

The Arabian Sea is unique among other tropical ocean gyres (Pacific or Atlantic) which are located within the similar latitudinal extent as they are permanently oligotrophic (Wiggert et al. 2005). Being land-locked to the North by Asian land-mass, unequal heating of land over ocean creates a thermal gradient. This results in bi-annual Indian monsoon winds: the summer or South-West (June-September) monsoon and the winter or North-East (December – February) monsoon (Wyrtki 1973). The hydrographic changes associated with these monsoon-driven circulation and mixing processes have been known to seasonally govern phytoplankton growth and periods of elevated productivity (Wiggert et al. 2005, Banse 1987). During the summer monsoon, wind driven circulation causes strong upwelling along coasts of Somalia and Oman. Along the west-coast of India, surface currents moves equatorward and promotes upwelling along the West-coast which begins at the southern tip of India by June and keeps shoaling northwards (Shetye 1990). The intrusion of colder nitrate rich slope waters in the shelf and coastal waters, triggers blooms of diatoms by August (Sawant and Madhupratap 1996, Goes 1992). The growth of diatoms depletes nitrate in the upper-ocean. During this period blooms of several dinoflagellates have also been reported in recent times from various harmful genera, such as *Gymnodinium* sp., *N miliaris*, *Cochlodinium* sp., *Gonyaulax* sp., *Ceratium* sp. etc (Padmakumar 2012). As the system moves towards more oligotrophic conditions of the intermonsoon

periods of November, blooms of the nitrogen fixing cyanobacteria *Trichodesmium* spp. are commonly detected (Parab et al. 2006).

During the cool-dry northeast monsoon (December – February) surface currents along west-coast of India moves northward towards Saurashtra. High grazing during the early periods of north-east monsoon (December) keeps phytoplankton biomass under check (Landry et al. 1998). The winter cooling leads to convective mixing in off-shore waters, enriching the upper-ocean with nutrients from the base of the thermocline (Wiggert et al. 2005) and favouring blooms of diatoms (Sawant and Madhupratap 1996; Madhupratap et al. 1996). In recent times, however, large scale blooms of *Noctiluca miliaris* have been reported to emerge in the northern Arabian Sea during these winter-monsoon periods (Matondkar et al. 2004, Gomes et al. 2008). Blooms of the cyanobacteria *Trichodesmium* spp. are favoured in the oligotrophic spring intermonsoon months of April, extending in the open-waters, Laccadives Sea and along west-coast of India (Matondkar et al. 2006, Parab and Matondkar 2012).

Hence, based on historical records from the Arabian Sea, the two most important bloom forming species from the Arabian sea appears to be: (a) an emerging open-ocean bloom of the dinoflagellate *Noctiluca miliaris* and (b) cyanobacterial blooms of the *Trichodesmium* spp.

The high organic nature of these blooms (Ferreira et al. 2011) calls for examination of the associated micro-flora and their relationship to bloom

ecosystem. The occurrence of high-biomass blooms of *Noctiluca miliaris* can have important biogeochemical implications on processes such as the biological pump and on the expansion of the Arabian sea oxygen minimum zone (OMZ) (Morrison et al. 1999) and intensifying denitrification, already spreading into the continental shelf of the Arabian Sea (Naqvi et al. 2000).

Earlier studies on the significance of bacteria in carbon-flux during the Joint Global Ocean Flux study of the Arabian Sea (1994-1996) suggested a strong 'microbial-loop' following the diatoms dominated winter monsoon period (Madhupratap et al. 1996, Ramaiah et al. 2005, Ducklow 2001[a]), while their phylogenetic diversity was noted by Reimann et al. 1999. Barring a single study from *Noctiluca miliaris* red tide off Mangalore (Nayak et al. 2000), bacterial/microbial diversity with respect to bloom ecosystem components remains unaddressed.

In light of the above, the present research study was undertaken with the **aim** to: (i) to observe the **microflora** and **retreive culturable bacteria** associated with the recently emerging **blooms** of the dinoflagellate ***Noctiluca miliaris*** occuring in the open-ocean of the Northern Arabian Sea the cyanobacterium ***Trichodesmium erythraeum*** occuring in the coastal region of the Arabian Sea; (ii) to unveil their **identity and diversity** of the retreived bacteria through morphological, biochemical and phylogenetic analysis and (iii) to decipher **implications** of the presence of these bacteria to the bloom and evaluation of their metabolism in **relationship with bloom ecosystem components** (physico-chemical charactersitics and food-chain). The

observations and the experimental results of this study and the inferences derived thereof are recorded in this thesis entitled "***Microbial Ecology of Phytoplankton Blooms of the Arabian Sea and their implications***".

Chapter II

Microbial Ecology of *Noctiluca miliaris* bloom

Noctiluca miliaris Suriray 1836 (synonym *N scintillans* MaCartney 1810) are large sized dinoflagellates (dia. ~ 400-1200 μm), and are an important bloom forming species (Harrison et al. 2011). They have two distinct physiological forms: (i) The phagotrophic red *Noctiluca* and (ii) the mixotrophic green *Noctiluca* containing endosymbiotic photosynthetic prasinophytes, the *Pedinomonas noctilucae* (dia. ~5μm) (Elbrachter and Qi 1998). Blooms of *Noctiluca* are distributed globally and also show an environmental preference as orange-red blooms of *Noctiluca* (red) are more restricted to cooler (10-25 °C), temperate and sub-tropical coasts, whereas, the green-tides of *Noctiluca* (green) are favored in the warmer waters of South-east Asia (25-30°C) (Harrison et al. 2011). In the Arabian Sea, both these forms have been known for some time to appear as sporadic blooms, restricted solely to coastal waters off India, Pakistan and Oman (Devassy and Nair 1987, Harrison et al. 2011).

The present chapter examines bacterial distribution in the ecosystem of *Noctiluca miliaris* blooms of the Northeastern Arabian Sea (NEAS) in relation to physico-chemical charactersitics.

2.1 Materials and Methods

2.1.1 Study Site and Cruise Tracks

Two research vessels - *ORV Sagar Kanya (SK)* and *FORV Sagar Sampada (SS)* (Plate 2.1) were used to study the dinoflagellate *Noctiluca miliaris* bloom in the Northeastern Arabian Sea (16-22°N and 64-72°E; Goa-Porbander sector) during the winter-monsoon period (Feb-Mar) of 2009-2011. Navigation to sampling locations during these cruises were guided by remotely sensed high Chlorophyll *a* areas as indicator of bloom using Indian remote sensing satellite (IRS-P4) ocean color monitor sensors (OCM and OCM-2). Cruise tracks and sampling stations from four oceanographic cruises are as shown in Fig. 2.1: Cruises *SK-256* (9th –23rd February 2009), *SS-263* (28th Feb – 13th March 2009), *SS-273* (5th – 13th Mar-2010) and *SS-286* (5th – 23rd Mar-2011).

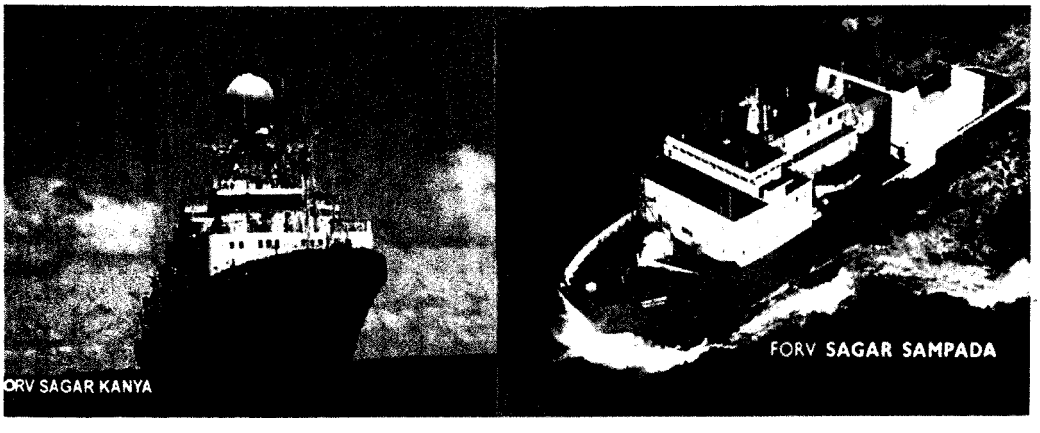

Plate 2.1 Oceanography research vessels ORV *Sagar Kanya* and FORV *Sagar Sampada* used for the present study.

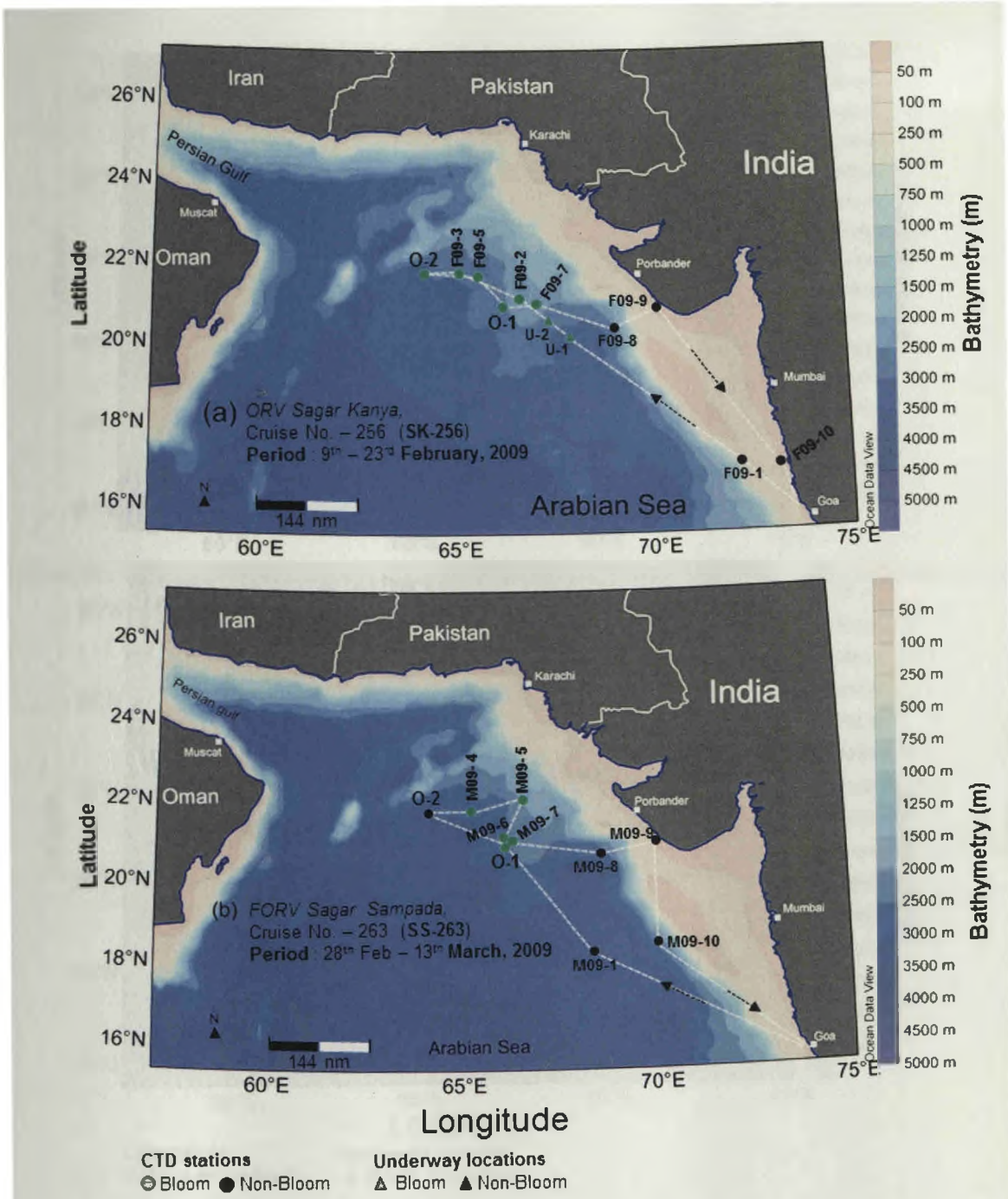

Fig. 2.1 Cruise tracks showing sampling stations for study of the dinoflagellate *Noctiluca miliaris* (green) in the Arabian Sea during: (a) February-2009 (b) March-2009 (c) March-2010 (d) March-2011.

Fig. 2.1 (c-d)

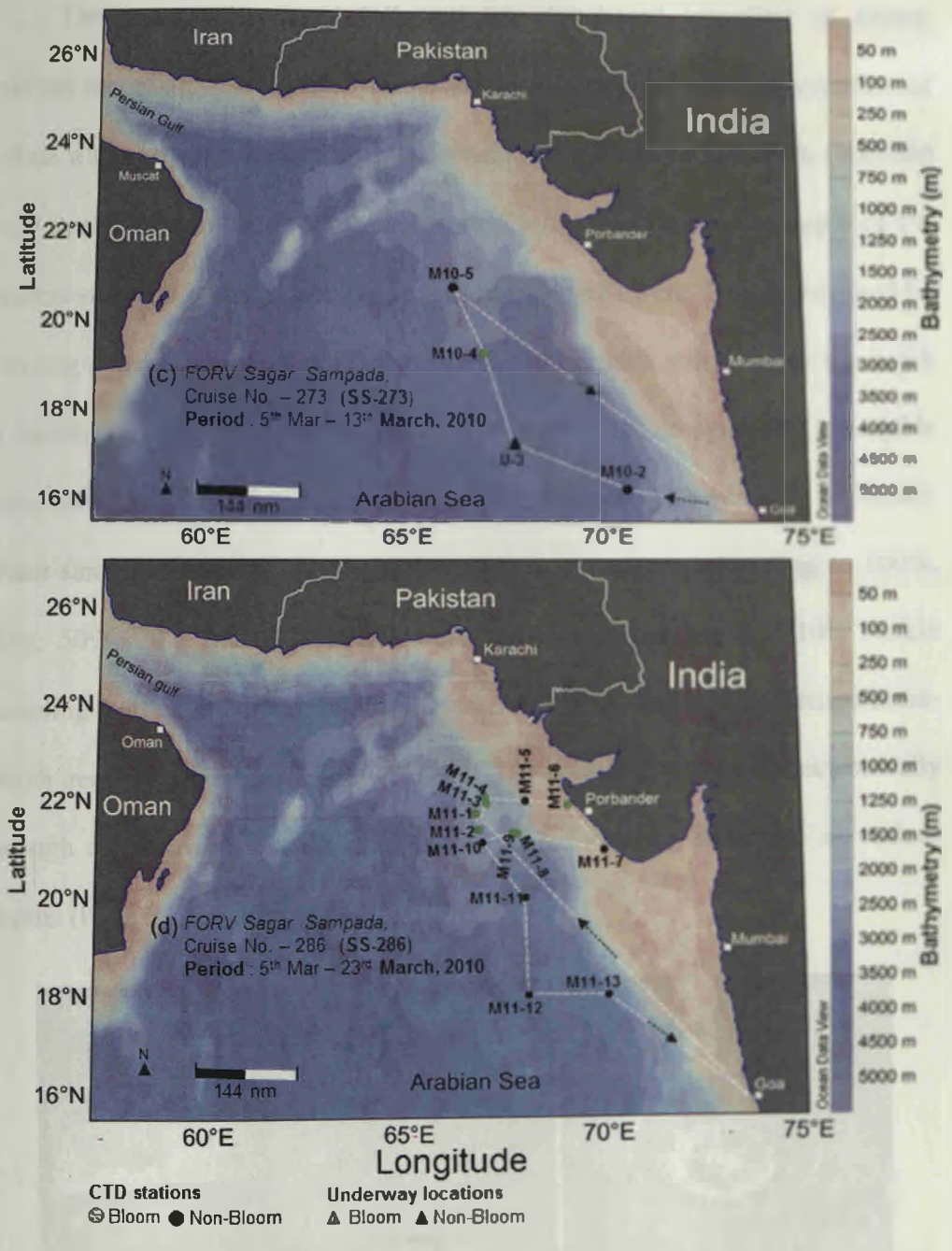
Iran
Pakistan
India
Karachi
Persian Gulf
Muscat
Oman
Porbander
Mumbai
Goa
M10-5
M10-4
M10-3
M10-2
(c) FORV Sagar Sampada,
Cruise No. – 273 (SS-273)
Period : 5th Mar – 13th March, 2010
Arabian Sea
144 nm
N
26°N
24°N
22°N
20°N
18°N
16°N
60°E
65°E
70°E
75°E
Latitude
Bathymetry (m)
50 m
100 m
250 m
500 m
750 m
1000 m
1250 m
1500 m
2000 m
2500 m
3000 m
3500 m
4000 m
4500 m
5000 m
Ocean Data View
Iran
Pakistan
India
Karachi
Persian gulf
Oman
Oman
Porbander
Mumbai
Goa
M11-1
M11-2
M11-3
M11-4
M11-5
M11-6
M11-7
M11-8
M11-9
M11-10
M11-11
M11-12
M11-13
(d) FORV Sagar Sampada,
Cruise No. – 286 (SS-286)
Period : 5th Mar – 23rd March, 2010
Arabian Sea
144 nm
N
26°N
24°N
22°N
20°N
18°N
16°N
60°E
65°E
70°E
75°E
Latitude
Longitude
Bathymetry (m)
50 m
100 m
250 m
500 m
750 m
1000 m
1250 m
1500 m
2000 m
2500 m
3000 m
3500 m
4000 m
4500 m
5000 m
Ocean Data View
CTD stations
Bloom Non-Bloom
Underway locations
Bloom Non-Bloom

2.1.2 Collection of bloom

The common protocol followed for ship-board sampling of bloom involved recording visual observations of the ocean-color and examination of surface waters at each station in the morning from plankton net hauls (100-200 µm) / steel bucket to check for presence of *Noctiluca miliaris*. The depth of 1% incident sun-light in the upper ocean (euphotic depth) were then determined by lowering either a Secchi-disk (Depth of 1% light equals ~three times the depth of Secchi disk visibility), or recorded from a PAR (Photosynthetic avaialable radiation in the visible spectrum) biospherical sensor (Dwivedi et al. 2006). Water samples from 5-7 depths in the euphotic zone (corresponding to 100%, 80%, 50%, 20% and 1% PAR) were then collected using 5-10L Niskin sampling bottles mounted on a 911 *plus* CTD (Conductivity-Temperature-Depth recording profiler) rosette. The CTD rosette controlled electronically through a hydrowire from a deck-unit, enabled closing of bottles at various depths (Plate 2.2).

Plate 2.2 Collection of *Noctiluca miliaris* bloom: (a) Deck controlling unit (*FORV Sagar Sampada*); (b) CTD rosette (*ORV Sagar Kanya*).

2.1.3 Bloom and Non-bloom sampling stations

Bloom and non-bloom sampling stations were differentiated based on Chl *a* and microscopic counts of *Noctiluca miliaris*.

2.1.3.1 Chl *a* as indicator of bloom

Satellite study

Chl *a* images from Indian remote sensing satellite (IRS-P4) ocean color monitor sensor (OCM) was used for routine detection and tracking of the bloom during shipboard sampling (Dwivedi *et al.* 2006). Chl *a* estimated by OCM-II and avaialable as level 2c images from the National Remote Sensing Centre (NRSC), Hyderabad, India was extracted for the bloom locations using ERDAS 9.5 or ENVI 4.4 image analysis softwares at Space Application Centre (ISRO), Ahmedabad. 8-day and monthly composite (method of choosing best value pixel) freely available Chl *a* data generated by other satellites sensors such as Sea-viewing Wide Field-of-view Sensor (SeaWiFS, 9km resolution) and the Aqua-Moderate Resolution Imaging Spectroradiometer (MODIS-Aqua, 4km resolution) were obtained from the NASA Giovanni DISC website (http://oceancolor.gsfc.nasa.gov) and used extensively during this study to corroborate ship-board observations of the bloom.

In situ study

For analysis of Chl *a*, water-samples were drained from Niskin sampler into acid-cleaned 5L carboys and were immediately filtered onto 25mm GF/F filters (0.5 – 1L) (Plate 2.3a), frozen in liquid nitrogen on the ship at sea and

transported to the shore laboratory for analysis by HPLC (Wright et al. 1991). HPLC analysis was performed following the method of Parab et al. (2006). Filters were immersed in 90% acetone-water, extracted under cold and dark conditions overnight and finally filtered through 0.2μm, 13mm PTFE (Polytetrafluoroethylene, Millipore) filters to free the sample from any particulate debris. Aliquots of 1ml of the extract were then mixed with 0.3ml of distilled water in a 2ml amber vial and allowed to equilibrate for 5min prior to its injection into an Agilent® 1100 series HPLC (Plate 2.3b), equipped with a diode array detector. Pigments separation was achieved in a C-18 column, flow rate of 1 ml per min. The gradient mobile phase consisted of Solvent A (80:20 v/v methanol: 0.5M ammonium acetate, pH 7.2 and 0.01% butylated hydroxytoluene w/v), Solvent B (87.5:12.5 v/v acetonitrile: water and 0.01% butylated hydroxytoluene w/v) and Solvent C as ethyl acetate. Chl *a* was identified based on retention time of (Rt ~21.6 mins) and concentration determined from peak area of spectrophotometrically estimated standard Chl *a* (Sigma-Aldrich) run alongwith samples during the analysis.

2.1.3.2 Concentration of *Noctiluca miliaris*

Identification and enumeration of *Noctiluca miliaris* was carried out by microscopy (Parab et al. 2006). 500 ml of seawater from various depths were fixed with 1% Lugol's iodine and preserved in 3% buffered formaldehyde. Water samples for microscopic analysis were concentrated to 5–10 ml by carefully siphoning the top layer with a tube covered by a 20 μm Nytex mesh on one end. Replicates of 1ml sample concentrates were transferred to a

Sedgwick-Rafter slide and counted using an Olympus Inverted microscope (Model IX 50) at 200X magnification.

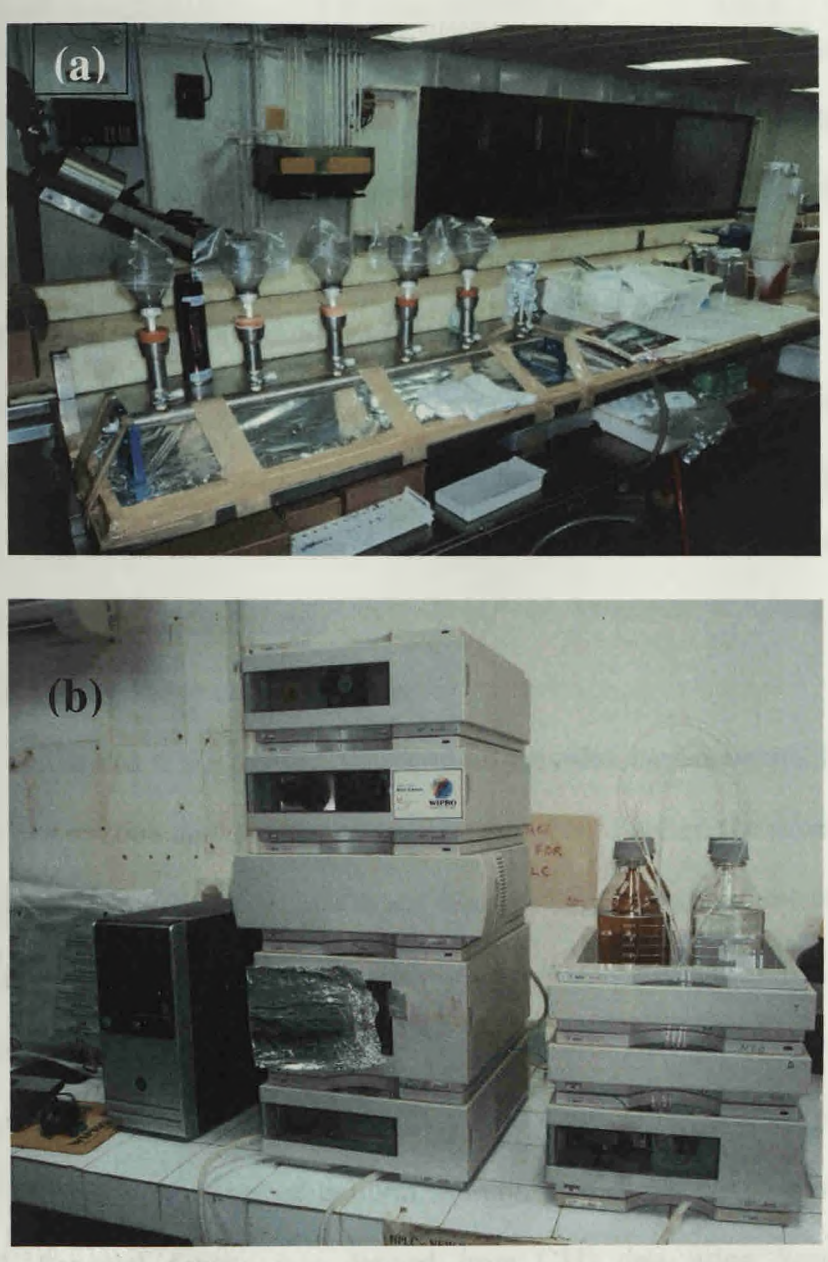

Plate 2.3 (a) Work space for filtration of water samples on board; and (b) Agilent 1100 HPLC facility used at National Institute of Oceanography (CSIR-India), Goa.

2.1.4 Physical Characersitics

2.1.4.1 Wind-speed

In situ wind-speed and direction was recorded from ship-board anemometers. Wind-vector images (daily, monthly and weekly averages) from the NASA's sea-wind Scatterometer satellite (QuickSCAT) available upto 2009 were downloaded from the website http:// www.remss.com/qscat/qscat browse.html.

2.1.4.2 Photosynthetic available radiation (PAR)

Monthly averages and 8-day composite MODIS-Aqua (4km and 8km resolution) satellite estimates of PAR were obtained for the area between 64-69°E and 19-23°N from NASA Giovanni DISC website http://oceancolor.gsfc.nasa. gov.

2.1.4.3 Hydrographic characteristics

Processed CTD profiles from cruises provided measurements for sea-water temperature and salinity of the water-column. Further, the mixed-layer *(homogenous layer of temperature, salinity and, hence sea-water density)* was calculated as the depth where, potential density, σ_Θ (*density of sea-water parcel when raised to surface without exchange of heat and change in salinity*), increased by 0.2 kg m^{-3} than the surface value, representing both isothermal (layer of uniform temperature, T_{mld}) and isohaline (layer of uniform salinity, T_{sal}) conditions (Shetye et al. 1996). Potential density was derived from CTD data using Seasave-V7 software (Seabird electronics, USA), which has inbuilt functions for calculating physical variables using thermodynamic equations of sea-water.

2.1.4.4 Mesoscale features

In order to check the spatial location of the bloom stations with respect to mesoscale (10 -500 km) eddies, daily and weekly composite images of changes in sea-surface height measured by satellite based altimetry were obtained on request from ftp site of Colorado center for astrodynamical research, USA (eddy.colorado.edu/ccar/data-viewer/index). Corresponding satellite images during Feb-Mar, 2009 for Historical sea-surface height anomaly maps (SSHA), absolute geostrophic velocity (*Ocean currents resulting from the balance between 'pressure gradient due to changes in sea-surface heights' and 'rotation of the earth'*), sea-surface temperatures (SST) and Chl *a* were compared with respect to bloom locations to check the presence of eddy during the bloom period.

2.1.5 Chemical characersitics

2.1.5.1 Dissolved Oxygen

On return of the CTD rosette to deck after hydrographic cast, samples for dissolved oxygen were always drawn first from the Niskin. Dissolved oxygen was estimated using the modified Winkler titration method which importantly involved whole bottle-titrations to reduce loss of iodine due to volatilization (Carpenter 1965). While end-point detection using starch as an indicator were used on cruises *SK-256*, an amperometric (Langdon) winkler titrator (Langdon 2010) was used during the cruises *SS-263, SS-273* and *SS-286* for precision measurements (Plate 2.4). This method essentially followed the winkler titration. 1 ml each of Winkler A ($MnCl_2$ -3M) and Winkler B (NaOH

– 5M; NaI – 8M) were added using repeater pipettes with long-tips immediately after water samples were drawn from Niskin into gravimetrically corrected 125 ml nominal capacity (pyrex) flared-neck Iodine titration flasks. Fresh water was added around rim and sealed with parafilm to prevent atmospheric contamination. After incubation for 3-4 hours in dark, the precipitated dissolved oxygen as hydrated tetravalent oxide of manganese was dissolved with acidified 5M H_2SO_4 to liberate Iodine from iodide ions in stoichiometric proportions (2 moles of Iodine for 1 mole of Oxygen). The flask was placed on the magnetic stirrer and titrated using an automated amperometric (Langdon) titration assembly. On starting the titration, a potential of 100mV was applied between two platinum electrodes dipped in the titration flask. At the cathode (negative electrode) Iodine gained electrons from the electrode to form Iodide (oxidation) and at the anode (positive electrode) Iodide lost electrons (reduction) to the electrode to form Iodine, resulting in flow of electrons from anode to cathode and a stable current proportional to Iodine was measured by the titrator assembly. From a motorized 2 ml piston burette 0.11 M sodium thiosulfate dispensed (in µl quantity) reacted with Iodine (2 moles of thiosulfate for 1 mole of Iodine) to form Iodide decreasing the current. The current ceased following the exhaustion of Iodine and recorded as the end-point. Oxygen concentrations were calculated following blank titrations for reagents and standardization of thiosulfate with 0.00167 M in oven-dried potassium iodate and expressed as µM or ml L^{-1}. The pickling

reagents were further flushed periodically with Nitrogen to prevent contamination during cruises and obtain appropriate blanks.

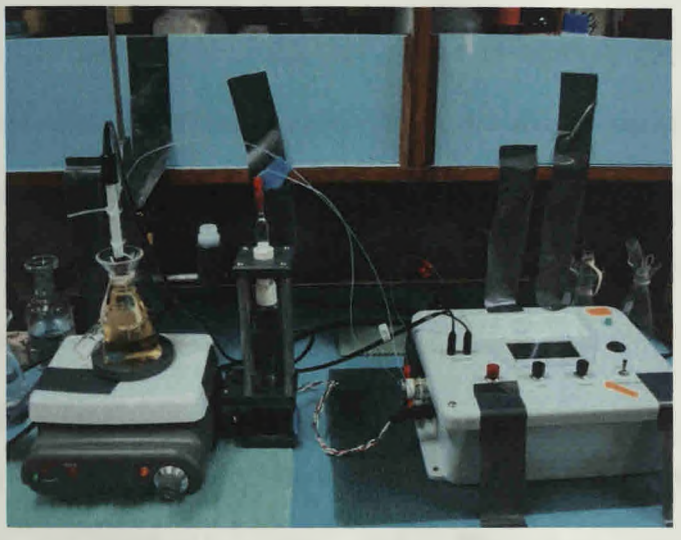

Plate 2.4 Amperometric titration for estimating dissolved oxygen.

2.1.5.2 Dissolved inorganic nutrients

For estimation of dissolved inorganic nutrients (Nitrate-N, Nitrite-N, Phosphate-P and Silicate-Si), 500 ml water samples were filtered through GF/F fraction (<0.7 micron) and frozen in acid-cleaned plastic bottles prior to spectrophotometric analysis, essentially following methods of sea-water analysis as detailed in Grasshoff et al. (1999). Spectrophotometric analysis was carried out using a Perkin Elmer Lambda 40 UV/Vis spectrophotometer using quartz cuvette of 10 cm path length (Plate 2.5). Prior to analysis frozen sea-water samples were thawed and brought to room-temperature prior to analysis.

Dissolved inorganic N-Nitrite

For estimation of dissolved Nitrite-N in sea-water, 0.5 ml of sulphanilamide was added to 25 ml aliquots of sample taken in 50 ml graduated glass tubes to react with nitrite for ~1min to form a diazonium compound. On addition of 0.5 ml of n-(1-napthyl)-ethylenediamine dihydrochloride and ~15-20 mins reaction time, the absorbance of the azo dye (magenta colour) formed was recorded at 540 nm. Absorbance by anhydrous sodium nitrite (2 μM) was used as standard to calculate calibration factor (F) as concentration of Nitrite-N per unit absorbance.

Dissolved inorganic N-Nitrate

Prior to sample analysis Nitrate was reduced to Nitrite by Copperized Cadmium granules packed in a glass column. The column was activated by passing 100μM Nitrate standard in 250 ml saturated buffer of ammonium chloride solution. During analysis, three aliquots of 25 ml sample was passed through the column to prevent contamination among samples and the fourth aliquot was collected for estimation of Nitrite-N as described earlier. Potassium Nitrate (2 - 10μM) was used as the standard to calculate calibration factor as concentration per unit absorbance. Nitrite-N estimated after reduction was subtracted from the actual Nitrite-N to obtain concentration of Nitrate-N (μM).

Dissolved Inorganic P-Phosphate

Dissolved inorganic Phosphate-P in sea-water was estimated by adding 0.5 ml of an acidified ascorbic acid reagent (reductant) to a 25 ml aliquot of the sea-water sample, followed by addition of 0.5 ml of an acidified mixed reagent

containing ammonium heptamolybdate tertrahydrate and potassium antimony tartarate. The reaction of phosphate ions with an acidified 'mixed reagent' resulted in a blue phosphorous complex and absorbance of sample was measured at 880 nm after ~10-15 mins reaction time against reagent blanks. Standards of 1 μM Phosphate-P aliquots were prepared by diluting a 10 μM stock of acidified oven dried (110°C) KH_2PO_4. Calibration factor (F) was expressed as the concentration of Phosphate–P per unit absorbance.

Dissolved inorganic Si-Silicate

For estimation of dissolved Silicate-Si all samples and reagents used for analysis were contained in plastic bottles to prevent contamination from glass-wares. 0.5 ml of a mixed reagent of acid molybdate was added to 25 ml sea-water samples taken in a plastic reagent bottle followed by immediate addition of 0.5 ml oxalic acid and 0.5 ml of ascorbic acid as the reductant. The absorbance of blue silicomolybdic acid was measured after 30-40 mins at 810 nm using a cuvette of 1 cm path length. 15 μM of aqueous solution of disodium hexafluorosilicate was used as the silicate standard to calculate the silicate-Si calibration factor (F) as concentration per unit absorbance.

On cruises SS-263, SS-273 and SS-286, dissolved nutrients were also measured onboard using a segmented flow autoanalyzer (SKALAR) essentially following the same principles as described above (Knap et al. 1996).

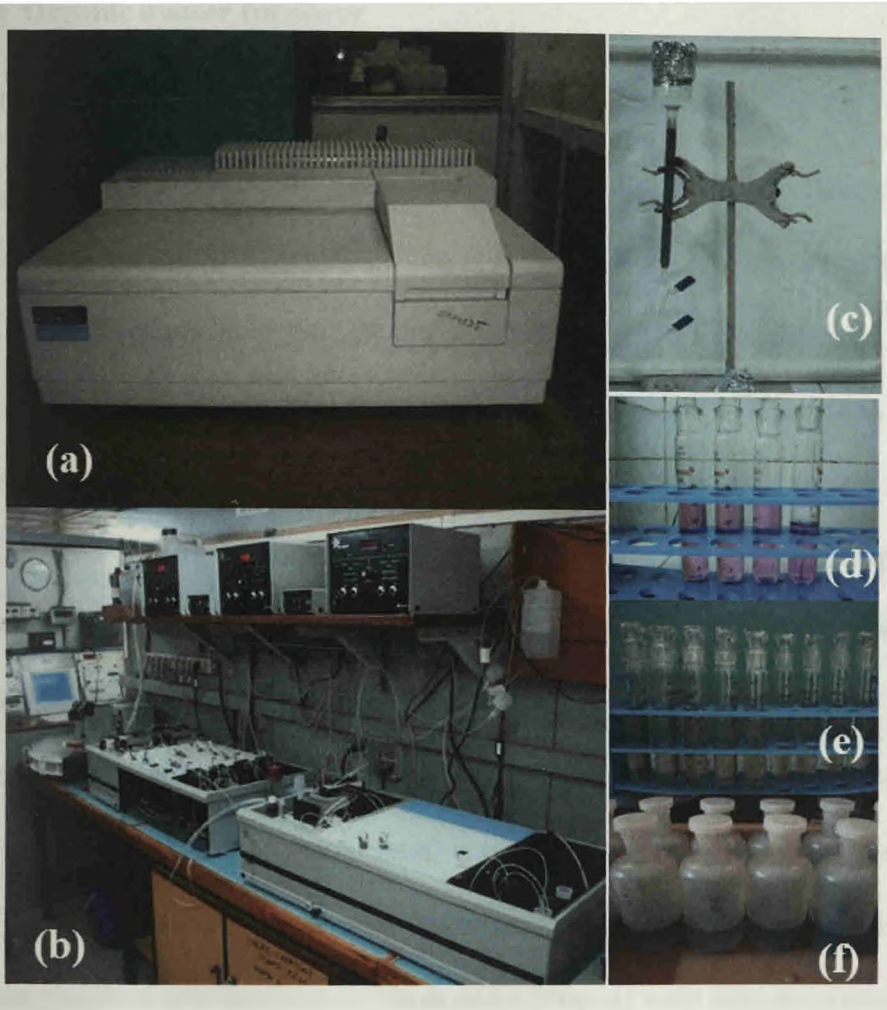

Plate 2.5 Dissolved nutrients analysis: (a) Perkin Elmer lambda 40 UV/Vis spectrophotometer; (b) SKALAR autoanalyzer (FORV Sagar Sampada); (c) Cd-Cu column for Nitrate reduction, and complexes of (d) Nitrite-N (e) Phosphate-P and (f) Silicate-Si estimated spectrophotometrically.

2.1.6 Organic matter turnover

2.1.6.1 Photosynthetic carbon-fixation

Primary productivity was measured for the Northern Arabian Sea cruises during bloom of dinoflagellate *N miliaris* from ^{14}C-uptake as exactly detailed by (Knap et al. 1996). Water samples collected from euphotic depths were injected with ^{14}C-bicarbonate (5μci) obtained from BRIT, India to 250ml capacity Nalgene Polycarbonate bottles. Incubation for uptake was done for 10-12 hrs on deck in a circulating sea-water tub (Plate 2.6) using appropriately calibrated light cut-off screens. Following incubation, water-samples were filtered through GF/F filter to retain fixed-biomass and acidified with 0.5N HCl to get rid-off inorganic Carbon in 7 ml scintillation vials. In laboratory, scintillation cocktail-W (Spectrochem) was added and activity was determined with a Wallac Scintillation counter (model no. 1409). Primary Productivity of surface plankton size-fractions (<20μm and <200μm) were also determined.

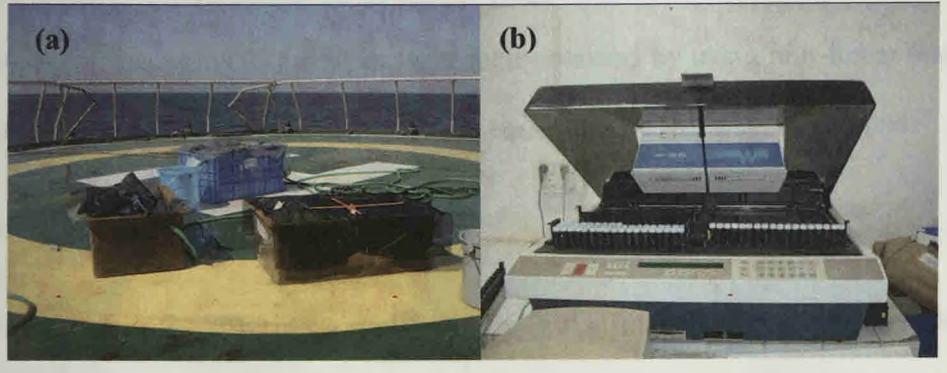

Plate 2.6 Estimation of carbon-fixation rates: (a) Circulating sea-water tubs with light cut-off screens on board *Sagar Sampada*; (b) Wallac liquid scintillation counter at NIO, Goa.

2.1.6.2 Chromophoric dissolved organic matter (C-DOM)

Water samples for CDOM analysis were filtered through a 0.22μm nucleopore polycarbonate membrane filter using clean techniques (Plate 2.7). CDOM samples were stored in 100ml amber colored bottles at 4°C in dark till spectrophotometric analysis on return to shore. CDOM absorption was measured in a Perkin Elmer lambda 40 spectrophotometer using quartz cuvette of 10cm path-length. Characteristic exponentially decaying CDOM spectra were obtained for the 250-800 nm region. Any baseline offsets due to temperature drift or scattering effects were corrected following Helms et al. (2008) and CDOM absorption coefficients (m^{-1}) were calculated from absorbance as below:

$$Ac_{\lambda} = 2.303A/l$$

where, Ac_{λ} is the absorbtion coefficient (m^{-1}) corresponding to absorbance A at wavelength λ and l is the optical path length (m). The exponential spectral slopes for the region 325-650nm were then obtained by using non-linear least squares fit of the CDOM spectrum to the equation (Twardowski et al. 2004)

$$Ac_{\lambda} = Ac_{\lambda o} e^{S(\lambda o - \lambda)}$$

Where, Ac_{λ} is the absorption coefficient (m^{-1}) at a final wavelength, $Ac_{\lambda o}$ is the absorbtion coefficient (m^{-1}) at any reference wavelength and S is the exponential slope (nm^{-1}).

The CDOM concentrations were expressed in terms of Ac_{300} and Ac_{325} (Nelson et al. 2002) as proxy for dissolved organic matter. The $Ac_{250:365}$ ratio

(De Haan and De Boer et al. 1987) and the slope-ratios (S_{ratio}), defined as $S_{275-295}$:$S_{350-400}$ was calculated as indicators of CDOM molecular-size following Helms et al. (2008). The $Ac_{465:665}$ ratio was further calculated as an indicator of CDOM aromaticity/general tracer of humicity (Summers et al. 1987).

Plate 2.7 Filtration set-up for C-DOM analysis on board *Sagar Sampada* (Cruise SS286, Mar-2011).

2.1.7 Microbial analysis

2.1.7.1 Evaluation of bacterial distribution

Water samples for all microbiological analysis were directly drained from the Niskin sampler. For estimating total bacterial counts, 100 ml water samples were immediately fixed with 2% final concentration (v/v) of glutaraldehyde and stored at 4 °C. Slides for cruises SK256, SS263 and SS273 were prepared in shore-laboratory at National Institute of Oceanography, Dona-Paula, Goa and during the cruise of SS286 they were prepared onboard ship. For preparation of slides, 1-5 ml water samples were first stained using 1 $\mu g\ ml^{-1}$ concentration of 4', 6-diamidino-2-phenylindole (DAPI) (Porter and Feig 1980) for 15 mins, filtered with gentle suction onto 25mm diameter 0.22μm black nuclepore polycarbonate filter (keeping shiny face up) with a GF/F filter at base to obtain even distribution of cells. The filter piece was lifted using forcep at one end and mounted on grease-free slide thinly smeared with non-fluorescent immersion oil (Type NF, Nikon). ~15 μl of immersion oil was placed on the filter and a 25 mm cover-slip was mounted, allowed to settle and slide inverted on a paper-towel with a gentle press. The slides were wrapped in alumunium foil and stored at 2-4°C for counting. Counting was done under 100X (oil immersion) objective lens in a Nikon-80i epifluorescent microscope (Plate 2.8) under UV filter-sets for DAPI using an eyepiece fitted with 100×100 μm calibrated occular grid (Appendix I). Images were captured from the eye-piece using a hand-held Sony-digital camera (12.5 mega-pixel) under low-light. Bacterial carbon biomass was calculated from total bacterial counts using the conversion of 20 fg C $cell^{-1}$ as it is an average standard

conversion which was employed for several previous studies from the Arabian Sea (Ducklow et al. 2001[a]).

Counts of photoautotrophs (picocyanobacteria) were determined on unstained samples from autofluorescence of picocyanobacterial pigments and slides were prepared exactly as above (Kemp et al. 1993). Under green excitation total picoplankton counts were obtained and under blue wave band excitation (450-500 nm), phycoerythrin containing pico-cyanobacteria fluoresced orange-yellow, *Prochlorococcus* as fading red dots and Phycocyanin containing picocyanobacteria as deep-red could be differentiated (Kemp et al.1993). Total counts of picocynaobacteria were calculated and expressed as Cells L^{-1} as described above.

2.1.7.2 Heterotrophic Nanoflagellates (HNF)

Heterotrophic nanoflagellate population were estimated during Cruise *SS-286* of Mar-2011. Samples for Nanoflagellates enumeration were at first size fractionated through 20µm nytex mesh. 100 ml of sea water was fixed in a three step procedure: 0.05% final concentration of alkaline Lugol's solution, followed by addition of 0.1% final concentration of 3% sodium thiosulfate and 2% final concentration of borate buffered formalin (Sherr and Sherr 1993). 25-30 ml of preserved sub-samples used for slide preparation were stained with 50 µg ml^{-1} DAPI (4'6' diamidino-2-phenylindole) for 7-10 mins and filtered through 0.8 µm pore-size Nuclepore polycarbonate filters. Slides were prepared in the same way as described in the above section.

Plate 2.8 Nikon 80i epifluorescent microscope.

2.1.7.3 Bacterial Production rates

The rate of synthesis of cellular DNA by heterotrophic bacteria were estimated from selected bloom and non-bloom stations, from the uptake of ^{3}H-methyl thymidine and converted to rates of synthesis of cellular carbon (Bacterial Production) using mean oceanic standard factors (Knap et al. 1996). 20 ml replicates from each depth were collected directly from the Niskin sampler in 50 ml graduated sterile centrifuge tubes (Tarsons, India). ^{3}H-methyl thymidine (Specific activity 52 Ci mM^{-1}, ICN aquous) was added to a final concentration of 20 nM (v/v). Tubes were wrapped up in alumunium foils and incubated in a circulating sea-water tub to provide ambient temperature in the dark for 1 hour. The uptake of thymidine was terminated by adding 1ml formaldehyde. Samples were filtered through 0.22 μm Millipore filters (Millipore India Ltd, Bangalore) on a chilled filtration unit kept over ice-packs and the thymidine incorporated into cellular DNA was extracted by rinsing

with cold trichloroacetic acid (5 ml) and cold ethanol (3 ml for each rinse). The filters were immersed in ethyl-acetate, stored in 7 ml scintillation vials. Killed blanks by adding formaline immediately after addition (time-zero) of ^{3}H-methyl thymidine were estimated simultaneously as control. In laboratory, scintillation fluid (cocktail-W, Spectrochem, Mumbai) was added to the samples and dpm (disintegrations per minute) and counts were deduced in a Wallac Scintillation counter (model no. 1409). Average conversion factor of 2.17×10^{18} cells $mole^{-1}$ of thymidine incorporated and 20 fg C $cell^{-1}$ for the Arabian Sea was used to calculate bacterial production (Ducklow 2000). The ratio of BP to the standing biomass was expressed as the population growth rates.

2.1.8 Data analysis

Maps and contours of the euphotic section were plotted using Ocean data View (ODV 4.5.3) software (Schlitzer 2002). The data from the euphotic zone (upto depth of 1% light) were integrated (trapezoidal integration) and expressed as euphotic 'Column' estimates per m^2. Principal component classification analysis (PCA) projecting Pearson's product moment correlations among variables from matching depth-wise dataset for the seasons Feb-09, Mar-09 and Mar-11 were performed using Statistica-6. Correlation graphs and correlation coefficients were obtained using excel (Microsoft).

2.2 Results

2.2.1 Detection and tracking of bloom

Detection and tracking of algal blooms in off-shore waters of the northeastern Arabian Sea was facilitated by Chl *a* images from Indian space borne sensors IRS-P4 -OCM and OCM-II (Fig. 2.2). The bloom was also detected from MODIS-Aqua derived averaged 8-day composites of Chl *a* in the study area, between 19 – 23°N and 64 – 69°E in the northeastern Arabian sea (NEAS) for January-April (2009-2011). As seen in Fig. 2.3, the bloom was initiated during late January, reached active or peak stage during the month of February and declined during March. The average Chl *a* in the area for the period 2009-2011 increased from 0.8 ± 0.17 mg m^{-3} during January to 2.47± 0.33 mg m^{-3} during February and dropped to 0.75± 0.26 mg m^{-3} during the month of March.

Ship-board observations mirrored the satellite trends as massive blooms (green-tides) were observed (Plate 2.9) during the cruises of February-2009 in the NEAS. Microscopic analysis revealed the bloom forming organism as the dinoflagellate *Noctiluca miliaris* (green) harbouring the symbiotic prasinophytes *Pedinomonas noctilucae* (cell diameter 0.5 - 1mm). During the cruises of March-2010 – 2011 bloom of *N miliaris* was detected in the same area during the receeding phase.

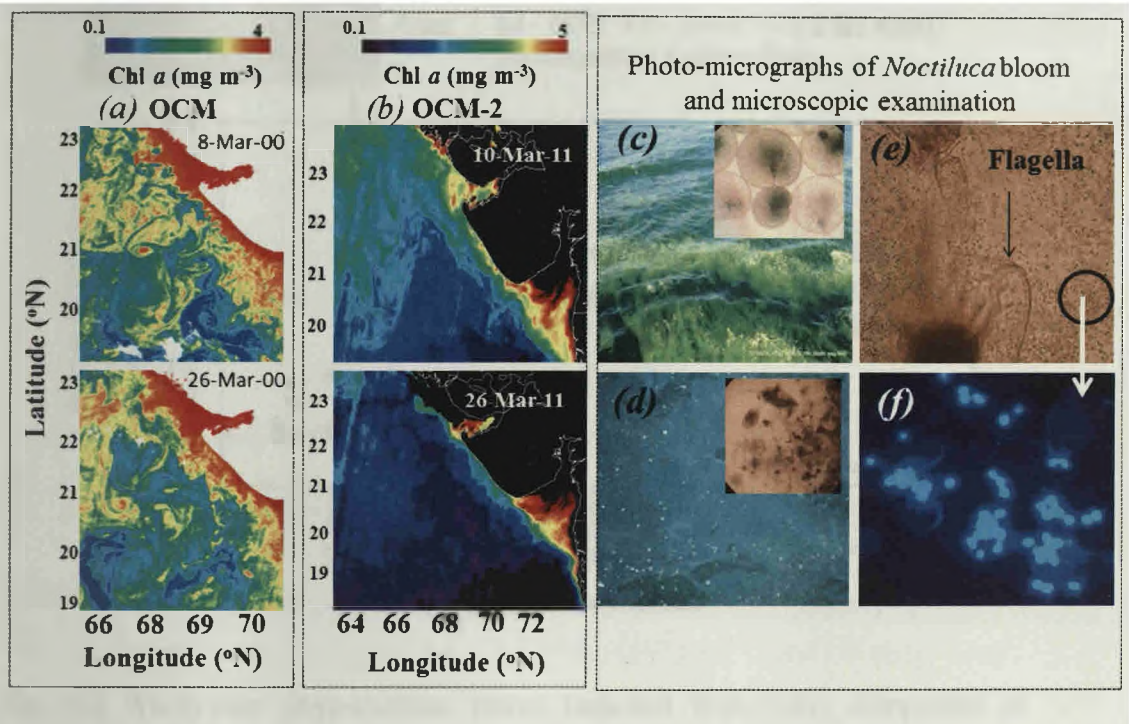

Fig. 2.2 Detection of bloom in off-shore waters of the northeastern Arabian Sea facilitated by Indian space borne sensors: *(a)* IRS-P4 OCM and *(b)* IRS-P4 OCM-2. Shipboard observations of the dinoflagellate green *Noctiluca miliaris* bloom during its: (*c*) peak/active phase of Feb-09 (*inset*) green *Noctiluca* cells and (*d*) declining phase of Mar-09 (*inset*) clumped *Noctiluca* cells. Microscopic examination of *Noctiluca* showing (e) green endosymbiontic prasinophytes (40X); (*f*) DAPI stained bi-flagellated endosymbionts (100X).

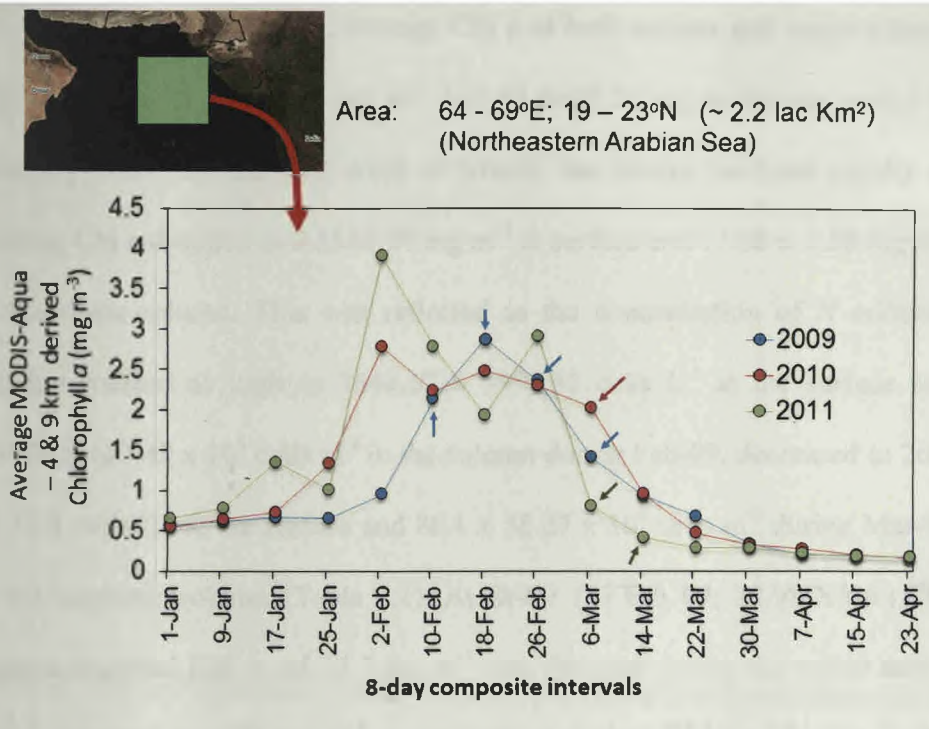

Fig. 2.3 Winter-time phytoplankton bloom indicated from 8-day composites of MODIS-Aqua (4 & 9km resolution) sensor derived estimates of Chl *a* in the northeastern Arabian Sea during the study period. Cruise periods falling during the bloom periods are indicated as arrows on starting days of 8-day composite. *(Data source: NASA DISC, Giovanni)*

2.2.2 Bloom and Non-bloom sampling stations

Noctiluca miliaris counts in the euphotic-water column (>10 cells L^{-1}) and open-water surface Chl *a* exceeding 0.5 mg m^{-3} were selected as locations of the *N miliaris* bloom in the NEAS. As seen in Fig. 2.4b, bloom was detected in a total of 19 sampling stations during 2009-2011 between 19-22°N and 64-69°E in the NEAS (station locations as shown in cruise tracks Fig. 2.1).

As seen in Table 2.1, average Chl *a* at both surface and water-column was as high as 5.33±10.96 mg m^{-3} and 43.5±28.23 mg m^{-2}during cruise of February 2009. By the first week of March, the bloom declined rapidly as average Chl *a* dropped to 0.55±0.30 mg m^{-3} at surface and 11.88 ± 3.88 mg m^{-3} in the water-column. This was reflected as the concentration of *N miliaris*, which remained as high as 1644.67 ± 3897.55 cells L^{-1} at the surface and 346.93 ± 683.49 x 10^4 cells m^{-2} in the column during Feb-09, decreased to 26.2 ±0.32.8 cells L^{-1} at the surface and 86.1 ± 58.27 x 10^4 cells m^{-2} during Mar-09 in the euphotic column (Table 2.1). At St-O1 (17Feb 09; 20.98°N/66.18°E) highest recorded Chl *a* of 27.7 mg m^{-3} was detected during the entire study, which dropped to 0.99 mg m^{-3} at the surface during 2nd Mar 09 (Fig. 2.4a). Surface *N miliaris* counts at St-O1 was also the highest and varied from 9600 cells L^{-1} during Feb-09 and decreased to 80 cells L^{-1} during Mar-09 as the bloom was declining (Fig. 2.4b). During Mar-10, bloom was detected at the single location (M09-10) and reflected similar intensity to that during Mar-09. During declining bloom phases of March-2011 high concentrations of cells were detected at stations M11-1 to M11-4 at depths below 20 m, however average Chl *a* still remained lower than Feb-09 indicating the receeding phase of bloom (Table 2.1). From the average distribution of *N miliaris* it is seen that bloom remained well distributed in the water-column upto 35-40 m (Fig. 2.4b). In comparison, Chl *a* at non-bloom stations remained <0.5 mg m^{-3}. In the coastal sites off Veraval, Gujrat (St F09-9), *N miliaris* remained undetectable in Feb-09 and Chl *a* was as low as 0.86 mg m^{-3} which further decreased to 0.2

mg m^{-3} in the same area during Mar-09 (St M09-9) in comparison to off-shore bloom (Table 2.1). However, during Mar-11, high Chl *a* was detected in the coastal station M09-7, and *N miliaris* was present even at the coastal station M09-6, at depths of 30m (42 cells L^{-1}).

Table 2.1 Chl *a* and *Noctiluca miliaris* cell counts as indicator of bloom in the Northeastern Arabian Sea.

Cruise Period (Stations)	Chl *a*		*Noctiluca miliaris* counts	
	Surface (mg $m^{-3)}$	**Column** (mg m^{-2})	**Surface** (cells L^{-1})	**Column** (10^4 cells m^{-2})
Active Bloom				
Feb-2009 (n=6)	5.33 ± 10.96	43.50 ± 28.23	1644.67 ± 3897.55	346.93 ± 683.49
Declining Bloom				
Mar-2009 (n=6)	0.55 ± 0.30	11.88 ± 3.88	26.2 ± 32.85	86.1 ± 58.27
Mar-2010 (n=1)	0.64	20.27	60	74.5
Mar-2011 (n=7)	1.25 ± 1.12	35.25 ± 19.60	520.29 ± 748.43	1429.49 ± 2474.19
Non-Bloom (Off-shore/Slope /Shelf)				
Feb-2009(n=3)	0.33 ± 0.06	16.81 ± 2.83	Nd	2.07 ± 2.15
Mar-2009 (n=3)	0.23 ± 0.03	13.01 ± 1.68	0.50 ± 1.00	0.10 ± 0.12
Mar-2010 (n=2)	0.45 ± 0.27	28.51 ± 11.65	Nd	Nd
Mar-2011 (n=5)	0.39 ± 0.46	22.69 ± 4.24	Nd	Nd
Non-Bloom (Coastal)				
Feb-2009 (n=1)	0.86	8.46	Nd	Nd
Mar-2009 (n=1)	0.20	23.98	Nd	Nd
Mar-2011 (n=1)	3.09	65.01	Nd	Nd

nd - not detected or absent.

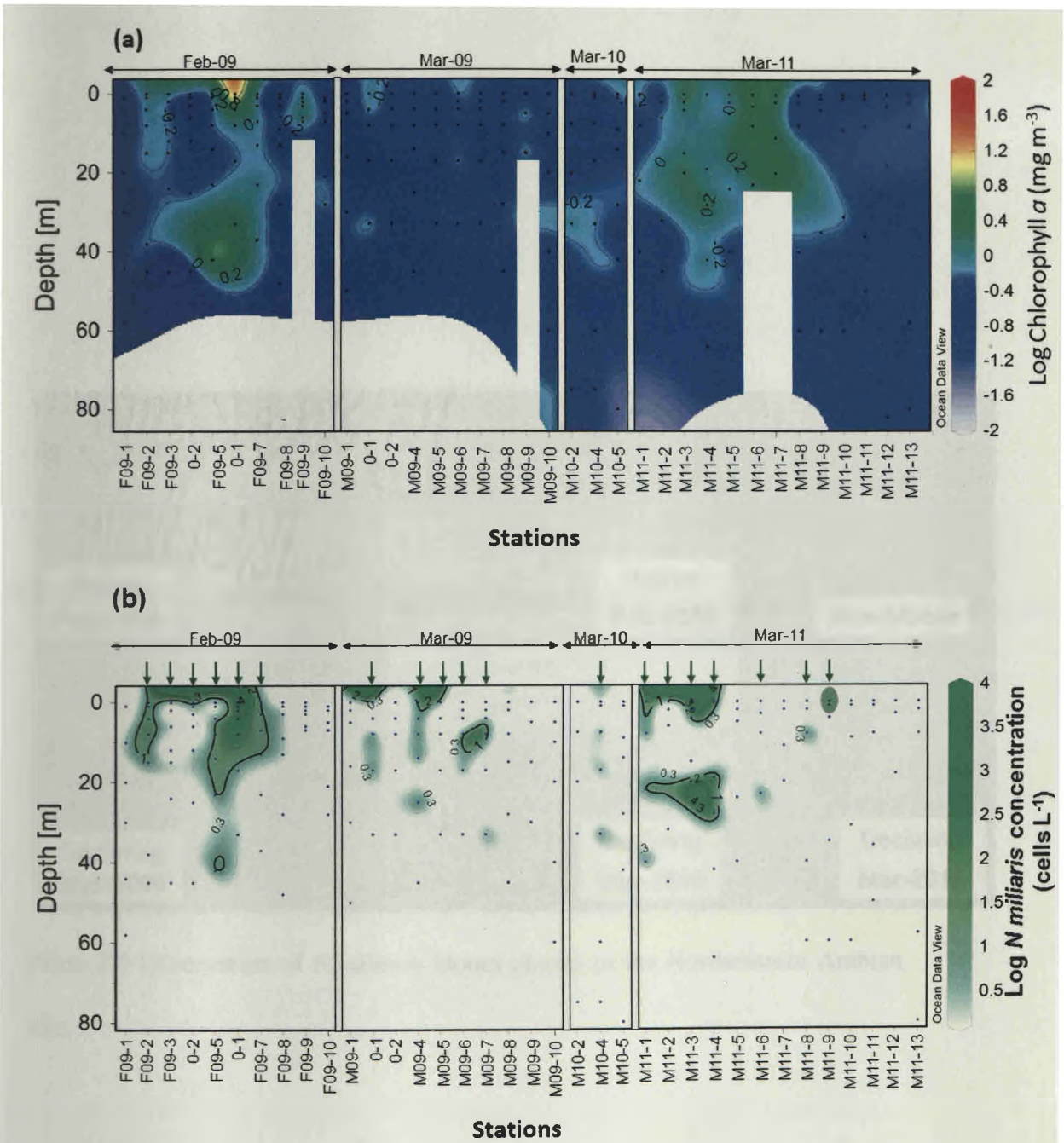

Fig. 2.4 *In situ* distribution of: (a) Chlorophyll *a* and (b) *Noctiluca miliaris* (green) as indicator of NEAS winter bloom during 2009-2011. Sampling depths indicated as dots in the sections and bloom stations designated by arrows. Station positions indicated as in map (Fig. 2.1)

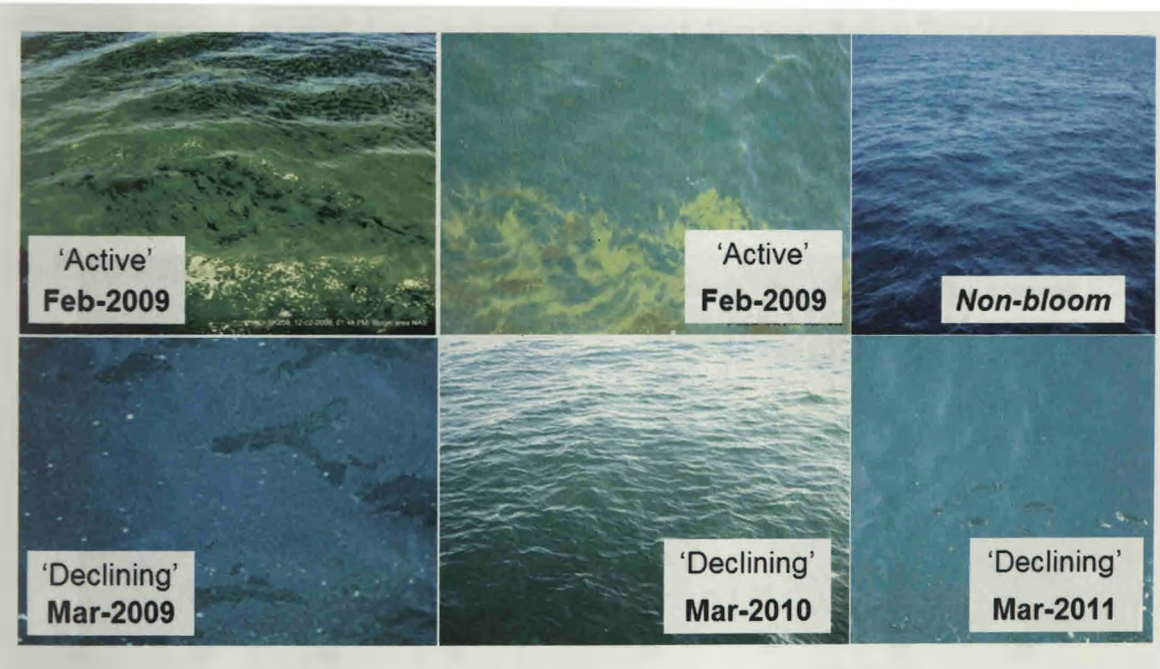

Plate 2.9 Observation of *N miliaris* bloom phases in the Northeastern Arabian Sea.

2.2.3 Physical characersitics

2.2.3.1 Wind-speed

In-situ wind-speed recorded at the time of morning CTD casts in the bloom area varied from 6.53±1.8 m sec^{-1} during Feb-09, 6.62±1.14 m sec^{-1} during Mar-09, 5.1± 1 m sec^{-1} during Mar-10. Scatterometer images from QuickScat V-4 wind vectors showed that wind was North-east direction during February-09 and reversed to South-west during Mar-09. The wind-vectors for the most intense bloom location at St-O1 is shown below (Fig. 2.5).

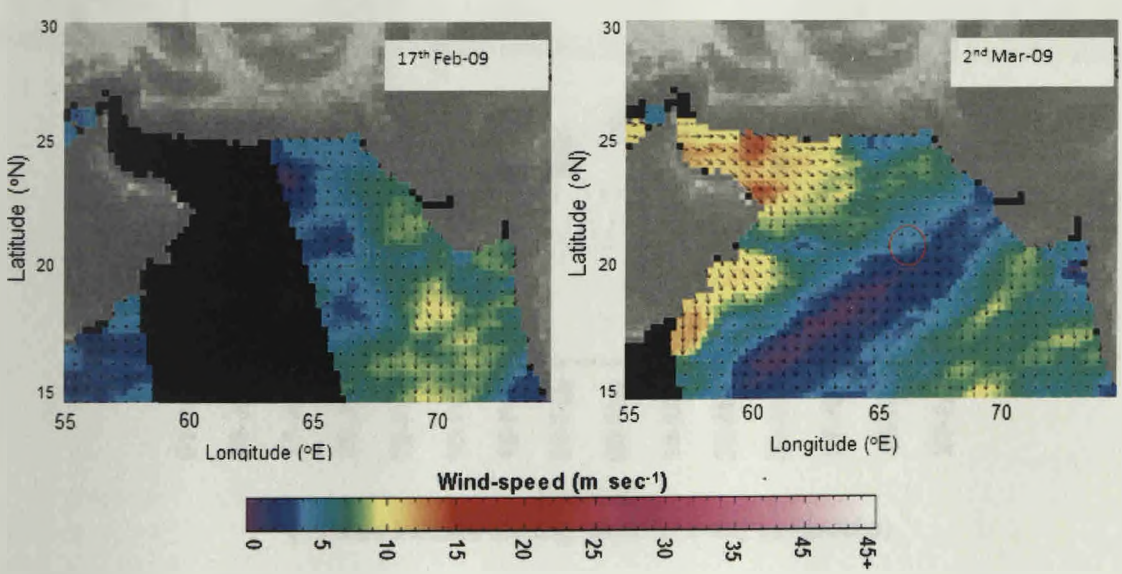

Fig. 2.5 Reversal in quickscat-V4 morning daily wind-vectors over an intense bloom area at St-O1 during Feb-Mar 2009 (*Source: www.remss.com*).

2.2.3.2 Photosynthetic avaialable radiation (PAR)

8-day composites of the satellite derived PAR obtained from MODIS-Aqua (4km resolution) in the NEAS bloom area (19-23°N and 64-69°E) showed that averaged PAR increased from January to April (Fig. 2.6). PAR varied as

35.83±2.59 Em^{-2} day^{-1} during Jan-09, 35.83±2.88 Em^{-2} day^{-1} during Jan-10 and was slightly higher as 37.58±1.71 Em^{-2} day^{-1} during Jan-11. The average PAR available during the month of February for 2009-2011 remained similar as 43.79±0.25 Em^{-2} day^{-1}. PAR was slightly higher during Mar-2011 and averaged 51.35±1.73 Em^{-2} day^{-1}, in comparison to 49.2 ±2.5 Em^{-2} day^{-1} during 2009 and 49.2 ±0.85 Em^{-2} day^{-1} during 2010.

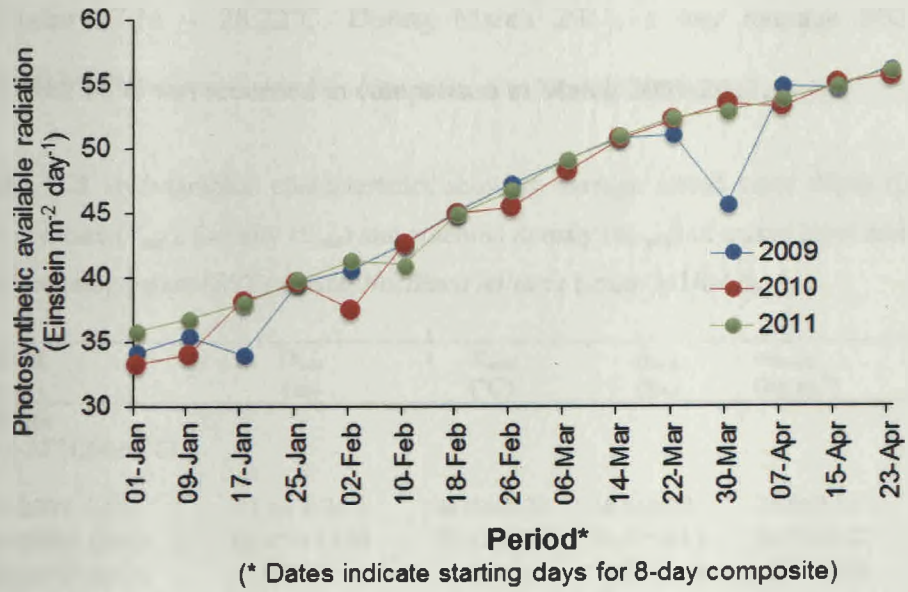

Fig. 2.6 8-day composite estimates of photosynthetic active radiation (PAR) obtained from MODIS-Aqua (4km resolution) in the NEAS (19-23°N; 64-69°E). *(Data source: NASA DISC, Giovanni)*

2.2.3.3 Hydrography

The hydrographic characteristics conditioning bloom and non-bloom locations are summarized below (Table 2.2). The average mixed layer during active bloom of February-09 (north of 19°N), varied around 71.67±24.5 m and decreased to 35.16 – 38 m during the month of March. The active bloom of February was characterized by a cooler sea-surface temperature (SST), averaging 24.96±0.49°C which increased to 25.15 – 26.07°C during March (Fig. 2.7, Table 2.2). Below 19°N temperature remained higher and varied between 27.16 – 28.22°C. During March 2011, a low average SST of 25.15±0.26°C was recorded in comparison to March 2009-2011.

Table 2.2 Hydrographic charactersitics showing average mixed layer depth (D_{mld}), temperature (T_{mld}), Salinity (S_{mld}) and potential density ($\sigma_{\Theta\text{-}mld}$) of mixed layer and sea-surface temperature (SST) during *Noctiluca miliaris* bloom in NEAS.

Period (Area)	**D_{mld} (m)**	**T_{mld} (°C)**	**S_{mld} (‰)**	**$\sigma_{\Theta\text{-}mld}$ (kg m^{-3})**	**SST (°C)**
Bloom (19-22°N;64-69°E)					
Feb-2009 (n=6)	71.67 ± 24.5	24.93±0.23	36.5±0.09	24.5±0.13	24.96±0.49
Mar-2009 (n=6)	35.67 ± 13.91	25.65±0.27	36.47±0.11	24.31±0.22	26.07±0.80
Mar-2010 (n=1)	38	25.76±0.35	36.06±0.04	23.92±0.08	26.06
Mar-2011 (n=6)	35.16 ± 10.30	24.98±0.45	36.04±0.14	24.14±0.07	25.15±0.26
Non-bloom					
Feb-2009 (n=1)	101	25.99±0.08	36.25±0.02	24.06±0.13	26.05
Mar-2009 (n=1)	34	26.66±0.18	36.22±0.008	23.75±0.05	26.28
Mar-2010 (n=1)	39	26.47±0.26	36.39±0.02	23.93±0.06	26.65
Mar-2011 (n=2)	48.5 ± 16.26	25.59±0.23	35.93±0.007	23.86±0.07	25.88±0.17
Non-bloom (16 -19°N; 68-70°E)					
Mar-2009 (n=2)	40.5 ± 28.99	27.15±0.007	35.89±0.02	23.35±0.007	27.23±0.06
Mar-2010 (n=1)	22	28.21±0.04	35.87±0.04	23.34±0.05	28.22
Mar-2011 (n=2)	30 ± 14.14	26.97±0.53	35.82±0.12	23.35±0.26	27.16±0.21

n- Sampling stations.

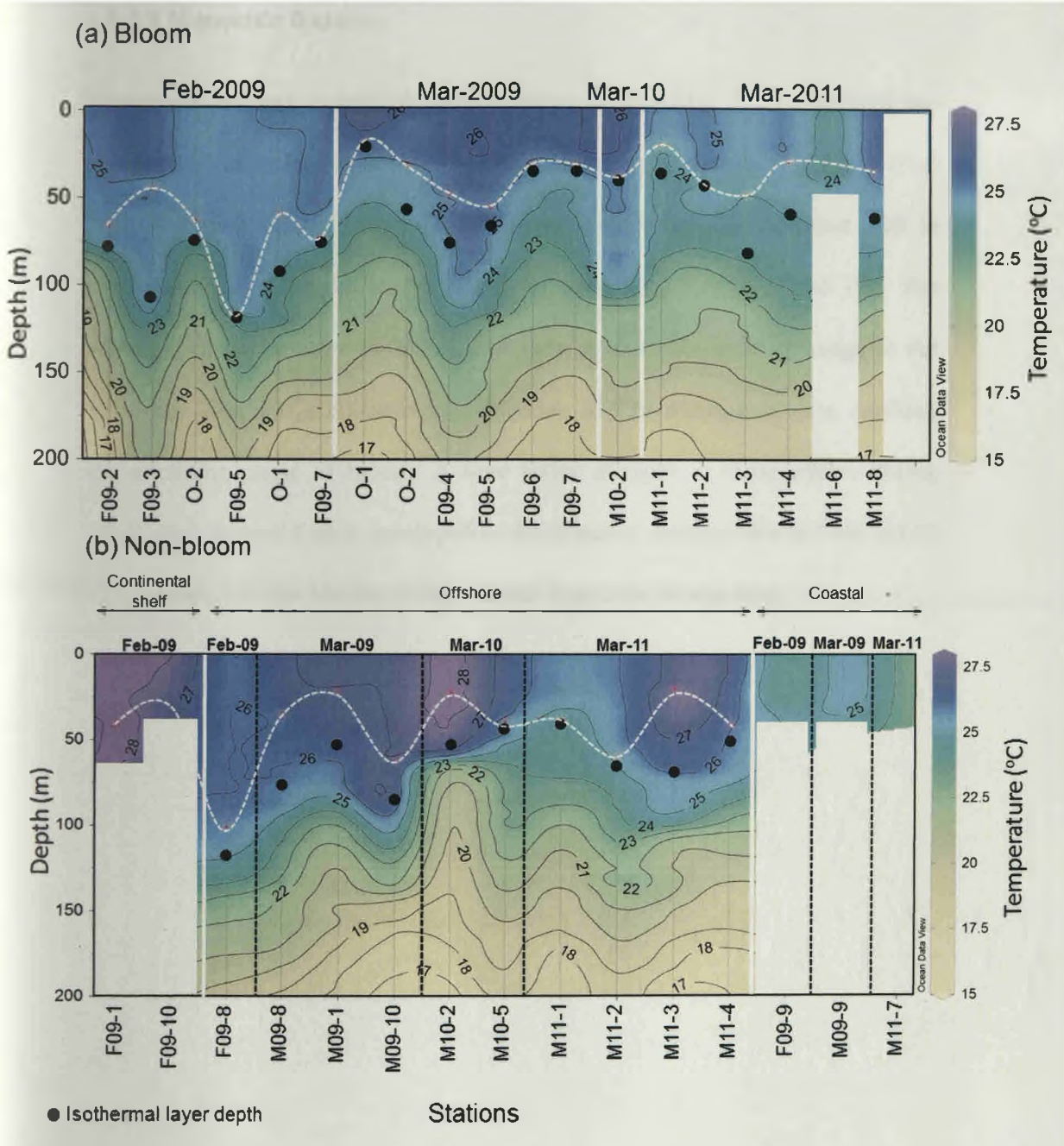

Fig. 2.7 Temperature distribution at: (a) bloom and (b) non-bloom stations during the study period. White dashed lines marks the depth of mixed layer (D_{mld}). Station positions indicated as in map.

2.2.3.4 Mesoscale features

Mesoscale features examined during bloom of Feb-Mar 2009 indicated the presence of anti-clockwise rotating cold-core eddy (diameter ~ 200km) (Fig. 2.8). The distribution of high Chl *a* plumes around the eddy matched with *in situ* observations of the major bloom at stations O1, F09-2 and O2. The warming of temperature in March was seen to coincide with a change in the wind-direction and a simultaneous decrease of Chl *a* concentration, marking the declining phase of bloom. A time series analysis of these eddies during 2009, also showed that it developed in the Western Arabian Sea and moved by late January into the Northeastern Arabian Sea in the bloom area.

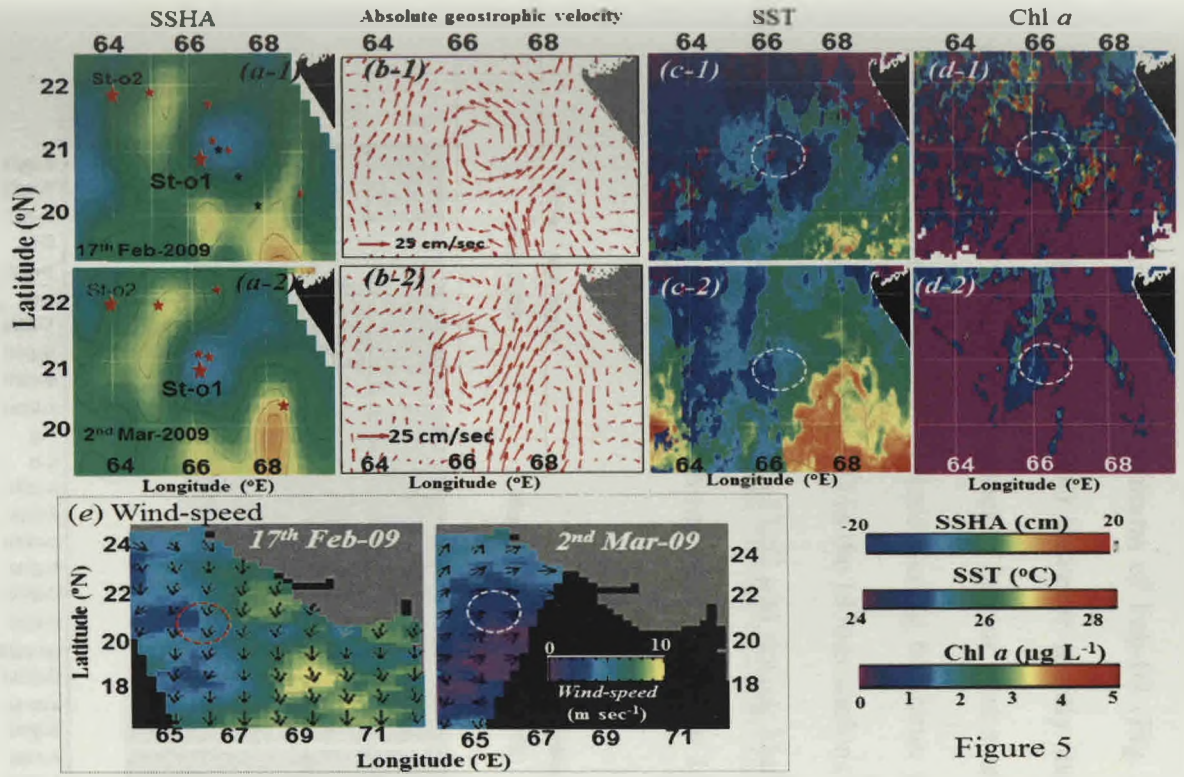

Figure 5

Figure 2.8 Mesoscale features *Noctiluca* bloom (active and declining phases) detected during consecutive cruises of Feb-Mar. Superimposed sampling stations on: (*a1-a2*) historical sea-surface height anomalies (SSHA). Corresponding panels show: (*b1- b2*) Absolute geostrophic velocities and 7-day averaged (future) level-3 MODIS-Aqua (4km) derived (c*1-c2*) sea-surface temperature (SST) and (*d1-d2*) Chl *a* concentration (*e*) Quick-Scat V4 wind is shown during the two phases.

2.2.4 Chemical characersitics

2.2.4.1 Dissolved oxygen (DO)

As seen in the water-column section, dissolved oxygen remained <150µM (<3.6 ml L^{-1}) during the active bloom of Feb-09 (Fig. 2.9). In the declining bloom phases of Mar-09, the DO however mostly increased to > 150 µM, except at St-O1, where large patches of bloom were seen to be declining (Plate 2.9). Similar trend was also noticed during the latter cruises of Mar-10 and Mar-11. The averaged surface DO in the bloom stations increased from 134.9± 5.81 µM during Feb-09 to 192.97±37.52 µM during Mar-09, 217.54 µM during Mar-10 and 198.78 ± 08.49 µM during Mar-11 (Table 2.3)

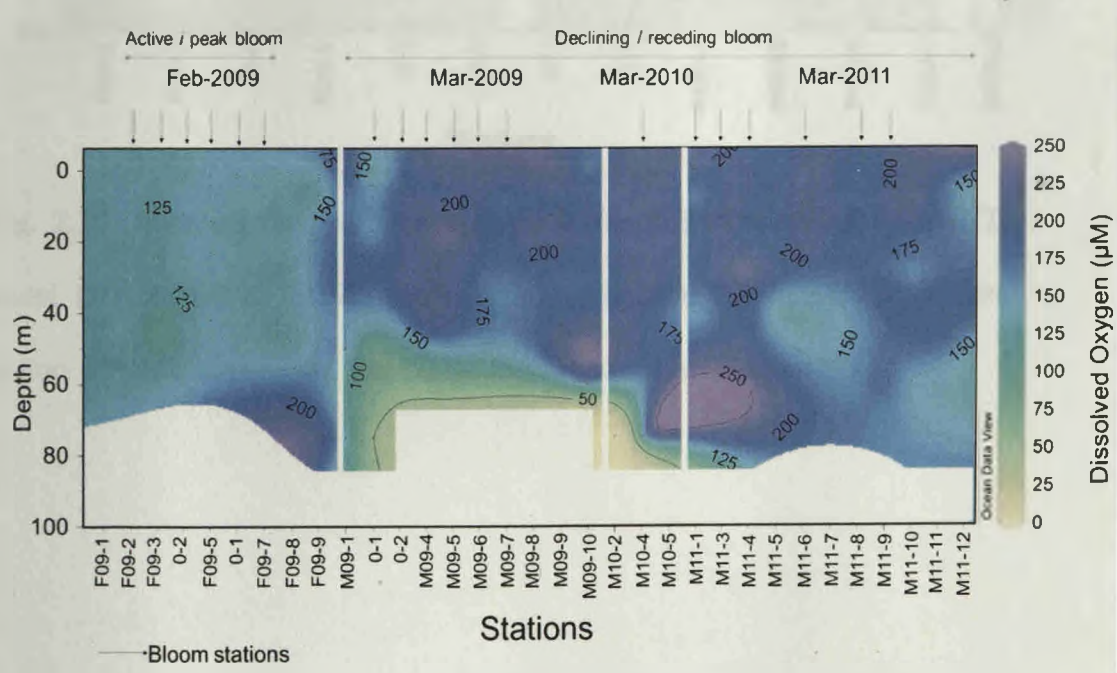

Fig. 2.9 Distribution of dissolved oxygen estimated in the bloom and non-bloom stations during the study period.

A comparative plot of the February-2009 cruises from a CTD based dissolved oxygen sensor suggests similar trends of low oxygen during the cruise of Feb-09. At the major bloom areas of Feb-09, advection of anoxic waters from the bottom was seen (Fig. 2.10).

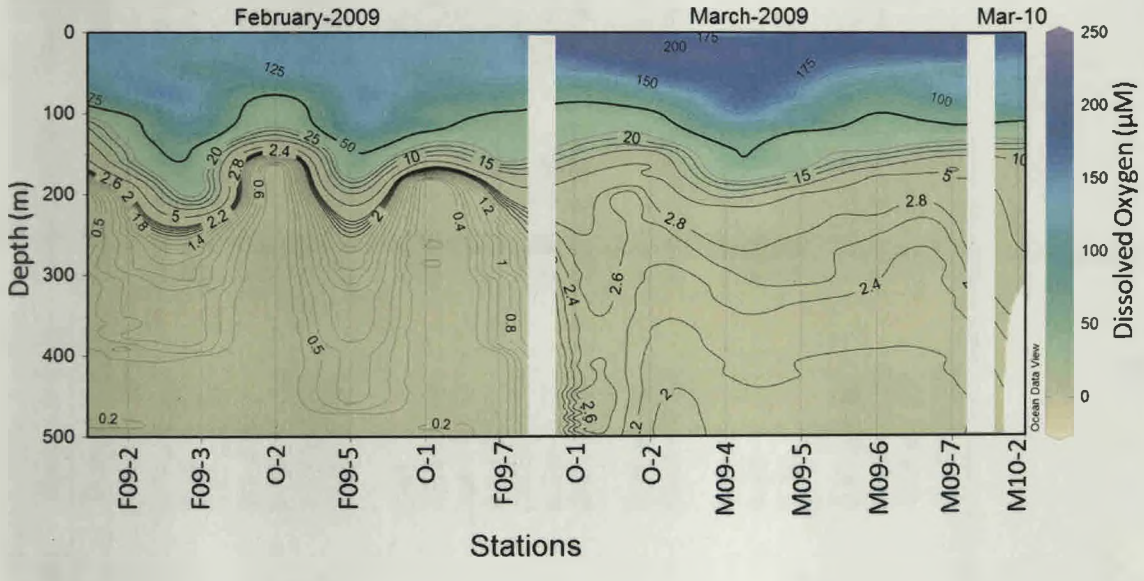

Fig. 2.10 Dissolved oxygen concentration in the NEAS recorded from CTD based DO sensor. Reference stations falling outside the major bloom area (below 19°N) is not shown. The 50µM DO contour is marked as bold.

Table 2.3 Chemical characteristics of the Northeastern Arabian Sea at the sea-surface during bloom of *N miliaris.*

Period	Dissolved Oxygen (µM)	Nitrate-N (µM)	Nitrite-N(µM)	Phosphate-P(µM)	Silicate-Si(µM)
	Surface (range)	Surface (range)	Surface (range)	Surface (range)	Surface (range)
Bloom					
Feb-09 (n=6)	134.90 ± 05.81 (126.86 - 143.39)	0.88 ± 0.5 (0.48 -1.8)	0.68 ± 0.32 (0.19 -1.1)	1.64 ± 1.77 (0.8 - 5.23)	15.09 ± 4.35 (9.64 – 20.87)
Mar-09 (n=6)	192.97 ± 37.52 (121.06 - 216.2)	0.03 ± 0.03 (nd -0.09)	0.07 ± 0.03 (0.03 - 0.11)	0.49 ± 0.17 (0.35 – 0.76)	1.34 ± 0.41 (0.73 – 1.77)
Mar-10 (n=1)	217.54	0.13	Nd	0.67	0.78
Mar-11 (n=6)	198.78 ± 08.49 (185.83 - 212.63)	0.26 ± 0.24 (0.03 -0.65)	0.04 ± 0.07 (nd – 0.19)	1.02 ± 1.6 (0.21 – 4.24)	2.45 ± 1.89 (0.4 – 5.05)
Non-bloom ***Off-shore, NEAS***					
Feb-09 (n=1)	137.37	0.44	0.22	0.67	9.07
Mar-09 (n=2)	196.87± 28.67 (164.65-219.58)	0.04 ± 0.06 (nd – 0.11)	0.07 ± 0.04 (0.03 – 0.11)	0.53 ± 0.36 (0.25 – 0.94)	1.14 ±0.28 (0.87 – 1.42)
Mar-10 (n=2)	205.39 ± 6.76 (200.61 – 210.17)	0.1 ± 0.02 (0.09 – 0.12)	0.02 ± 0.03 (nd – 0.05)	0.62 ± 0.07 (0.57 – 0.67)	0.9 ± 0.12 (0.82 – 0.98)
Mar-11 (n=2)	194.92 ± 0.85 (194.31 -195.52)	0.24 – 0.31 (0.01 – 0.46)	0.06 – 0.09 (nd – 0.13)	0.16 ± 0.03 (0.14 – 0.18)	0.35 ± 0.04 (0.32 – 0.38)
Continental shelf, EAS					
Feb-09 (n=2)	135.14±0.4 (142.1 – 132.02)	0.25 ±0.03 (0.23 – 0.27)	0.3 ± 0.1 (0.23 – 0.38)	0.56 ±0.03 (0.54 – 0.58)	26.41±3.92 (23.64-29.19)
Coastal (Off Gujrat)					
Feb-09 (n=1)	137.28	1.42	1.57	1.08	62.28
Mar-09 (n=1)	223.56	0.40	0.52	0.99	3.16
Mar-11 (n=1)	294.31	0.35	0.02	0.44	3.07
Historical-data[1]					
Jan-1995 (n=6)	198.02±4.70 (190.60 - 205.20)	2.81 ± 0.59 (1.67 – 3.33)	0.26 ± 0.05 (0.2 – 0.34)	0.62 – 0.05 (0.52 -0.68)	2 ±0.47 (1.5 – 2.8)
Mar-1995 (n=7)	210.83±8.06 (197.79 – 221.91)	1.08 ± 1.38 (0.16 – 4.23)	0.2 ± 0.09 (0.02 – 0.36)	0.46 ± 0.18 (0.28 – 0.77)	1.95 0.76 (1.0 – 3.0)

n= not-detected; [1]Data source - JGOFS Arabian Sea Process study (http://usjgofs.whoi.edu); Contributing PI, L Codispoti.

2.2.4.2 Dissolved inorganic nutrients

The distribution of dissolved inorganic nutrients is shown as in Table 2.3 for all the cruises.

Dissolved inorganic N-Nitrate

Dissolved inorganic nitrate at surface remained high at the bloom stations during Feb-2009 and averaged 0.88 ± 0.5 μM at the surface. Nitrate decreased during the latter phases of bloom in March and varied from as low as 0.03 ± 0.03 μM in Mar-09, 0.13 μM during Mar-10 and 0.26± 0.24 μM during March 2011 (Table 2.3). In the non-bloom stations, surface nitrate ranged from 0.44 μM during Feb-09, 0.04 ± 0.06 μM during Mar-09, 0.1 ± 0.02 μM during Mar-10 and was slightly higher as 0.24±0.31 μM during Mar-2011. Historical dataset compiled from 1995 JGOFS cruises in the NEAS showed that surface Nitrate in the bloom area between 19 – 22°N averaged 2.81± 0.59 μM during Jan-1995 and decreased to 1.08± 1.38 μM during Mar-1995 following bloom of diatoms. Examination of nitrate concentration in the euphotic column mirrored similar trends as the surface (Fig. 2.11). During bloom of Feb-09, Nitrate concentration always remained >0.5μM and ranged between 0.8 – 6 μM at the base of the euphotic zone. During March-09, nitrate was mostly depleted from the upper ocean as it dropped to <0.5μM in the bloom area in the upper 20m of the water-column and remained enriched in the bottom waters as >1μM in both bloom and non-bloom areas (Fig. 2.12).

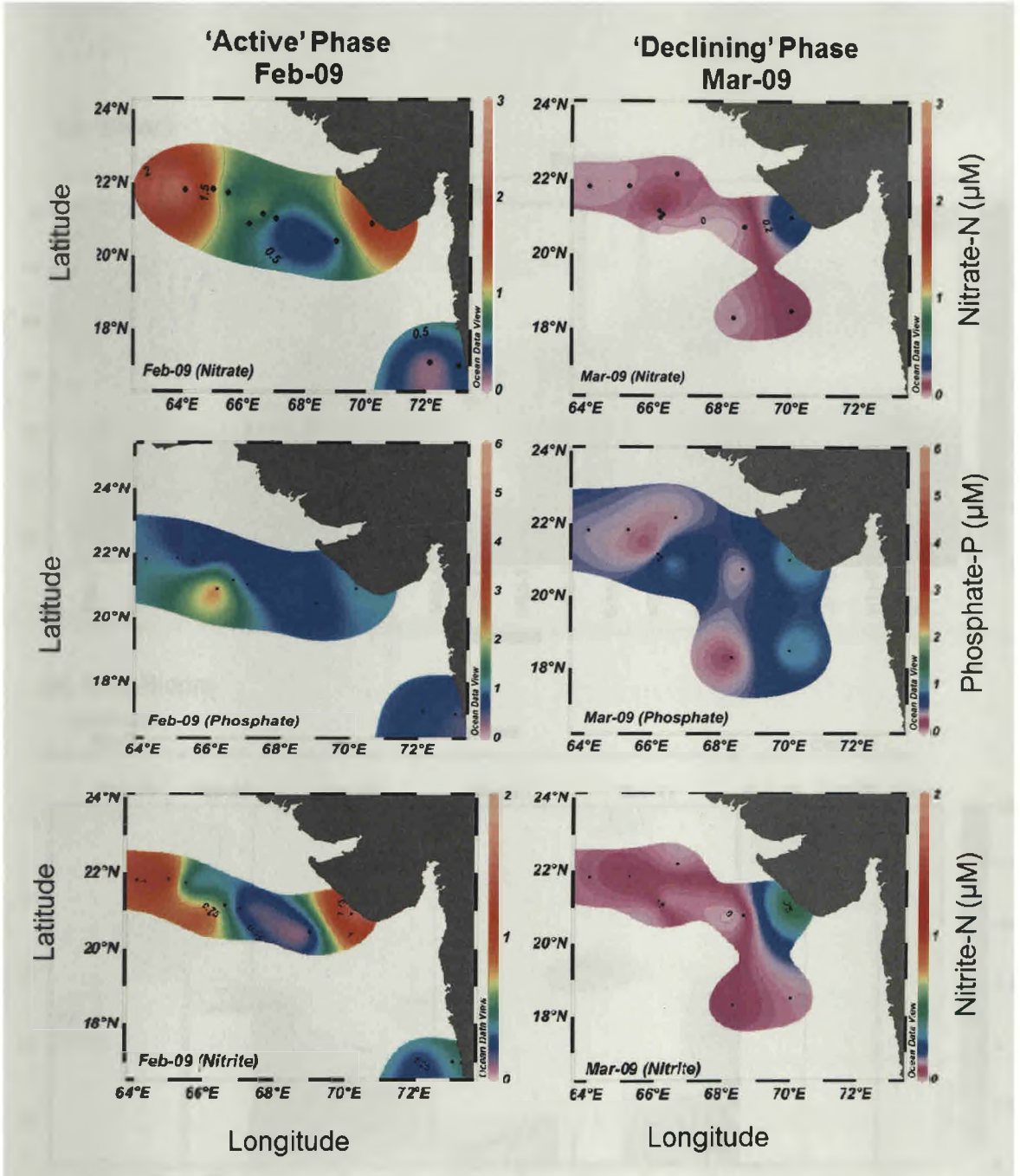

Fig. 2.11 Distribution of dissolved inorganic nutrients at the surface during consecutive cruises of Feb-Mar 2009 in the NEAS. All bloom stations fall between 64 -68°E.

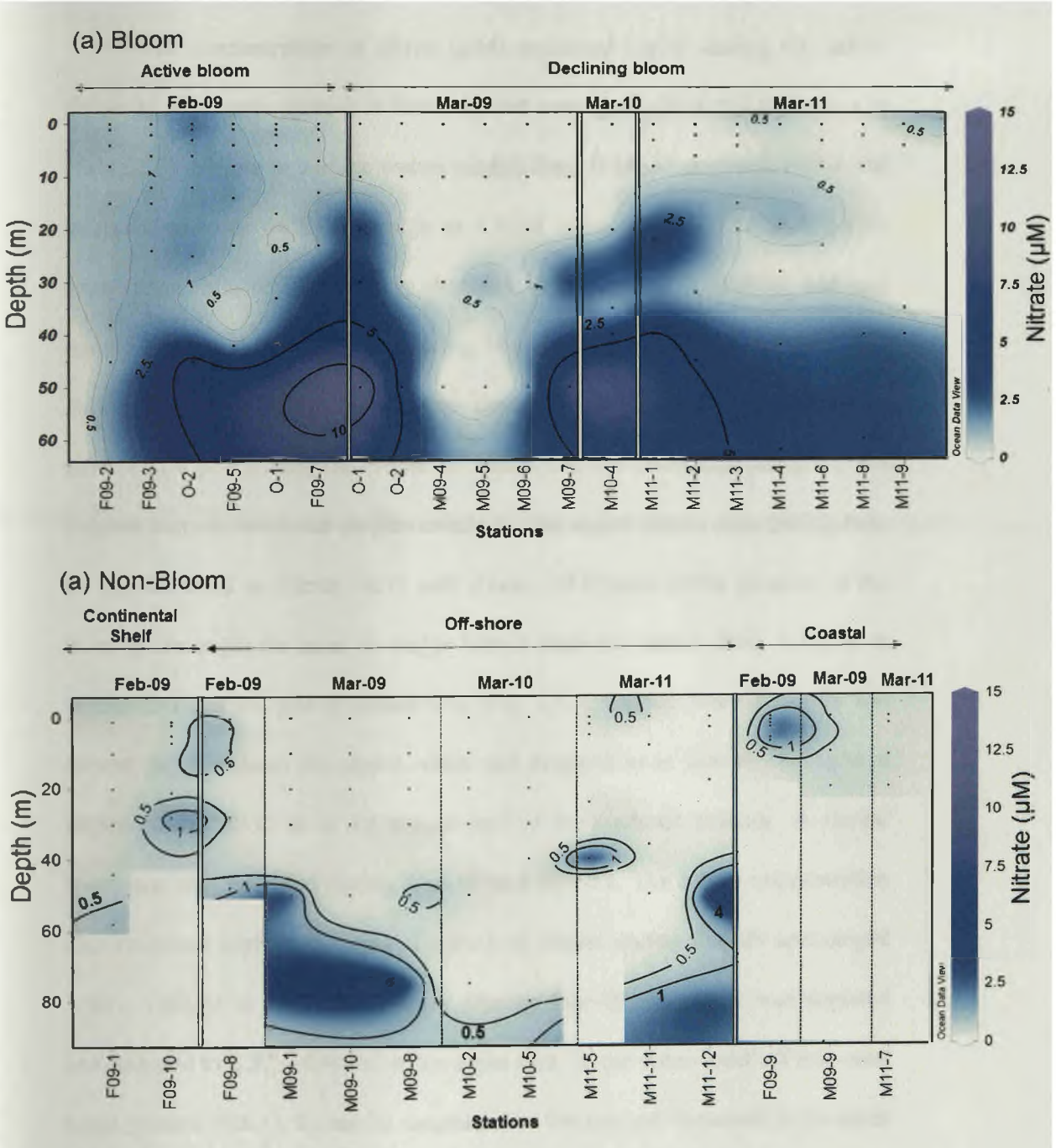

Fig. 2.12 Dissolved inorganic Nitrate-N concentrations in the water-column of:

(a) *N miliaris* bloom and (b) Non-bloom stations during 2009-2011.

Dissolved inorganic N-Nitrite

The concentration of nitrite (μM) remained higher during the active bloom of *N miliaris* (green) in February and averaged 0.88±0.5 μM as seen in (Table 2.3). Nitrate in surface waters ranged from 0.48μM at station F09-7 and increased towards 64°E to as high as 1.1μM at station F09-3 (Fig. 2.11). In comparison, Nitrite substantially declined to as low as 0.07±0.03 μM and ranged between 0.03 - 0.11 μM during Mar-09. A similar trend was also seen during Mar-10 when Nitrite was non-detectable at the surface and varied as 0.04 – 0.07 μM during the bloom of Mar-11 in the receeding period. Water column sections mirrored similar trends as the major bloom area during Feb-09 was enriched in Nitrite >0.75 μM. Zones of highest nitrite detected at the base of the euphotic zone in major bloom stations, varied from 1.19μM at station O-1 and 1.7 μM at station O-2 (Fig. 2.13). During Mar-09, nitrite was almost depleted from the upper ocean and dropped to as low as <0.25μM at depths below 20-30 m at the bottom-half of the euphotic column A similar trend was also reflected during Mar-10 and Mar-11. The nitrite concentration also remained high in the coastal waters of Gujrat during Feb-09 and ranged 1.42 – 1.89μM in the water-column. During Mar-09, the nitrite was depleted and dropped to 0.37 – 0.4 μM in the same area. In the outer-shelf off mid-west coast (station F09-1), the nitrite ranged 0.34 - 0.4 μm and increased in the inner shelf (station F09-10) and varied between 0.23 - 1.17 μM. At the off-shore non-bloom sites nitrite remained <0.25μM. Historical data from the Arabian Sea indicates that average surface nitrite concentrations of March (0.2±0.09

μM) was ~5 times higher than during the declining bloom of March (Table 2.3).

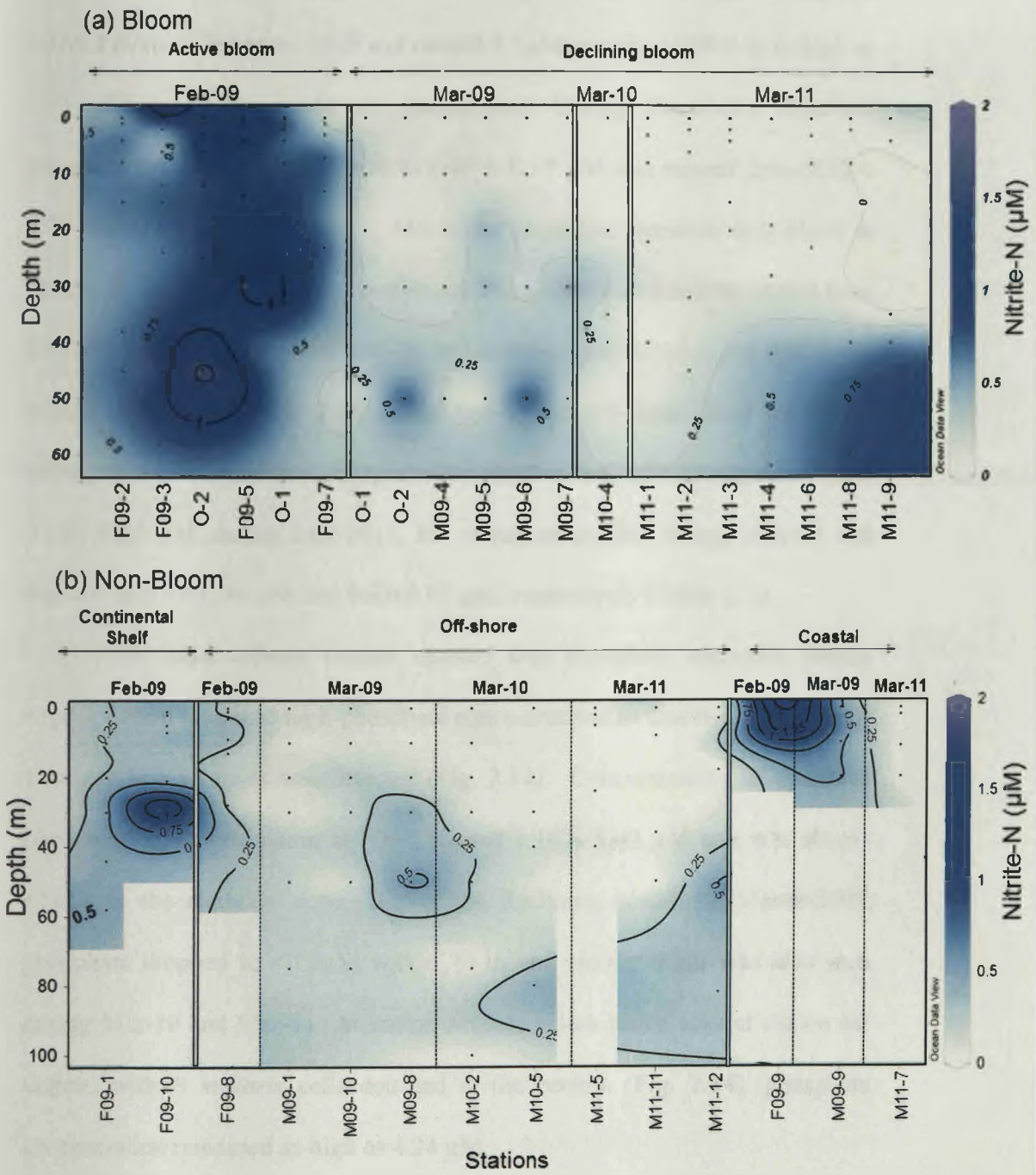

Fig. 2.13 Dissolved inorganic Nitrite-N concentrations in the water-column of:

(a) *N miliaris* bloom and (b) Non-bloom stations during 2009-2011.

Dissolved inorganic P-Phosphate

Dissolved phosphate at surface averaged 1.64 ± 1.77 μM during the active bloom of February-2009 and ranged 0.7μM at station F09-7 to as high as 5.23 μM at the major bloom station O-1. During March-09, dissolved phosphate concentration declined to 0.49 ± 0.17 μM and ranged from 0.35 – 0.76 μM. At station O-1, during March the phosphate declined to 0.64μM at station O-1 in the declining bloom-phase. Phosphate concentration varied from 0.67μM during the bloom of Mar-10 and increased to 1.02±1.6 μM during the bloom of Mar-11 (Table 2.3). In the non-bloom off-shore areas of NEAS, averaged surface dissolved phosphate decreased to 0.67 μM during Feb-09 and 0.16± 0.03 μM during Mar-2011, but remained similar during Mar-09 and Mar-10 as 0.53±0.36 μM and 0.62±0.07 μM, respectively (Table 2.3).

The water-column section showed that phosphate remained mostly <1μM, except localized high-phosphate concentrations as detected at station O-1, where heavy bloom was detected (Fig. 2.14). Concentrations of dissolved phosphate in water-column at F09-2 ranged 1.16 – 1.49 μM and was always <1μM in the euphotic zone. During the declining bloom of March-2009, phosphate dropped to <0.5μM within 30 m and similar trend was also seen during Mar-10 and Mar-11. At station M09-6, which was a coastal station off Gujrat, with *N miliaris* cells detected at the bottom (Fig. 2.14), phosphate concentration remained as high as 4.24 μM.

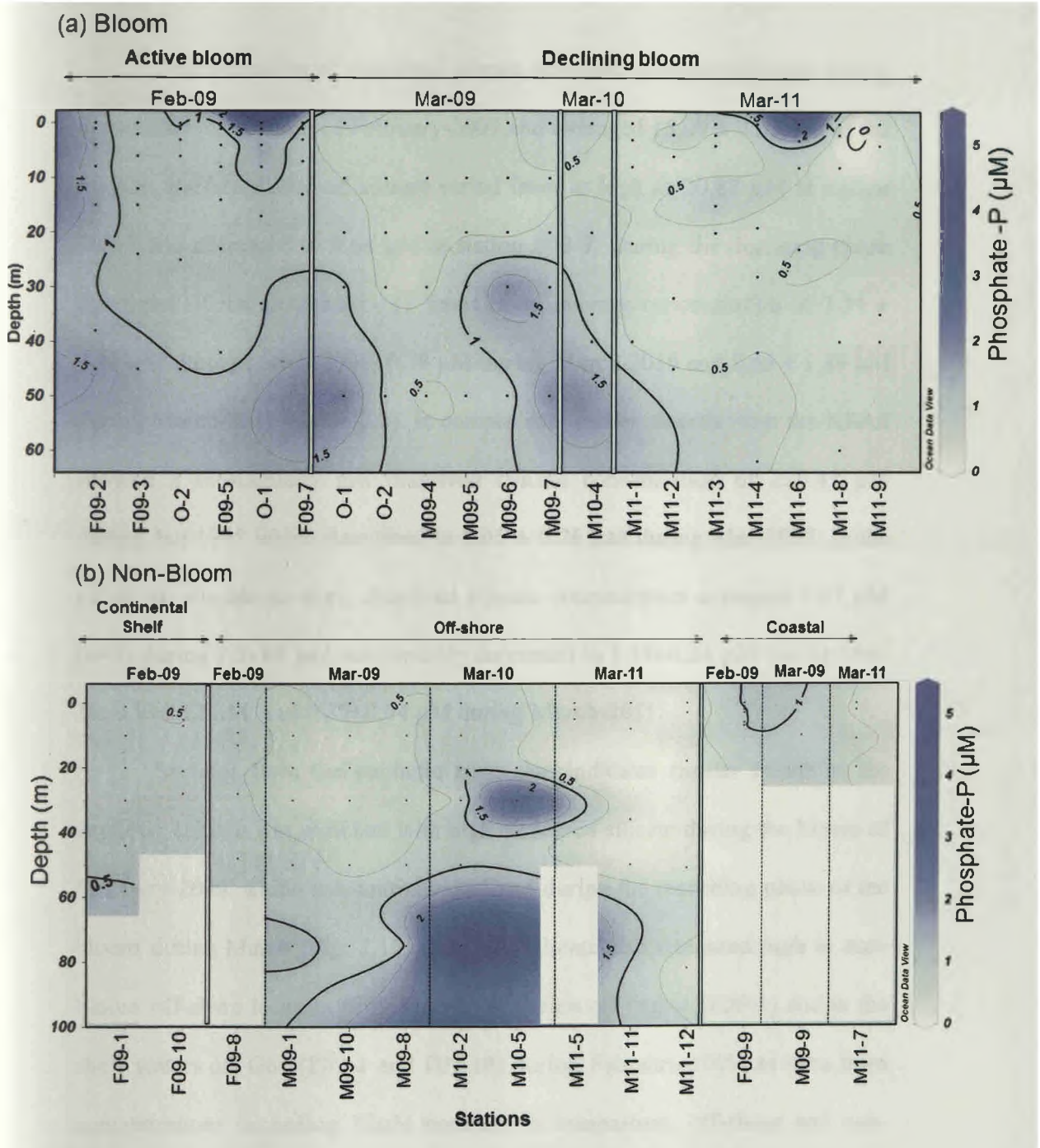

Fig. 2.14 Dissolved inorganic Phosphate-P concentrations in the water-column of: (a) *N miliaris* bloom and (b) Non-bloom stations during 2009-2011.

Dissolved inorganic Si-Silicate

Concentrations of dissolved silicate remained substantially high during the active bloom phase of February-2009 and averaged 15.09 ± 4.35 μM at the surface. Surface dissolved silicate varied from as high as 20.87 μM at station F09-3 and decreased to 9.64 μM at station F09-7. During the declining phase dissolved silicate decreased ~11 times to an average concentration of 1.34 ± 0.41 μM during March-2009, 0.78 μM during March-2010 and 2.45 ± 1.89 μM during March-2011 (Table 2.3). In comparison, earlier records from the NEAS showed a substantially low dissolved silicate concentration of 2±0.47 μM during Jan-1995 which decreased to 1.95 ± 0.76 μM during Mar-1995. In the off-shore non-bloom sites, dissolved silicate concentration averaged 9.07 μM (n=1) during Feb-09 and substantially decreased to 1.14±0.28 μM during Mar-10, 0.9±0.12 μM and 0.35±0.04 μM during March-2011.

Sections from the euphotic zone also indicates similar trends as the euphotic column was enriched with high dissolved silicate during the bloom of February-2009, which substantially declined during the receeding phase of the bloom during March (Fig. 2.15) dissolved silicate also remained high in non-bloom off-shore location (F09-8), coastal station off Gujrat (F09-1) and in the shelf waters off Goa (F09-1 and F09-10) during February-2009, as seen from concentrations exceeding 10μM contour. In comparison, off-shore and non-bloom sampling sites during March2009 indicates silicate depletion below 5μM (Fig. 2.15).

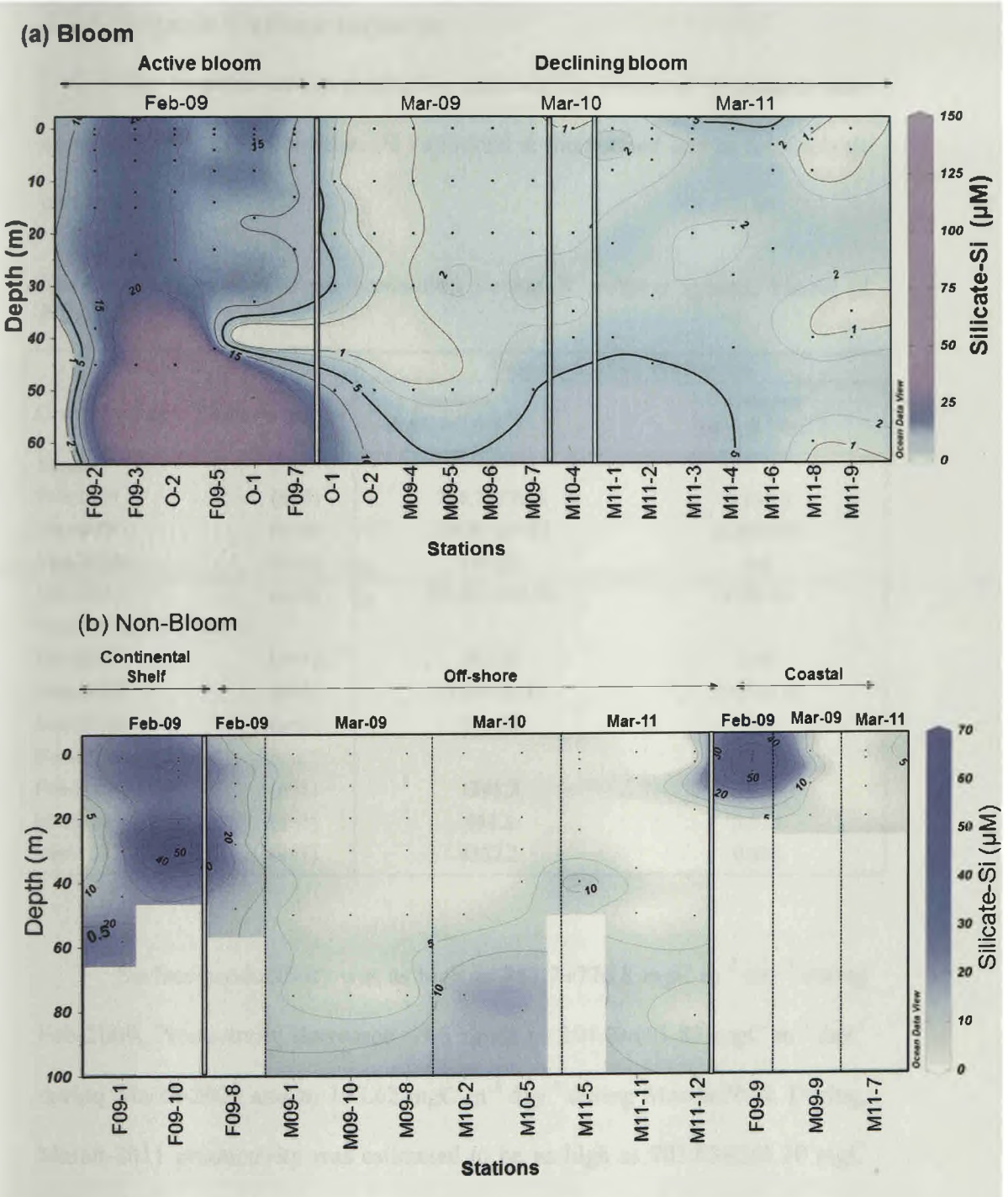

Fig. 2.15 Dissolved inorganic Silicate-Si concentrations in the water-column of: (a) *N miliaris* bloom and (b) Non-bloom stations during 2009-2011.

2.2.5 Organic Carbon turnover

The Organic carbon production rates during bloom of *N miliaris* were extremely high, with considerable variations at the surface and in the euphotic column (Table 2.4).

Table 2.4 Organic Carbon production during *N miliaris* (green) bloom of NEAS.

Cruise Period	Stations (n)	Organic Carbon Production	
		Surface ($mgC\ m^{-3}\ day^{-1}$)	**Column** ($g\ C\ m^{-2}\ day^{-1}$)
Bloom			
Feb-2009	(n=6)	751.7±776.8	4.1±4.6
Mar-2009	(n=6)	204.0±161.82	2.28±0.86
Mar-2010	(n=1)	193.62	4.6
Mar-2011	(n=4)	703.83±255.30	9.08±10
Non-Bloom (Off-shore)			
Feb-2009	(n=1)	285.26	1.85
Mar-2009	(n=3)	75.44±18.53	2.13±2.36
Mar-2010	(n=1)	268.88	3.35
Non-Bloom (Coastal)			
Feb-2009	(n=1)	1345.3	1.5
Mar-2009	(n=1)	484.3	0.012
Mar-2011	(n=1)	4337.2	0.016

Surface productivity was as high as 751.7±776.8 mgC m^{-3} day^{-1} during Feb-2009. Productivity decreased ~3.6 times to 204.0±161.82 mgC m^{-3} day^{-1} during March-2009 and to 193.62 mgC m^{-3} day^{-1} during March-2010. During, March-2011 productivity was estimated to be as high as 703.83±255.30 mgC m^{-3} day^{-1} due to the high concentration of *Noctiluca* cells detected in the mid-euphotic column. Overall, column productivity was also highest during March-2011 as 9.08±10 g C m^{-2} day^{-1} and decreased to 4.6 g C m^{-2} day^{-1} during Mar-

2010, 4.1±4.6 g C m^{-2} day^{-1} during Feb-2009 and to a minimum of 2.28±0.86 g C m^{-2} day^{-1} during Mar-2009. In comparison, productivity at non-bloom off-shore locations were at least ~2-3 times lower than in the bloom area for the corresponding season.

2.2.6 Chromophoric Dissolved Organic Matter (C-DOM)

Charactersitic C-DOM absorbtion signature for *Noctiluca miliaris* (green) bloom was detected at 337 nm during the active phase of Feb-09 at station O-1 (Fig. 2.16). C-DOM absorbtion coefficient at 300 nm, used as a proxy for dissolved organic matter content was highest during the bloom of February-2009 as 1.1±0.57 m^{-1} and decreased to 0.65 ±0.30 m^{-1} during March-2009 and remained similar as 0.4 m^{-1} during March-2010 and 0.41±0.09 m^{-1} during March-2011. Strong peaks at 337 nm at station O-1 lead to further high absorbtion coefficients at 325 nm. Hence, at station O-1, slope ratio was calculated from best fit curves after ignoring the peak. Slope ratio characteristics revealed a significant decrease to 1.13±0.51 in comparison to 2-3 times higher slope ratios obtained during the receeding phases of bloom during March-2009-11. The lower slope-ratio during active bloom of Feb-2009 (Table 2.5) resulted due to steeper 275-295 nm slope and a shallower 350-400 nm slope, characteristic feature of coastal/estuarine water-bodies with high dissolved organic content. In contrast, higher slope-ratios (2.25 – 6.29) of non-bloom waters in the NEAS showed a more marine character, although the

values of 2.25 and 2.74 as estimated during Feb-09 and Mar-11 were much lower in comparison to true off-shore systems.

Table 2.5 Chromophoric dissolved organic matter (C-DOM) absorbtion charactersitics during bloom of *N miliaris* (green) in the Arabian Sea.

C-DOM Absorbtion Charactersitics	Bloom			
	Feb-09 (n=6)	**Mar-09 (n=6)**	**Mar-10 (n=1)**	**Mar-11 (n=6)**
Ac254 (m^{-1})	2.08±0.53	1.79±0.83	1.6	1.45±0.09
Ac300 (m^{-1})	1.10±0.57	0.65±0.30	0.40	0.41±0.09
AC325 (m^{-1})	1.18±1.36	0.46±0.29	0.23	0.25±0.08
(S1) Slope $_{275\text{-}295}$ (nm^{-1})	0.0186±0.002	0.0255±0.010	0.0372	0.0331±0.003
(S2) Slope $_{350\text{-}400}$ (nm^{-1})	0.0237±0.020	0.0117±0.003	0.0122	0.0129±0.003
S_{ratio} (S1:S2)	1.13±0.51	2.27±0.1	3.04	2.81±1.00
(S_{nlf}) Slope $_{325\text{-}650}$ (nm^{-1})	0.0175±0.007	0.0238±0.034	0.0169	0.0118±0.002
	Non-Bloom (Off-shore)			
	Feb-09 (n=1)	**Mar-09 (n=3)**	**Mar-10 (n=2)**	**Mar-11 (n=2)**
Ac254 (m^{-1})	1.1377	1.63±0.82	1.33±0.02	1.85±.0.18
Ac300 (m^{-1})	0.3616	0.65±0.54	0.40±0.09	0.72±0.14
AC325 (m^{-1})	0.2741	0.42±0.42	0.27±0.09	0.31±0.09
(S1) Slope $_{275\text{-}295}$ (nm^{-1})	0.02	0.0257±0.008	0.03±0.01	0.0255±0.00
(S2) Slope $_{350\text{-}400}$ (nm^{-1})	0.0089	0.0065±0.003	0.0063±0.004	0.0114±0.007
S_{ratio} (S1:S2)	2.2514	4.87±3.20	6.29±3.47	2.74±1.65
(S_{nlf}) Slope $_{325\text{-}650}$ (nm^{-1})	0.01	0.0084±0.003	0.0096±0.003	0.0100±0.004

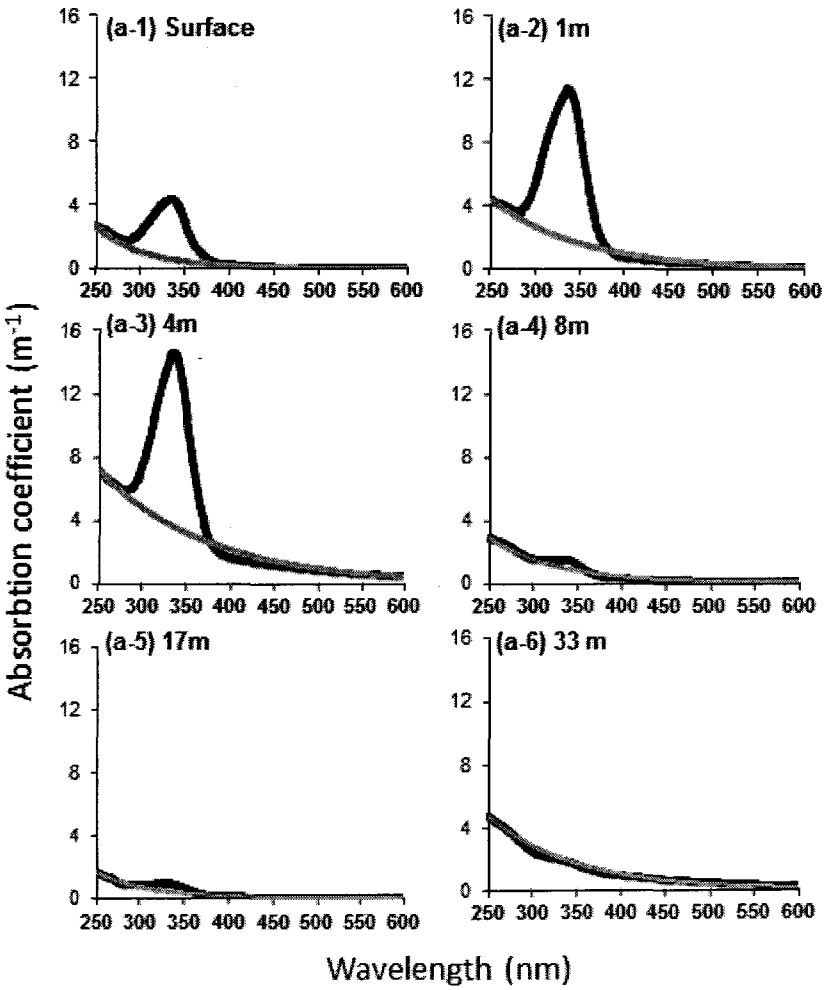

Fig. 2.16 CDOM absorbtion during *Noctiluca miliaris* bloom of Feb-09 at St-O1. (*a1- a6*) Peaks of Mycosporine like amino acids (λ_{max} 336-337 nm) and non-linear exponential fits to the spectrum (*in blue*) indicating 250-600 nm slope.

2.2.7 Bacterial distribution in *N miliaris* bloom

2.2.7.1 Total bacteria

A massive inflation of total bacterial counts was recorded in the euphotic zone of NEAS during the off-shore blooms of *Noctiluca miliaris* (green) (Fig. 2.17). Overall trends of bacterial distribution showed highest counts during the active phase bloom of February-2009, averaging $5.71\pm6.93\times10^{9}$ cells L^{-1} at the surface and $11.73\pm7.55\times10^{13}$ cells m^{-2} in the water-column, although with significant variations. As the bloom progressed to the declining phase of March-2009, averaged bacterial counts surprisingly decreased (~5 times) to $1.66\pm1.26\times10^{9}$ cells L^{-1} at the surface and $4.14\pm1.22\times10^{13}$ cells m^{-2} in the euphotic zone (Table 2.6). During March 2010, surface counts of 1.35×10^{9} cells L^{-1} was similar to that of March-2009, although water-column counts increased to 5.41×10^{13} cells m^{-2}. Bacterial load during bloom of March-2011 was ~ 2 times higher in comparison to that of March-2009 and 2010. Significantly high column bacterial counts of $10.26\pm3.79\times10^{13}$ cells m^{2} during this season was however, still lower than the active bloom of Feb-09 (Table 2.6).

In comparison to bloom, surface bacterial counts at non-bloom off-shore/shelf areas were much lower and varied from $0.89\pm0.24\times10^{9}$ cells L^{-1} during Feb-2009 to $1.46\pm0.36\times10^{9}$ cells L^{-1} during Mar-2011 (Table 2.6). Counts from the euphotic zone also mirrored the same trend and was atleast 2-3 times lower, varying from $3.09\pm0.85\times10^{9}$ cells m^{-2} during Mar-09 to $4.26\pm0.84\times10^{13}$ cells m^{-2} during Mar-2011. Importantly, baeterial counts in the

off-shore bloom area were ~15 times high than the coastal waters off Gujrat during Feb-2009 (Table 2.6).

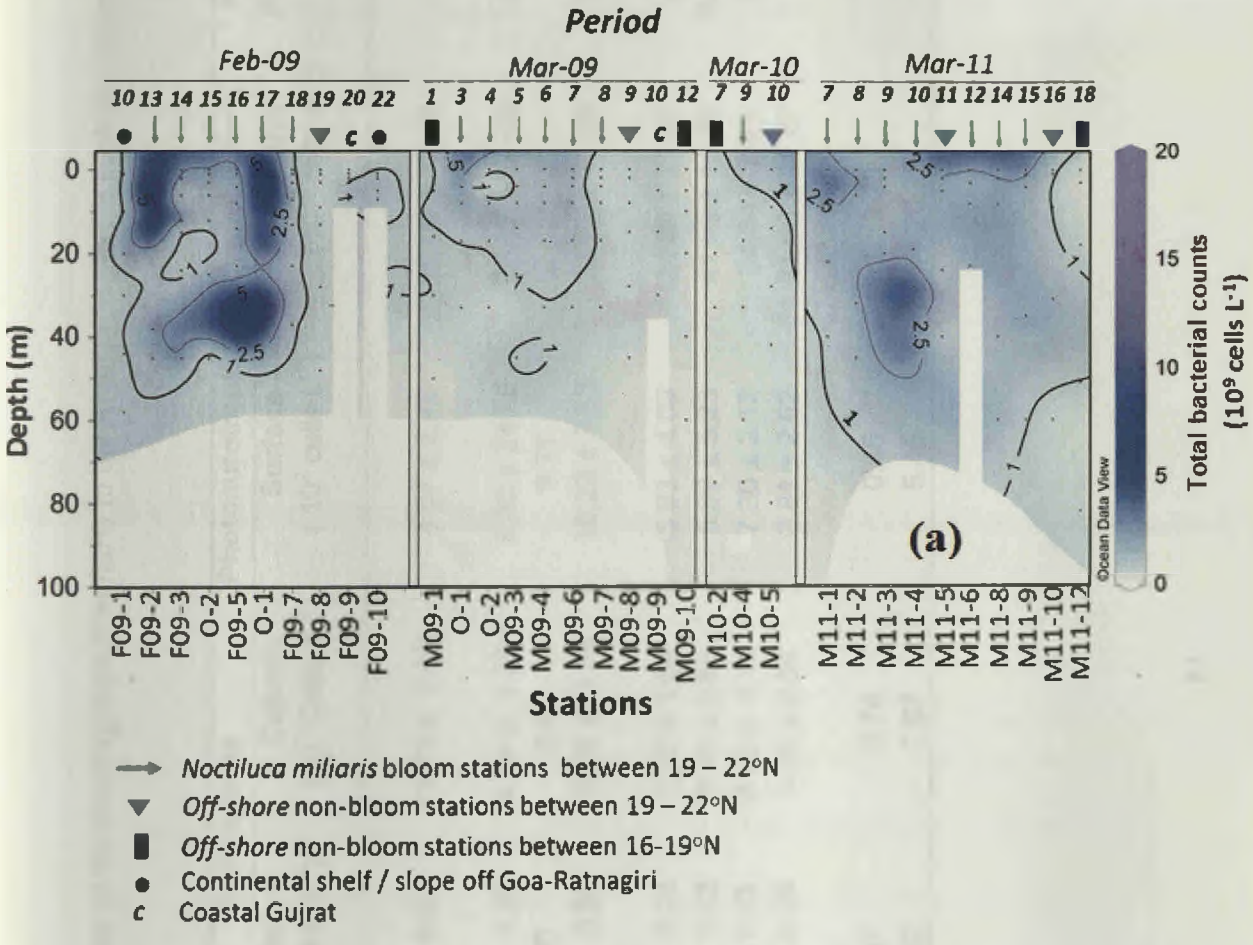

Fig. 2.17 Euphotic section showing distribution of total bacterial counts in NEAS during bloom of *N miliaris*.

Table 2.6 Bacterial distribution during bloom of the dinoflagellate *N miliaris* in the Arabian Sea in the euphotic column.

Cruise Period	Stations (n)	Total bacteria		Photoautotroph (Picocyanobacteria)		Percentage of Photoautotrophs
		Surface (10^9 cells L^{-1})	Column (10^{13}Cells m^{-2})	Surface (10^7 cells L^{-1})	Column (10^{11} cells m^{-2})	
Active Bloom						
Feb-2009	(n=6)	5.71 ± 6.93	11.73 ± 7.55	4.57 ± 2.42	19.06 ± 12.19	2.22 ±1.63
Declining Bloom						
Mar-2009	(n=6)	1.66 ± 1.26	4.14 ± 1.22	8.30 ± 24.48	37.07 ± 24.48	8.54 ± 5.09
Mar-2010	(n=1)	1.35	5.41	9.71	35.52	6.53
Mar-2011	(n=7)	2.87 ± 0.54	10.26 ± 3.79	10.23 ± 7.63	32.57 ± 15.34	3.54 ± 1.76
Non-Bloom (Off-shore, Slope, Shelf)						
Feb-2009	(n=3)	0.89 ± 0.24	3.86 ± 1.69	5.93 ± 4.09	29.89 ± 28.27	6.78 ± 3.63
Mar-2009	(n=3)	0.67 ± 0.23	3.09 ± 0.85	5.99 ± 5.23	41.03 ± 11.39	10.63 ± 10.07
Mar-2010	(n=2)	1.09 ± 0.63	3.83 ± 1.15	7.30 ± 2.12	34.84 ± 7.04	9.80 ± 4.78
Mar-2011	(n=2)	1.46 ± 0.36	4.26 ± 0.84	3.81 ± 2.62	21.60 ± 11.37	4.9 ± 0.99
Non-Bloom (Coastal)						
Feb-2009	(n=1)	0.37	0.74	0.45	3.23	4.37
Mar-2009	(n=1)	0.82	2.87	5.46	20.28	7.05

n= number of sampling stations

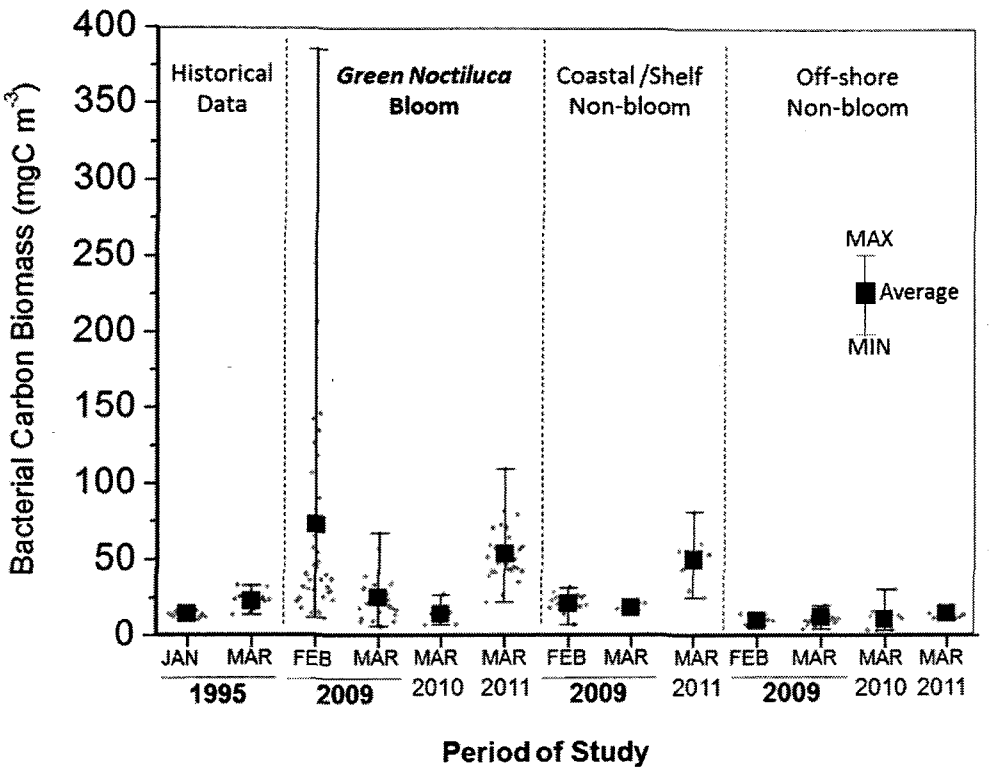

Fig. 2.18 Comparison of estimated bacterial carbon-biomass during green *Noctiluca miliaris* bloom with historical dataset of the Arabian Sea obtained within the bloom area of the northeastern Arabian Sea. The dots represent values upto depth of 1% light for present study and 0-50 m from the historical dataset. Carbon biomass calculated for all data using conversion factor 20fgC $cell^{-1}$.

Reflecting the trends in total bacterial counts, a major inflation of bacterial carbon biomass was detected during Feb-2009 (Fig. 2.18). At the stations O-1 and F09-2, located on massive green-tides of *N miliaris* (Fig. 2.19), bloom associated bacterial counts inflated to 19.3×10^{9} cells L^{-1} at O-1 and to 6.8×10^{10} cells L^{-1} at station F09-2. The shallow euphotic zone of 33-45 m resulting from heavy bloom was enriched in bacteria as high as 22.7×10^{13} cells m^{-2} at O-1 to 19.7×10^{13} cells m^{-2} at F09-2. During the consecutive cruise of March-2009, there was a dramatic decline of the total bacterial load in this area. Counts at the overlapping station O-1 during Mar-09 dropped ~6 times at the surface to 3.36×10^{9} cells L^{-1} and ~4 times in the water column to 5.09×10^{13} cells m^{-2}. At the other major bloom locations during Feb-09 (except F09-7), surface counts ranged between 2.04×10^{9} cells L^{-1} at F09-5 to 2.86×10^{9} cells L^{-1} at O-2. East of 67°E, the bloom was moderate at station F09-7. Surface Chl *a* of 0.77 μg L^{-1} and *N miliaris* concentration of 34 cells L^{-1} were low in comparison to other bloom stations, but so were the ~6 times lower bacterial load of 0.9×10^{9} cells L^{-1} at the surface and 4.74×10^{13} cells m^{-2} in the euphotic column (Fig. 2.17). Such variations in bacterial distributions with *N miliaris* distribution was reflective in the significant overall correlation with both Chl *a* (R^2=0.65, n=42) and *N miliaris* counts (R^2=0.49, n=42), during the active bloom period of Feb-09 (Fig. 2.21). By Mar-2009, the correlation between *N miliaris* counts and bacteria, turned as insignificant as R^2=0.09, n=33 and also remained similar during Mar-11 (R^2=0.09, n=33) (Fig. 2.20 and 2.21).

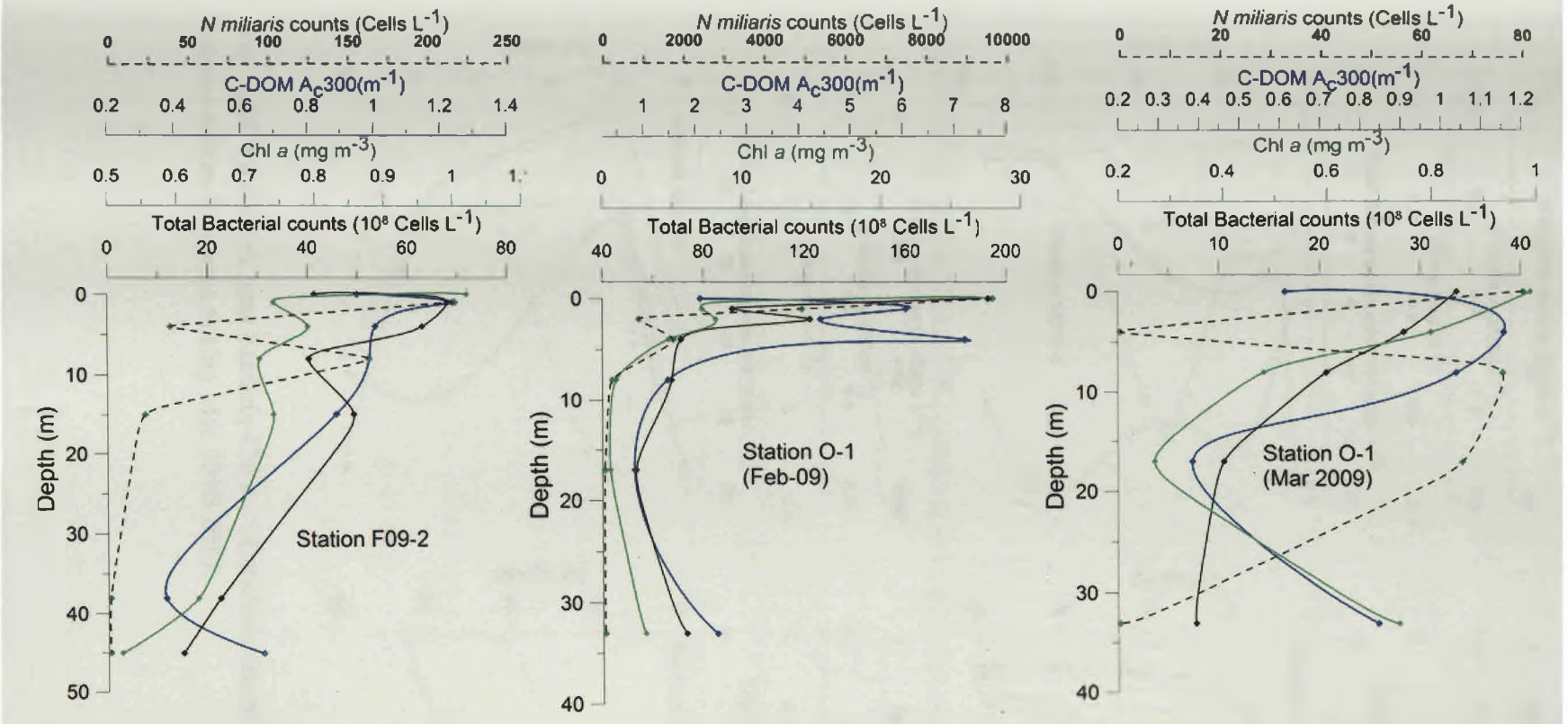

Fig. 2.19 Profiles of total bacteria-Chl *a* – N *miliaris* counts - C-DOM at most intense bloom locations during Feb-Mar 2009.

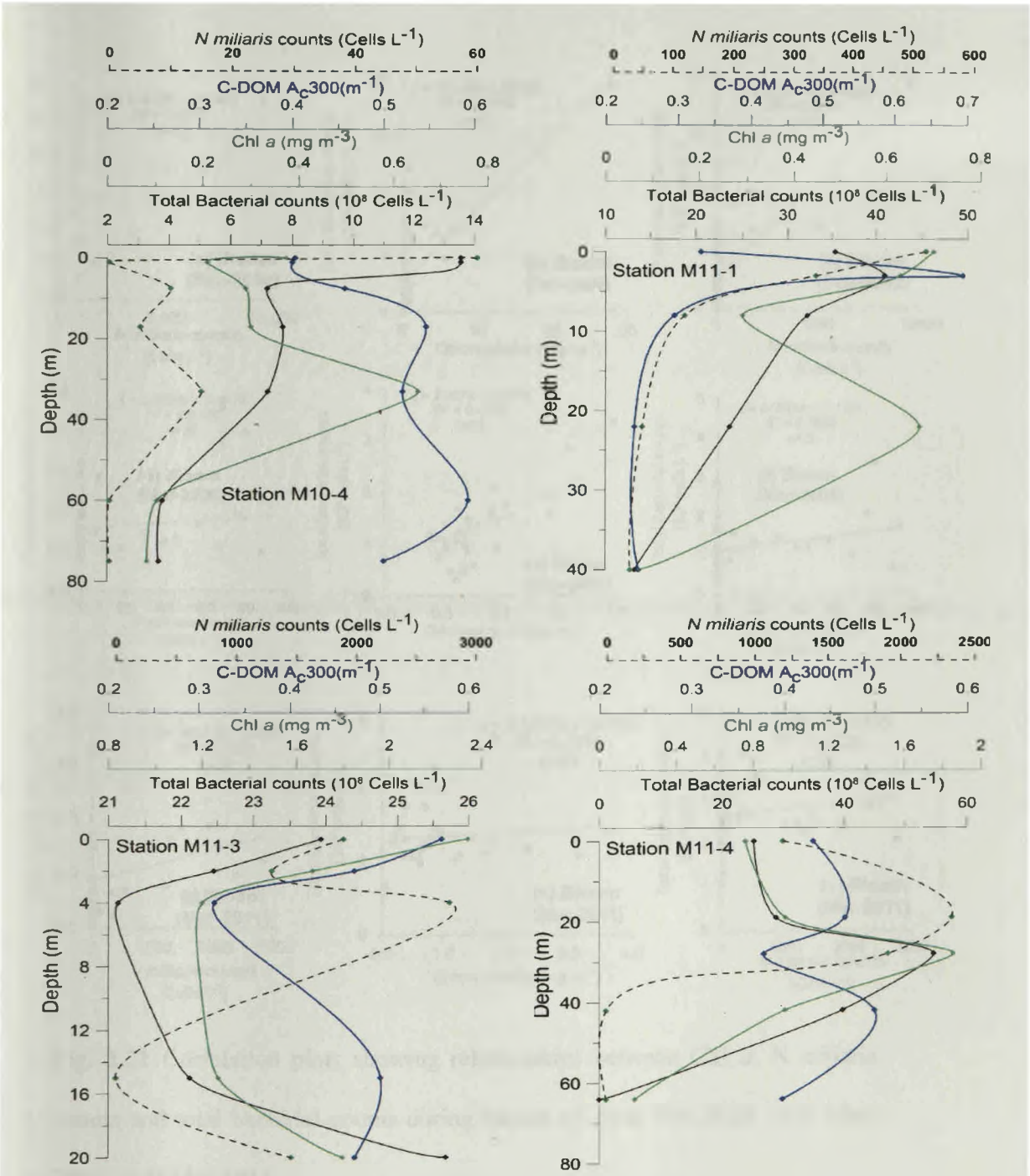

Fig. 2.20 Profiles of total bacteria-Chl *a* – N *miliaris* counts - C-DOM at most intense bloom locations during Mar 2010-2011.

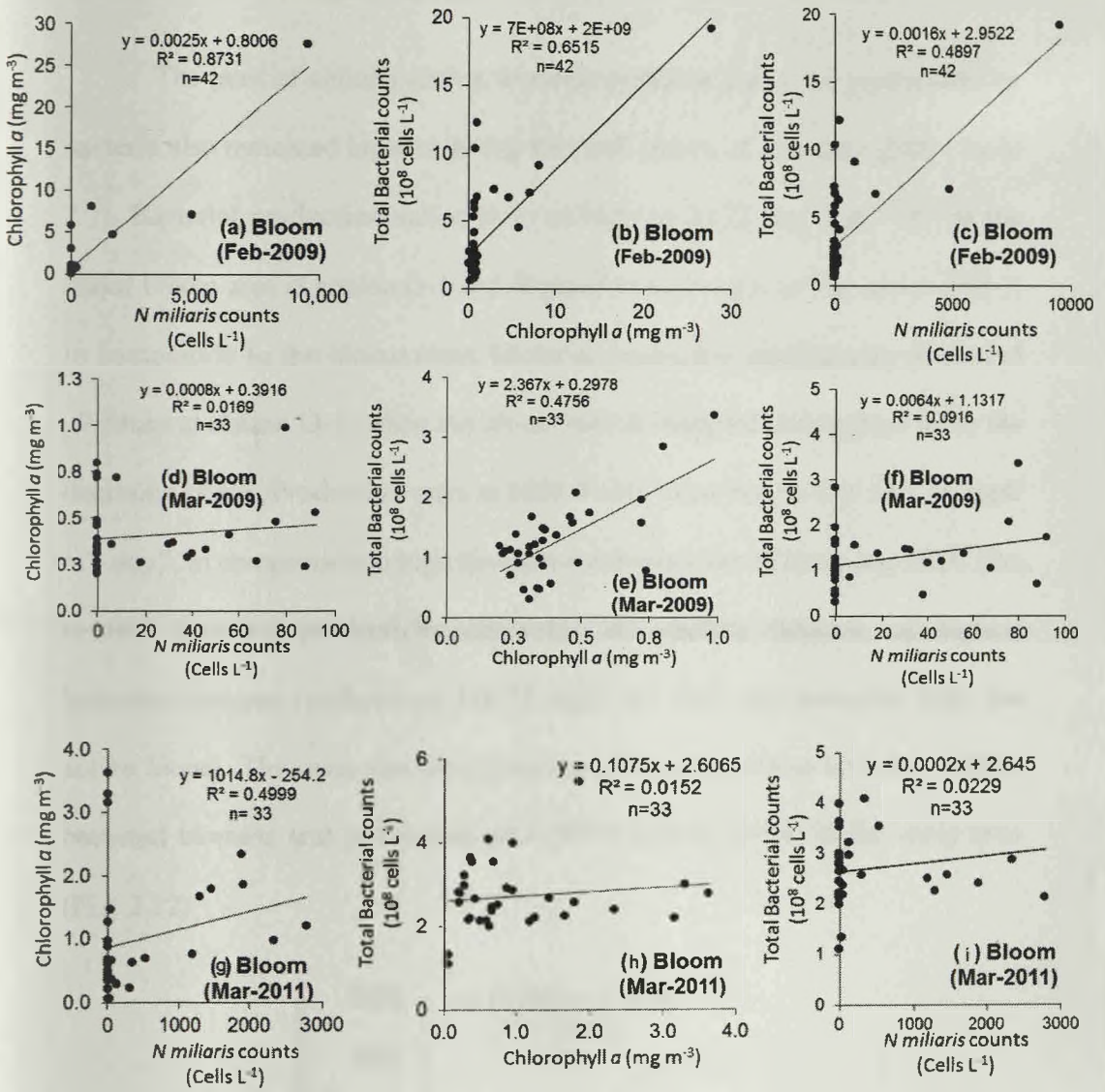

Fig. 2.21 Correlation plots showing relationships between Chl *a*, N miliaris counts and total bacterial counts during bloom of: (a-c) Feb-2009, (d-f) Mar-2009, (g-i) Mar-2011.

2.2.7.2 Bacterial Production rates

The rates of cellular carbon biomass synthesis (bacterial production) by bacteria also remained highest during the peak bloom of February-2009 (Table 2.7). Bacterial production varied from as high as 21.72 mg C m^{-3} Hr^{-1} at the major bloom area at station O-1 and dropped to 0.47 mg C m^{-3} at station F09-7. In comparison to the bloom areas, bacterial production significantly decreased ~7 times at station O-1, when the bloom was re-sampled during Mar-09 in the declining phase. Production rates at M09-4 also remained as low as 1.54 mgC m^{-3} day^{-1}, in comparison to high biomass synthesis rates of February-2009. The column bacterial productivity supported the surface features, as highest bacterial biomass synthesis of 148.72 mgC m^{-2} Hr^{-1} was recorded from the active bloom. This was also seen from the strong correlation between surface bacterial biomass and production rates (R^2 = 0.9847, n=14) in the study area (Fig. 2.22)

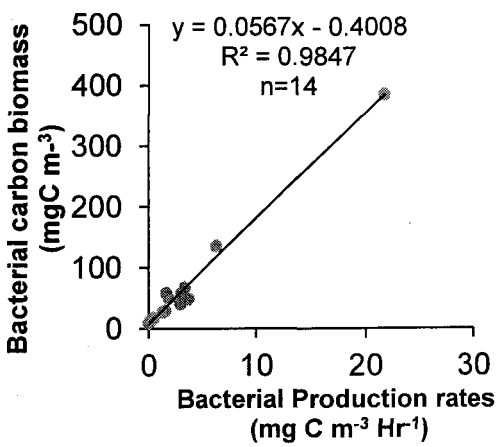

Fig. 2.22 Correlation between bacterial biomass and bacterial production at the surface during the NEAS bloom.

In comparison to February 2009, bacterial production rates of 1.32 mg m^{-3} hr^{-1} and 1.75±0.15 mg m^{-3} hr^{-1} during March-2010 and March-2011, were found to be significantly low by ~4 times. At the non-bloom off-shore sites, bacterial production remained <1 mgC m-3 hr^{-1} and remained lowest at station M09-10, located below 19°N in the NEAS.

Tritiated thymidine tracer added to measure DNA synthesis rates, was utilized by the bacterial population at ultra-high concentrations of 500.31 pM L^{-1} hr^{-1} at station O-1, which significantly dropped to 78 pM L^{-1} hr^{-1} during March-2009 (Table 2.7). Population growth rates calculated from ratios of standing bacterial biomass to bacterial production rate ratios mirrored this trend. Averaged over the euphotic zone, high growth rates of 0.05±0.01 hr^{-1} were recorded during the month of February-2009 for the entire study. The population growth rates marginally declined to 0.051±0.0016 hr^{-1} during Mar-09, and further to 0.048 hr^{-1} during Mar-10 and to 0.032±0.006 hr^{-1}. At the non-bloom sites, growth rates varied between 0.003 – 0.009, implying a generation time of 73.72 – 210 hours.

Table 2.7 Heterotrophic bacterial production during bloom of *Noctiluca miliaris* (green) in the NEAS at selected major bloom and non-bloom stations.

Period of Study		Bacterial Carbon Biomass		^{3}H-Thymidine uptake		Bacterial Production (BP)		Population Growth rate (Hr^{-1})
		Surface ($\mu g\ C\ L^{-1}$)	Column ($g\ C\ m^{-2}$)	Surface ($pM\ L^{-1}\ Hr^{-1}$)	Column ($nM\ m^{-2}\ Hr^{-1}$)	Surface ($mg\ C\ m^{-3}Hr^{-1}$)	Column ($mg\ C\ m^{-2}Hr^{-1}$)	
Bloom								
Feb-2009	(n=6)	114.27 ± 138.65	2.39±1.57	146.93±178.54	1.92±0.92	6.38±7.75	83.33±39.95	0.055±0.018
Mar-2009	(n=2)	48.13±27.01	1.07±0.08	56.87±30.40	1.33 ±0.57	2.47±1.32	57.68±24.81	0.051±0.0016
Mar-2010	(n=1)	27.05	0.94	30.5	1.05	1.32	45.4	0.048
Mar-2011	(n=2)	54.19±5.82	2.69±0.58	40.43±3.46	1.87±0.90	3.91±1.80	89.31±21.86	0.032±0.006
Non-Bloom								
Feb-09	(n=1)	12.64	0.54	2.74	0.26	0.12	11.43	0.0094
Mar-09	(n=1)	8.58	0.56	0.65	0.18	0.03	7.74	0.0033
Mar-11	(n=1)*	11.60	nd	1.97	nd	0.09	Nd	0.007

n= number of CTD stations; *Surface estimate, nd – not determined;

2.2.7.3 Picocyanobacteria

In comparison to total bacteria, counts of photoautotrophic picocyanobacteria showed an exactly opposite trend and significantly increased as the bloom started to decline during the month of March. Picocyanobacterial load remained $<5\times10^{7}$ cells L^{-1} during the active bloom of February-2009 in the NEAS (Fig. 2.18). Averaged distribution during this period showed lowest counts of $4.57\pm2.42\times10^{7}$ cells L^{-1} at the surface and $19.06\pm12.19\times10^{11}$ cells m^{-2} in the water column. In comparison, during March-2009, the declining bloom area became enriched in picocyanobacteria, with ~2 times increase to $8.3\pm24.48\times10^{7}$ cells L^{-1} at the surface and $37.07\pm24.48\times10^{11}$ cells m^{-2} in the water-column, respectively. During the later cruises of March 2010-11, picocyanobacterial counts remained similar and varied as 9.71×10^{7} - $10.23\pm7.63\times10^{7}$ cells L^{-1} at the surface and 35.52×10^{11} – $32.57\pm15.34\times10^{11}$ cells m^{-2} in the euphotic column (Table 2.6).

In the non-bloom stations of Feb-Mar 2009, surface picocyanobacterial counts of $5.93\pm4.09\times10^{7}$ – $5.99\pm5.23\times10^{7}$ cells L^{-1} were similar. However, counts of the euphotic column reflected the general trend with a ~1.5 times increase from $29.89\pm28.27\times10^{11}$ cells m^{-2} during February to $41.03\pm11.39\times10^{11}$ cells m^{-2} in March. Non-bloom counts during March 2010-11 were found to be low in comparison to 2009 and varied as $34.84\pm7.04\times10^{7}$ – $21.60\pm11.37\times10^{7}$ cells L^{-1} at the surface to $9.8\pm4.78\times10^{11}$ – $4.9\pm0.99\times10^{11}$ cells m^{-2} in the water column. In the coastal Gujrat, picoplankton counts recorded during Feb-Mar 2009 also reflected the general trend and showed a significant increase of ~12

times at the surface from 0.45×10^7 cells L^{-1} to 5.46×10^7 cells L^{-1} (Table 2.6).

Autofluorescence charactersitics revealed that yellow-orange fluorescing picocyanobacteria belonging to the *Synechococcus* spp. were the dominant forms and also detected as colonies. Microscopic enumeration of groups during bloom of March-2011 showed that *Synechococcus* spp. comprised an average of 98.5% of the total picocyanobacterial population, whereas 1.46% belonged to dark red /fading red fluorescing phycocyanin and *Prochlorococcus* groups.

Station-wise trends further showed that at the overlapping station O-1, the highest inflation of picocyanobacterial counts had occurred as the bloom progressed from the active to the declining phase during Feb-Mar 2009. At this location, surface counts increased ~8 times from 1.94×10^7 cells L^{-1} during Feb-09 to 8.9×10^7 cells L^{-1} in March, which was also reflected in the water-column.

HPLC analysis at the overlapping stations O-1 and O-2, further reflected an increase in Zeaxanthin from Feb-09 to Mar-09, suggesting an increase in the cyanobacterial population following decline of the bloom (Fig. 2.24). Zeaxanthin concentrations at St-O2 remained undetected during active bloom of 17th Feb-09, while it increased to 0.23 μg L^{-1} during 3rd Mar-09 at the same location. At st-O1, the high concentration of Chl *b* (23.59 μg L^{-1}) during Feb-09, was due to the due to the symbiotic flagellates (prasinophytes) *Pedinomonas noctiluca* which decreased to as low as 0.41 μg L^{-1} during Mar-09, showing the demise of the bloom. Further, rates of photosynthetic carbon-fixation of plankton size-fractions from surface bloom waters during Mar-09

also reflected a similar trend, as the productivity of <20μm size-fraction containing the microbial-population substantially increased to 47.9%. This was indicative of the picoplankton contribution to overall productivity during the later stages of the bloom.

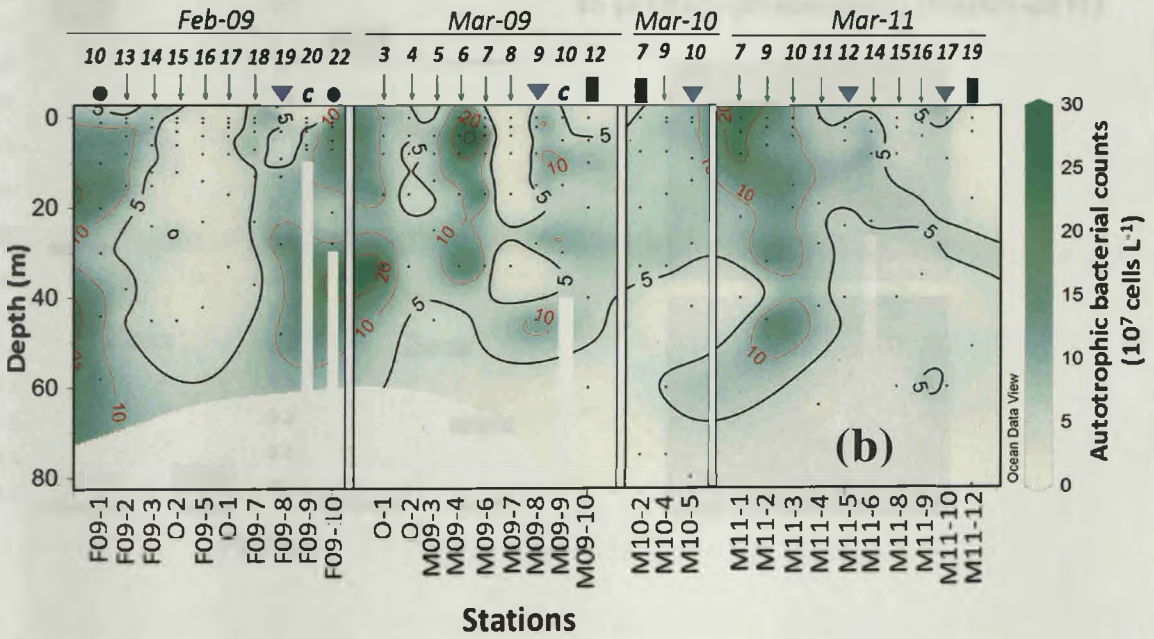

Fig. 2.23 Euphotic section showing distribution of total picocyanobacteria (autotrophic) in NEAS during bloom of *N miliaris*.

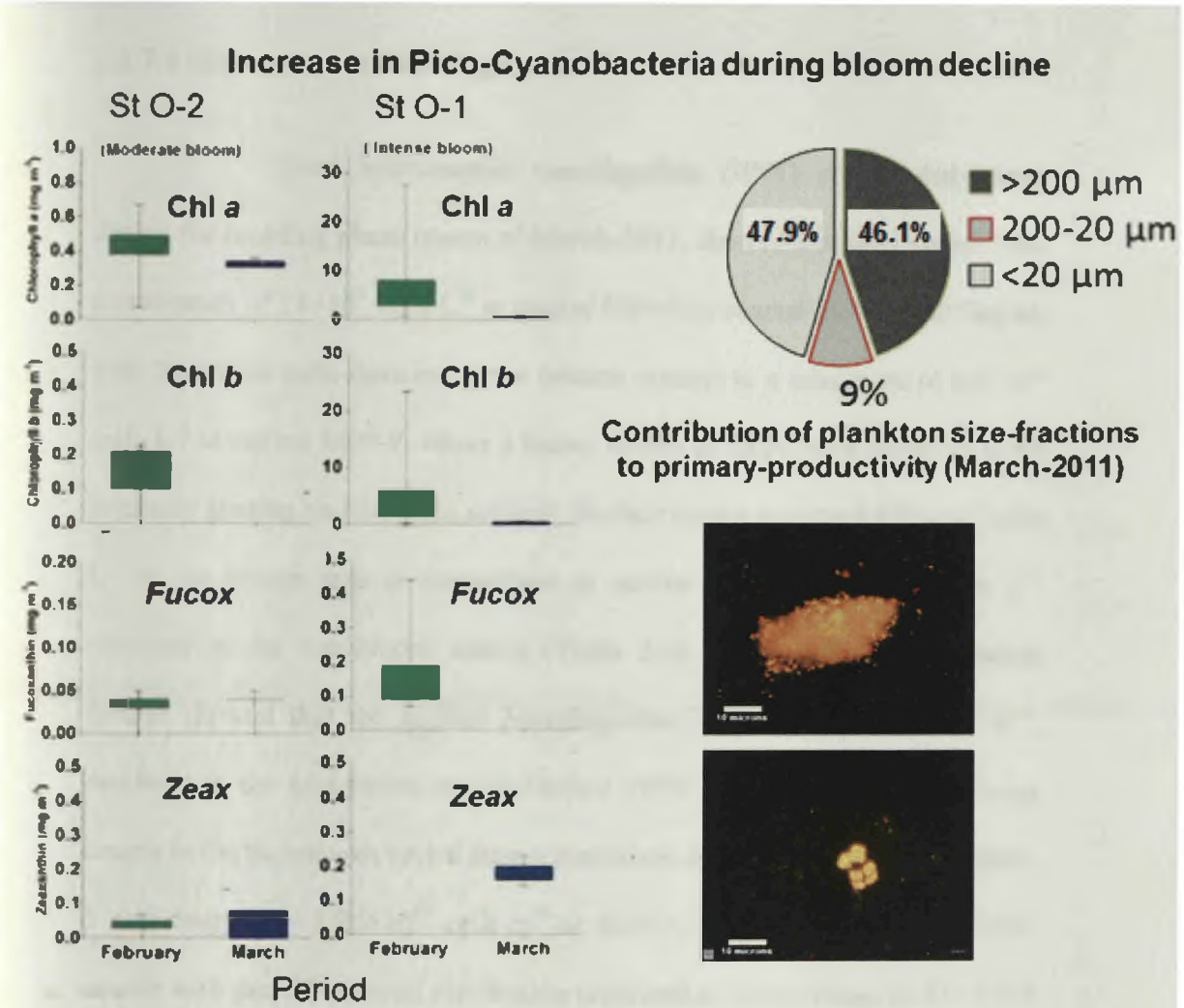

Fig. 2.24 Increase in pico-cyanobacteria at stations O-1 and O-2 during the declining phase bloom of March-2009, in comparison to active bloom of Feb-2009. Also seen is the increase in <20µm primary productivity and epifluorescent images confirming as the phycoerythrin containing picocyanobacteria.

2.2.7.4 Heterotrophic Nanoflagellates

Total heterotrophic nanoflagellate (HNF) counts determined during the receding phase bloom of March-2011, showed that they varied from a maximum of 14×10^5 cells L^{-1} at station M09-6 (a coastal location off Gujrat, with *Noctiluca* cells detected in the bottom waters) to a minimum of 6.5×10^6 cells L^{-1} at station M09-9, where a heavy bloom of Salps were observed to be intensely grazing on *Noctiluca miliaris*. Surface counts averaged 9.81×10^6 cells L^{-1} in the bloom area in comparison to similar counts of 10×10^5 cells L^{-1} obtained in the non-bloom station (Table 2.8). Water column distribution further showed that the highest *Nanoflagellate* load of 5.02×10^8 cells m^{-2}, occurred in the non-bloom station, below 19°N at station M09-11. Column counts in the bloom area varied from a maximum of 4.34×10^8 cells m^{-2} at M09-2 and dropped to 1.95×10^{12} cells m^{-2} at M09-3. Overall correlation of HNF counts with that of bacterial distribution remained as insignificant as $R^2=0.015$ (n=32). Relationship with Chl *a* also remained insignificant, as $R^2=0.09$ (n=32) and with *N miliaris* counts as $R^2=0.09$ (n=32). Interestingly, a pattern of negative relation with HNF counts decreasing in case of higher N miliaris counts was observed as marked in Fig. 2.25c.

Table 2.8 Total Nanoflagellates distribution during bloom of March-2011

Station	Surface (10^6 cell L^{-1})	Column (10^8 cells m^{-2})
M09-1	5.1	3.51
M09-2	12.5	4.34
M09-3	8.0	1.95
M09-4	12.6	3.30
M09-6	14.0	2.77
M09-8	10.0	3.43
M09-9	6.5	2.76
M09-11	10.0	5.02

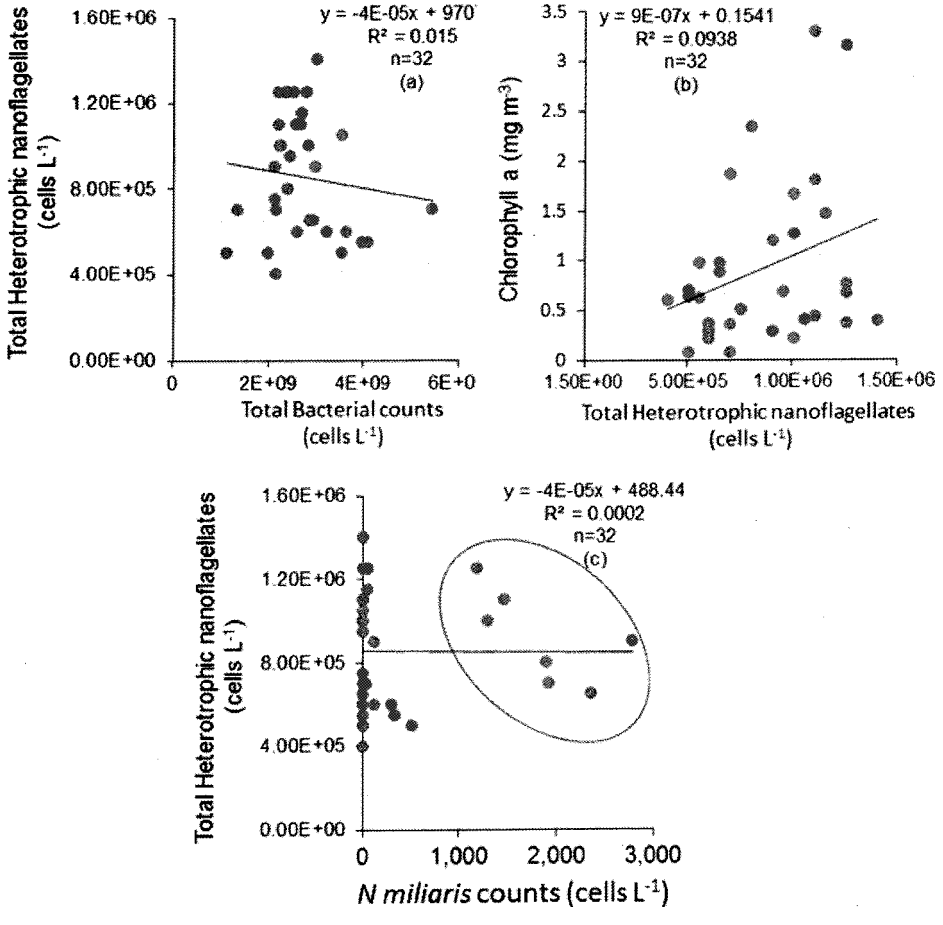

Fig. 2.25 Relationship of HNF population with: (a) total bacteria (b) Chl *a* and (c) *N miliaris* counts from bloom areas of March-2011 in the NEAS.

2.2.7.5 Bacterial relationship with bloom ecosystem components

To discriminate patterns of variations in the distribution of bacteria with the bloom phases, PCA analysis was undertaken with physico-chemical charactersitics, photosynthetic carbon production, C-DOM absorbtion characteristics as proxy for bloom DOM nature and concentration (Fig. 2.26). Matching datasets from euphotic depths with detectable presence of *N miliaris* was selected to run the analysis. The first two principal components (PC) explained the maximum variations which together varied from 54.31% during the active bloom phase of Feb-2009, 43.87% during Mar-2009 and 50.56% during Mar-2011 (Fig. 2.26). A seen in Fig. 2.26, during active bloom of Feb-2009, the distribution of bacteria remained strongly correlated (positive) with Chl *a, N miliaris* counts, C-DOM concentration (Ac300), slope-ratio (Sratio), 465:665 nm absorbtion coefficient ratio (e4:e6) and dissolved inorganic phosphate on the first principal component, explaining the maximum variation of 36.16% on the first PC axis. Bacterial counts also showed almost equally strong positive correlations at $p<0.05$ with Chl *a* ($r = 0.69$) and C-DOM Ac_{300} ($r = 0.62$) (Table 2.9). Strongest correlation was obtained between bacteria and phosphate ($r=0.71$), which was also reflected in the overall data (Fig. 2.26). On the other hand, inverse indicators of the molecular size of C-DOM as S-ratio and s1 (275-295 nm slope) and e1 (250:365 nm absorbtion coefficient), showed strong negative correlations with bacteria and the indicators of the bloom, implying higher molecular size C-DOM consistent with observations of the mucus/slime produced by the bloom.

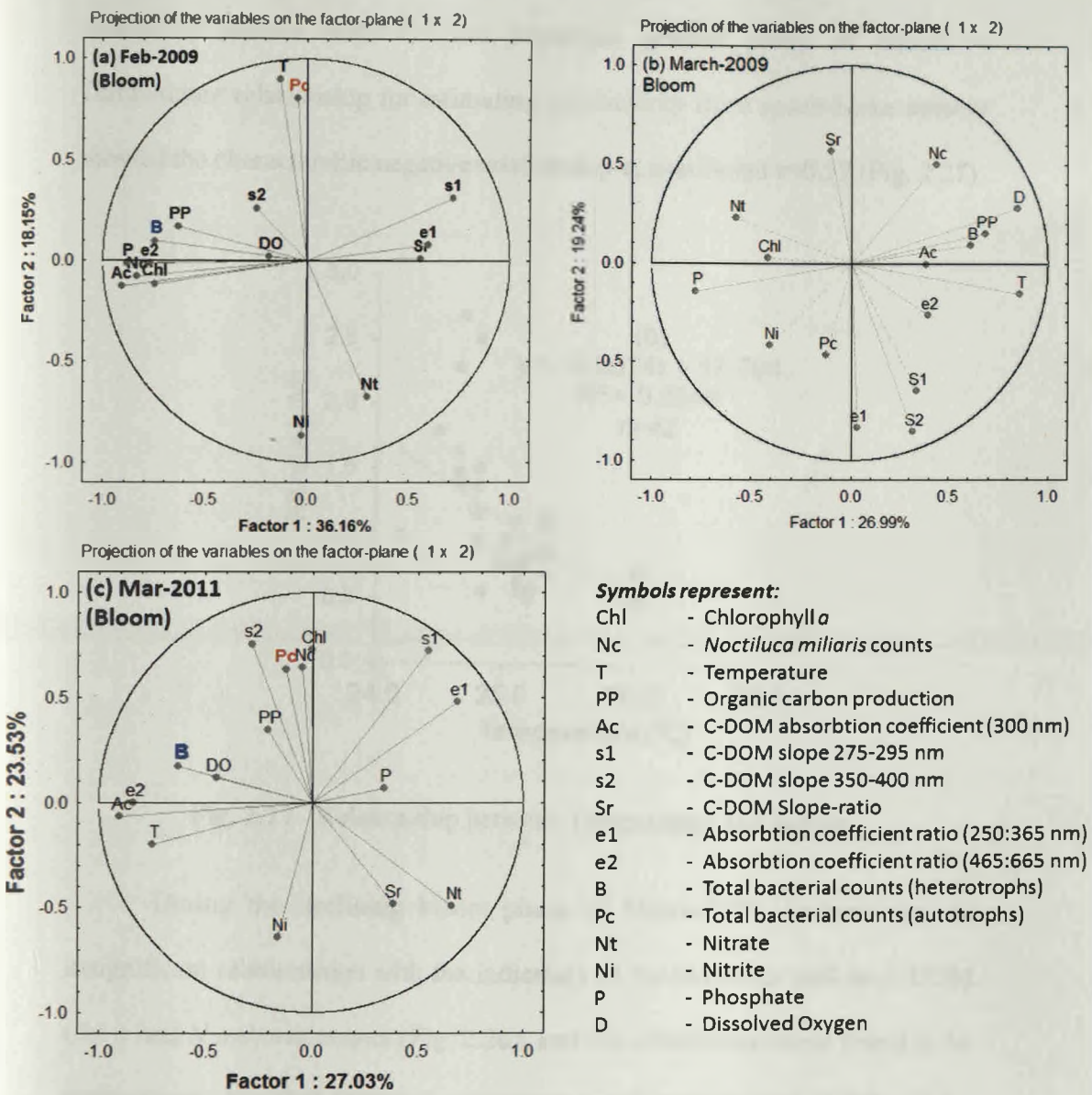

Fig 2.26 Principal-component ordination analysis of bacterial distribution with biological and physico-chemical characterestics of bloom of the dinoflagellate *N miliaris,* during (a) Feb-2009 (b) Mar-2009 and (c) Mar- 2011 in the NEAS.

On the other hand, the picocyanobacterial population showed strong correlations with temperature (r=0.67), whereas they remained inversely

related to Nitrate (r=0.57). The important general proxy of Nitrate – Temperature relationship for estimating productivity from space-borne sensors showed the charactersitic negative relationship at significant r=0.57 (Fig. 2.27).

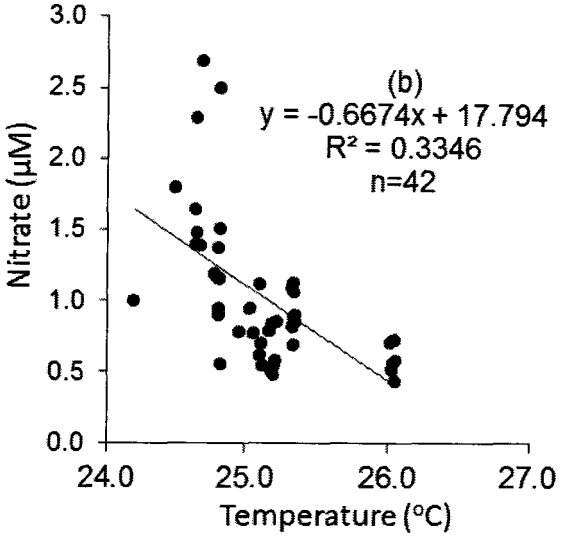

Fig. 2.27 Relationship between Temperature and Nitrate.

During the declining bloom phase of March-2009, bacteria showed insignificant relationships with the indicators of the bloom as well as C-DOM Chl *a* and *N miliaris* counts (Fig. 2.26), and the correlations were found to be insignificant. The first principal component could explain only 26.99% of the variations. Productivity and Temperature remained well correlated during this phase (r=0.54) and both showed positive relationship to dissolved oxygen and were negatively related to Nitrate (Table 2.9b). Although, primary-productivity decreased significantly almost 2-3 times, during the latter half of the bloom, bacteria was correlated with PP as r=0.53. Dissolved phosphate showed negative correlation with PP (r= -0.52) and dissolved oxygen (r = - 0.83) and

the charactersitic negative Temperature-Nitrate relationship (r=-0.44) was seen. The C-DOM Ac300 did not show any significant relationship with bacteria or with Chl *a*. Change in charactersitics or nature of C-DOM was observed from changing interrelationships between the slopes.

During the bloom of March 2011, the first principal component could explain only 27.03% of the variations, and the second component explained 23.53% variations, reflecting the nature of more complex relationships at the trophic levels with their environmental variables, in comparison to the active bloom of Feb-2009 (Fig. 2.26c). The significantly higher *N miliaris* concentrations and Chl *a* recorded during this period was explained by the second component as r=0.67. The relationship between Picoplankton and Chl *a* remained as r=0.32, while the relationship was stronger between Bacteria and Picocyanobacteria as r= 0.57. PP remained positively correlated with DO (r=0.59), whereas the charactersitic Temperature-Nitrate relationship was again observed as, r = - 0.66. The first principal component was explained by an unusually strong relationship between e2 (465:665 nm ratio) and the overall concentration of C-DOM measured at 300 nm (Ac300) as r=0.91 and also a strong relationship with bacteria as r=0.67.

Table 2.9 Correlation matrix showing Pearson's product moment correlation (r) among variables during: **(a)** active bloom of Feb-2009 (n=35); declining bloom of **(b)** Mar- 2009 (n=20) and **(c)** Mar-2011 (n=20), in the NEAS. Coefficients marked as red are significant at p<0.05. (**Symbols in table represented by**: ***Chl****- Chlorophyll a;* ***Nc*** *– N miliaris counts;* ***B****- Total bacterial counts;* ***Pc*** *– Picocyanobacterial counts;* ***PP*** *– Primary productivity;* ***T****- Temperature;* ***D****- Dissolved Oxygen;* ***Nt*** *– Dissolved Nitrate-N;* ***Ni*** *– Dissolved Nitrite;* ***P*** *– Dissolved Phosphate; and C-DOM absorbtion parameters as* ***Sr*** *–Slope ratio;* ***Ac*** *–Absorbtion coefficient 300 nm;* ***s1*** *– 275-295 nm slope;* ***s2****- 350-400 nm slope;* ***e1*** *– 250:365 nm absorbtion coefficient ratio;* ***e2*** *– 465:665 nm absorbtion coefficient ratio).*

(a)

Variable	Chl	Nc	PP	Sr	Ac	s1	s2	e1	e2	B	Pc	T	D	Nt	Ni	P
Chl	1.00	0.67	0.37	-0.36	0.75	-0.56	-0.01	-0.34	0.39	0.69	-0.23	0.04	0.22	-0.20	0.08	0.16
Nc	0.67	1.00	0.45	-0.38	0.79	-0.49	0.09	-0.35	0.66	0.48	-0.14	0.10	0.16	-0.20	0.05	0.63
PP	0.37	0.45	1.00	-0.27	0.71	-0.44	-0.02	-0.29	0.18	0.21	0.08	0.17	0.19	-0.32	-0.27	0.43
Sr	-0.36	-0.38	-0.27	1.00	-0.45	0.38	-0.67	0.15	-0.40	-0.43	0.16	0.02	-0.24	0.19	-0.06	-0.39
Ac	0.75	0.79	0.71	-0.45	1.00	-0.73	0.05	-0.55	0.60	0.62	-0.15	0.05	0.22	-0.15	0.09	0.50
s1	-0.56	-0.49	-0.44	0.38	-0.73	1.00	0.11	0.62	-0.51	-0.59	0.12	0.18	-0.17	0.04	-0.26	-0.32
s2	-0.01	0.09	-0.02	-0.67	0.05	0.11	1.00	0.02	0.35	0.04	0.13	0.20	0.02	-0.15	-0.13	0.32
e1	-0.34	-0.35	-0.29	0.15	-0.55	0.62	0.02	1.00	-0.58	-0.47	-0.12	0.01	-0.01	0.06	-0.08	-0.36
e2	0.39	0.66	0.18	-0.40	0.60	-0.51	0.35	-0.58	1.00	0.58	0.10	0.18	-0.15	-0.00	0.09	0.69
B	0.69	0.48	0.21	-0.43	0.62	-0.59	0.04	-0.47	0.58	1.00	0.12	0.22	0.12	-0.22	0.06	0.71
Pc	-0.23	-0.14	0.08	0.16	-0.15	0.12	0.13	-0.12	0.10	0.12	1.00	0.67	-0.01	-0.40	-0.60	0.15
T	0.04	0.10	0.17	0.02	0.05	0.18	0.20	0.01	0.18	0.22	0.67	1.00	-0.15	-0.57	-0.71	0.05
D	0.22	0.16	0.19	-0.24	0.22	-0.17	0.02	-0.01	-0.15	0.12	-0.01	-0.15	1.00	-0.46	0.10	-0.01
Nt	-0.20	-0.20	-0.32	0.19	-0.15	0.04	-0.15	0.06	-0.00	-0.22	-0.40	-0.57	-0.46	1.00	0.50	-0.10
Ni	0.08	0.05	-0.27	-0.06	0.09	-0.26	-0.13	-0.08	0.09	0.06	-0.60	-0.71	0.10	0.50	1.00	0.03
P	0.16	0.63	0.43	-0.39	0.50	-0.32	0.32	-0.36	0.69	0.71	0.15	0.05	-0.01	-0.10	0.03	1.00

(b)

Variable	Chl	Nc	PP	Sr	S1	S2	Ac	e1	e2	B	Pc	T	D	Nt	Ni	P
Chl	1.00	0.05	-0.19	-0.25	-0.49	-0.03	-0.07	0.04	-0.58	0.23	0.30	-0.28	-0.36	0.33	-0.06	0.31
Nc	0.05	1.00	0.43	0.09	-0.23	-0.14	0.28	-0.32	-0.25	0.38	-0.10	0.43	0.41	-0.03	-0.43	-0.20
PP	-0.19	0.43	1.00	-0.11	0.02	0.16	0.38	-0.17	0.27	0.53	0.00	0.54	0.55	-0.10	-0.30	-0.32
Sr	-0.25	0.09	-0.11	1.00	0.10	-0.81	-0.24	-0.37	0.02	-0.05	-0.24	-0.09	0.12	0.26	-0.01	-0.06
S1	-0.49	-0.23	0.02	0.10	1.00	0.45	0.12	0.52	0.60	0.02	0.24	0.44	0.11	-0.17	0.34	-0.18
S2	-0.03	-0.14	0.16	-0.81	0.45	1.00	0.16	0.68	0.25	0.15	0.34	0.37	0.01	-0.38	0.17	-0.06
Ac	-0.07	0.28	0.38	-0.24	0.12	0.16	1.00	-0.29	0.38	0.19	-0.02	0.42	0.07	0.05	0.05	-0.17
e1	0.04	-0.32	-0.17	-0.37	0.52	0.68	-0.29	1.00	-0.12	0.01	0.47	0.21	-0.15	-0.41	0.12	0.11
e2	-0.58	-0.25	0.27	0.02	0.60	0.25	0.38	-0.12	1.00	-0.06	-0.09	0.25	0.27	0.04	0.21	-0.35
B	0.23	0.38	0.53	-0.05	0.02	0.15	0.19	0.01	-0.06	1.00	0.20	0.55	0.41	-0.31	-0.34	-0.37
Pc	0.30	-0.10	0.00	-0.24	0.24	0.34	-0.02	0.47	-0.09	0.20	1.00	0.04	-0.23	0.28	-0.06	0.16
T	-0.28	0.43	0.54	-0.09	0.44	0.37	0.42	0.21	0.25	0.55	0.04	1.00	0.64	-0.44	-0.24	-0.52
D	-0.36	0.41	0.55	0.12	0.11	0.01	0.07	-0.15	0.27	0.50	-0.23	0.64	1.00	-0.44	-0.43	-0.83
Nt	0.33	-0.03	-0.10	0.26	-0.17	-0.38	0.05	-0.41	0.04	-0.31	0.28	-0.44	-0.44	1.00	0.31	0.52
Ni	-0.06	-0.43	-0.30	-0.01	0.34	0.17	0.05	0.12	0.21	-0.34	-0.06	-0.24	-0.43	0.31	1.00	0.39
P	0.31	-0.20	-0.32	-0.06	-0.18	-0.06	-0.17	0.11	-0.35	-0.37	0.16	-0.52	-0.83	0.52	0.39	1.00

Table 1.9 (Continued)

(c)

Variable	Chl	Nc	PP	Sr	Ac	s1	s2	e1	e2	TBC	Pc	T	D	Nt	Ni	P
Chl	1.00	0.67	0.27	-0.52	-0.04	0.27	0.45	0.12	-0.12	-0.12	0.32	-0.26	0.19	-0.39	-0.27	0.28
Nc	0.67	1.00	0.41	-0.34	0.04	0.30	0.33	0.05	-0.06	-0.12	0.25	-0.20	0.04	-0.36	-0.22	-0.10
PP	0.27	0.41	1.00	-0.11	0.02	0.10	0.09	-0.00	0.04	-0.26	-0.11	0.19	0.59	-0.46	-0.27	-0.29
Sr	-0.52	-0.34	-0.11	1.00	-0.52	-0.07	-0.81	0.03	-0.38	-0.12	-0.02	-0.06	-0.06	0.20	-0.07	-0.18
Ac	-0.04	0.04	0.02	-0.52	1.00	-0.59	0.37	-0.66	0.91	0.54	0.08	0.49	0.23	-0.37	0.35	-0.11
s1	0.27	0.30	0.10	-0.07	-0.59	1.00	0.45	0.88	-0.43	-0.03	0.43	-0.43	-0.27	-0.01	-0.64	0.01
s2	0.45	0.33	0.09	-0.81	0.37	0.45	1.00	0.29	0.43	0.38	0.49	-0.07	-0.09	-0.30	-0.24	0.10
e1	0.12	0.05	-0.00	0.03	-0.66	0.88	0.29	1.00	-0.46	-0.10	0.24	-0.58	-0.28	0.32	-0.40	0.08
e2	-0.12	-0.06	0.04	-0.38	0.91	-0.43	0.43	-0.46	1.00	0.67	0.24	0.38	0.19	-0.32	0.25	-0.26
TBC	-0.12	-0.12	-0.26	-0.12	0.54	-0.03	0.38	-0.10	0.67	1.00	0.57	0.46	-0.01	-0.47	-0.02	-0.36
Pc	0.32	0.25	-0.11	-0.02	0.08	0.43	0.49	0.24	0.24	0.57	1.00	-0.12	-0.14	-0.44	-0.41	0.11
T	-0.26	-0.20	0.19	-0.06	0.49	-0.43	-0.07	-0.58	0.38	0.46	-0.12	1.00	0.46	-0.66	0.01	-0.46
D	0.19	0.04	0.59	-0.06	0.23	-0.27	-0.09	-0.28	0.19	-0.01	-0.14	0.46	1.00	-0.53	-0.41	-0.09
Nt	-0.39	-0.36	-0.46	0.20	-0.37	-0.01	-0.30	0.32	-0.32	-0.47	-0.44	-0.66	-0.53	1.00	0.42	0.28
Ni	-0.27	-0.22	-0.27	-0.07	0.35	-0.64	-0.24	-0.40	0.25	-0.02	-0.41	0.01	-0.41	0.42	1.00	0.02
P	0.28	-0.10	-0.29	-0.18	-0.11	0.01	0.10	0.08	-0.26	-0.36	0.11	-0.46	-0.09	0.28	0.02	1.00

2.3 Discussion

The Indian remote sensing ocean color sensor, IRS-P4-1 (OCM) generated the first image of the unusually high Chl *a* conditions during 2000 in the northeastern (NEAM) Arabian Sea (Fig. 2.2), however, the type of organisms causing the bloom were not known. Subsequent studies reported extensive blooms of an invasive dinoflagellate *Noctiluca miliaris* (green) containing photosynthetic prasinophytes, giving deep green coloration to the off-shore waters in the NEAS (Matondkar et al. 2004, Parab et al. 2006, Gomes et al. 2008, Dwivedi et al. 2008).

Based on satellite Chl *a* and shipboard observations during consecutive cruises of Feb-Mar 2009, two phases of this bloom are discernible. During the month of February-2009, massive blooms are detected in the 'active or peak' phase, associated with cooler temperatures averaging 24.96±0.49°C under the influence of the northeast winter monsoon winds and a nutrient-rich deep mixed layer of 71.67 ±24.5 m. During March-2009, ~4 times decrease of Chl *a* and *N miliaris* counts in the euphotic column is seen to be accompanied by the weakening and reversal of the northeast monsoon winds. This resulted in warming of sea-surface temperature to 26.07±0.8 °C with shoaling of a nutrient-depleted mixed layer to 35.67±13.91m, creating unfavorable conditions for the bloom, and hence referred to as the 'declining/receeding' phase. Although, a similar trend is detected during March-2010, the bloom of Mar-2011 is seen to be associated with a much lower temperature of 25.15±0.26°C. This probably favored the higher concentration of *N miliaris*

which is detected at depths even in the coastal waters off Gujrat and higher nutrient concentrations in comparison to the earlier seasons of March.

As the major bloom stations during February 2009 are seen to be located on the edges of the mesoscale cold-core eddies which tends to bring up nutrient-rich waters from the deep, they probably play an important role in supporting the 'active' bloom phase of February. The isotherms of these bloom stations (O-1, F09-2, F09-4) also show pushing up of the thermoclines which are an important feature of such mesoscale features (McGillicudy and Robinson 1997). In light of recent findings that these eddies can promote seasonal blooms in the Arabian Sea (Balcerak 2012) their role needs to be further investigated. Earlier, Gomes et al. (2008) had reported the occurrence of such eddies during blooms of *N miliaris* in the NEAS and also suggested the advection of hypoxic waters into the euphotic zone. During this study, the oxygen readings from dissolved oxygen sensor of CTD revealed clear signs of such advection from the oxygen minimum zone (Morrison et al. 1999), known to be intensified at intermediate depths (150-800 m) during winter (Desousa et al. 1999). The surface dissolved oxygen remained <3.6 ml L^{-1} during Feb-09 and increased to > 4 ml L^{-1} during March.

Of particular importance is the higher concentrations of nitrite detected during the month of February in the euphotic zone which exceeded surface concentrations of nitrate as in station O-1. During assimilative uptake of nitrate, blooms of phytoplankton can excrete nitrite and such a feature has been

earlier detected by Naqvi et al (2002), during the northeast monsoon of Feb-1997 in our study area.

The high organic turnover of the active *N miliaris* bloom ecosystems and the abundnace of dissolved organic matter excreted into the sea-water as mucilage is further reflected from C-DOM absorbtion coefficients at 300 nm averaging >1 m^{-1} and slope-ratios values falling close to 1.13±0.51, indicative of high molecular size/colloidal DOM. The C-DOM of heavy *Noctiluca miliaris* bloom waters of the NEAS is further charactersitic of an absorbtion maxima at 337 nm indicative of the mycosporine like amino-acids similar to the red physiotype (Carreto et al. 2005).

The dissolved organic matter from the 'active' phase bloom of Feb-2009 supported a massive inflation of ***'oceanic bacterial counts'*** at the major bloom stations and averaged ~ 7 times higher than the historical dataset of the JGOFS cruises when the bloom forming community used to be dominated by diatoms (Ducklow et al. 2001a, Ramaiah et al. 2005, Garrison et al. 2000). However, the high standard deviations indicated significant variations in total bacterial counts in both the water-column as well as from the intense to the moderate / weak bloom areas. This suggests a bloom specific response as total bacterial counts remained significantly correlated with Chl *a* and also C-DOM absorbtion coefficients, as indicator of the bloom dissolved organic matter. During the declining phase bloom of March-2009, the total bacterial counts drastically declined to ~5 times within a space of 8-10 days, along with sharp decrease in the C-DOM and depletion of nutrients from the upper-ocean. It is

well known that following the blooms of phytoplankton, there is significant release of dissolved organic matter which supports the increase in bacterial counts during the latter phases of the bloom (Cole 1982, Azam et al. 1983). Historical results from the Arabian Sea suggests that following the winter blooms of diatoms the build-up of DOC supports an active 'microbial-loop' pathway wherein, heterotrophic nanoflagellates actively clear bacterial population to sustain the zooplankton/salps biomass during the intermonsoon phases of March (Madhupratap et al. 1996). The counts of bacteria are also highest during this phase as they utilize the residual organic matter of the winter bloom. However, during the declining bloom of March-2011, estimation of the population of heterotrophic nanoflagellates suggests that they remained uncorrelated with the total bacterial counts and also with that of *N miliaris*, and a negative trend is discernible at high concentrations of *N miliaris*.

In comparison to the heterotrophic bacteria, the autotrophic picocyanobacteria increased in population during the latter phases of the bloom under nitrate depleted condition. The picocyanobacterial population consisted almost entirely of the phycoerythrin containing *Synechoccus* spp. as free-living or in several colonial forms. In comparison to the *Prochlorococcus* spp. which pefers oligotrophic conditions and deeper depths at the base of the euphotic zone, the distribution of *Synechococcus* sp. has been known to be more restricted to the upper sun-lit and comparatively nutrient rich ecosystems (Zwirglmaier et al. 2008). Their importance to the bloom ecosystem in this study may be asserted from the fact as the productivity of the <20μm fraction

~47.9% to the total surface primary-productivity of the system during March 2009.

The inflation in total bacterial counts and bacterial production rates as noted in this study clearly suggests an actively growing flora which is specific to *Noctiluca* and hence their identity needs to be further deciphered in order to study their relationship with these unique seasonally appearing tropical open-ocean blooms of the Arabian Sea.

2.4 Salient results

Winter blooms in the northeastern Arabian Sea (NEAS) were tracked using Indian satellite IRS-P4 (OCM and OCM-II) during four oceanographic cruises from 2009-2011. *In situ* observations of the euphotic zone from a total of 36 CTD stations showed occurence of the dinoflagellate *Noctiluca miliaris* (green variant) as high-biomass bloom at 18 open-ocean sites (19 – 22°N; 64 - 69°E) in the NEAS and also at depths of one coastal site off Gujrat during March 2011, with considerable variations in intensity. MODIS-Aqua (4km and 9 km resolution) derived Chl *a* showed that the progression of bloom during the winter monsoon could be broadly divided into the **'active' phase of February and the 'declining' phases of March**. This was supported by *in situ* estimates of Chl *a*, *N miliaris* concentrations and visual observations of the bloom during the cruises. During February 2009 average Chl *a* estimated at both surface and water-column was as high as 5.33±10.96 mg m^{-3} and 43.5±28.23 mg m^{-2}. During consecutive cruise of March 2009, the bloom declined rapidly as average Chl *a* dropped to 0.55±0.30 mg m^{-3} at surface and 11.88 ± 3.88 mg m^{-3} in the water-column. This was reflected as the decrease in *N miliaris* cell concentration from 1644.67±3897.55 cells L^{-1} at the surface and 346.93± 683.49x10^4 cells m^{-2} in the euphotic column during Feb-09, to 26.2±0.32.8 cells L^{-1} at the surface and 86.1±58.27x10^4 cells m^{-2} during Mar-09 in the euphotic column. During Mar-10, bloom was detected at the single location and reflected similar intensity to that during Mar-09. During declining bloom phases of March-2011 high concentrations of cells were detected at

major bloom areas at depths below 20 m, however average Chl *a* still remained lower than Feb-09 indicating the receeding phase of bloom. In comparison, Chl *a* at all non-bloom off-shore stations remained <0.5 mg m^{-3}.

The **'active' bloom phase of Feb-2009** was under influence of northeasterly winds (6.53±1.8 m sec^{-1}), cooler sea-surface temperature (24.96±0.49°C), low dissolved oxygen and a nutrient rich deeper mixed layer (71.67 ± 24.5 m). The major active bloom stations O-1, F09-2, F09-4 were found to be associated with cold-core eddies, wherein advection of low-oxygen waters from the anoxic depths into the euphotic zone were observed. The dissolved oxygen at the surface averaged 134.9±5.81µM during this period. The surface nutrient concentrations during this period averaged 0.88±0.5µM of Nitrate-N, 0.68±0.32 µM of Nitrite-N, 1.64±1.77 µM of Phosphate-P and 15.09±4.35µM of Silicate-Si. The high organic turnover of the bloom during active phase was reflected from photosynthetic carbon fixation rates averaging 751.7±776.8 mgC m^{-3} at the surface to 4.1±4.46 mgC m^{-2} in the euphotic column. The C-DOM absorbtion coefficient (300nm) supported the observations of high mucilaginous character of the bloom patches with Ac300 values increasing to 1.10±0.57 m^{-1} in comparison to 0.3616 m^{-1} at the non-bloom off-shore site. The C-DOM produced by *N miliaris* active bloom was characterized by a sharp peak at 337 nm, indicative of the mycosporine like amino acids. The active bloom organic matter supported inflation in oceanic bacterial counts as high as 19.3x10^{9} cells L^{-1} at the surface and averaged11.73±7.55 x10^{13} cells m^{-2} in the euphotic column. The high counts

were accompanied by high bacterial production rates of 6.38±7.75 mgC m^{-3} H^{-1} at the surface to 83.3±39.9 mgC m^{-2} H^{-1} in the euphotic column. Principle component analysis based on correlations showed that total bacterial counts remained significantly correlated ($p<0.05$) with chlorophyll *a*, *N miliaris* counts, C-DOM in terms of the absorbtion coefficient at 300 nm, photosyntehtically fixed carbon and dissolved inorganic phosphate.

The **'declining' bloom phase of March (2009-2011)** was accompanied by withdrawal of the Northeast monsoon, increase in sea-surface temperature (25.15 – 26.07°C) and shallowing of average mixed layer (35.16 – 38m) with depletion of nutrients and increase in dissolved oxygen in comparison to the active bloom phase. The dissolved oxygen at the surface averaged as 192.97±37.52 µM during March 2009, 217.54 µM during March 2010 and 198.78±8.49µM during March 2011. The average surface nutrient concentrations during this declining bloom period varied from 0.03 - 0.26 µM of Nitrate-N, 0.04 – 0.07 µM of Nitrite-N, 0.49 – 1.02 µM Phosphate-P and 0.78 – 2.45 µM of Silicate-Si. The average rates of photosynthetic carbon-fixation varied from 193.62 – 703.83 mgC m^{-3} H^{-1} at the surface to 2.28 – 9.08 mgC m^{-2} H^{-1} in the euphotic column. C-DOM absorbtion coefficients at 300 nm decreased ~2 times from active phase and varied from 0.41 – 0.65 m^{-1}. Total bacterial counts at the surface decreased significantly from 5.71 ± 6.93x10^9 cells L^{-1} in Feb-2009 to 1.66 ± 1.26 x10^9 cells L^{-1} during consecutive cruise of Mar-2009, 1.35 x10^9 cells L^{-1} during Mar-2010 and 2.87±0.54 during Mar-2011. The rates of bacterial production also decreased almost ~2 -4 fold

and average bacterial production rates varied from 1.32 - 3.91 mgC m^{-3} H^{-1} at the surface to 45.4 – 89.3 mgC m^{-2} hr^{-1} in the euphotic column. With the concentration of nutrients (nitrate, nitrite and phosphate) depleted in the upper-ocean rise in picocyanobacterial population was observed and they were dominated by phycoerythrin containing *Synechococcus* sp. Average counts of autotrophic picoplanktons increased from: 4.57±2.42 cells L^{-1} at the surface to 19.06±12.19 cells m-^{2} in the water column during February 2009 to 32.57 – 35.52 cells L^{-1} at the surface to 3.54 – 8.54 cells m^{-2} in the euphotic column. Their importance to the system is further indicated from an average 47.9% contribution to the total surface carbon fixation rates by the <20μm plankton size fractions during declining bloom of Mar-2009.

Principle component analysis based on correlations showed that total bacterial counts remained were more strongly correlated ($p<0.05$) with chlorophyll *a*, *N miliaris* counts, C-DOM in terms of the absorbtion coefficient at 300 nm, photosyntehtically fixed carbon and dissolved inorganic phosphate during the active phase of bloom, whereas their relationships remained insignificant during the declining phases. Estimates of heterotrophic Nanoflagellates during March-2011 by epifluorescent microscopy remained uncorrelated with total-bacterial counts and showed negative relationships with *N miliaris* population.

Chapter III

Microbial Ecology of

Trichodesmium erythraeum bloom

The cyanobacteria *Trichodesmium* spp. is of global significance owing to their efficiency in fixing atmospheric nitrogen (Capone et al. 1997, Parab and Matondkar 2012). *Trichodesmium* blooms appear seasonally in the tropical Eastern and Southern Arabian Sea basin during oligotrophic conditions of late March, extending till May (Devassy 1987, Matondkar et al. 2006). Decomposition of the bloom biomass leads to nutrient regeneration, indicating the strong involvement of water column microbes (Devassy et al. 1979). Although bacterial colonization and association with *Trichodesmium* blooms have been previously recognized in other oceans (Sellner 1992, Sheridan et al. 2002, Renaud et al. 2005), data from the Arabian Sea is not available. The lack of bacteriological studies led us to enumerate bloom associated bacteria and study their relationship with chromophoric dissolved organic matter (C-DOM).

Spectral characteristics of C-DOM, the dynamic pool of photo-reactive dissolved organics (Nelson and Siegel 2002) can reveal distinct differences in the C-DOM nature (Carder et al. 1989), and the nature can further indicate a different C-DOM source, as algal (Romera-Castillo et al. 2010; Steinberg et al. 2004), microbial (Nelson et al. 2004; Ogawa et al. 2001), or photochemical (Miller and Moran 1997). This makes it useful as a potential biogeochemical marker (Helms et al. 2008). The biogeochemically responsive Arabian Sea basin thus provided an important environment to explore the distribution of bacteria and C-DOM and understand their relationships from the bloom and non-bloom areas of *Trichodesmium* respectively.

3.1 Materials and Methods

3.1.1 Study Site and Cruise track

Study of the spring intermonsoon bloom was carried out during the cruise *Sagar Manjusha* (Sama-06) from 1st – 8th April 2008 in the Eastern Arabian Sea (mid- West coast of India). As shown in the bathymetric features of the below cruise track, three transects monitored were off Bhatkal, Goa and Ratnagiri from coastal, continental shelf and continental slope waters (Fig. 3.1).

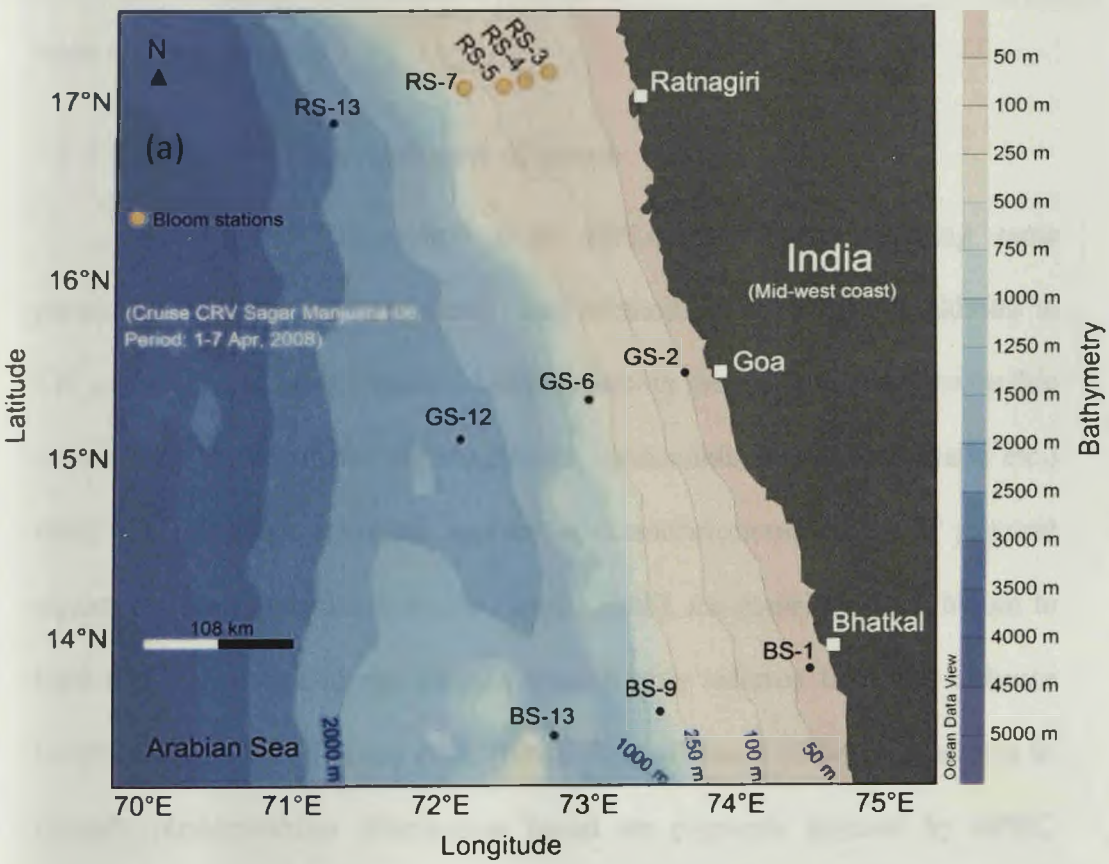

Fig. 3.1 Sampling locations during cruise CRV *Sagar Manjusha*-06 for study of *Trichodesmium* spp. bloom along west coast of India.

3.1.2 Collection of bloom

Water samples were collected from fixed depths between surface – 100 m. The procedure for collection of bloom/water samples was as described earlier in Materials and Methods, section 2.1.

3.1.3 Bloom and Non-bloom sampling stations

Bloom and non-bloom sampling stations were differentiated based on *in situ* Chlorophyll *a* and microscopic counts of *Trichodesmium* filaments. Cloud cover during this period over the study area prevented availability of remotely sensed Chl *a*. Further, other parameters from satellite such as photosynthetic avaialable radiation in the visible electromagnetic spectrum were also unavailable.

3.1.3.1 Chlorophyll *a* as indicator of bloom

Analysis of Chlorophyll *a* by HPLC was followed using same procedure as described in Materials and Methods, section 2.1. In addition to Chl *a*, other signature pigments of phytoplankton groups (such as Fucoxanthin for diatoms, Peridinin for dinoflagellates, Zeaxanthin for Cyanobacteria etc.) were run alongwith standards enabled a chemotaxonomic study of pigment signatures. During cruise *Sama-06* (April, 2008), the contribution of bloom to total Chl *a* at major bloom stations were further inferred from the software CHEMTAX V1.95 (Mackey et al. 1996). The software CHEMTAX enables to identify phytoplankton distribution based on pigments derived by HPLC analysis and expressed as proportions of signature pigments in algae with respect to total Chl *a*. This enables detection of bloom in a study area.

3.1.3.2 Concentration of *Trichodesmium*

Concentration of *Trichodesmium* were determined by microscopy as described earlier (Section 2.1, Materials and Methods) and counts expressed as Trichomes per Liter.

3.1.4 Physical Characterisitics

3.1.4.1 Wind-speed

Wind-speed data was obtained as earlier described for the northern Arabian Sea cruises (Materials and Methods, section 2.1).

3.1.4.2 Sea-surface temperature

CTD data remained unavialable for this cruise. The sea-surface temperature during the cruise period was obtained from the MODIS-Aqua ~4km satellite which is based on micro-wave and infrared imaging method.

3.1.5 Chemical characterisitics

3.1.5.1 Dissolved Oxygen

Dissolved oxygen was measured as described earlier (Materials and Methods, section 2.1) using the winkler's titration method. End-point was detected using starch as the indicator with a Dosimat titrator routinely used for ship-board analysis.

3.1.5.2 Dissolved inorganic nutrients

Dissolved inorganic nutrients (Nitrate-N, Nitrite-N, Phosphate-P and Silicate-Si) were estimated spectrophotometrically as described earlier (Materials and Methods, section 2.1).

3.1.6 Chromophoric dissolved organic matter (C-DOM)

Analysis for C-DOM was carried out from major bloom and non-bloom areas and detailed in (Materials and Methods, section 2.1).

3.1.7 Evaluation of Bacterial distribution

Epifluorescent microscopic analysis to estimate total bacterial counts were performed as detailed in (Materials and Methods, section 2.1). The DNA stain Acridine orange (0.01% w/v) was used instead of DAPI (Hobbie et al.1977). Images obtained were enlarged to detect frequency of dividing cells instead of enriching with the antibiotic Nalidixic acid (Hagstrom et al. 1979).

3.1.8 Data analysis

Correlation and regression analysis was performed using Microsoft Excel 2003 to study relationship and their significance among bloom, bacteria, C-DOM concentration and C-DOM slope charactersitics as indication of their nature.

3.2 Results

3.2.1 Distribution of bloom

Water samples collected off Ratnagiri (RS) shelf harbored visible saw-dust slicks of algal bloom at stations RS-7, RS-5, RS-4 and RS-3 (Fig. 3.1 and 3.2). The highest surface biomass of phytoplankton in terms of Chl *a* occurred in these bloom waters and varied from 107.49 mg m^{-3} at RS-3 to 0.56 mg m-3 at RS-7 (Table 3.1). Microscopic observations showed characteristic "puffs and tufts" arrangement, conforming to the description of cyanobacteria *Trichodesmium spp.* At these stations, *Trichodesmium* spp. comprised upto 99.9% of the phytoplankton population.

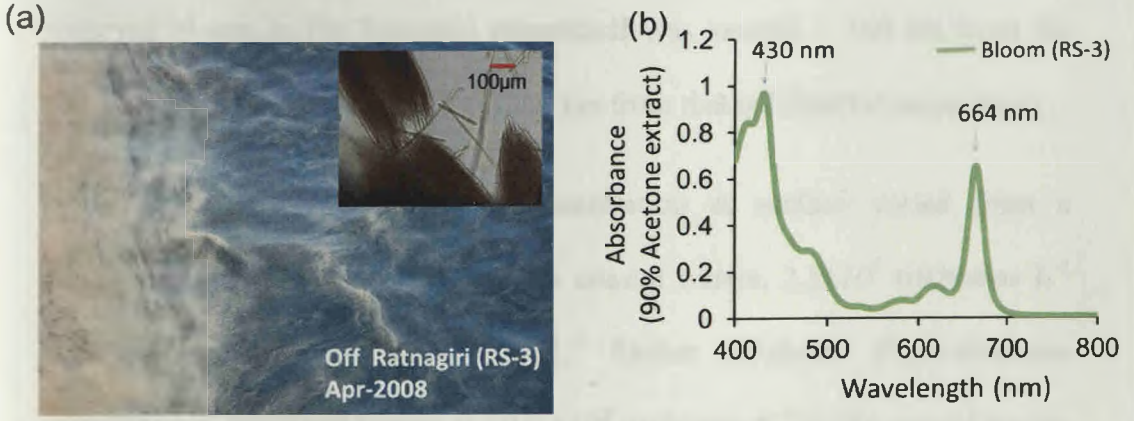

Fig. 3.2 *Trichodesmium erythreaum* bloom: (a) Saw-dust slicks off Ratnagiri (EAS) (inset) *Trichodesmium erythreaum* colonies, (b) Chlorophyll *a* absorbtion of 90% acetone-water bloom extracts.

Both *Trichodesmium erythraeum* and *Trichodesmium thieabautii* were observed in surface waters at all stations in the Ratnagiri transect except at RS-3, where *Trichodesmium erythraeum* was only present. *Trichodesmium* spp. concentrations varied from as high as 3.05 x 10^6 trichomes L^{-1} at station RS-3 and decreased to 3.24 x 10^2 trichomes L^{-1} at 50m depth of RS-5 (Table 3.1).

Surface phytoplankton biomass, in terms of Chl*a*, decreased from 107.49 mg m^{-3} at RS-3 to 0.56 mg m^{-3} at RS-7, as the bloom gradually weakened on moving towards the open-ocean area (Table 3.1). Although, presence of *Trichodesmium* was detected in other stations off Bhatkal (BS-1, BS-9, BS-13), Goa (GS2, GS6, GS12) and in the open-ocean area off Ratnagiri at RS-13, the filament concentrations were much lower (Fig. 3.3). The observed bloom in the Ratnagiri slope/shelf was located ~ 560 km from the non-bloom transect off Goa and ~ 1560 km from that off Bhatkal respectively.

Off Goa, *Trichodesmium* concentration at surface varied from a maximum of 11.4 x10^2 cells L^{-1} in the coastal waters, 2.5x10^2 trichomes L^{-1} and increased to 10.0 x10^2 cells L^{-1} further off-shore. *Trichodesmium* concentration remained lowest as 10.0 x10^2 trichomes L^{-1} in the coastal waters off Bhatkal, but increased to 5.2 x10^2 L^{-1} in the shelf and to 18.80 x10^2 trichomes L^{-1} further off-shore. Distribution of *Trichodesmium* in the water-column reflected the same trend (Table 3.1).

Table 3.1 Quantitation of Phytoplankton biomass indicator (Chl*a*), *Trichodesmium* spp. concentration (TC) and Total Bacterial Counts (TBC) in the Eastern Arabian Sea basin during April 2008

Location	Chl *a*		TC		TBC	
	Surface mgm^{-3}	**Column** mgm^{-2}	**Surface** 10^2 trichomes L^{-1}	**Column** 10^4 trichomes m^{-2}	**Surface** 10^8 cells L^{-1}	**Column** 10^{13} cells m^{-2}
Off Ratnagiri						
*RS-3	107.4	-	30533	-	94.09	-
*RS-4	32.34	-	447.6	-	56.82	-
*RS-5[c]	8.8	121.63	195.2	13.6	59.04	16.1
*RS-7[a]	0.56	7.65	4.0	1.03	6.94	1.11
ΨRS-13[d]	0.55	30.60	15.96	2.83	4.92	3.15
Off Goa						
GS-2[b]	1.10	42.05	11.40	0.80	6.52	1.42
GS-6[c]	0.26	12.7	2.50	0.99	9.86	3.47
ΨGS-12[e]	0.24	25.83	10.0	1.29	4.27	2.13
Off Bhatkal						
BS-1[a]	0.96	5.6	1.0	0.13	13.35	1.38
BS-9[c]	0.30	13.8	5.20	9.4	6.72	3.28
ΨBS-13[d]	0.25	20.48	18.80	2.38	6.38	3.61

Column: [a] 0-10 m and [b] 0-25 m (coastal), [c] 0-50 m (shelf), [d] 0-75 m and [e] 0-100 m (open-ocean)

* *Trichodesmium spp.* bloom area

Ψ Open-ocean stations

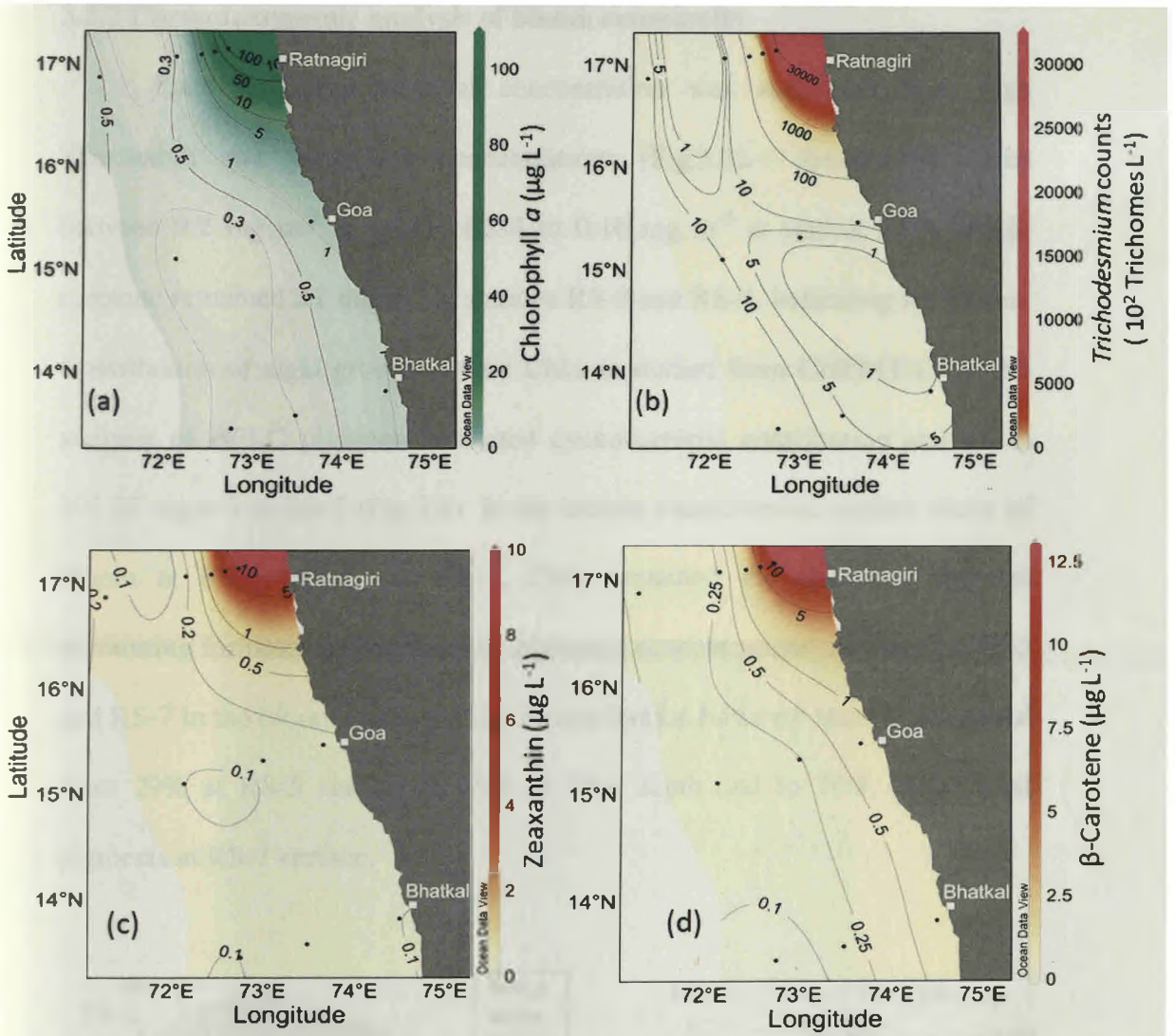

Fig. 3.3 Bloom of cyanobacteria *Trichodesmium* spp. along mid-west coast of India is indicated from distribution of: (a) Chlorophyll *a* (b) *Trichodesmium* spp. counts (c) Zeaxanthin and (d) *β*-carotene.

3.2.2 Chemotaxonomic analysis of bloom community

The high cyanobacterial concentration was supported from high Zeaxanthin and β-carotene concentrations (Fig.3.3). Zeaxanthin varied between 9.2 mg m^{-3} at station RS-3 to 0.16 mg m^{-3} at station RS-7 and β-carotene remained >1 mg m^{-3} at stations RS-3 and RS-4, indicating the bloom. Contribution of algal groups to total Chl*a* as studied from CHEMTAX V1.95 analysis of HPLC pigments indicated cyanobacterial contribution as high as 101.97 mgm-3 at RS-3 (Fig.3.4). In the intense charactersitic surface slicks of bloom at RS-5, RS-4 and RS-3, Chl*a* remained the dominant pigment accounting for upto 76% of the total pigments concentrations. At stations RS-5 and RS-7 in the bloom areas, the Chl *b* contribution however steadily increased from 29% at RS-5 surface to 75% at 25m depth and to 76% of the total pigments at RS-7 surface.

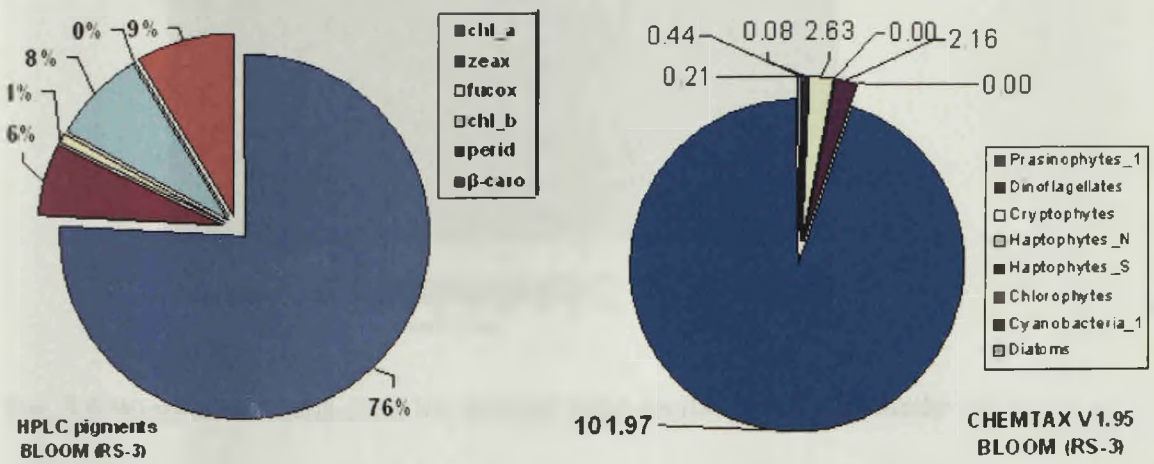

Fig. 3.4 Contribution of algal groups to total Chl*a* as studied from CHEMTAX V1.95 analysis of HPLC pigments.

3.2.3 Physico-chemical environment of bloom

3.2.3.1 Wind-speed

Wind-speed varied between 4-12 m sec^{-1} in the eastern Arabian Sea. *In situ* wind-speed remained lowest off Ratnagiri shelf (~4-6 $msec^{-1}$), where the aggregation of slicks near ship were observed. Quick Scat V4 wind-vectors during the first week of April, suggested North-westerly winds in the Eastern Arabian Sea (Fig. 3.5).

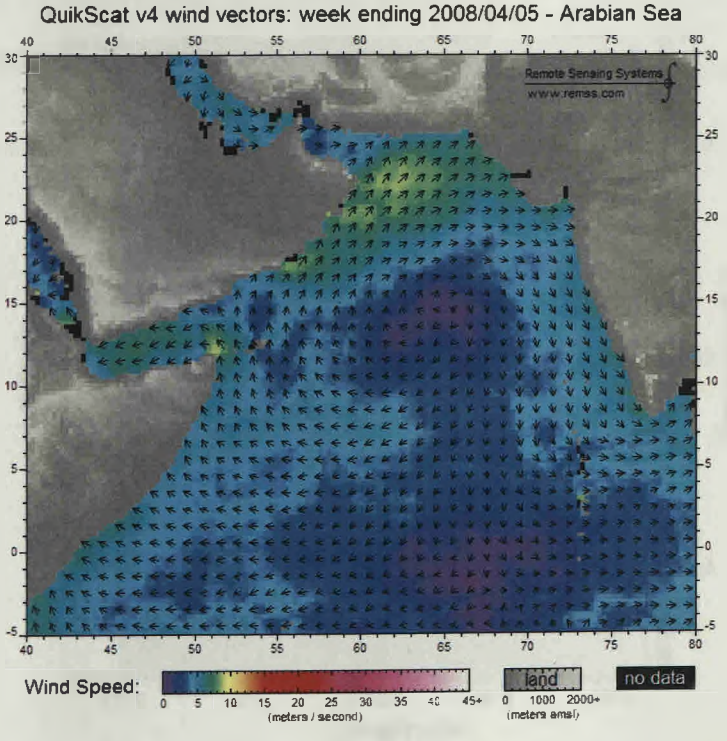

Fig. 3.5 Wind-speed Quik-Scat V4 derived wind-vectors during the study period.

3.2.3.2 Sea-surface temperature

Sea-surface temperature (SST) conditions measured by satellite (Fig. 3.6) for the first week of April shows decrease in SST on moving off-shore. In comparison to the open-waters off Bhatkal (BS-13) where SST remained relatively high (>29°C) and had the highest concentration of *Trichodesmium* in off-shore waters among all the three transects, off-shore locations of Goa and Bhatkal showed SST varying between 28.5 – 29°C for the first week of April. In the coastal waters however, temperature recorded was highest off Goa (29.5 – 30.01°C).

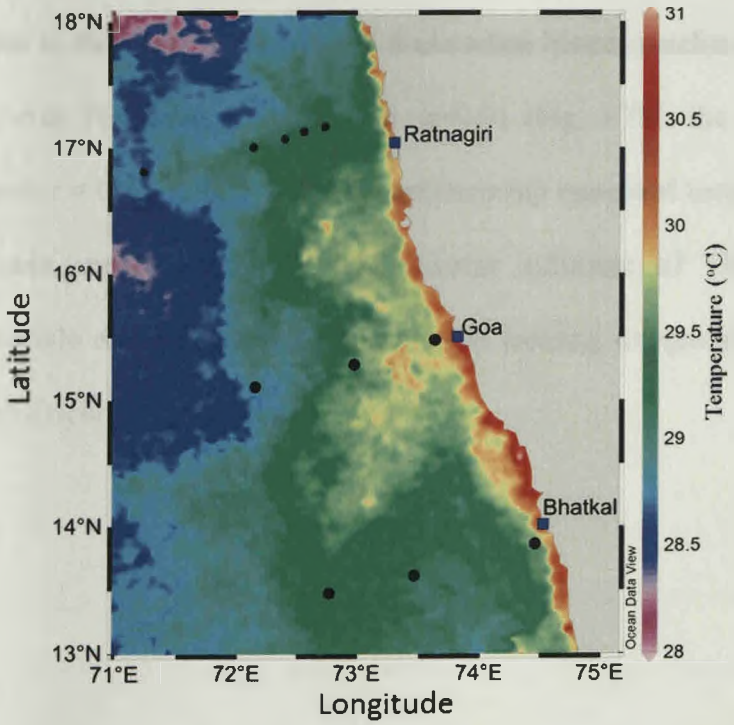

Fig. 3.6 Sea-surface temperature for the study period (1st -7th April 2008) measured from MODIS-Aqua (4micron, day time) sea-surface temperature.

3.2.3.3 Dissolved Oxygen

The distribution of dissolved oxygen with reference to the *Trichodesmium* bloom and non-bloom water types showed marked variations. The surface DO increased from coastal to further offshore in open-ocean areas (Fig. 3.7a) and varied between 201.4 - 123.4 µM in the *Trichodesmium* bloom to 195.42 - 110.43 µM in the non-bloom areas respectively. Off Goa, the highest recorded DO was 248.92 µM in the shelf at GS6 (25m) while it decreased to 80.16 µM (100m) at station GS12.

A significantly strong negative correlation of both TBC and Chl*a* with DO was seen in the areas harboring *Trichodesmium* bloom patches. While the correlation with TBC was r = 0.81, n=8, p=0.01 (Fig. 3.7b), the correlation with Chl*a* was r = 0.83, n=8, p=0.01. The relationship remained insignificant in the non-bloom areas respectively. The inverse influence of TBC on DO suggests possible role of bacterial respiration in creating oxygen poor micro-zones within *Trichoesmium* colonies.

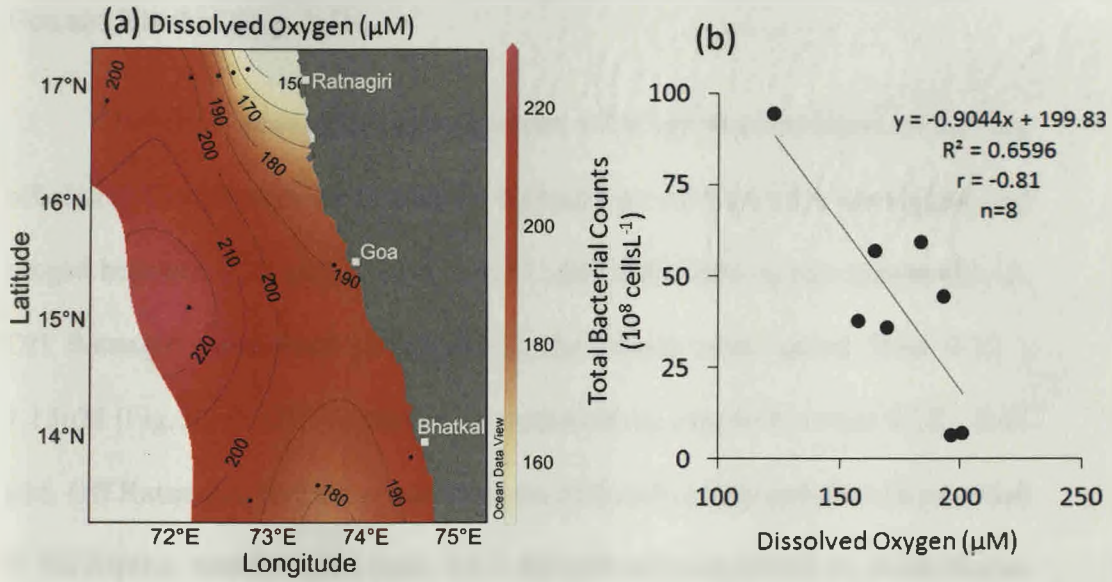

Fig. 3.7 Distribution of (a) dissolved oxygen and (b) relationship of bacteria with dissolved oxygen in the bloom.

3.2.3.4 Dissolved Inorganic nutrients

The distribution of inorganic nitrate revealed prevailing oligotrophic conditions in the study area. The surface nitrate concentrations remained mostly depleted (Fig.3.7a), and varied from remaining undetected at BS-1 off Bhatkal to 0.3µM off Ratnagiri. Nitrate concentrations significantly increased at the depths in the off-shore sites off Goa and Ratnagiri. At station RS-13, Nitrate at depths of 50-75 m ranged 1.25 - 2.7 µM which further increased to 4.7µM off Goa (Fig. 3.8). The comparative distribution of Nitrate with that of *Trichodesmium* concentration in the water-column reflected an inverse

relationship (Fig. 3.8). Dissolved inorganic nitrite remained mostly undetected at the surface, and ranged between 0.15 – 0.39μM at the off-shore locations off Goa and Bhatkal (Fig. 3.7b).

Dissolved phosphate concentrations at the surface decreased on moving off-shore. Concentrations of dissolved phosphate off Goa were the highest and ranged between 2.26 μM at GS-6 – 0.41 μM in the open-ocean station GS-12. Off Ratnagiri, dissolved phosphate in the bloom area varied from 0.22 - 1.13μM (Fig.3.7c). Off Bhatkal the concentrations ranged between 0.15 – 0.47 μM. Off Ratnagiri, highest concentrations of dissolved phosphate was recorded at the depths, which varied from 3.5 – 4.9 μM between 25-50 m in the bloom stations at RS-5. Comparatively off Goa and Bhatkal, dissolved phosphate remained as low as 0.36 – 0.82 μM and 0.17 – 0.56 μM, respectively.

Dissolved silicate was highest at the off-shore stations off Goa, Bhatkal and Ratnagiri and decreased on moving towards shelf to coastal stations. Surface Silicate ranged from 5.96μM off Ratnagiri (RS-13) to 4.12 μM (off GS-12) (Fig.3.7d). Highest concentrations of water-column silicate was detected off Goa (off-shore station GS-12) at depths of 50-100m and ranged from 3.56 – 11.72 μM (Fig. 3.8). Dissolved silicate at similar depths were low off Bhatkal (1.1 – 1.7μm) and off Ratnagiri (1.13 – 1.74 μM). This was reflected in a higher concentration of Fucoxanthin (indicating presence of diatoms) at depths enriched in nitrate and silicate (Fig. 3.8).

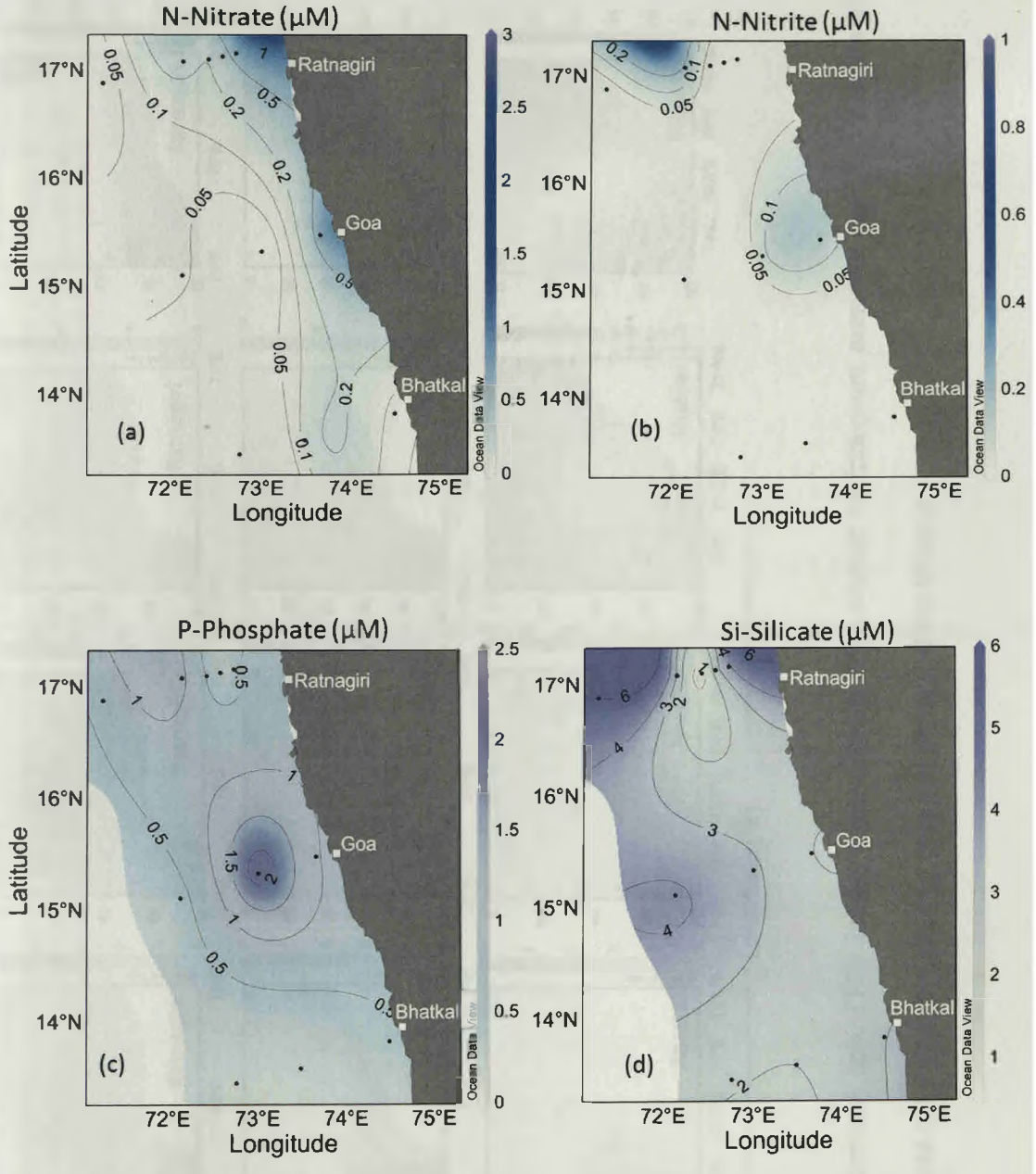

Fig. 3.7 Surface distribution of inorganic nutrients: (a) N-Nitrate, (b) N-Nitrite (c) P-Phosphate and (d) Si-Silicate in the study area.

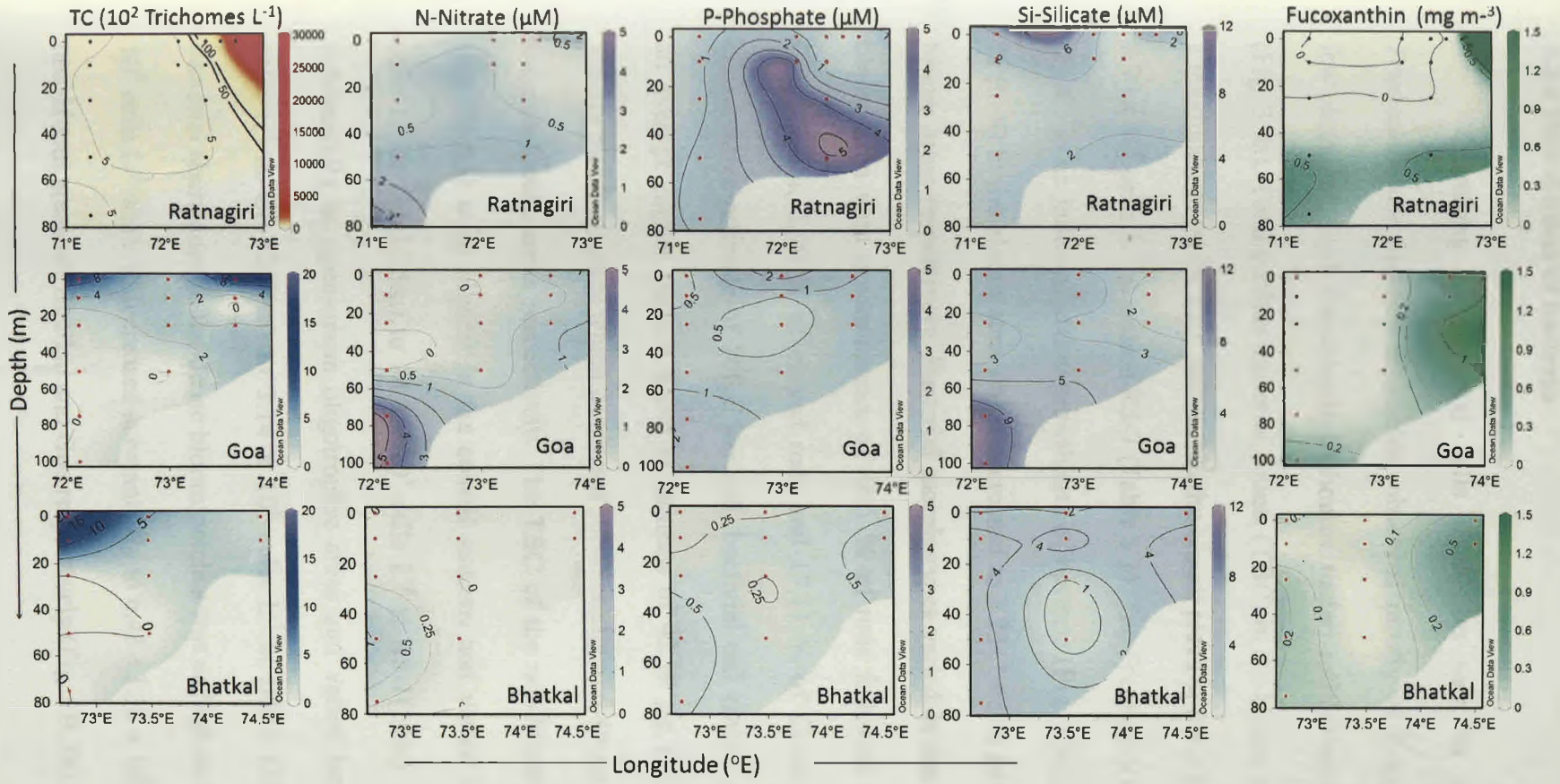

Fig. 3.8 Distribution of *Trichodesmium* spp. (TC) in the water-column with respect to inorganic nutrients and Fucoxanthin as indicator of diatoms in the study area off Ratnagiri (bloom), Goa and Bhatkal (Non-bloom).

3.2.4 Distribution of bacteria

Clustering of bacterial cells could be seen in micro-zones of *Trichodesmium* filament fragments, observed mostly as living (stained) and few damaged/dead (unstained) trichomes under eplifluorescent microscope (Fig. 3.9a). Total surface bacterial counts (TBC) in the bloom area varied from a maximum of 94.09 x10^8 cells L^{-1} in the bloom patch at RS-3 to a minimum of 6.94 x 10^8 cells L^{-1} at station RS-7 (Table 3.1). The Frequency of dividing cells (FDC) as an index of active growth rate of bacteria (Fig. 3.9c), was 8.33±1.83 % (n=8) in the bloom area which decreased to 3.23±1.48 % (n=29) in the non-bloom areas respectively. Bacterial morphotypes varied in the *Trichodesmium* bloom area with predominance of 48.5 % of rods followed by 31.54 % of Coccobacilli, 2.99 % of curved rods and 17.11 % of Cocci. Considering a conservative estimate of 10fgC per cell, bacterial cell counts corresponded to an average higher surface bacterial biomass of 42.59 µg C L^{-1}(n=8) in the intense bloom patches which decreased substantially to 6.49 µg C L^{-1} (n=29) in the non-bloom areas respectively. The TBC of the non-bloom areas off Goa and Bhatkal were highest in the coastal stations and varied between 12x10^8 cells L^{-1} at GS-2(25m) to 14.3 x 10^8 cells L^{-1} at BS-1(10m). TBC decreased substantially in open-ocean oligotrophic areas and varied between 1.34x10^8 cells L^{-1} at GS-12(50m) to 3.14 x 10^8 cells L^{-1} at BS13 (75m). The mean bacterial abundance in the dense bloom patches was as high as 54.59 ± 21.61 x 10^8 cells L^{-1} while it decreased substantially to 6.48 ±3.30 x 10^8 cells L^{-1} in the non-bloom areas off Bhatkal and Goa respectively (Fig. 3B.7b).

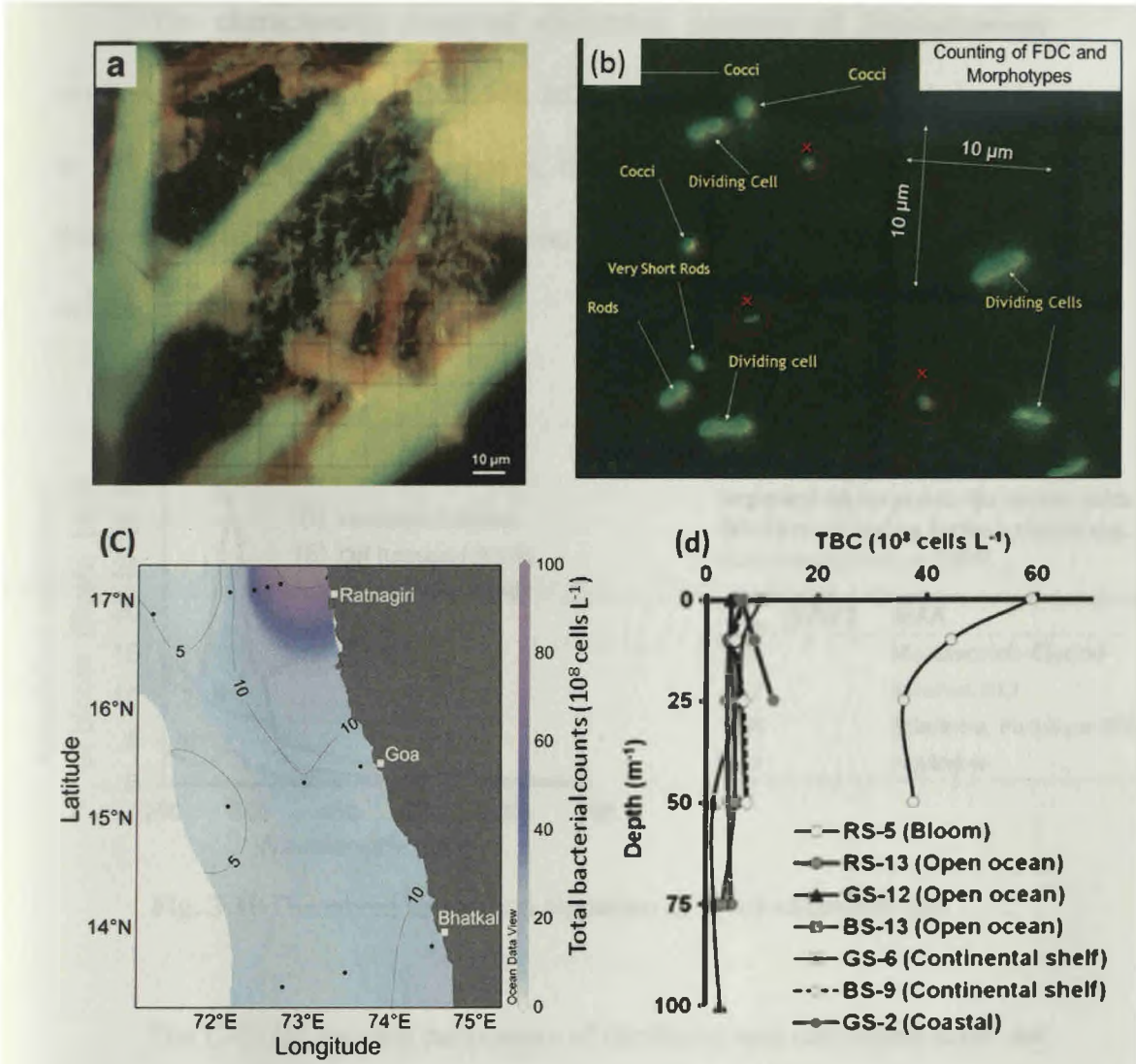

Fig. 3.9 Acridine orange stained photomicrographs showing: (a) Clustering of bacterial cells around *Trichodesmium erythraeum* trichomes; (b) Dividing cells and morphotypes; (c) distribution of total bacteria (TBC) during bloom of *T erythraeum* off Ratnagiri; and (d) TBC profiles of bloom and non-bloom stations.

3.2.5 C-DOM characersitics

The characersitic dissolved absorbtion signature of *Trichodesmium erythraeum* is seen below (Fig. 3.10). Intact colonies of RS-3 showed shoulder at 365 nm. On vortexing the colonies, the twin absorbtion features indicating the presence of Mycosporine-like amino acids at 330 nm and 365 nm became evident.

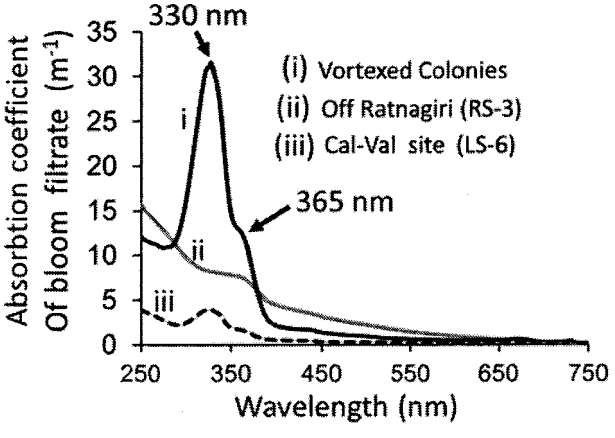

Reported Mycosporine like amino acids (MAA) produced by *Trichodesmium* spp. *(Subramaniam et al. 1999)*

λ_{max} (HPLC)	MAA
310	Mycosporine-Glycine
332	Asterina-332
334	Shinorine, Porphyra-334
360	Palythene

Fig. 3.10 Dissolved absorbtion signature of *Trichodesmium* spp.

The C-DOM spectral parameters of the bloom and non-bloom areas are summarized in Table 3.2. C-DOM concentration averaged as high as 2.2789 ± 3.02 m^{-1} in the *Trichodesmium* bloom to as low as 0.28 ± 0.07 m^{-1} in the non-bloom waters respectively. The bloom was characterized by a significantly low mean $Ac_{250:365}$ ratio of 5.54 ± 3.57 and S_{Ratio} of 2.05 ± 1.4. In comparison, the non-bloom area was characterized by $Ac_{250:365}$ ratio of 20.17 ± 13.75 and S_{ratio} of 4.09 ± 2.05. As both these parameters inversely relate to C-DOM molecular size, it indicates a predominance of higher molecular size C-DOM present in

the bloom. The S_{Ratio} decrease in the bloom was due to an overall decrease in the mean $S_{275-295}$ slope to 0.0156 ± 0.0041 nm^{-1} in the bloom from 0.03 ± 0.004 nm^{-1} in the non-bloom area, since the average $S_{350-400}$ remained relatively constant at 0.0099 nm^{-1} in both the bloom and non-bloom areas respectively. Interestingly, in the most intense *Trichodesmium* bloom area (RS-3 and RS-4), the $S_{275-295}$ was shallower than $S_{350-400}$ which is a characteristic feature of terrestrially dominated estuarine C-DOM. As the averaged $Ac_{465:665}$ ratio decreased significantly from 4.46 ± 0.9 in the *Trichodesmium* bloom to 1.68 ± 0.9 in the non-bloom area, the more refractile nature of C-DOM present in the non-bloom waters were reflected. The mean $S_{250-350\ nm}$ C-DOM spectral slope varied from 0.0138 nm^{-1} (± .0037, n=6) in the *Trichodesmium* bloom area to 0.0255 nm^{-1} (± 0.0027, n=9) in the non-bloom area respectively. The 300-700 nm spectral slopes averaged 0.0168± 0.0155 nm^{-1} in the bloom to 0.0385± 0.0556 in the non-bloom waters.

3.2.6 Bloom C-DOM-bacterial relationships

The relationship between TBC and Chl*a* in the *Trichodesmium* bloom area was significant as R^2 = 0.6599, n=8, p=0.01; whereas, in the non-bloom areas the relationship remained as insignificant as R^2=0.1751, n=29, p=0.02 (Fig. 3.11c). The strong relationship indicates bloom specific flow of carbon and energy to lower trophic levels ie. bacteria. Correlations between C-DOM absorbtion coefficients and Chl*a* varied from R^2=0.9831 (n=6, p<0.0001) in the bloom to R^2=0.9831 (n=9, p=0.51) in the non-bloom area (Fig. 3.11c,f). Similar strong relationship (r = 0.9150, p<0.0001) between Ac_{325} and TBC

indicated a significant increase in TBC as C-DOM concentration and insignificant in the non-bloom area (r=-0.2806, p=0.46, n=9) (Fig. 3.11b, e).

An overall inverse relationship of TBC with the C-DOM molecular size indicators - S_{ratio} increased in the bloom (Fig.3.11g). TBC and Ac_{443} relationship also showed strong correlations in the bloom area (r=0.9066, p=0.01, n=6), which was however negative and $Ac_{250:365,}$ was seen in both the bloom and non-bloom areas. The overall correlation between TBC and S_{ratio} was r=0.5354, p=0.03, n=15. Similar relationships were obtained between TBC and $Ac_{250:365}$ ratio of r =0.5362, p=0.04, n=15 which became more insignificant as r=0.207, p=0.592, n=9 in the non-bloom area respectively (Fig. 3.11g). Further, a strong overall positive correlation of r = 0.8417, p<.001, n=15 were noted between $Ac_{465:665}$ ratios, as a proxy for C-DOM aromaticity and TBC (Fig. 3.11h).

Table 3.2 Comparative mean C-DOM spectral parameters in *Trichodesmium spp* bloom and non-bloom areas and their relationship with Bacteria.

C-DOM Spectral Parameters	Bloom (n=6)	Non-Bloom (n=9)	Relationship with TBC		
			Overall	Bloom	Non-Bloom
$S_{350\text{-}400}$ nm^{-1}	0.0099 ± 0.0043	0.0099 ± 0.0056	r =- 0.8951 p < 0.0001	r = - 0.7059 p = 0.11	r = - 0.02 p=0.95
$S_{275\text{-}295}$ nm^{-1}	0.0156 ± 0.0041	0.03 ± 0.004	r =-0.8492 p <0.0001	r = - 0.4041 p=0.43	r = - 0.0831 p = 0.83
S_{Ratio}	2.0539 ± 1.4091	4.09 ± 2.05	r =-0.5354 p=0.03	r = - 0.4187 p=0.41	r = - 0.2274 p = 0.56
$S_{250\text{-}350}$ nm^{-1}	0.0138 ± 0.0037	0.0255 ± 0.0027	r = -0.8948 p < 0.0001	r = -0.7083 p =0.11	r = - 0.0166 p = 0.96
$S_{300\text{-}700}$ nm^{-1}	0.0168± 0.0155	0.0385±0.0556	r = -0.2659 p = 0.34	r = - 0.4087 p = 0.42	r = -0.1475 p = 0.70
Ac250:365 (E2:E3)	5.54 ± 3.57	20.17 ± 13.75	r =-0.5362 p=0.04	r = - 0.5306 p = 0.278	r = - 0.207 p = 0.592
Ac465:665 (E4:E6)	4.46 ± 0.9	1.68 ± 0.9	r = 0.8412 p<0.0001	r = 0.2279 p = 0.66	r = -0.4986 p= 0.17
Ac325 m^{-1}	2.2789 ± 3.02	0.28 ± 0.07	r = 0.7965 p < 0.001	r = 0.9150 p=0.01	r = 0.3239 p = 0.39
Ac443 m^{-1}	0.9094 ± 1.26	0.78 ± 0.02	r = 0.8034 p<0.0001	r = 0.9066 p = 0.01	r = -0.280 p =0.46

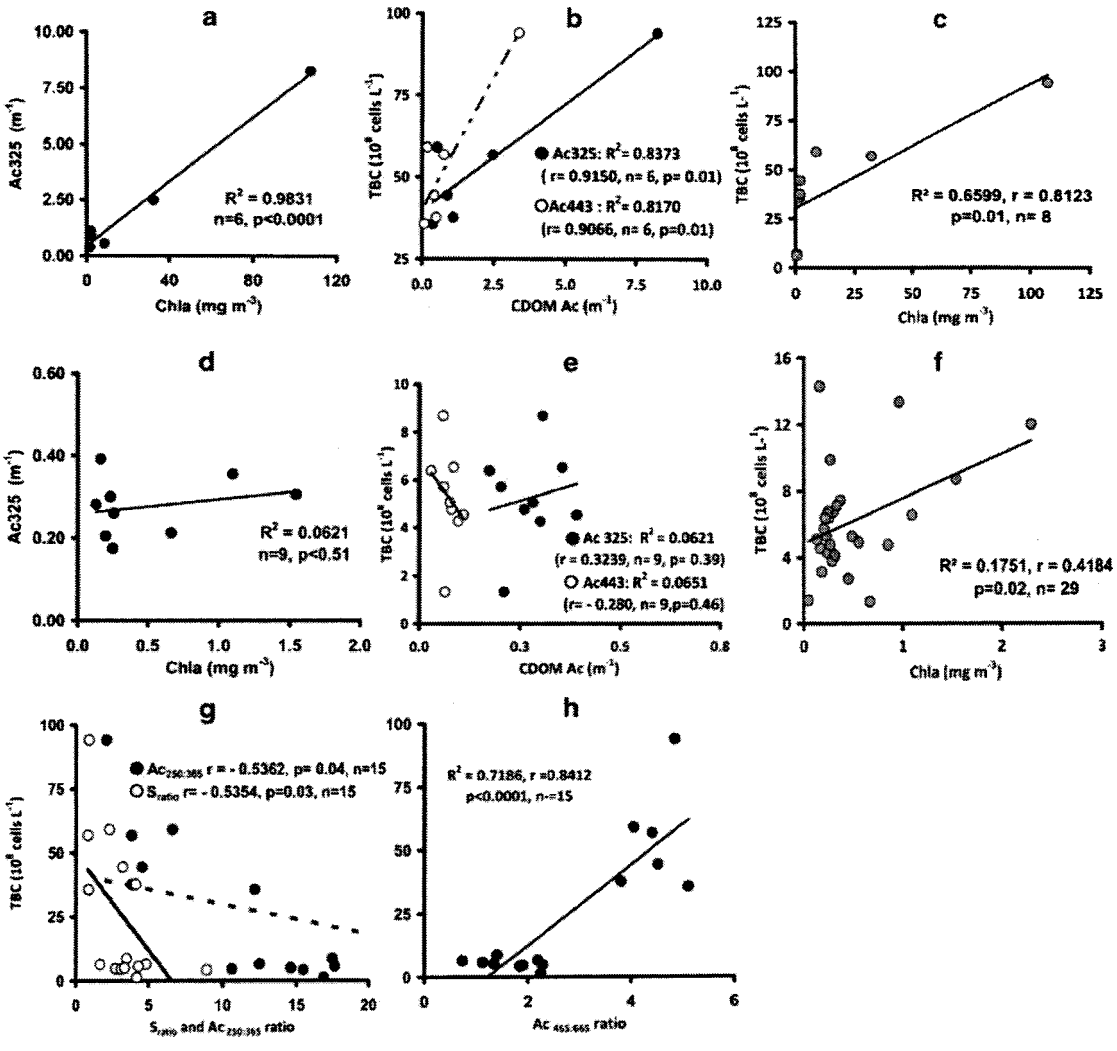

Fig. 3.11 Comparative relationship of Chl*a*, C-DOM concentration (Ac_{325}) and Total bacterial counts (TBC) in the *Trichodesmium spp* bloom and non-bloom areas respectively: (a) Ac325 and Chl*a* (Bloom) (b) TBC with Ac_{325} and Ac_{443} (bloom) (c) TBC and Chl*a* (bloom) (d) Ac_{325} and Chl*a* (non-Bloom) (e) TBC and C-DOM concentration (non-bloom) (f) TBC and Chl*a* (non-bloom). Overall relationship of TBC with (g) C-DOM molecular size indicators (S_{ratio} and $Ac_{250:365}$) and (h) $Ac_{465:665}$ ratio.

3.3 Discussion

A study of C-DOM – bacterial interactions from the *Trichodesmium* bloom was necessary, as they tend to be seasonally more predictable in the Arabian Sea.

Study of C-DOM-bacterial dynamics as a potential biogeochemical marker can be advantageous in detecting possible water quality changes, albeit imperceptible at times, but significant for the marine environment. As recent trends of intensifying coastal anoxia (Naqvi et al. 2000), increasing productivity (Goes et al. 2005) and unusual algal blooms (Gomes et al. 2008) are raising concern about the response of the Arabian Sea to climatic and eutrophication effects, such monitoring of C-DOM-bacterial relationships may provide valuable understanding of her biogeochemistry.

Results of interrelationship between bloom, C-DOM and bacteria showed a strong dependence of: (a) C-DOM concentration on Chl*a* (R^2=0.9831, $p < 0.01$) implying C-DOM production almost entirely from the bloom (Fig. 3a); (b) bacteria on C-DOM (R^2 = 0.8373, p=0.01) implying significant increase in bacterial counts in response to higher C-DOM concentrations (Fig 3b) and (c) bacteria on Chl*a* (R2 = 0.6599, p=0.01) implying a bloom-specific increase in bacterial counts (Fig. 3c). An anticipated decrease in C-DOM concentration in response to active bacterial utilization is not reflected in these results. This possibly is because an active bloom continues to be a constant source of C-DOM. However, the significantly higher biomass of bacteria in the bloom strongly suggests the role of C-DOM in

supporting it (b). It may be further argued, such a possibility of actual decrease in C-DOM concentration following active bacterial utilization would exist, but only when the rate of newly produced C-DOM from an active bloom (source) decreases as the bloom declines (Zhang et al., 2009). In such cases, the correlation of Chl*a* (aging/post bloom) with C-DOM concentration will be weak, unlike in our study. Higher C-DOM concentrations during these post-bloom periods will not mean a higher Chl*a*. If bacterial consumption still predominates during these post-bloom stages, C-DOM uptake may be reflected as a negative relationship with TBC; but not always, as other possible sources of C-DOM, such as extracellular products of microbial hydrolysis or even viral lysis of bacteria (Balch et al. 2002, Nelson et al. 2004, Ogawa et al. 2001, Miller and Moran 1997) may be important during these stages.

The nature of C-DOM produced by *Trichodesmium* bloom at RS-3 and RS-4 was characterized by $S_{350\text{-}400} > S_{275\text{-}295}$ and an absorbtion peak (λ_{max}, 360 nm) of the mycosporine-like amino acid palythene (Subramaniam et al. 1999). The shallower slopes of the spectral regions $S_{275\text{-}295}$, $S_{250\text{-}350}$ and $S_{300\text{-}700}$ in the bloom (Table 3), reflected a possible increase in absorption by colloidal dissolved organics >1KD (Simeon et al. 2003, Chin et al. 1994). In comparison, C-DOM quality was a mix of low molecular - higher aromatic compounds with steeper slopes, from the larger area covering non-bloom locations in the Eastern Arabian Sea. C-DOM nature supporting lower bacterial counts in these areas were possibly of a more refractile/semi-refractile nature. Such intermediate pools of C-DOM in the water column can be

climatologically important sinks of photo-oxidization to CO (Zuo and Jones 1995) or export to the deep (Druffel et al. 1992), as they evade bacterial degradation.

Reported bacterial count of 94.09 $x10^8$ cells L^{-1} from the intense *Trichodesmium* bloom patch at RS-3 (Table 1) was much higher in comparison to that reported from New Caledonia, Bay of St Marie (Renaud et al. 2005). Significantly low bacterial counts of $9.3x10^6$ cells ml^{-1} were recorded in this area during blooms of *Trichodesmium spp.* In contrast, bacterial counts averaged as high as 8.2 x 10^{11} cells ml^{-1} per *Trichodesmium* colony in the Sargasso Sea (Sheridan et al. 2004). Such heterogeneity in bacterial distribution associated with *Trichodesmium* reflects the influence of geographic habitat and conditions. A comparison of TBC in the bloom and non-bloom areas in the present study, further revealed a ~ 19-fold decline of TBC at non-bloom RS-13, located only ~ 120 km offshore from the intense bloom at RS-3 (Fig 2b). Influence of bacteria in reducing dissolved oxygen in the *Trichodesmium* bloom area was seen from our results (Fig 5b). Higher respiration rates by these bacteria perhaps create such oxygen poor zones and may actually benefit *Trichodesmium spp* to fix nitrogen. Although any hypoxic conditions developing at depths were not detected, the surface dissolved oxygen of the entire study area mostly remained lower than 200z μM and interestingly decreased on moving from the coastal to the open-ocean stations (Fig 5a). Bacterial mineralization of the decaying bloom and dissolved organic matter is likely to leave the system finally enriched in nitrate at depths

(Devassy 1987). In this context, the study of Naqvi et al. (2000) provides insight. As sub-oxic waters shoal into the Western Indian shelf and coasts during upwelling, vigorous denitrification occurs. Appearance of intense *Trichodesmium* blooms just prior to the monsoonal upwelling (late March-May) has therefore important implications. Production of more bio-refractile C-DOM, through a combination of bacterial and photochemical processing of bloom exudates (Brophy and Carlson 1989, Ogawa et al. 2001), could also be important in naturally mitigating such processes. However, no available datasets to quantify such effects are available and requires exhaustive post-bloom observations.

The C-N flux can split through multiple pathways, involving unknown intermediates in the marine environment (Druffel et al. 1992, Chin et al. 1998). Flow of carbon from algal blooms via C-DOM ↔ bacterial interactions, is an important step in this direction. In summary, our study contributes new and valuable information on bacterial distribution, C-DOM characteristics and C-DOM - bacterial relationship during a seasonal *Trichodesmium spp* bloom in the Eastern Arabian Sea. While bacterial utilization of *Trichodesmium spp* bloom generated C-DOM is indicated, occurrence of relative bio-refractile C-DOM was detected in non-bloom waters during this period. Studies monitoring C-DOM-bacterial dynamics during post-bloom conditions will be important to strengthen above observations.

3.4 Salient results

Blooms of the cyanobacteria *Trichodesmium erythraeum* were detected off Ratnagiri shelf and coastal waters during the spring-intermonsoon cruise of April 2008 on search for algal blooms from 11 stations, located in the coastal, shelf and open-ocean/slope areas off Ratnagiri (16°59'N, 73°17'E), Goa (15°30'N, 73°48'E) and Bhatkal (13°58'N, 74°33'E) coasts respectively. Distinctively visible bloom of "saw-dust" color in the Ratnagiri shelf showed dominant presence of cyanobacteria *Trichodesmium erythraeum* with trichome concentrations remained as high as 3.05×10^6 trichomes L^{-1}. The highest surface biomass of phytoplankton in terms of Chl *a* occurred in these bloom waters and varied from 107.49 – 0.56 mg m^{-3}. Although, presence of *Trichodesmium erythraeum* as well as *T thieabautii* were detected in other stations off Bhatkal, Goa and in the open-ocean area off Ratnagiri, the filament concentrations were much lower. Microscopic examination of bloom and HPLC based signature pigments of phytoplankton analyzed using software CHEMTAX V1.95 indicated cyanobacterial contribution to total Chl *a* as high as 101.97 mgm-3 at RS-3. The surface dissolved oxygen increased from coastal to further offshore in slope areas and varied between 201.4 - 123.4 μM in the *Trichodesmium* bloom to 195.42 - 110.43 μM in the non-bloom areas respectively. Blooms of *Trichodesmium* were associated with complete depletion of nitrate in the surface waters and favored by high average temperature during the period of ~27.5°C. The distribution of Nitrate-N with that of *Trichodesmium* concentration was reflected as an inverse relationship. The surface nitrate

concentrations varied from remaining undetected in coastal waters off Bhatkal to 0.3μM off Ratnagiri. Nitrate concentrations significantly increased at the depths in the off-shore sites and varied from 2.7 μM off Ratnagiri which further increased to 4.7μM off Goa. Nitrite-N remained mostly undetected at the surface, and ranged between 0.15 – 0.39μM at the off-shore locations off Goa and Bhatkal. Highest concentration of dissolved phosphate was recorded at the depths, which varied from 3.5 – 4.9 μM between 25-50 m in the bloom area off Ratnagiri. At the surface Phosphate concentrations remained highest in coastal waters off Goa (2.26 μM). Dissolved silicate was highest at the off-shore stations off Goa, Bhatkal and Ratnagiri and decreased on moving towards shelf to coastal stations. Surface Silicate at off-shore sites ranged from 5.96μM off Ratnagiri to 4.12 μM off Goa. This was reflected in a higher concentration of Fucoxanthin (indicating presence of diatoms) at depths enriched in nitrate and silicate. Total bacterial counts (TBC) varied between 94.09 x 10^8 cells L^{-1} in the bloom to 1.34 x 10^8 cells L^{-1} in the non-bloom area. C-DOM concentrations averaged 2.27± 3.02 m^{-1} in the bloom to 0.28 ± 0.07 m^{-1} in the non-bloom waters respectively. The C-DOM of *Trichodesmium erythraeum* were characterized by peaks of mycosporine like amino acids at 365 nm. The C-DOM composition varied from a higher molecular size in the bloom to lower molecular size and increased aromaticity in the non-bloom areas respectively. Strong positive relationship of TBC with Chlorophyll *a* (R^2=0.65, $p<0.01$) and C-DOM concentrations (R^2=0.8373, p=0.01) in the bloom area indicated hydrolysis and/or uptake of C-DOM by bacteria. The

results demonstrated bloom specific flow of Carbon to bacteria via C-DOM from field measurements. Further, absorbtion by mycosporine like amino acid was recorded in the filtrate of the bloom. High bacterial aggregation in inter-colonial spaces of *Trichodesmium erythraeum* was seen as a factor to affect oxygen content of the bloom patches / slicks.

Chapter IV

Phylogenetic characterization of retrieved bacterial flora from the Arabian Sea phytoplankton blooms

The bacterial flora developing with algal-blooms are known to be highly specific in the 'phycosphere', the region immediately surrounding the phytoplankton cells (Sapp et al. 2007, Goecke et al. 2013). It has also noted that some phytoplankton, e.g, the *Trichodesmium* sp. have been difficult to maintain under axenic conditions, implying the importance of associate bacteria (Sellner 1992). Earlier in this study, microscopic estimates have established high bacterial counts during blooms of *Noctiluca miliaris* in the northern Arabian Sea and *Trichodesmium erythraeum* in the eastern Arabian Sea (off Ratnagiri) (Chapter 2 and 3). The present chapter therefore attempts to isolate and study the dominant bacterial flora associated with these bloom forming phytoplankton.

4.1 Materials and Methods

4.1.1 Collection of bloom samples

(a) Bloom of Noctiluca miliaris

N miliaris bloom samples were collected from an overlapping bloom station (station O-1) during two consecutive ship-cruises of Feb-Mar 2009 (Chapter 2, Fig. 2.1). At station O-1, *Noctiluca* counts decreased from 9600 cells L^{-1} on 17th Feb-09 to 80 cells L^{-1} on 2nd Mar 09, within a span of 13 days and represented the '*active*' and the '*declining*' phase of the bloom. 1-2 L of surface bloom water collected using Niskin water sampler were pre-screened on a 100 µm nytex mesh to retain the thick biomass and transferred to sterile 50 ml conical centrifuge tubes (Tarsons, India) for isolating associated bacteria. Non-bloom surface water samples below 19°N at stations M09-1 and M09-10 (Chapter 2, Fig. 2.1) were also collected for obtaining comparative culturable bacterial load.

(b) Bloom of Trichodesmium erythraeum

"Saw-dust" patches of *Trichodesmium erythreaum* bloom observed off Ratnagiri (stations RS-5, RS-4 and RS-3) during cruise Sagar Manjusha-06 of April -2008 were collected using plankton-net from surface waters. Buoyant filaments of *Trichodesmium erythreaum* were pre-screened through a 20 µm Nytex mesh followed by filtration on sterile 0.22 µm Nuclepore filters with a gentle vacuum to collect the *Trichodesmium* filaments. The <20µm bloom filtrates were also collected at station RS-3 for isolation of free-living bacteria.

4.1.2 Enumeration and retrieval of bacterial flora

(a) Bloom of Noctiluca miliaris (green)

Triplicate sub-samples of *N miliaris* bloom were serially diluted in filtered-sterilized (0.22 μm nuclepore) sea-water prepared from the bloom itself and plated on: (a) Zobell's marine agar 2216E (ZB) (b) 1/10 strength ZB (ZB1/10) and (c) Sea-water agar (SWA). Plates were incubated at 25°C (average temperature of bloom area) for 72-120 hours. Incubations were prolonged upto two weeks to retrieve any slow growing types. 70 well isolated colonies (34 isolates from 'active' and 36 isolates from 'declining' bloom phase) were randomly selected from the 10^{-5} dilution to represent the dominant growing bacteria at St-O1. All 'active' phase isolates were coded with the prefix '^{GU}*SK256*' for active phase and '^{GU}*SS263*' for 'declining' phase bloom.

(b) Bloom of Trichodesmium erythraeum

Trichodesmium filaments collected on 0.22 μm filters were further suspended in sterile 3.5% NaCl solution and triplicate dilutions were plated separately on 2216E Zobell's full strength and Zobell's 1/10 strength media. For the filament-free bloom filtrates, 0.1 ml were plated separately on 2216E Zobell's full strength and Zobell's 1/10 strength media. 29 well isolated colonies (21 as filament associated and 6 as free-living/phycospheric) were randomly selected from the 10^{-5} dilution to represent the dominant growing bacteria.

Morphotypes of all retreived isolates were recorded and further purified by streaking for further characterization.

4.1.3 Phenotypic and biochemical characterization

Morphological and biochemical studies of all the isolates were carried out following standard protocols (Gerhardt et al. 1981).Gram staining was performed by both traditional and the KOH method (Buck 1982).

Scanning electron microscopy

The morphology of potentially new strain from *N miliaris* bloom was examined using scanning electron microscopy Cellular dimensions of the bacterial isolates growing at 20% (w/v) NaCl were recorded using scanning electron microscopy (JEOL-5800LVSEM). A thin smear of a culture suspension (A600= 0.8) was made on square cover slips, air dried, fixed in 2% (v/v) of glutaraldehyde, overnight at room temperature. Smear was subjected to 10 minutes each of an increasing gradient of acetone: water solution (30%, 50%, 70%, 90% and 100% (v/v) respectively followed by air drying. The coverslips were mounted onto aluminium stubs which were in turn fixed on a sputter coater (SPI module specimen holder) for coating the cells with a 10-15 nm gold film before visualization.

Key phenotypic characters of endospore staining, catalase, oxidase, anaerobic growth in thioglycollate broth, Nitrate reduction and motility were examined as described previously (Smibert and Krieg 1994). Tests for citrate utilization, lysine decarboxylase, Ornithine decarboxylase, phenylalanine deaminase, urease and H_2S production were determined using KB-002 biochemical-kit of Himedia Lab Pvt Ltd., India. Acid from the

carbohydrates D-glucose, D-adonitol, D-lactose, D-arabinose, L-arabinose, D-Sorbitol, D-maltose, D-fructose, D-galactose, D-raffinose, D-trehalose, D-melibiose, D-sucrose, D-mannose, inulin, sodium gluconate, D-salicin, D-dulcitol, D-glycerol, D-inositol, D-sorbitol, D-mannitol, D-arabitol, D-erythritol, α-methyl-d-glucoside, D-rhamnose, D-cellobiose, D-xylitol and D-sorbose were determined using KB-009 kit of Himedia labs Pvt Ltd. India following manufacturer's instructions.

The ability of isolates to produce extracellular enzymes amylase, protease, lipase, cellulase and phosphatase were determined by spotting cultures on prepared plates of starch agar, casein agar, tributyrin agar, CMC (carboxymethyl cellulose) agar and Pikovskaya's media (Smibert and Krieg 1994), respectively. All plates were incubated at 25°C. Zones of amylase and protease were observed by flooding starch plates with iodine solution and casein plates with 3% tricarboxylic acid. Cellulose degradation were checked after a week's incubation by flooding plates with 1% Congo-red for 15 mins and then destaining the agar with 1.5M NaCl solution. Lipase and phosphatase activity could be determined by visible zones of clearance against turbid background of media. Liquefaction of gelatin stabs at 4°C indicated gelatinase activity (Smibert and Krieg 1994).

Utilization of carbohydrates and amino-acids by isolates retreived from *N miliaris* bloom were further determined by suitably modifying a micro-titre well plate method incorporating the respiratory dye tetrazolium chloride (TTC) as indicator. 150μl of a mineral salts basal media (MSM)

was dispensed into the micro-titre wells and filter-sterilized (sterile 0.2 micron hydrophilic HDPE syringe filters) stocks of carbohydrates (D-glucose, D-fructose, D-ribose, D-mannose, D-xylose, D-maltose and D-sucrose), carboxylic acids (succinate, citrate), and complex organics (starch, casein, tween-80 and carboxy methyl cellulose) were added at 0.5% v/v final concentrations to the basal medium. For studying utilization of amino-acids as sole source of carbon and Nitrogen, the NH_4Cl was excluded from basal media and 2mM amino-acids (L-alanine, L-methionine, L-leucine, L-isoleucine, L-threonine, L-lysine, L-tryptophan, L-serine, L-phenylalanine, L-histidine) were added to each well. Micro-titre plates were inoculated with 2% culture suspension in 1% sterile saline with an OD of 0.8-0.9 at 600 nm. All micro-titre plates were incubated for 36 hours and 20μl of 1% TTC dye (Hi-media, India) were added to each well and incubation continued overnight. Positive wells showed pinkish-red color against negative control wells without any added substrates. Positive controls of the same tests using 5ml volume of broth were run randomly to verify the results using standard protocol (Smibert and Krieg 1994). Denitrifying potential among the isolates were screened on a Giltay-Nitrite (GN) medium (Matsuzaka et al. 2003). Isolates were inoculated in GN broth and left shaking at 220 rpm and 25°C to provide adequate aeration. The change in color of GN broth from blue to green with gas collected in Durham's tubes indicated denitrifying potential among the isolates. Growth was also

checked using 0.2% Acetamide as sole carbon and nitrogen source on Verstraete and Alexander broth (VA) (Matsuzaka et al. 2003).

Resistance of isolates to 18 different antibiotics were checked by spreading a growing suspension of each culture on Mueller-Hinton agar plates (Himedia-India) with 3.5 % w/v NaCl over which antibiotic discs (Ampicillin – 10mcg; Ciprofloxacin – 5 mcg; Chloramphenicol – 30 mcg; Clindamycin – 2 mcg; Erythromycin – 15mcg; Furazolidone – 50 mcg; Gentamycin – 10 mcg; Kanamycin – 30 mcg; Methicillin – 30 mcg; Norfloxacin – 10 mcg; Novobiocin – 5 mcg; Neomycin – 30 mcg; Nalidixic acid - 30 mcg; Oxytetratcycline – 30 mcg; Polymyxin B – 30 mcg; Streptomycin - 300 mcg; Tetracycline – 30 mcg and Penicillin-G – 50U) manufactured by Hi media Labs, India were placed. Appearance of zones of inhibition were recorded after 36-48 hours of incubation at 25°C and referred using the Kirby-Bauer susceptibility chart to determine resistance.

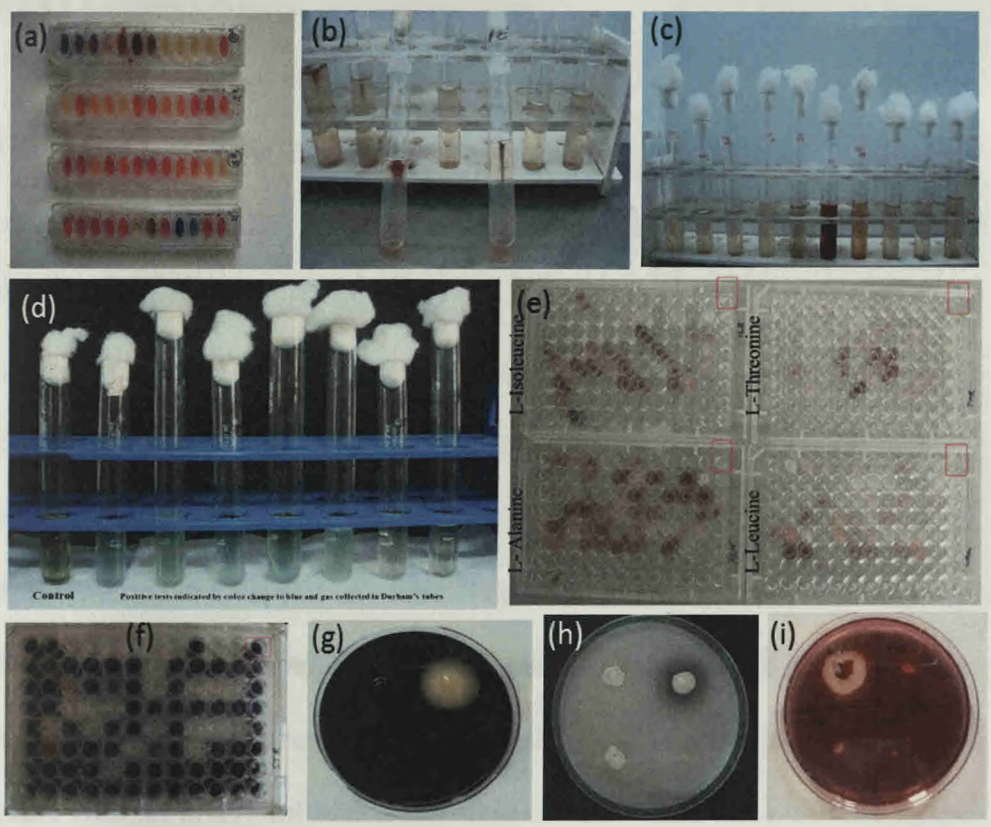

Plate 4.1 Phenotypic, biochemical/metabolic characterization of bloom associated bacterial cultures: (a) Use of KB002 and KB009 test kits Hi media (India) Pvt Ltd kits; (b) Motility tests; (b) Nitrate reduction test; (c) Denitrification of Nitrite-giltay's broth; (d) Carbohydrates/amino-acids/complex substrate utilization tests in micro-titre plates using TTC indicator; (f) utilization of starch; and plate assays demosntrating zones on (g) Starch, (h) Casein (i) Carboxymethyl cellulose.

4.1.4 Chemotaxonomic characterization

Five bacterial isolates from the *N miliaris* bloom, showing less than 97% 16SrDNA gene homology were selected to study their Fatty-acid methyl esters 'FAME' characteristics and match with the Library (MIDI Sherlock; Library-RTSBA6), using the MIDI protocol (Sasser 2009): Pure cultures were streaked on Zobell's marine agar at 28°C for 24 hours. With a sterile-loop ~80-90 mg cells were gently scraped from plates and mixed with 1 ml of Saponification reagent (NaOH-45g; Methanol-150 ml; Distilled water-150 ml) in a capped test-tube. The tubes are briefly heated for 5 mins in a boiling water bath, vigorously vortexed and again heated for 25 mins in the water bath. Test-tubes were cooled and 2ml of methylating reagent (6N HCL – 325 ml in 275 ml Methanol) were added to each test-tube. The tubes were briefly vortexed and heated for 10 mins at 80°C. Extraction of FAME was done by adding 1.25 ml of Hexane: Methyl-tert butyl ether (1:1) with gentle vortexing for 10 mins and the lower aquous phase was pipetted out and discarded. 3 ml of 0.3M NaOH was finally added to the organic phase, mixed for 5 mins and then 1.5 ml of the organic phase was pipetted into a GC vial for analysis. The FAME extracts were analyzed using a Gas-Chromatograph (Model Agilent 6850), with a silica capillary column. The temperature set –up was adjusted to increase from 170-270°C at 5°C increment per minute and peaks were detected using the FID (Flame Ionization detector). H_2 was used as the carrier gas, Nitrogen was the make-up gas with air to support the flame. The FAME composition was compared

using the Sherlock pattern recognition software (Midi-Sherlock; Library RTSBA6) and peaks were identified with respect to the Sherlock external calibration standard.

4.1.5 Molecular characterization

A single colony of purified cultures was inoculated in Zobell's marine broth 2216E and genomic DNA was extracted from a 24 hour growing culture (OD ~1) using the Gen-Elute bacterial genomic DNA spin extraction kit NA2110 (Sigma-Aldrich) following manufacturer's instructions. Genomic DNA was amplified using the universal bacterial primers 27f (5' AGA GTT TGA TCC TGG CTC AG 3') and 1492R (5 ' ACGGCTACCTTGTTACGACTT 3') (Green et al. 2004). 50µl PCR reaction mixture was prepared with 25 µl of 2X red-dye PCR master-mix (Genei, India), 20 µl PCR-grade water (Genei, India), 10pM each of primer (8f and 1522r) and 10-30 ng of DNA template. The thermocycler (Takara-Japan) was programmed to denaturation at 95 ^{0}C for 3 minutes, 35 cycles at 95 ^{0}C for 1 min, primer annealing at 48 ^{0}C for 1 min and strand extension at 72 ^{0}C for a brief period of 90s. This was followed by a final elongation step at 72 ^{0}C for 5 mins. The amplified DNA was purified using the PCR-purification kit (Genei, India). 16SrDNA amplicons corresponding to ~ 1.5 kb were then bi-directionally sequenced using the Big-dye terminator sequencer method (Applied Biosystems) in Bangalore Genei, India. The

reactions were analyzed through automated sequencer (ABI-3730 DNA analyser) and electropherograms were imported in Chromas-pro, ver 1.5.

Plate 4.2 16SrDNA gene amplicons from genomic DNA of isolates separated on 1.2% agarose. Lane numbers represented by: 4 - ^{GU}SK256-20; 5 - ^{GU}SK256-33; 6 - ^{GU}SK256-5; 7 - ^{GU}SK256-38; 10 - ^{GU}SK256-17; 12 - ^{GU}SK256-30; 13 - ^{GU}SK256-19; 17- ^{GU}SK256-22; 21 - ^{GU}SK256-15; ^{GU}SK256-N4; 23 - ^{GU}SK256-N7; 24 - ^{GU}SK256-N1; 25 - ^{GU}SK256-N8.

4.1.6 16SrDNA gene sequence analysis

Partial sequences (300 - 1000 bp) were obtained for 99 isolates. Among these sequencing of 18 isolates were repeated to obtain near-full-length (≥1300 bp) sequences to ensure procedural reliability and quality-control. All sequence electropherograms were manually curated to remove few extra nucleotides flanking the sequences, checked for their query

coverage (100%) using BLASTn (http://blast.ncbi.nlm.nih.gov) and then uploaded in the Ribosomal Database Project (Cole et al. 2009) for alignment using 'infernal' secondary structure alignment of RDP-10 (http://rdp.cme.msu.edu).

4.1.7 Bacterial identification

The 'naive Bayesian classifier' algorithm of RDP-II (Wang et al., 2007) was used to identify the aligned sequences. To reach the best possible generic/species level taxonomic assignments and select the closest phylotype/s to our sequences, we followed a common frame-work based upon: (a) Isolates referred reliably to 'species' level in cases of > 97 % 16SrDNA gene sequence homology to a 'single nearest described Type strain' in both RDP-II and EZtaxon-e (Kim et al. 2012) database with supporting phenotypic characteristics. (b) At >97% homology, isolates referred to 'genus' level when species level distinction based on 16SrDNA gene and phenotypic characters were unreliable (c) At >97% homology, isolates referred to 'groups' of genus when generic level distinction based on 16SrDNA gene and phenotypic characters were unreliable. (d) Sequences showing <97% match with nearest Type strains referred to as unclassified family/genus level for further characterization.

4.1.8 Phylogenetic and community analysis

A neighbor-joining phylogenetic tree was constructed after multiple-alignment of only partial sequences using Clustal-X and MEGA-5 (Tamura et al. 2011). The Uni-Frac distance metric (Lozupone et al. 2011) web-based test was run to compare whether 16SrDNA gene sequences representing 'active' and 'declining' bloom phases differed significantly. Further, partial sequences of the cultured red *Noctiluca* endocytic bacterial community reported from Helgoland roads, North Sea (Seibold et al. 2001) were also incorporated in the phylogenetic tree to examine phylotype differences with our present study and represented as a UNIFRAC computed principal coordinate analysis (PCoA)-biplot. The diversity of bacterial 'genus' occurring during the bloom phases were compared from the Shannon-wiener diversity index (H′), calculated using Primer-6 (http://www.primer-e.com). Strain level proximity/dissimilarity of isolates showing similar biochemical characteristics were deciphered based on a Non-metric Multidimensional scaling of zone –sizes using NMDS module of XLStat^{2007} (Addinsoft).

Accession number

Sequences submitted to GenBank were assigned accession numbers:

(a) For *Noctiluca miliaris* associated bacterial flora: JX429828-JX429861 (Active bloom) and JX429792 – JX429827 (Declining bloom).

(b) For *Trichodesmium erythreaum* associated bacterial flora: KF495537 – KF495563.

4.2 Results

4.2A Bacterial flora of *Noctiluca miliaris* bloom phases

4.2A.1 Culturable Bacterial load

Cultivable bacterial counts during active and declining phases of *Noctiluca* (green) bloom did not differ significantly (Fig. 4.1). Culturable bacterial load at the overlapping station St-O1 was highest among all other stations during both the active and declining bloom phases. Plate counts at this location during active bloom varied from $6.84x10^5$ CFU ml^{-1} on ZB, $5.21x10^5$CFU ml^{-1} on ZB1/10 and $5.2x10^5$ CFU ml^{-1} on SWA medium. During declining bloom a culturable load of $6.73x10^5$ CFU ml^{-1} obtained on ZB was similar to that of active phase. Plate counts however, slightly increased to $5.51x10^5$ CFU ml^{-1} on ZB1/10 and $5.42x10^5$ CFU ml^{-1} on SWA during the declining phase. Counts at other active bloom waters of Feb-09 (Fig. 1) varied from $4.73x10^4 - 5.1x10^5$ CFU ml^{-1} on ZB, $3.23x10^3 - 5.3x10^5$ CFU ml^{-1} on ZB1/10 and $8.7\ x10^4$ - $3.95x10^5$ - CFU ml^{-1} on SWA. As the bloom declined by Mar-09 plate counts varied from $3.73x10^4 - 6.7x10^5$ CFU ml^{-1}on ZB, $2.96x10^4 - 5x10^5$ CFU ml-1 on ZB1/10 and $3.97x10^4 - 4.9x10^5$ CFU ml^{-1} (Fig. 2a). In comparison, a significantly ~2-3-fold lower culturable count was obtained at the non-bloom locations which ranged $2.1\times10^3 - 1.1\times10^3$ CFU ml^{-1} on ZB, $5.1\times10^3 - 5.8\times10^3$ CFU ml^{-1} ZB1/10 and $5.65\times10^3 - 4.99\times10^2$ CFU ml^{-1} on SWA (Fig. 2a).

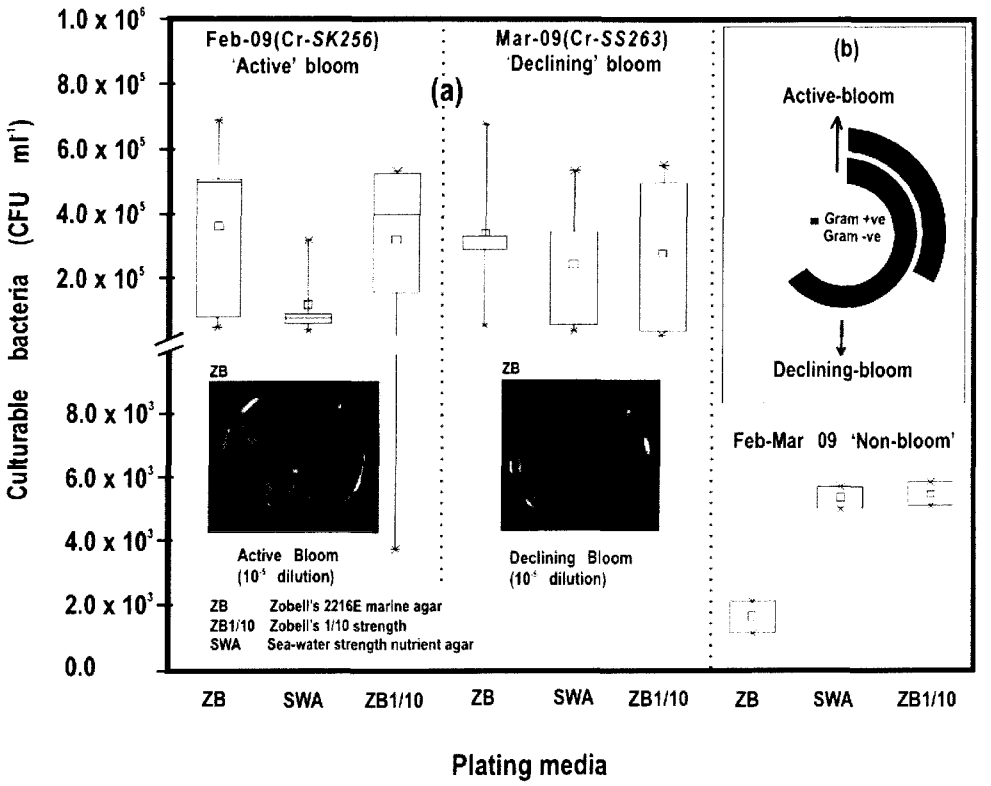

Fig. 4.1 Statistical box (25-75 percentile) and whisker (min-max) plots shows response of open-ocean bacteria to *Noctiluca* (green) bloom of NAS in Feb-Mar 2009: (a) Plate counts of active and declining bloom against 'non-bloom' waters; (inset) plate images of flora at St-O1 on ZB and SWA (b) Shift in percent gram-character of flora.

4.2A.2 Description of flora: active and declining phase

Of the total 70 bacterial isolates retreived, several were pigmented, which increased from 25% in the active bloom to 38.7% in the declining bloom. Pigmentation varied from yellow (SK256-34; SK256-15; SK256-28;

SK256-35; SK256-37; SK256-N8; SS263-17), pink (SK256-5), orange (SK256-17; SS263-26; SS263-4; SS263-2; SS263-9; SS263-14; SS263-28; SS263-29; SS263-30; SS2363-33), brick-red (SS263-19); reddish-pink (SS263-23) to cream (SK256-8; SK256-12; SK256-16; SK256-29; SS263-5; SS263-10; SS263-12; SS263-24;SS263-31) and the rest were white.

4.2A.3 Phenotypic and Biochemical charactersitics

While the dominant isolates during the active phase were Gram-positive (70.59%), Gram-negative forms (61.11%) increased in the declining phase. Majority of these isolates were motile during both the bloom phases (Table 4.1). Key phenotypic charactersitics which showed significant variations from the active to the declining bloom were the endospore producers which decreased from 44.12% during the active bloom to 19.44% during the declining bloom. While the majority of isolates expressed catalase (100-97.2%), 50% of isolates during active bloom and 47.22% during the declining bloom could also grow in anaerobic conditions, indicating their facultative nature. A significantly high fraction could also reduce nitrate, which varied from 73.33% during the active phase to 83.33% during th Belonging to these nitrate reducing groups, 50% isolates during the active phase also demonstrated denitrifying ability under aerobic conditions which decreased to 47.22% during the declining bloom (Table 4.3).

Table 4.1 Phenotypic and biochemical / metabolic charactersitics of bacterial flora from **'active'** phase bloom of *Noctiluca miliaris*: [Mph- Morphology; Gram- gram character Mot – Motility; Ang – Anaerobic growth in thioglycollate; End-endospores; Oxi – Oxidase, LDC – Lysine decarboxylase, ODC- Ornithine decarboxylase, H_2S –Desulfurase, NR – Nitrate reductase, DNR – Nitrite reductase (Denitrifier), Ure – Urease, Phs – phosphatase, Amy – Amylase, Cell – Cellulase, Prot – Protease, Gel- Gelatinase, Lip – Lipase]. Tentative identity of genera assigned from Bergey's manual of determinative bacteriology are indicated as: *Psd - Pseduomonas*; *Prv-Providencia; Hal -Halomonas; Mic - Microbacterium; Mcr - Micrococcus; Stp-Staphylococcus; Vrg-Virgibacillus; Bac-Bacillus.*

Isolate code	Colony Color	Mph	Gram	End	Mot	AnG	Cat	Oxi	LDC	ODC	H_2S	NR	DNR	Ure	Phs	Amy	Cell	Prot	Gel	Lip	Genera
GU SK256-25A	Orange	Rods	-	-	+	±	+	+	-	-	-	+	+	-	+	-	-	+	-	-	*Psd*
GU SK256-N3	White	Rods	-	-	+	±	+	-	-	-	-	+	+	-	+	-	-	-	-	+	*Psd*
GU SK256-N5	White	Rods	-	-	+	±	+	-	+	+	-	+	+	+	+	+	+	-	+	+	*Psd*
GU SK256-N7	White	Rods	-	-	+	±	+	-	+	+	-	+	+	+	+	-	-	-	-	+	*Psd*
GU SK256-N6	White	Rods	-	-	+	±	+	+	-	-	-	+	+	-	-	-	-	-	-	+	*Psd*
GU SK256-N2	White	Rods	-	-	+	±	+	-	-	+	-	+	+	-	+	-	-	+	-	+	*Psd*
GU SK256-N1	White	Rods	-	-	+	±	+	-	-	+	-	+	+	+	+	-	-	-	-	+	*Psd*
GU SK256-33	Orange	Rods	-	-	+	±	+	+	+	+	+	+	+	+	-	+	-	-	-	+	*Psd*
GU SK256-16A	White	Rods	-	-	+	±	+	-	-	+	-	+	-	-	-	-	-	+	-	+	*Psd*
GU SK256-29	Cream	Rods	-	-	+	±	+	+	-	+	+	-	-	+	+	+	-	-	-	+	*Hal*
GU SK256-N4	Yellow	Rods	+	-	-	+	+	-	-	+	+	+	-	+	+	+	-	-	-	-	
GU SK256-N8	White	Rods	+	-	+	-	+	-	-	-	+	-	-	-	+	+	-	-	+	-	*Mic*
GU SK256-37	Yellow	Cocci	+	-	-	±	+	+	-	-	-	-	-	+	+	+	-	-	+	+	*Mic*
GU SK256-35	Yellow	Cocci	+	-	-	±	+	+	-	-	-	+	-	+	+	+	-	-	+	+	
GU SK256-28	Yellow	Rods	+	-	-	±	+	-	-	-	-	+	+	+	+	+	-	-	+	+	
GU SK256-15	Yellow	Rods	+	-	-	±	+	+	-	-	-	-	-	-	-	+	-	+	+	-	

± Weak positive

Table 4.1 Continued (Phenotypic characteristics and enzyme expressions by bacterial flora from **'active'** phase bloom)

Isolate code	Colony Color	Mph	Gram	End	Mot	AnG	Cat	Oxi	LDC	ODC	H_2S	NR	DNR	Ure	Phs	Amy	Cell	Prot	Gel	Lip	Genera
GU SK256-25B	Orange	Rods	+	-	+	+	+	-	-	-	-	+	-	-	+	+	+	+	+	-	
GU SK256-38	White	Rods	+	-	+	+	+	+	-	-	-	-	-	-	-	+	-	+	+	+	
GU SK256-30	White	Cocci	+	-	-	-	+	-	-	-	-	-	-	+	-	-	-	-	+	+	*Stp*
GU SK256-19	Beige	Rods	+	+	+	+	+	+	-	-	-	+	+	-	-	-	-	+	+	-	*Vrg*
GU SK256-18	Beige	Rods	+	+	+	+	+	+	-	-	-	+	+	-	-	-	-	+	+	-	*Vrg*
GU SK256-21	White	Rods	+	+	+	-	+	+	+	-	-	+	-	-	-	-	-	+	+	+	
GU SK256-20	White	Rods	+	+	+	+	+	-	-	-	-	+	+	-	+	-	+	+	+	+	*Bac*
GU SK256-S7	White	Rods	+	+	+	+	+	+	-	-	-	-	-	-	-	-	-	-	+	-	*Bac*
GU SK256-32	White	Rods	+	+	+	±	+	+	-	-	-	+	+	-	-	+	-	+	+	+	*Bac*
GU SK256-22	White	Rods	+	+	+	+	+	-	-	-	-	-	+	+	-	-	+	+	+	-	*Bac*
GU SK256-5	Pink	Rods	+	+	+	+	+	+	-	-	-	-	-	-	-	+	-	+	+	+	*Bac*
GU SK256-17	White	Rods	+	+	+	+	+	-	-	-	-	+	+	-	+	-	+	+	+	-	*Bac*
GU SK256-16	White	Rods	+	+	+	+	+	-	-	-	-	-	-	-	-	+	-	+	-	-	*Bac*
GU SK256-S9	White	Rods	+	+	+	+	+	-	-	-	-	-	-	+	-	+	-	-	-	-	*Bac*
GU SK256-14	White	Rods	+	+	+	+	+	-	-	-	-	+	+	+	+	-	-	+	+	+	*Bac*
GU SK256-13	White	Rods	+	+	-	+	+	-	-	-	-	+	-	+	+	+	+	+	+	+	*Bac*
GU SK256-12	White	Rods	+	+	+	+	+	-	-	+	-	+	+	+	-	-	+	-	-	-	*Bac*
GU SK256-8	White	Rods	+	+	+	+	+	-	-	-	-	+	+	+	+	+	-	+	+	+	*Bac*

Table 4.2 Phenotypic and biochemical/metabolic charactersitics of bacterial flora from **'declining'** phase bloom of *Noctiluca miliaris*: [Mph- Morphology; Gram- gram character Mot – Motility; Ang – Anaerobic growth in thioglycollate; End-endospores; Oxi – Oxidase, LDC – Lysine decarboxylase, ODC- Ornithine decarboxylase, H_2S –Desulfurase, NR – Nitrate reductase, DNR – Nitrite reductase (Denitrifier), Ure – Urease, Phs – phosphatase, Amy – Amylase, Cell – Cellulase, Prot – Protease, Gel- Gelatinase, Lip – Lipase]. Tentative identity of genera assigned from Bergey's manual of determinative bacteriology is indicated as: Psd - *Pseduomonas*; *Vbr - Vibrio, Hal - Halomonas; Shw - Shewanella; Stp- Staphylococcus; Vrg- Virgibacillus; Bac- Bacillus.*

Isolate code	Colony Color	Mph	Gram	End	Mot	AnG	Cat	Oxi	LDC	ODC	H_2S	NR	DNR	Ure	Phs	Amy	Cell	Prot	Gel	Lip	Genera
^{GU}SS263-38	White	Rods	-	-	+	±	+	+	-	+	+	-	-	+	+	+	-	+	-	+	*Hal*
^{GU}SS263-24	White	Rods	-	-	+	+	+	+	-	-	-	+	-	+	-	+	-	+	-	-	*Hal*
^{GU}SS263-30	White	Rods	-	-	+	-	+	+	-	-	+	+	-	+	+	-	-	-	-	-	
^{GU}SS263-11	White	Rods	-	-	-	±	+	-	-	-	-	+	-	-	+	-	-	+	-	-	
^{GU}SS263-N5	White	Rods	-	-	-	±	+	-	-	-	-	-	-	-	+	+	-	+	-	-	
^{GU}SS263-13	White	Rods	-	-	-	±	+	-	-	-	-	+	-	-	+	-	-	+	-	-	
^{GU}SS263-29	White	Rods	-	-	-	±	+	-	-	-	-	+	-	-	+	-	-	+	-	-	
^{GU}SS263-1	White	Rods	-	-	-	±	+	+	-	-	-	+	+	+	+	-	-	+	-	+	
^{GU}SS263-36	White	Rods	-	-	-	±	+	+	-	-	-	+	+	+	+	-	-	+	-	+	
^{GU}SS263-21	White	Rods	-	-	-	±	+	+	-	-	-	+	+	+	+	-	-	+	-	+	
^{GU}SS263-3	White	Rods	-	-	+	±	+	+	-	+	-	+	+	-	+	-	-	-	-	+	*Psd*
^{GU}SS263-6	White	Rods	-	-	+	±	+	-	-	+	-	+	+	-	+	+	+	+	-	+	*Psd*
^{GU}SS263-8	White	Rods	-	-	+	±	+	+	-	+	-	+	+	-	+	-	-	-	-	+	*Psd*
^{GU}SS263-31	White	Rods	-	-	+	+	-	+	+	+	-	+	-	+	+	+	-	-	+	+	*Vib*
^{GU}SS263-28	White	Rods	-	-	+	-	+	+	-	-	-	-	-	-	-	+	-	+	+	+	
^{GU}SS263-N4	Orange	Rods	-	-	+	+	+	+	-	+	+	+	-	-	+	-	-	-	+	+	*Shw*

± Weak positive

Table 4.2 Continued (Phenotypic characteristics and enzyme expressions by bacterial flora from **'declining'** phase bloom)

Isolate code	Colony Color	Mph	Gram	End	Mot	AnG	Cat	Oxi	LDC	ODC	H_2S	NR	DNR	Ure	Phs	Amy	Cell	Prot	Gel	Lip	Genera
SS263-9	Pale Orange	Rods	-	-	+	+	+	+	-	+	+	+	-	-	+	-	+	+	+	+	*Shw*
SS263-33	Orange	Rods	-	-	+	+	+	+	-	+	+	+	+	+	+	-	-	-	+	+	
SS263-28A	Pale orange	Rods	-	-	+	+	+	+	-	+	+	+	+	+	-	-	-	-	+	+	*Shw*
SS263-2	White	Rods	-	-	+	+	+	+	-	+	+	+	+	+	+	-	-	+	+	+	
SS263-14	White	Rods	-	-	+	+	+	+	-	+	+	+	+	+	+	-	-	+	-	+	
SS263-38A	Beige	Rods	-	-	+	-	+	+	-	-	-	+	+	+	-	-	+	+	-	+	
SS263-19	Red	Rods	+	-	-	-	+	-	+	+	-	+	-	+	-	-	-	-	-	+	
SS263-17	Yellow	Rods	+	-	-	-	+	-	-	-	-	-	-	-	-	+	-	-	-	-	
SS263-4	Yellow	Rods	+	-	-	+	+	-	-	+	+	+	-	+	+	+	-	+	-	-	
SS263-16	Pale yellow	Rods	+	-	-	+	+	-	-	+	+	+	-	+	+	+	-	-	-	-	
SS263-27	White	Rods	+	-	-	-	+	-	-	-	-	-	-	+	-	-	-	-	+	+	
SS263-23	Deep-red	Rods	+	-	±	+	+	-	-	-	-	+	-	-	+	+	+	+	-	-	
SS263-26	Cream	Rods	+	-	±	+	+	-	-	-	-	+	+	-	-	-	-	+	+	-	
SS263-34	White	Rods	+	+	+	-	+	-	-	-	-	+	+	-	+	-	-	+	+	+	*Bac*
SS263-12	White	Cocci	+	-	-	-	+	-	-	-	-	+	-	+	-	+	-	-	+	+	*Stp*
SS263-37	White	Rods	+	+	+	-	+	+	-	-	-	+	+	-	-	+	-	-	+	-	*Vrg*
SS263-20	White	Rods	+	+	+	-	+	+	-	-	-	-	-	-	+	+	+	+	-	+	*Bac*
SS263-5	White	Rods	+	+	+	-	+	-	-	-	-	+	+	+	-	+	-	+	+	+	*Bac*
SS263-10	White	Rods	+	+	+	-	+	+	-	-	-	+	-	+	-	-	-	+	+	+	*Bac*
SS263-7	White	Rods	+	+	+	+	+	-	+	-	-	+	-	-	-	-	-	-	-	+	*Bac*

Table 4.3 Comparative metabolism of 'active' and 'declining' bloom flora

Phenotypic/Metabolic characteristics	**Percentage of flora**	
	Active (N=34)	**Declining (N=36)**
Gram-Character (+ve)	70.59	38.88
Motility	76.47	58.33
Endospores	44.12	19.44
Anaerobic growth in thioglycollate	50.00	47.22
Catalase	100.00	97.22
Oxidase	41.18	55.56
β-galactosidase (ONPG)	20.59	13.89
Lysine decarboxylase	8.82	8.33
Ornithine decarboxylase	26.47	38.89
Phenylalanine deaminase	5.88	8.33
H_2S (Desulfurase)	11.76	27.78
Nitrate reduction	73.53	83.33
Denitrification (Aerobic)	50.00	41.67
Extracellular Hydrolysis of:		
Urea	35.29	52.78
Esculin	47.06	30.56
Starch	50.00	38.89
Carboxy-methyl Cellulose	20.59	13.89
Casein	55.88	58.34
Gelatin	61.76	38.89
Tributyrin	26.47	30.56
Tween-80	52.94	61.11
Tricalcium Phosphate	52.94	63.89
Carbon source utilization:		
Citrate	41.18	61.11
Succinate	82.35	86.11
Acetamide	44.12	63.90
D-Glucose	100.00	80.56
Sucrose	44.12	75.00
Maltose	73.53	83.33
D-Xylose	38.24	47.22
D-Fructose	76.47	83.33
L-Arabinose	23.53	27.78
D-Mannose	32.35	50.00
Trehalose	29.41	61.11
Amino-acids as sole C&N source:		
Alanine	47.06	41.67
Methionine	17.65	19.44
Lysine	41.18	27.78
Threonine	32.35	33.33
Leucine	38.24	66.67
Iso-leucine	35.29	22.22
Valine	26.47	44.44
Phenylalanine	20.59	52.78

Table 4.3 continued.

Phenotypic/Metabolic characteristics	Percentage of flora	
	Active (N=34)	Declining (N=36)
Tryptophan	14.71	13.89
Histidine	41.18	41.67
Serine	55.88	63.89
Acid from Carbohydrates (Aerobic)		
Glucose	64.71	66.67
Adonitol	17.65	8.33
Lactose	11.76	19.44
L-Arabinose	35.29	27.78
Sorbitol	2.94	13.89
Xylose	20.59	33.33
Maltose	44.12	30.56
Fructose	41.18	44.44
Galactose	29.41	16.67
Raffinose	8.82	ND
Trehalose	44.12	22.22
Melibiose	14.71	8.33
Sucrose	41.18	16.67
Mannose	47.06	25.00
Inulin	8.82	ND
Na-gluconate	11.76	13.89
Glycerol	29.41	22.22
Salicin	11.76	5.56
Glucosamine	23.53	5.56
Inositol	14.71	5.56
Sorbitol	5.88	8.33
Mannitol	41.18	13.89
alpha-methyl D Glucoside	2.94	ND
Ribose	52.94	30.56
Rhamnose	11.76	2.78
Cellobiose	20.59	8.33
Melezitose	8.82	5.56
alpha-methyl D Mannoside	5.88	ND
Xylitol	2.94	19.44
Sorbose	2.94	2.78
Erythritol	14.71	ND
Arbutin	17.65	2.78

4.2A.4 Fatty-acid characersitics

Fatty-acid methyl esters (FAME) were determined for the isolates SK256-38, SS263-38, SS263-30, and SK256-15 for match-up with the 16SrDNA gene sequence based identifications. The characteristic FAME and match-up with the Sherlock version 6B, RTSBA6.6 library is shown in Table 4.4. The results indicated that identification of isolates based on FAME characersitics correlated with 16SrDNA based identity. The isolate SS263-30 was placed under *Halomoans vensuta.* The isolate SS263-28 showed a FAME similarity of 0.58 with *Pseudoalteromonas nigrifaciens,* while 16SrDNA gene showed a major similarity to *Pseudoalteromonas elyakovii* KMM162^{T} [AF082562] as (99.3%), which are very closely related to each other phylogenetically. The isolates SK256-38 and SK256-15 did not show any good-match with the known FAME characersitics of any species and this is also reflected in the 16SrDNA gene based homology as Unclassified strains belonging to Planococcaceae and Microbacteriaceae.

Table 4.4 Fatty-acids (FAME) charactersitics of selected strains for match-up with 16SrDNA sequence based identity.

Major fatty acids	Fatty acid percentage of isolates (%)			
	SK256-38	***SS263-30***	***SS263-28***	***SK256-15***
10:0		2.16		
11:0 3OH			2.73	
12:0		1.25	4.38	
12:0 3OH		7.0		
12:0 iso 3OH			2.11	
14:0		2.53		
14:0 iso	5.21			
15:0 anteiso	36.05			40.28
15:0 iso	18.32			8.55
15:1 iso H/13:0 3OH			1.26	
16:0 iso	11.87		1.82	24.43
16:1 w7c alcohol	6.15			
16:0	1.19	8.47	14.15	5.63
16:1 w11c	1.53			
16:1 w7c/16:1 w6c		13.90	30.01	
17:0 anteiso	11.94			13.54
17:0 iso				2.72
17:1 w8c				14.54
17:0			2.46	
18:1 w7c		62.17	3.36	
RTABA6.6 Library	*Bacillus* GC group-22	*Halomonas Venusta*	*Pseudoalteromonas nigrifaciens*	*Microbacterium laevaniformans*
Similarity (FAME)	0.5	0.802	0.58	0.46
16SrDNA analysis **(Table 4.5 and 4.6)**	*Unclassified Planococcaceae*	*Halomonas venusta*	*Pseudoalteromonas* sp.	*Unclassified Microbacteriaceae*

4.2A.5 Phylogenetic composition

Based on 16SrDNA gene sequence relatedness, the taxonomic assignments of isolates were determined (Table 4.5 and 4.6) with supporting phenotypic characteristics (Fig. 4.2). The neighbor-joining boot-strap consensus tree grouped all 70 isolates, belonging to 21 classified genera and 5 unclassified genera under 4 different phylum of *Firmicutes, Actinobacteria, γ-proteobacteria and α-proteobacteria.* Members of *Firmicutes* were represented by the genera *Bacillus* spp. (SK256-8; SK256-12; SK256-13; SK256-14; SK256-S9; SK256-16; SK256-17; SK256-21; SK256-5; SK256-22; SK256-32; SK256-S7; SK256-20; SS263-20; SS263-5; SS263-34), *Oceanobacillus* sp. (SK256-21), *Brevibacillus* sp. (SS263-26), *Virgibacillus* spp. (SK256-18; SK256-19; SS263-37); *Staphylococcus* spp. (SK256-30; SS263-12), *Exiguobacterium* sp. (SK256-25/2) and unclassified members of Planococcaceae and order Bacillales (SK256-38; SS263-7; SS263-10). Representative genus of phylum *Actinobacteria* belonged to *Micrococcus* spp. (SK256-35; SK256-37), *Microbacterium* spp. (SK256-N8; SS263-4), *Brachybacterium* sp. (SK256-N4; SS263-16), *Dietzia* spp. (SS263-17; SS263-19), *Kocuria* sp. (SS263-23), *Leucobacter* sp. (SS263-27), Unclassified Micrococcaceae (SK256-15) and Unclassified Intrasporangiaceae (SK256-28). The Phylum *γ-proteobacteria* were represented by members of the *Pseudomonas* spp. (SK256-25/1; SK256-N3; SK256 N5; SK256 N7;SK256 N6; SK256 N2; SK256-N1; SK256-33; SS263-3; SS263-6; SS263-8), *Halomonas* spp. (SK256-29; SS263-24; SS263-38; SS263-30), *Psychrobacter* spp. (SS263-1; SS263-21; SS263-36), *Shewanella* spp. (SS263-2; SS263-9; SS263-14; SS263-N4; SS263-28A;SS263-33), *Cobetia* spp. (SS263-N5; SS263-29; SS263-13; SS263-11), *Vibrio* sp. (SS263-31),

P*seudoalteromonas* sp. (SS263-N4) and *Providencia* sp. (SK256 16/1). Members of Phylum *α-proteobacteria* was represented by the sole genus *Ochrobactrum* sp. (SS263-38A).

A compilation of the relative abundance of these bacterial genera showed that bacteria belonging to *Bacillus* spp. were by far the most dominant during the active phase and comprised 35.29% of the flora with several other genera constituting the minor fractions (Table 4.8). During the declining phase, *Shewanella* spp. emerged as the dominant forms, constituting 16.67% of the flora, followed by *Cobetia* spp. constituting 11.11% and an equal dominance of species belonging to *Pseudomonas-Psychrobacter-Halomonas* consortium comprising 24.9 % of the flora (Table 4). Species belonging to the genus *Micrococcus, Exiguobacterium, Providencia* and the unclassified bacteria of families *Intrasporangiaceae and Micrococcaceae* were exclusively present during the active phase of bloom; whereas, those belonging to genera *Ochrobactrum, Shewanella, Cobetia, Psychrobacter, Pseudoalteromonas, Vibrio, Dietzia, Leucobacter, Kocuria, Brevibacillus* and unclassified *Planococcaceae* were retreived exclusively during the declining bloom at St-O1. Common species present during both phases of the bloom were *Bacillus flexus, Bacillus cereus, Virgibacillus halodentrificans, Brachybacterium paraconglomeratum* and *Halomonas meridiana.* The common phylotypes of the dominant genera *Pseudomonas* belonged to the highly coherent 'Fluorescent *Pseudomonas'* cluster of bacteria, and hence their unclear distinction at the species level restrained further conclusions. The comparative list of bacteria species detected during 'active' and 'declining' phases of the bloom at St-O1 is shown in Table 4.7.

Table 4.5 Identification of bacteria isolated from 'active' *Noctiluca* bloom phase of Feb-2009 at station O-1.

Isolate code*[a]	**Species identity**	**Accession**	**Nearest strain/s in RDP-II and/or Eztaxon-e database**	**Pair-wise similarity (%)**	
SK256-25A	*Pseudomonas xanthomarina*	JX429828	*Pseudomonas xanthomarina;* KMM 1447^{T} [AB176954]	99.6	(2/512)
SK256-N3	*Pseudomonas* sp.[b]	JX429829	*Pseudomonas chlororaphis*; 4.4.1[FR682804]	100.0	(0/226)
SK256-N5	*Pseudomonas* sp.[b]	JX429830	*Pseudomonas merdiana ;* KJPB15 [FM213379]	99.0	(4/384)
SK256-16A	*Providencia rettgeri*	JX429831	*Providencia rettgeri;* IITRP2 [GU193984]	100.0	(0/867)
SK256-29	*Halomonas meridiana*	JX429832	*Halomonas meridiana; DSM 5425*^{T} [AJ306891]	99.8	(1/826)
SK256-N7	*Pseudomonas* sp.[b]	JX429833	*Pseudomonas spp.* [AJ492830; AY509898; AF374472]	100.0	(0/326)
***SK256-N6**	*Pseudomonas gessardii*	JX429834	*Pseudomonas gessardii;* CIP105469^{T} [AF074384]	99.6	(5/1405)
SK256-N2	*Pseudomonas* sp.[b]	JX429835	*Pseudomonas spp.;* [AJ492830; AY509898;AF268029]	100.0	(0/366)
SK256-N1	*Pseudomonas* sp.[b]	JX429836	*Pseudomonas sp.,* PILH1 ; AY456708	99.7	(0/394)
SK256-33	*Pseudomonas stutzeri*	JX429837	*Pseudomonas stutzeri* ATCC 17588^{T} [CP002881]	99.0	(4/409)
SK256-N4	*Brachybacterium paraconglomeratum*	JX429838	*Brachybacterium paraconglomeratum;* CT24 [EU660352]	99.3	(3/417)
SK256-N8	*Microbacterium oxydans*	JX429839	*Microbacterium oxydans;* NJ6 [DQ403811]	100.0	(0/476)
SK256-37	*Micrococcus luteus*	JX429840	*Micrococcus luteus;* CV39 [AJ717368]	100.0	(0/696)
***SK256-35**	*Micrococcus luteus*	JX429841	*Micrococcus sp.;* HB241 [GU213502]	99.9	(1/1323)
SK256-28	*Intrasporangiaceae*[c]	JX429842	*Phycicoccus bigeumensis; MSL03*^{T} [EF466128]	97.3	(17/640)
***SK256-15**	*Micrococcaceae*[c]	JX429843	Micrococcaceae K2-66; [AY345408]	93.7	(89/1418)
SK256-25/2	*Exiguobacterium aurantiacum*	JX429844	*Exiguobacterium aurantiacum* DSM 6208^{T}; [DQ019166]	99.4	(5/844)

Table 4.5 Continued. (Active *Noctiluca* bloom phase)

Isolate code*[,a]	Species identity	Accession	Nearest strain/s in RDP-II and/or Eztaxon-e database	Pair-wise similarity (%)	
SK256-20	*Bacillus cereus*	JX429845	*Bacillus cereus; ATCC 14579*[T][AE016877]	100.0	(0/1014)
SK256-S7	*Bacillus* sp.[c]	JX429846	*Bacillaceae bacterium; KVD-unk-34* [DQ490422]	97.2	(11/386)
SK256-32	*Bacillus subtilis*	JX429847	*Bacillus subtilis subsp. subtilis*; GH44 [AB301013]	99.3	(3/418)
SK256-22	*Bacillus cereus*	JX429848	*Bacillus cereus*; CICC10185 [AY842872]	99.8	(1/419)
***SK256-5**	*Bacillus* sp.[c]	JX429849	*Bacillus* sp.; 53-11 [FJ607050]	99.9	(2/1413)
SK256-38	*Planococcaceae*[c]	JX429850	*Bacillus* sp.; M71_N104b [FM992794]	99.8	(2/920)
SK256-30	*Staphylococcus arlettae*	JX429851	*Staphylococcus arlettae;* P2S4 [EU221385]	100	(0/765)
SK256-19	*Virgibacillus halodenitrificans*	JX429852	*Virgibacillus halodenitrificans ;* DSM 10037[T] [AY543169]	99.5	(3/701)
SK256-18	*Virgibacillus halodenitrificans*	JX429853	*Virgibacillus halodenitrificans;* DSM 10037[T] [AY543169]	99.8	(1/535)
SK256-21	*Oceanobacillus* sp.	JX429854	*Oceanobacillus* sp.; VE-2-10-82 [EU604320]	100.0	(0/817)
SK256-17	*Bacillus cereus*	JX429855	*Bacillus cereus;* RIVM BC00068 [AJ577283]	100.0	(0/833)
SK256-16	*Bacillus flexus*	JX429856	*Bacillus flexus;* MDLD1 [FJ861081]	99.3	(3/429)
SK256-S9	*Bacillus* sp.	JX429857	*Bacillus firmus;* XJSL1-9 [GQ903388]	99.8	(1/474)
SK256-14	*Bacillus* sp.	JX429858	*Bacillus firmus;* 87-7 [FJ607055]	99.6	(1/284)
SK256-13	*Bacillus mycoides*	JX429859	*Bacillus mycoides;* BGSC1[DN3] [EU285664]	100.0	(0/793)
SK256-12	*Bacillus* sp.	JX429860	*Bacillus sp.;* BA-54 [AY557616]	100.0	(0/821)
***SK256-8**	*Bacillus* sp.	JX429861	*Bacillus sp.*; ARCTIC-P30 [AY573046]	99.5	(7/1490)

*Near complete (> 1200bp) sequences obtained for 'bold-faced' isolate codes
[a] GU (Goa University) – isolate code
[b] Fluorescent Pseudomonads group (8.33%)
[c] Unclassified strains with nearest Type strain match <97% and significantly different phenotypic characteristics from nearest Type strain

Table 4.6 Identification of bacterial isolates retreived from 'declining' *Noctiluca* bloom phase of Mar-2009 at station O-1.

Isolate code*,[a]	**Species identity**	**Accession**	**Nearest strain/s in RDP-II and/or Eztaxon-e database**	**Pair-wise similarity (%)**	
SS263-38A	*Ochrobactrum* sp.	JX429792	*Ochrobactrum* spp. [AY776289; CP000758; AY457038]	99.3	(2/305)
SS263-2	*Shewanella* sp.	JX429793	*Shewanella* sp.; KJW23 [HM016085]	99.7	(2/645)
SS263-24	*Halomonas axialensis*	JX429794	*Halomonas axialensis;* Althf1^T [AF212206]	99.5	(2/409)
SS263-28A	*Shewanella* sp.	JX429795	*Shewanella sp.;* W3 [GQ280385]	99.5	(2/692)
***SS263-N5**	*Cobetia marina*	JX429796	*Cobetia marina;* DSM 4741^T [AJ306890]	99.8	(2/1413)
***SS263-N4**	*Shewanella haliotis*	JX429797	*Shewanella haliotis;* DW01^T [EF178282]	100.0	(0/1414)
***SS263-38**	*Halomoans meridiana*	JX429798	*Halomonas meridiana;* DSM 5425^T [AJ306891]	99.8	(2/1374)
SS263-31	*Vibrio campbellii*	JX429799	*Vibrio campbellii;* ATCC 25920^T [X74692]	99.7	(1/430)
SS263-36	*Psychrobacter* sp.	JX429800	*Psychrobacter sp.;* B-5151 [DQ399761]	98.8	(7/613)
SS263-33	*Shewanella* sp.	JX429801	*Shewanella upenei;* 20-23R^T[GQ260190]	99.8	(1/630)
***SS263-30**	*Halomonas venusta*	JX429802	*Halomonas venusta;* DSM 4743^T[AJ306894]	99.8	(2/1430)
***SS263-29**	*Cobetia marina*	JX429803	*Cobetia marina;* DSM 4741^T[AJ306890]	99.7	(3/1305)
***SS263-28**	*Pseudoaltermonas* sp.	JX429804	*Pseudoalteromonas elyakovii* KMM162^T [AF082562]	99.3	(13/1437)
SS263-21	*Psychrobacter* sp.	JX429805	*Psychrobacter sp.;* B-5151 [DQ399761]	99.0	(6/629)
SS263-14	*Shewanella* sp.	JX429806	*Shewanella algae;* ATCC 51192^T [AF005249]	97.6	(7/296)
SS263-13	*Cobetia marina*	JX429807	*Cobetia marina DSM 4741*^{T} [AJ306890]	99.6	(2/633)
SS263-11	*Cobetia marina*	JX429808	*Cobetia marina DSM 4741*^{T} [AJ306890]	99.3	(4/648)
***SS263-9**	*Shewanella* sp.	JX429809	*Shewanella* spp. [EF028091; EU252498]	100.0	(0/1452)

Table 4.6 Continued. (Declining *Noctiluca* bloom phase)

Isolate code*,[a]	**Species identity**	**Accession**	**Nearest strain/s in RDP-II and/or Eztaxon-e database**	**Pair-wise similarity (%)**	
SS263-8	*Pseudomonas* sp. [b]	JX429810	*Pseudomonas* spp. [AY486386; AF094729]	100.0	(0/619)
SS263-6	*Pseudomonas* sp. [b]	JX429811	*Pseudomonas* spp. [AY492830; AY509898; AF268029; AF37447]	99.4	(2/389)
SS263-3	*Pseudomonas* sp. [b]	JX429812	*Pseudomonas sp.*PILH1 [AY456708]	100.0	(0/392)
SS263-1	*Psychrobacter* sp.	JX429813	*Psychrobacter marincola*; KMM277^T [AJ309941]	98.5	(6/402)
SS263-27	*Leucobacter komagatae*	JX429814	*Leucobacter komagatae IFO 15245*^{T} [AJ746337]	100.0	(0/631)
***SS263-23**	*Kocuria* sp.	JX429815	*Kocuria* sp; C20 [AB330815]	100.00	(0/1396)
SS263-16	*Brachybacterium paraconglomeratum*	JX429816	*Brachybacterium paraconglomeratum*;CT24 [EU660352]	99.7	(2/798)
SS263-19	*Dietzia schimae*	JX429817	*Dietzia schimae;* YIM 65001^T [EU375845]	100.0	(0/433)
SS263-17	*Dietzia timorensis*	JX429818	*Dietzia timorensis; ID05-A0528*^{T} [AB377289]	100.0	(0/513)
SS263-4	*Microbacterium* sp.	JX429819	*Microbacterium* spp. [AJ853910; X77444]	99.6	(1/316)
SS263-26	*Brevibacillus borstellensis*	JX429820	*Brevibacillus borstelensis;* NRRL-NRS-818^T [D78456]	99.8	(1/775)
SS263-12	*Staphylococcus cohnii*	JX429821	*Staphylococcus cohnii* subsp. cohnii; ATCC29974^T [D83361]	99.7	(1/440)
SS263-37	*Virgibacillus halodenitrificans*	JX429822	*Virgibacillus halodenitrificans;* DSM 10037^T [AY543169]	99.8	(1/663)
SS263-10	Unclassified Bacillales [c]	JX429823	*Bacillus* sp.; Pd3T [GU391528]	96.2	(8/215)
***SS263-34**	*Bacillus cereus*	JX429824	*Bacillus cereus;* B204 [AJ577293]	100.0	(0/1503)
***SS263-5**	*Bacillus flexus*	JX429825	*Bacillus flexus IFO 15715(T)*	99.86	(2/1461)
SS263-20	*Bacillus sp.*	JX429826	*Bacillus firmus* IMAUB1032; BT5-2 [FJ641034]	99.6	(3/726)
SS263-7	Unclassified Bacillales [c]	JX429827	*Chryseomicrobium imtechense;* MW 10(T) [GQ927308]	92.57	(20/269)

*Near complete (> 1200bp) sequences obtained for 'bold-faced' isolate codes
[a] GU (Goa University) – isolate code
[b] Fluorescent Pseudomonads group (8.33%)
[c] Unclassified strains with nearest Type strain match <97% and significantly different phenotypic characteristics from nearest Type strain

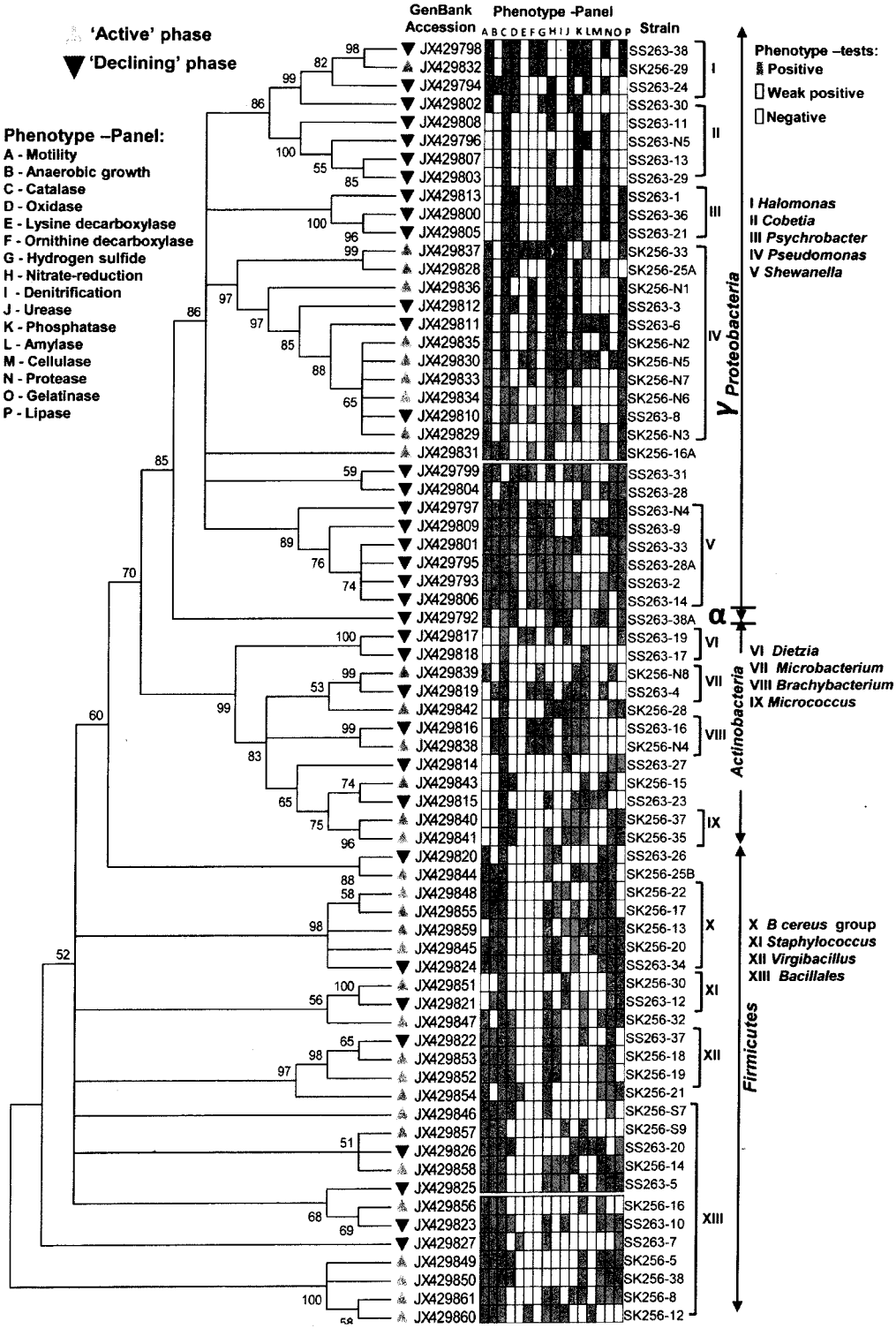

Fig. 4.2 Neighbor joining boot-strap (50% cut-off) consensus tree of partial 16SrDNA gene sequences depicts phylogenetic relationship among bacterial associates of *Noctiluca miliaris* (green) during active (*SK256*) and declining (*SS263*) bloom. Major generic clusters are indicated from tree. Key phenotypic characteristics of strains are merged as a heat-map of positive/negative tests.

Table 4.7 List of bacteria species from 'active' and 'declining' bloom at St-O1.

List of Bacterial species	Isolate codes	
	Active bloom (Cruise SK256)	**Decaying bloom (Cruise SS263)**
Bacillus cereus	SK256-17; SK256-22; SK256-20	SS263-34
Bacillus mycoides	SK256-13	Nd
Bacillus flexus	SK256-16	SS263-5
Bacillus subtilis subsp. subtilis	SK256-32	Nd
Bacillus sp.	SK256-8; SK256-12; SK256-14; SK256-S9; SK256-S7; SK256-5	SS263-30
Oceanobacillus sp.	SK256-21	Nd
Unclassified Planococcaceae	SK256-38	SS263-7
Virgibacillus halodenitrificans	SK256-18; SK256-19	SS263-37
Brevibacillus borstellensis	Nd	SS263-26
Staphylococcus cohnii	Nd	SS263-12
Staphylococcus arlettae	SK256-30	Nd
Exiguobacterium aurantiacum	SK256-25B	Nd
Microcobacterium oxydans	SK256-N8	
Microbacterium sp.		SS263-4
Micrococcus luteus	SK256-37, SK256-35	
Leucobacter komagate	Nd	SS263-27
Brachybacterium paraconglomeratum	SK256-N4	SS263-16
Kocuria sp.	Nd	SS263-23
Dietzia schimae	Nd	SS263-19
Dietzia timorensis	Nd	SS263-17
Unclassified Micrococcaceae	SK256-15	Nd
Unclassified Intrasporangiaceae	SK256-28	Nd
Shewanella haliotis	Nd	SS263-N4
Shewanella spp.	Nd	SS263-2; SS263-28A; SS263-33; SS263-14; SS263-9
Cobetia marina	Nd	SS263-11; SS263-13; SS263-N5; SS263-29
Providencia rettgeri	SK256-16A	Nd
Psychrobacter spp.	Nd	SS263-36; SS263-21; SS263-1
Halomonas meridiana	SK256-29	SS263-38
Halomonas axialensis	Nd	SS263-24
Halomonas venusta	Nd	SS263-30
Pseudoaltermonas sp.	Nd	SS263-28
Vibrio campbelli	Nd	SS263-31
Pseudomonas stutzeri	SK256-33	Nd
Pseudomonas xanthomarina	SK256-25A	Nd
Pseudomonas gessardii	SK256-N6	Nd
Fluorescent *Pseudomonas* group	SK256-N1; SK256-N2; SK256-N3; SK256-N5; SK256-N7	SS263-3; SS263-6; SS263-8
Ochrobactrum sp.	Nd	SS263-38A

Nd – not detected/absent

Table 4.8 Relative frequency of bacterial genera during 'active' and 'declining' bloom phases of *Noctiluca miliaris*.

Phylum	Bacterial Genera	Relative abundance (%)	
		Active phase (N=34)	Declining phase (N=36)
α-proteobacteria	*Ochrobactrum*	-	2.78
γ-proteobacteria	*Shewanella*	-	16.67
	Halomonas	2.94	8.33
	Providencia	2.94	-
	Cobetia	-	11.11
	Psychrobacter	-	8.33
	Pseudoalteromonas	-	2.78
	Vibrio	-	2.78
	Pseudomonas	23.53	8.33
Actinobacteria	*Leucobacter*	-	2.78
	Kocuria	-	2.78
	Brachybacterium	2.94	2.78
	Dietzia	-	5.56
	Microbacterium	2.94	2.78
	Micrococcus	5.88	-
	Unclassified *Micrococcaceae*	2.94	-
	Unclassified *Intrasporangiaceae*	2.94	-
Firmicutes	*Brevibacillus*	-	2.78
	Staphylococcus	2.94	2.78
	Virgibacillus	5.88	2.78
	Exiguobacterium	2.94	-
	Oceanobacillus	2.94	-
	Bacillus	35.29	11.11
	Unclassified *Planococcaceae and Bacillales*	2.94	2.78

(-) not detected / absent

4.2A.6 Community diversity analysis

The overall Shannon-Wiener diversity index (H′) of genera increased to 2.66 during declining phase from 2.07 during the active phase (Fig. 4.3). At the phylum level, this diversity shift was more prominent. Generic diversity of *Proteobacteria* increased from 0.64 during the active phase of bloom to 1.74 during the declining bloom with an increase in richness from 0.87 to 2.04. Although population size of Firmicutes during the active phase was numerically dominant (N = 18), diversity in genera was as low as 1.16. In comparison, a low-population size of Firmicutes (N=5) during declining phase was more diverse with an index of 1.33. Diversity of Actinobacterial genus remained unchanged during both phases as 1.56 (Fig. 4.3).

The Unifrac 'P-test' showed that bacterial phylotypes based on 16SrDNA gene sequences associated with *Noctiluca* (green) bloom phases did differ significantly from each other as $p = 0.03$. This was further reflected in the web-based Unifrac-PCoA plot which showed spatial separation of bacterial communities at St-O1 during active and declining phases of the bloom as well as with that of the reported endocytic bacterial flora of the red *Noctiluca* (Fig. 4.3).

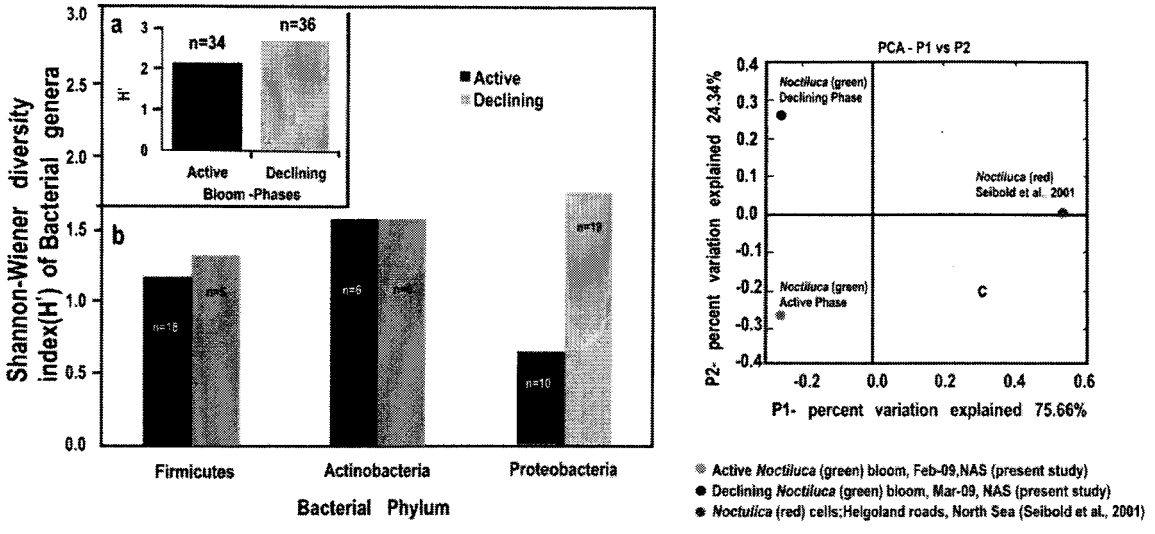

Fig. 4.3 Community analysis of bacterial-flora retreived from *Noctiluca* (green) bloom phases at St-O1 **(a)** Diversity of bacterial genera **(b)** Diversity of bacterial genera based on phylum representations **(c)** Unifrac drawn PCA plot showing bacterial communities based on 16SrDNA partial sequences. Bacterial community of *Noctiluca* (red) cells of Helgolands, North Sea (Seibold A et al., 2001) was included in the phylogenetic tree for comparison with active and declining phases of NAS *Noctiluca* (green) bloom in the present study.

4.2A.7Antibiogram

The strain level differentiation of the flora was aided from their dissimilarity in their antibiograms as seen in a NMDS plot (Fig. 4.4). Although, high resistance (>25% of isolates) to several antibiotics was exhibited by the micro-flora during both the phases of the bloom, decaying phase microflora showed a comparatively lower resistance to the antibiotics tested. During the active phase highest resistance of micro-

flora was to the antibiotics Nalidixic acid (94.12%), Penicillin (85.29%), Ampicillin (79.41%) and Oxytetracycline (73.53%). In the declining flora of the bloom, resistance to both Nalidixic acid and Ampicillin decreased to 47.22%. Penicillin-G resistance also decreased to 61.1%, whereas resistance to Oxytetracycline remained similar. However, the □-*proteobacteria* dominated declining flora showed higher resistance than active phase community to four different antibiotic classes: Clindamycin (beta-lactam), Kanamycin (amino-glycoside), Furanzolidone (nitro-furan) and Novobiocin (amino-coumarin) (Table 4.9).

Table 4.9 Resistance to antibiotics among active and declining bloom flora.

Antibiotics resistance	**Percentage of flora**	
	Active	**Declining**
Antibiotics Resistance:		
Ampicillin	79.41	47.22
Ciprofloxacin	11.76	2.78
Chloramphenicol	26.47	16.67
Clindamycin	58.82	77.78
Erythromycin	50.00	22.22
Furanzolidone	50.00	58.33
Gentamycin	11.76	11.11
Kanamycin	41.18	52.78
Methicillin	58.82	33.33
Norfloxacin	17.65	16.67
Novobiocin	38.24	58.33
Neomycin	14.71	16.67
Nalidixic acid	94.12	47.22
Oxytetracycline	73.53	75.00
Polymyxin B	52.94	38.89
Streptomycin	2.94	5.56
Tetracycline	55.88	47.22
Penicillin	85.29	61.11

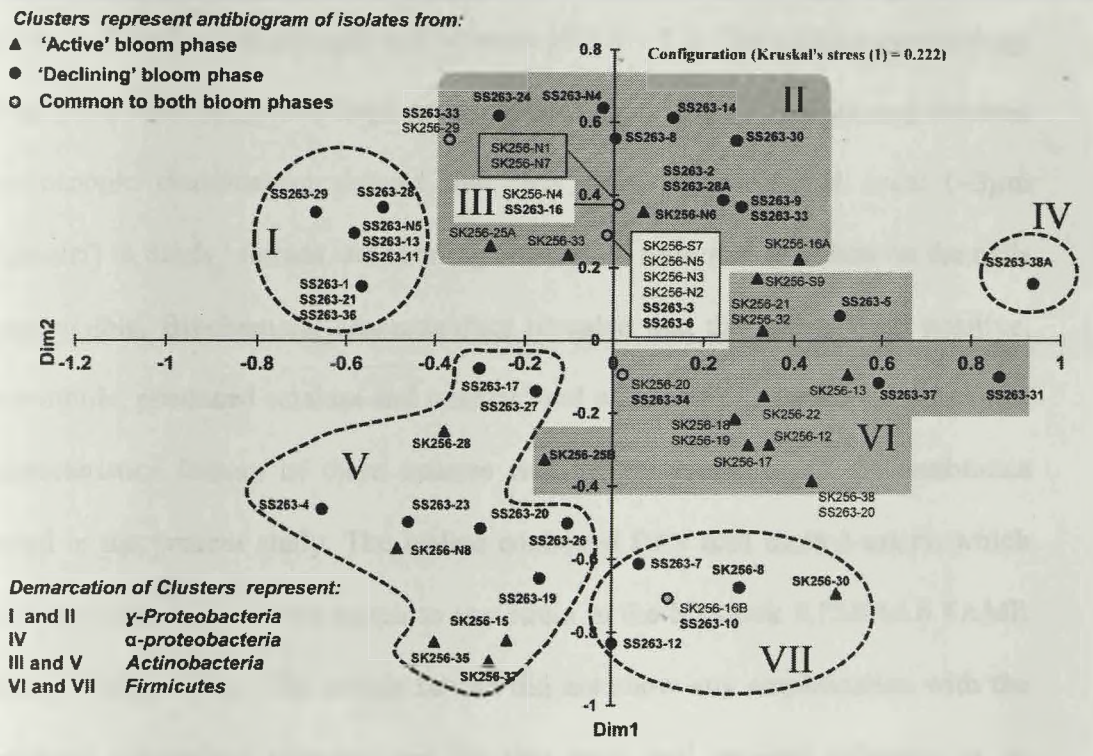

Fig. 4.4 Multi-dimensional scaling showing strain-level proximity/ dissimilarity based on antibiotics resistance among bacterial isolates. Identity of isolates is shown in Table 4A.2.2 and 4A.2.3.

4.2A.8 Isolate retreived on UV exposure to *Noctiluca*

On plating a *Noctiluca* cell concentrate after a brief UV exposure of 1 min in the laminar hood, on Zobell's 1/10 agar, an orange red pigmented isolate (^{GU}SK256-2) came up after ~48 hours and was retreived. The isolate could also grow on Zobell's full strength and between pH3.5 – 3.7. The cellular morphology from gram stain suggested large gram positive cocci (Fig. 4.5). Scanning electron microscopic examination showed that they were large colonial cocci (~3μm diameter) in diads / tetrads and forming clusters. A stalk and an indent on the cells were visible. Biochemical charactersitics revealed that they were gram positive, non-motile, produced catalase and oxidase, and were positive for citrate. The most characteristics feature of these isolates was the resistance to all the antibiotics tested in the present study. The isolate contained fatty acid methyl-esters, which further revealed no known match to any strain in the Sherlock RTSBA6.6 FAME library (Table 4.10). The isolate further did not show any amplification with the universal eubacterial primers used for this study and remains unknown in its phylogenetic placement.

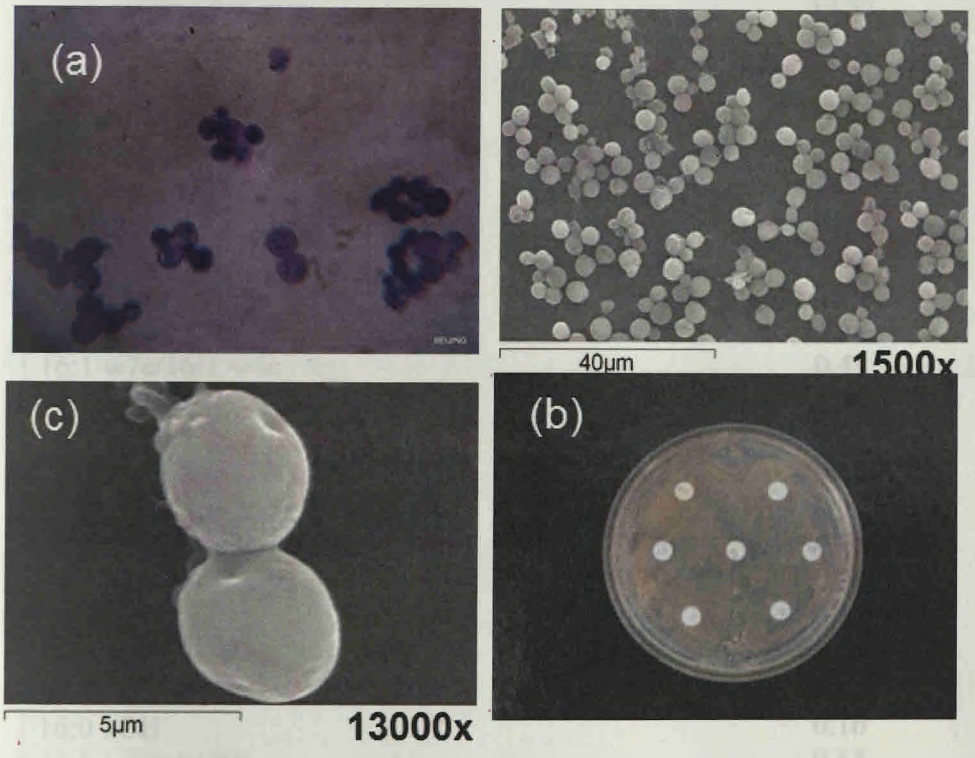

Fig. 4.5 Morphology and antibiotic resistance of isolate ^{GU}SK256-2, retrieved from cells of *N miliaris* (green) (a) Colony morphology (b) Gram stained cells (c) Resistance to antibiotics (d) SEM morphology.

Table. 4.10 Fatty acid characteristics of ^{GU}SK256-2.

Fatty-acid	Percentage (%)
18:2 w6,9c/18:0 ante	39.57
18:1 w9c	21.93
18:1 w7c/18:1 w6c	17.53
16:0	11.51
17:1 w8c	1.68
17:0	1.09
16:0 2OH	0.69
18:0	0.65
14:0	0.56
15:0 anteiso	0.51
16:1 w7c/16:1 w6c	0.48
17:0 anteiso	0.36
18:0 2OH	0.34
20:0 iso	0.32
12:0	0.30
20:4 w6,9,12,15c	0.29
19:1 w11c/19:1 w9c	0.28
18:1 2OH	0.26
17:0 2OH	0.24
19:0 iso	0.17
16:0 3OH	0.16
17:1 anteiso w9c	0.14
16:1 w9c	0.14

4.2B Bacterial flora of *Trichodesmium erythraeum* bloom

4.2B.1 Culturable Bacterial load

Culturable counts in the *Trichodesmium erythreaum* bloom waters off Ratnagiri averaged $36\pm18.4\times10^5$ CFU mL−1 on Zobell's and $13.4\pm6.43\times10^5$ CFU mL−1 on Zobell's 1/10 strength media. The dominant flora attached to *Trichodesmium erythreaum* tuft colonies could be retrieved along-with those isolated from the filtrate of colonies (loosely attached forms) and referred to as the phycospheric colonial forms.

4.2B.2 Description of flora: Colony associated and free-living

The method of bacterial isolation employed here, allowed us to separate the *Trichodesmium* bloom associated bacteria into the free –living and attached forms. Isolation of attached and free –living bacteria were done simultaneously on Zobell's and Zobell's 1/10 strength media containing 3.5% NaCl. Isolates with different morphological characteristics were picked up for further study and grouped into the free-living and attached forms. A total of 21 bacterial isolates were obtained which remained attached to *Trichodesmium* while 6 isolates were obtained as the free-living bacteria (Table. 4.11). The frequency of pigmented isolates varied from 33% cream, 19% orange/pale orangish, 4% each of wax-bead, yellow and beige types while the majority of 36% isolates were white and non-pigmented.

4.2B.3 Phenotypic and Biochemical characersitics

The morphological and biochemical characersitics of 27 isolates are given in Table 4.11. Interestingly, an overall predominance of gram-positive bacteria (85.18%) were observed among both the attached and free-living forms. The morphology of these isolates were dominated by rods (92.59%). All isolates were catalase positive, however around 55.5% of both attached and free-living isolates were able to grow anaerobically on thioglycollate media.

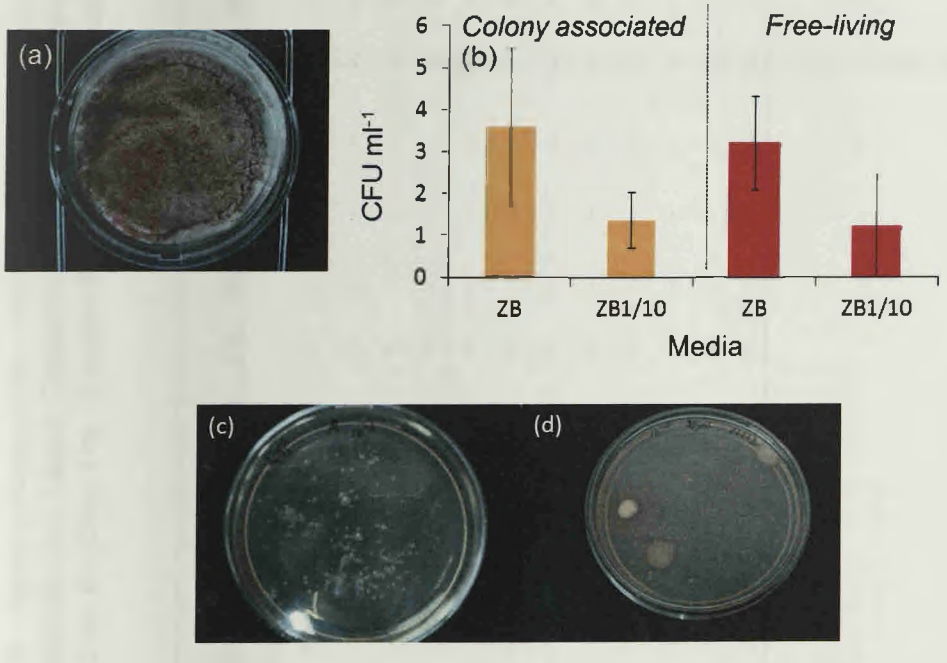

Fig. 4.6 Culturable bacterial load of *T erythraeum* bloom: (a) Trichomes retained on filter (b) plate counts on Zobell's (ZB) and 1/10 dilution of ZB (ZB1/10) (c) Bacterial flora on ZB1/10 plates of (c) Colony associated forms (b) Free-living forms.

Table 4.11 Phenotypic biochemical/metabolic charactersitics of bacterial flora from *T erythreaum* bloom: [Mph- Morphology; Gram-gram character Mot – Motility; Ang – Anaerobic growth in thioglycollate; End-endospores; Oxi – Oxidase, LDC – Lysine decarboxylase, ODC- Ornithine decarboxylase, H_2S –Desulfurase, NR – Nitrate reductase, DNR – Nitrite reductase (Denitrifier), Ure – Urease, Phs – phosphatase, Amy – Amylase, Cell – Cellulase, Prot – Protease, Gel- Gelatinase, Lip – Lipase]. Tentative identities of genera assigned from Bergey's manual of determinative bacteriology are indicated as: *Bac- Bacillus, Vrg –Virgibacillus, Hal - Halomonas, Psd - Pseduomonas, Mic- Microbacterium; Stp -Staphylococcus.*

Isolate code GUFB Sama06-	**Color**	**Mph**	**Gram**	**End**	**Mot**	**AnG**	**Cat**	**Oxi**	**LDC**	**ODC**	**H2S**	**NR**	**DNR**	**Ure**	**Phs**	**Amy**	**Cell**	**Prot**	**Gel**	**Lip**	Genera
Colony Associated																					
01/RS5	White	Rods	+	+	+	+	+	-	-	-	-	+	+	+	-	+	+	+	+	+	*Bac*
02/RS5	White	Rods	+	+	+	+	+	-	-	-	-	+	-	-	-	-	-	-	+	+	*Vrg*
03/RS5	Colorless	Rods	-	-	-	-	+	-	-	-	-	+	-	+	+	+	-	+	-	-	
04/RS5	White	Rods	+	-	-	+	+	-	-	-	-	-	-	-	-	+	-	-	+	+	
05/RS5	White	Rods	+	-	-	+	+	-	-	-	-	+	-	-	-	+	-	+	+	-	
06/RS5	Cream	Rods	+	-	-	-	+	-	-	-	-	+	-	-	-	-	-	+	-	+	*Bac*
08/RS5	White	Rods	+	-	-	-	+	-	-	-	-	+	-	+	-	-	-	+	-	-	
11/RS5	Cream	Rods	+	+	-	+	+	-	-	-	-	+	+	-	-	+	-	+	-	-	*Vrg*
12/RS5	Cream	Rods	+	+	+	+	+	-	-	-	-	+	-	-	+	+	+	+	-	-	*Bac*
13/RS5	White	Rods	+	-	-	-	+	-	-	-	-	-	-	-	-	+	-	-	-	+	
14/RS5	Cream	Rods	+	-	+	-	+	-	-	+	+	-	-	+	-	+	-	-	-	-	
15/RS5	Cream	Rods	+	-	+	+	+	+	-	-	-	-	-	-	-	+	-	+	-	-	

Table 4.11 Phenotypic biochemical/metabolic characersitics of bacterial flora from *T erythreaum* bloom: [Mph- Morphology; Gram-gram character Mot – Motility; Ang – Anaerobic growth in thioglycollate; End-endospores; Oxi – Oxidase, LDC – Lysine decarboxylase, ODC- Ornithine decarboxylase, H_2S –Desulfurase, NR – Nitrate reductase, DNR – Nitrite reductase (Denitrifier), Ure – Urease, Phs – phosphatase, Amy – Amylase, Cell – Cellulase, Prot – Protease, Gel- Gelatinase, Lip – Lipase]. Tentative identities of genera assigned from Bergey's manual of determinative bacteriology are indicated as: *Bac- Bacillus, Vrg –Virgibacillus, Hal - Halomonas, Psd - Pseduomonas, Mic- Microbacterium; Stp -Staphylococcus.*

Isolate code ^{GUFB}Sama06-	**Color**	**Mph**	**Gram**	**End**	**Mot**	**AnG**	**Cat**	**Oxi**	**LDC**	**ODC**	**H2S**	**NR**	**DNR**	**Ure**	**Phs**	**Amy**	**Cell**	**Prot**	**Gel**	**Lip**	Genera
Colony Associated																					
01/RS5	White	Rods	+	+	+	+	+	-	-	-	-	+	+	+	-	+	+	+	+	+	*Bac*
02/RS5	White	Rods	+	+	+	+	+	-	-	-	-	+	-	-	-	-	-	-	+	+	*Vrg*
03/RS5	Colorless	Rods	-	-	-	-	+	-	-	-	-	+	-	+	+	+	-	+	-	-	
04/RS5	White	Rods	+	-	-	+	+	-	-	-	-	-	-	-	-	+	-	-	+	+	
05/RS5	White	Rods	+	-	-	+	+	-	-	-	-	+	-	-	-	+	-	+	+	-	
06/RS5	Cream	Rods	+	-	-	-	+	-	-	-	-	+	-	-	-	-	-	+	-	+	*Bac*
08/RS5	White	Rods	+	-	-	-	+	-	-	-	-	+	-	+	-	-	-	+	-	-	
11/RS5	Cream	Rods	+	+	-	+	+	-	-	-	-	+	+	-	-	+	-	+	-	-	*Vrg*
12/RS5	Cream	Rods	+	+	+	+	+	-	-	-	-	+	-	-	+	+	+	+	-	-	*Bac*
13/RS5	White	Rods	+	-	-	-	+	-	-	-	-	-	-	-	-	+	-	-	-	+	
14/RS5	Cream	Rods	+	-	+	-	+	-	-	+	+	-	-	+	-	+	-	-	-	-	
15/RS5	Cream	Rods	+	-	+	+	+	+	-	-	-	-	-	-	-	+	-	+	-	-	

Table 4.11 Continued.

Isolate code GUFBSama06	Color	Mph	Gram	End	Mot	AnG	Cat	Oxi	LDC	ODC	H2S	NR	DNR	Ure	Phs	Amy	Cell	Prot	Gel	Lip	Genera
17/RS5	White	Rods	+	-	+	-	+	+	-	+	+	+	-	+	-	-	-	-	-	-	
18/RS5	White	Rods	+	+	+	+	+	-	-	-	-	+	+	-	-	-	-	-	+	-	*Vrg*
19/RS5	White	Rods	+	-	+	+	+	-	-	-	-	+	+	+	-	+	-	+	-	+	*Bac*
2.2/RS5	White	Rods	+	+	+	-	+	-	-	-	-	-	-	-	+	-	-	-	-	-	*Bac*
2.3/RS5	Cream	Rods	+	+	+	-	+	-	-	-	-	+	-	-	+	-	-	+	-	-	*Bac*
24/RS4	Orange	Rods	-	-	+	+	+	-	-	-	-	+	-	+	-	-	-	-	-	-	*Psd*
25/RS4	Orange	Rods	-	-	+	-	+	+	-	+	-	+	-	-	-	+	-	-	-	-	*Hal*
26/RS4	Orange	Cocci	+	-	-	+	+	+	-	-	-	+	+	+	-	+	-	-	-	+	*Stp*
27/RS4	Yellow	Cocci	+	-	-	+	+	-	-	+	+	+	+	+	+	-	-	-	-	-	
Free-living																					
07/RS-5	Cream	Rods	+	+	+	+	+	-	-	-	-	-	-	-	-	+	-	-	-	-	*Bac*
09/RS-5	Orange	Rods	+	+	+	+	+	-	-	-	-	-	-	-	-	+	-	-	-	-	*Bac*
10/RS-5	Cream	Rods	+	-	-	-	+	-	-	-	-	-	-	-	-	-	-	-	+	-	
16/RS-5	Cream	Rods	+	+	-	+	+	+	-	-	-	+	+	-	-	+	-	+	-	+	*Bac*
20/RS-5	Orange	Rods	-	-	+	-	+	-	-	+	+	-	-	+	-	-	-	-	-	-	
21/RS-5	Beige	Rods	+	-	+	-	+	-	-	-	-	-	-	+	-	+	-	+	-	+	

4.2B.3 Phylogenetic composition

Based on 16SrDNA phylogeny, 27 bacterial isolates retreived from *Trichodesmium erythreaum* colony and/or phycosphere could be grouped into three major phylum: (a) **The *Firmicutes*** (48.28%) represented by *Bacillus* spp. (^{GUFB}Sama06: 1; 6; 2.2; 2.3; 12 and 19), *Virgibacillus* spp. (^{GUFB}Sama06: 2; 11 and 18), *Staphylococcus* sp. (^{GUFB}Sama06 26) and Unclassified *Bacillaceae* (^{GUFB}Sama06-16). (b) ***The Actinobacteria*** *(34.48%)* represented *by Corynebacterium* spp. (^{GUFB}Sama06: 4; 5 and 10), *Salinibacterium* sp. (^{GUFB}Sama06-13), *Leucobacter* spp.(^{GUFB}Sama06-8; 21); *Microbacterium* spp. (^{GUFB}Sama06: 14; 17) *and Brachybacterium* spp.(^{GUFB}Sama06 27) and the *(c)* □-***Proteobacteria*** *(17.24%)* represented *by Halomonas* spp. (^{GUFB}Sama06: 25), *Pseudomonas* sp. (^{GUFB}Sama06 24), *Shewanella* sp. (^{GUFB}Sama06 20) and an Unclassified *Halomonadaceae* (^{GUFB}Sama06 3).

Of these 27 isolates, 11 isolates could be further referred to their species level, 14 isolates referred to the generic level and 2 isolates showed 16SrDNA homology of <97% with respect to their nearest Type Strains (Table 4.12).

Table 4.12 Identification of bacteria associated *T erythraeum* colonies

Isolate Code	Station	Identity	Accession	Nearest phylogenetic relative; Accession no.	Similarity (%)
Colony associated					
^{GUFB}Sama06-1	RS-5	*Bacillus cereus*	KF495537	*Bacillus cereus;* ATCC 27877; **Z84581**	100(0/466)
^{GUFB}Sama06-2	RS-5	*Virgibacillus* sp.	KF495538	*Virgibacillus dokdonensis* (T); DSW-10; **AY822043**	98.6(6/442)
^{GUFB}Sama06-3	RS-4	Unclassified *Halomonadaceae*	KF495539	*Halomonas* sp. KJ5-1-1; **AB305217**	95.1 (23/481)
^{GUFB}Sama06-4	RS-5	*Corynebacterium maris*	KF495540	*Corynebacterium maris* (T); Coryn-1; **FJ423600**	99.6(2/512)
^{GUFB}Sama06-5	RS-5	*Corynebacterium maris*	KF495541	*Corynebacterium maris* (T); Coryn-1; **FJ423600**	99.4(3/504)
^{GUFB}Sama06-6	RS-5	*Bacillus flexus*	KF495542	*Bacillus flexus;* MDLD1; **FJ861081**	99.8(1/524)
^{GUFB}Sama06-8	RS-5	*Leucobacter komagatae*	KF495543	*Leucobacter komagatae;* IFO15245T; **AJ746337**	99.9 (1/459)
^{GUFB}Sama06-11	RS-5	*Virgibacillus* sp.	KF495544	*Virgibacillus dokdonensis* (T); DSW-10; **AY822043**	98.2(7/393)
^{GUFB}Sama06-12	RS-5	*Bacillus licheniformis*	KF495545	*Bacillus licheniformis;* M1-1; **AB039328**	99.4(3/507)
^{GUFB}Sama06-13	RS-5	*Salinibacterium* sp.	KF495546	*Salinibacterium amurskyense;* KMM 3673(T) **AF539697**	99.8 (1/497)
^{GUFB}Sama06-14	RS-5	*Microbacterium* sp.	KF495547	*Microbacterium* sp. PAO-12; **EF514877**	99.8(1/460)
^{GUFB}Sama06-15	RS-5	*Corynebacterium* sp.	KF495548	*Corynebacterium pilosum* (T); ATCC 29592T; **X81908**	99.4(2/314)
^{GUFB}Sama06-17	RS-5	*Microbacterium* sp.	KF495549	*Microbacterium oxydans*; NJ6; **DQ403811**	99.8(1/385)
^{GUFB}Sama06-18	RS-5	*Virgibacillus halodenitrificans*	KF495550	*Virgibacillus halodenitrificans*; KL1-1; **AB697708**	98.3(9/534)
^{GUFB}Sama06-19	RS-5	*Bacillus* sp.	KF495551	*Bacillus* sp. RS-1; **HM179550**	98.6(6/421)
^{GUFB}Sama06-2.2	RS-5	*Bacillus licheniformis*	KF495552	*Bacillus licheniformis*; KL-176; **AY030335**	99.4 (3/469)
^{GUFB}Sama06-2.3	RS-5	*Bacillus licheniformis*	KF495553	*Bacillus licheniformis*; SDA1223; **JN998738**	100(0/495)
^{GUFB}Sama06-24	RS-5	*Pseudomonas* sp.	KF495554	*Pseudomonas* sp. MT03; **AY690685**	100 (0/582)
^{GUFB}Sama06-25	RS-4	*Halomonas* sp.	KF495555	*Halomonas meridiana* (T); DSM 5425; **AJ306891**	98.9 (6/560)
^{GUFB}Sama06-26	RS-4	*Staphylococcus* sp.	KF495556	*Staphylococcus sp.* R-20810; **AJ786778**	99.8 (1/502)
^{GUFB}Sama06-27	RS-4	*Brachybacterium* sp.	KF495557	*Brachybacterium* sp. I20-12; **EU181223**	99.8 (2/870)

Table 4.13 Identification of free-living (phycospheric) isolates of *T erythraeum*

Isolate Code	Station	Identity	Accession	Nearest phylogenetic relative; Accession no.	Similarity (%)
Free-living					
^{GUFB}Sama06-7	RS-5	*Bacillus* sp.	KF495558	*Bacillus persicus B48(T);HQ433471*	96.4 (22/616)
^{GUFB}Sama06-9	RS-5	*Bacillus* sp.	KF495559	*Bacillus sp.* RS-1; **HM179550**	98.8(5/409)
^{GUFB}Sama06-10	RS-5	*Corynebacterium maris*	KF495560	*Corynebacterium maris* (T); Coryn-1; **FJ423600**	99.4(3/496)
^{GUFB}Sama06-16	RS-5	Unclassified *Bacillaceae*	KF495561	*Bacillus firmus;* XJSL1-1; **GQ903380**	89.2 (54/500)
^{GUFB}Sama06-20	RS-5	*Shewanella algae*	KF495562	*Shewanella algae;* YJ06114; **EF542799**	99.9 (1/737)
^{GUFB}Sama06-21	RS-5	*Leucobacter komagatae*	KF495563	*Leucobacter komagatae*; IFO15245T; **AJ746337**	100(0/616)

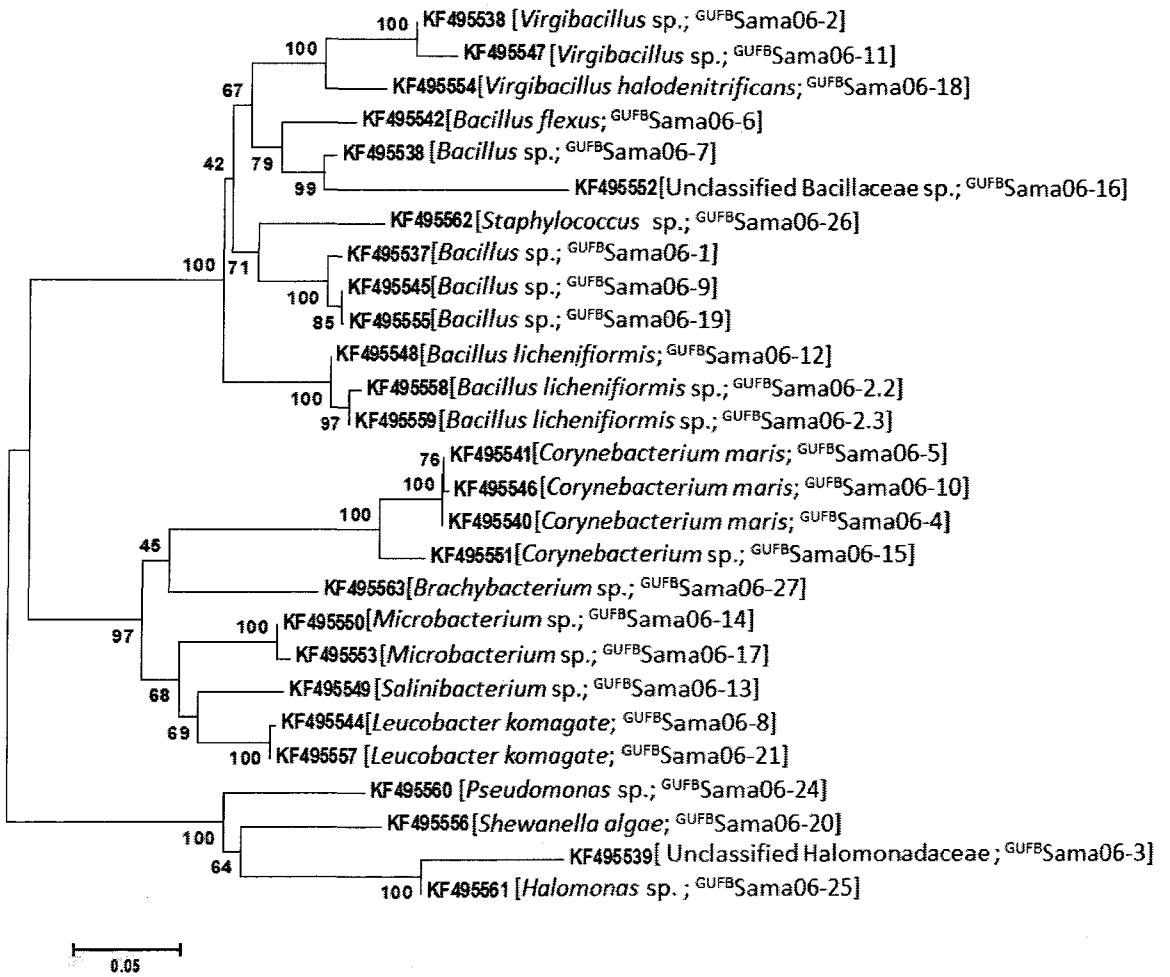

Figure. 4.7 Neighbor joining phylogenetic tree showing phylogenetic relationship among *T erythraeum* bloom associated bacterial strains. Gen bank Accession numbers [Identity, Isolate code] is indiacted on the branches. The optimal tree with the sum of branch length = 1.4503 is shown. The percentage of replicate trees in which the associated taxa clustered together in the bootstrap test (500 replicates) are shown next to the branches. The evolutionary distances were computed using the Jukes-Cantor method.

Table 4.13 Relative abundance of genera associated with *Trichodesmium* spp. bloom

Bacterial Genera	Relative abundance (%)	
	Colony associated	Phycospheric
Phylum *Firmicutes*		
Bacillus	28.57	33.33
Unclassified Bacillaceae	Nd	16.67
Virgibacillus	14.29	Nd
Staphylococcus	4.76	Nd
Phylum *Actinobacteria*		
Corynebacterium	14.29	16.67
Salinibacterium	4.76	Nd
Leucobacter	4.76	16.67
Microbacterium	9.52	
Brachybacterium	4.76	Nd
Phylum □-*proteobacteria*		
Halomonas	4.76	Nd
Unclassified Halomonadaceae	4.76	
Pseudomonas	4.76	Nd
Shewanella	Nd	16.67

Nd- Not detected

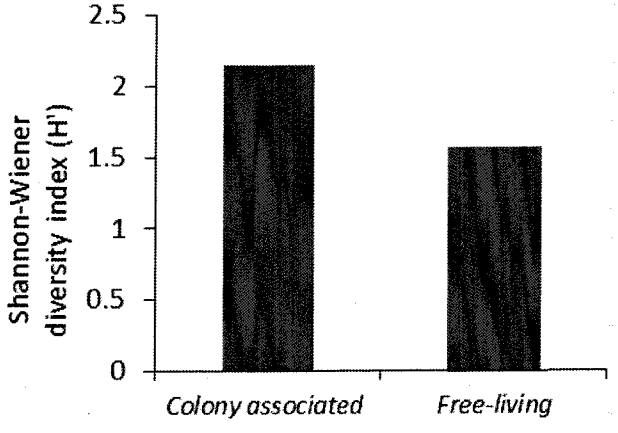

Fig. 4.8 Shannon-wiener diversity index of bacterial genera retreived from *Trichodesmium erythraeum* bloom off Ratnagiri.

The relative abundance of bacterial genera (Table 4.13) showed that *Bacillus* were by far the most dominant genera constituting 28.57% of the colony associated and 33.33% of the free-living bacterial population. Of the colony associated forms *Bacillus licheniformis* was the dominant species of the *Bacillus* group, while other identifiable species belonged to *Bacillus cereus* (^{GUFB}Sama06-6) and *Bacillus flexus* (^{GUFB}Sama06-1). *Virgibacillus* and *Staphylococcus* constituted 14.29% and 4.76% of the colony associated flora. The relative frequency of phylum *Actinobacteria* was 38.09% and the major representative genera were the *Corynebacterium* (14.29%) represented by *C maris,* followed by members of *Microbacterium* (9.52%) and equal percentages of *Salinibacterium, Leucobacter* and *Brachybacterium,* constituting 4.76% each of the flora. Members of the *γ-proteobacteria* were found to be the least dominant, constituting 14.28% of the flora, and represented by *Halomonas*, Unclassified Halomonadaceae and *Pseudomonas*. The free-living forms were also dominated by the *Bacillus* of Firmicutes (33.33%). Members of *Corynebacterium, Leucobacter and Shewanella* constituted equal percentages (16.67%) of the flora.

4.2B.4 Community diversity analysis

Diversity analysis of bacterial genera retreived from *T erythraeum* bloom further showed that The Shannon-wiener diversity index of bacterial genera showed that the colony associated forms are more diverse (H' = 2.15) with a higher richness (d=3.29) and low Pielou's specie evenness (J'=0.89). The generic diversity of free-living forms were low (H'=1.56), with low richness (d=2.23) but showing higher evenness (J'=0.96) (Fig 4.8).

4.3 Discussion

4.3A Bacterial flora of *N miliaris* bloom

Culturable bacterial load

The plate counts revealed ~ 2-3 fold increase in culturable bacterial load during active and declining phases of *Noctiluca* (green) bloom against 'non-bloom' waters, on both nutrient-rich (ZB and SWA) as well as nutrient-poor (ZB 1/10 strength) media (Fig. 2). In comparison, the red *Noctiluca* bloom of April 1993 in the coastal waters off Mangalore gave lower plate counts, varying between 6.5×10^3 CFU ml^{-1} - 3.3×10^2 CFU ml^{-1} (Nayak et al. 2000). Examination of red *Noctiluca* from Helgolands, North Sea further shows that a high population of bacteria can actually exist within *Noctiluca* cells and referred to as 'turbid' cells (Seibold et al. 2001) which also feeds on bacterial cells (Kirchner et al. 1996) or are toxic (Kirchner et al. 2001). The higher plate counts also supports our preliminary assessment of bloom waters during March 2007 in NAS and therefore, can only be explained as a *'natural enrichment'* of certain bacterial community during the course of the bloom. Further, as our flora is directly retreived from the bloom-biomass, screened from water-samples using a 100µm nytex-mesh, these isolates should be more intimate associates (phycospheric and/or intracellular) of the green *Noctiluca* cells itself. Hence, these bacteria must be important, not only to initially process the fresh exudates of the bloom and contribute to supplying this DOM to the free-living bacterial community in the surrounding water-column (Azam et al. 1994), but also as they are valuable and relevant forms which must be further examined for their role in the process of bloom formation and bloom-termination as well.

Taxonomic diversity of bacteria

Several factors are known to determine the bacterial-flora, which are specific to algal-blooms and can also change at different stages of the bloom (Sapp et al. 2007). Since, a large fraction of bacteria in the active phase are motile (76.47%), they can be chemotactic to the *Noctiluca* (green) DOM during its initial growth. The enzymatic repertoire of 'bacterial-forms' to grow on and utilize organic exudates (Haynes et al. 2007), along with 'antagonistic' interactions among them (Long et al. 2005) possibly shapes up the succession in bacterial community at later stages of the bloom.

The growth of bacteria on all the plating media conspicuously shows a stark contrast in colony morphologies appearing during the two bloom phases (Fig. 2a inset). While bacterial colonies appearing during active phase are mostly non-pigmented types, the declining phase consists of dominant orangish-mucoid colonies on all the plating medium used for isolation. Such a shift in bacterial flora has been distinctly emphasized in the results, referred to as the 'active' and 'declining' phase. In this regard, it is further important to note that an apparent peak-phase of bloom occurs when actively buoyant *Noctiluca* (green) cells rise to surface waters and form dense patches, after which the bloom can decline very quickly (Harrison et al. 2011). This is exactly what we observed at the overlapping station St-01, when the massive active bloom spreading over a large area on 17th Feb-09 suddenly crashed to aggregated lysed *Noctiluca* cells (declining' phase) on 2nd Mar-09. This makes the active phase bacterial community, just prior to bloom decline a strong suspect in the possible termination through 'algicidal' bacteria (Mayali and Azam 2004). This may

also be intricately timed with an aging *Noctiluca* (green) population as north-east monsoon cooling weakens, creating unfavorable conditions for the growth of the bloom (Dwivedi et al. 2006).

However, the most important features of the bacterial community representing these two distinct phases of the bloom are: (a) dominance of *Firmicutes* in the active phase, exclusively belonging to order *Bacillales* just before the bloom declines, (b) the emergence of a dominant and more diverse *γ-proteobacterial* forms in the declining bloom, (c) a diverse and consistent Actinobacterial population in both the bloom phases, although represented by mostly different species, and (d) culturable *alpha-proteobacteria* comprising a minor fraction and detected only during the declining phase.

The UNIFRAC-PCA plot based on partial 16SrDNA sequences clearly shows that flora of *Noctiluca* (green) differed significantly from the active to the declining phase as well as the one reported from the endocytic bacteria of red-*Noctiluca* from Helgoland roads, North-Sea (Seibold et al. 2001). The community also differed from the coastal red-*Noctiluca* bloom (April-May, 1993) off Mangalore, reporting a dominant *Moraxella* spp. population comprising 33%-54% of the flora and a dramatic decline in *Bacillus* spp. from 37.29% during the 'peak' stage to 3.92% on the subsequent day (Nayak et al. 2000). Although *Moraxella* spp. phylotypes remained undetected, those belonging to *Psychrobacter* spp. (8.33%) of the family *Moraxallaceae* are the only phylogentically close population recorded in this study during the declining phase of *Noctiluca* (green). The low frequency of cultured *α-proteobacterium* is surprising. Overwhelming evidence from culturable and

molecular analysis of bacterial community of several bloom forming dinoflagellate species(s) *Gymnodinium catenatum*, *Alexandrium tamarense*, *Karenia brevis*, *Scripsiella trachoidea*, the diatom *Pseudo-nitzchia* spp. as well as the green-algae *Enteromorpha prolifera* bloom off Qingdao in Yellow Sea show *alpha-proteobacterium* to be the dominant community with a high frequency of retreivable aerobic-anoxygenic phototrophic (AAP) bacteria, commonly referred to as the *Roseobacter* clade, also implicated in the dimethylsulfoniopropionate (DMSP) cycle (Fandino et al. 2001, Gonzalez et al. 2000, Green et al. 2004, Guo et al. 2011, Jones et al. 2010, Tada et al. 2011). A recent red *Noctiluca* bloom event in South China Sea also showed a similar high predominance of AAP's (Chen et al. 2011). However, the absence of such pigmented AAP bacterial morphotypes on both nutrient rich and nutrient poor media, amended with filtered sea-water from the bloom itself, does show absence of culturable types, atleast as the dominant culturable forms. The only retreived isolate belonging to *α-proteobacteria* is referred to *Ochrobactrum* sp., SS263-38A. Closest relatives of this strain in RDP.10 database shows ability to mineralize phenolic compounds and their derivatives (Strain As-12, AY662685) and also produce siderophores (Strain Sp-18) isolated from a coastal phytoplankton bloom (Martin et al. 2006).

Although a minor component of the Firmicutes flora, the isolate SK256-25B referred to as *Exiguobacterium aurantiacum* also belongs to an important group of bacterial species capable of degrading such complex hydrocarbons, phenolics and poly-aromatic hydrocarbons (Jeswani and Mukherji 2012). These bacteria are

important as they may break down complex hydrocarbons in the blooms and pave way for the other members in a consortium to grow on their products of metabolism.

Of the total 70 isolates, 21.42% belongs to *Bacillus*. Among these, 12 isolates belong to the active phase itself, whereas only 3 isolates are retreived from the declining phase. This is further confirmed by the dominance of *Bacillus* on all plated medium in active phase. Occurence of *Bacillus* is nearly ubiquitous in the marine environment, and they play an important role in biogeochemical cycling (Ettoumi et al. 2009). However, their strong association as a dominant culturable community with an open-ocean algal bloom is a very new finding. The high efficiency of the fast growing *Bacillus* community to degrade complex carbohydates and their highest abilities to reduce nitrate perhaps made them important constituents of the "active" phase bloom, rich in mucilage and fresh photosynthates. Further, the tropical environment of the Arabian Sea may also be responsible for natural selection of such forms. Recent studies in the mid-west coastal estuaries of India also show *Bacillus* as dominant with high abilities to efficiently degrade carbohydrates (Khandeparkar et al. 2011). Their role as an important fraction of the phosphate mineralizing bacteria in the coral-reefs of the Gulf- of Mannar, in southern peninsular India, has been documented quite recently (Kannipiran and Ravindran 2012). As the neighbor joining boot-strap consensus tree brings out their phylogenetic heterogeneity (Fig. 3), the source of nearest isolates to the retreived *Bacillus* forms are also seen to be equally diverse: from extreme deep-sea sediment habitat to highly efficient bio-remediating strains. Further, as many as five isolates (SK256-S7; SK256-5; SK256-38 from active bloom and SS263-10 from declining

bloom) are potential candidates for new species designations, all retreived from 1/10 strength Zobell's medium. A surprising result among this group however, is the inability of all *Bacillus cereus* isolates to express amylase. The closest phylogenetic relatives to our *Bacillus cereus* in RDP-II database indicated toxin "cereulide" producing phylotypes [RIVM BC00068 (AJ577283); OH599 (AJ577286); BC00067 (AJ577282); A4-20-12 (AB591768)] and B204 (AJ577292)]. A review of *Bacillus* literature led us to confirm their inability to produce acid from salicin, a key phenotypic identifying feature of the toxic 'cereulide' producing emetic *Bacillus cereus* biovars, although tentative (Altayar and Sutherland 2006, Holt et al. 1994). The role of these possible emetic *Bacillus* biovars therefore, needs to be further screened for possible toxic effects on cultured *Noctiluca* (green). We opine that if bacteria are to play a decisive role in terminating such a high-biomass open-water bloom, covering such large area in the Arabian Sea, the relative abundance of those species should be also be substantially higher, if not the dominant flora. Retreived flora from green *Noctiluca* of NAS is however, conspicuous in the absence of the major reported algicidal genera from *Noctiluca* (green) belonging to *Marinobacter* spp. (Keawtawee T et al. 2011), atleast as the dominant culturable flora. We however detected the occurence of *Pseudoalteromonas* spp. and *Vibrio* spp. with a very low frequency in the declining phase.

Members of *Pseudomonas* spp. form the next major group of bacteria in the active phase (24%) and with a low relative abundance (8.3%) in the declining 'phase' of the bloom. The close phylogenetic and phenotypic relatedness among various species refrains us from referring most of these isolates to species level. However, a

comparison of the recent examination of detailed *Pseudomonas* 16SrDNA phylogeny shows that our isolates belongs to 2 distinct lineages (Mulet et al. 2010): (a) *P aeruginosa* lineage, represented by the *P stutzeri* group with two species identifiable as *P stutzeri*; SK256-33 and *P xanthomarina*; SK256-25-1; and (b) *P fluorescens* lineage, represented by the *P fluorescens* group with 9 phylotypes. Based on their closest relatives, the most probable placement of these phylotypes should be under any of the three subgroups: the *P fluorescens* subgroup, *P gessardii* subgroup and the *P chlororaphis* subgroup. The closest relatives of SS263-N1 of active and SS263-3 of declining bloom shows that *Pseudomonas* sp. PIL-H1, a siderophore producing strain having 99.59% similarity with *P chlororaphis* subsp. *aurantiaca* and capable of producing the broad-spectrum antibiotic 2,4-diacetylphloroglucinol (PHL), a major determinant in the biological control of a range of plant pathogens by many fluorescent *Pseudomonas* spp. (Keel et al. 1996). Further, closest members belonging to our Fluorescent *Pseudomonas* group are capable of producing bio-active compounds, degrade a host of organic hydrocarbons as indicated from their nearest phylotypes and are well-known to produce siderophores (Isnansetyo and Kamei 2009).

The dominant forms during the declining phase of the bloom were the *Shewanella* spp. (16.7%), phylogentically close with *S algae* and *S haliotis* group, forming mucoid orange to beige colonies on Zobell's and NASW medium. All isolates of *Shewanella* produced H_2S and failed to produce amylase. Members of the genus *Shewanella* are known to be highly versatile in respiring over a suite of organic and inorganic compounds including several radionuclides and metals and

therefore play an important role in carbon cycling (Fredrickson et al. 2008). *Shewanella* sp. are mostly retreived from chemically stratified communities with changing redox environments (Hau and Gralnick 2007). As Nawata and Sibaoka (1976) reports a highly acidic pH of *Noctiluca* flotation vacuole, a gradient in redox-potentials created during *Noctiluca* cell lysis can be highly suitable for members of *Shewanella* sp. to out-compete other microbes (Fredrickson et al. 2008). A drop in the water-column pH from 8.3 - 8.4 during the active bloom phase to 8.1-7.9 duirng the declining bloom phase (Table 1) further supports such a succession in favor of *Shewanella*.

Although, *γ-proteobacteria* remained the dominant class during the declining phase, the most commonly reported dominant members from algal blooms belonging to *Alteromonas* sp., *Alcanivorax* spp. and *Marinomonas* spp. (Green et al. 2004) were missing among our isolates. Instead, members of the genera *Cobetia, Halomonas, Psychrobacter and Pseudomonas* were identified in almost equal fractions during the "declining" phase.

Both *Cobetia* and *Halomonas* belong to the family *Halomonadaceae*. The high ability of the *Cobetia marina* isolates to produce phosphatase corroborates with published strains which also produces alkaline-phosphatase with a high-specific activity and are also regarded as 'specialized bacteria' appearing during algal-thallus degradation, due to their versatility in assimilating several by-products of polysaccharides (Ivanova et al. 2005). Retrieval of several *Halomonas* isolates were interesting and their phylogenetic closeness to those strains occuring in deep-sea

hydrothermal vents (group-2B) and other extreme deep-sea habitat provokes further interest to study these osmotically flexible physiotypes (Kaye et al. 2011).

Antibiogram

Apart from a taxonomic use of the antibiogram to study strain level proximity or dissimilarity among closely related isolates (Fig. 5), the results also show that these bacteria tend to display strong resistance to several antibiotics (Table 5). The change in the overall bacterial community from a dominant gram positive to gram negative forms should have essentially different antibiograms and this is also reflected in the overall resistance to different antibiotics (Table 5). Multiple resistance to antibiotics can affect bacterial population dynamics (Martinez 2006) and are also known to spread through horizontal /lateral gene transfers (Frost et al. 2005). Thus, the seasonal emergence of this bloom can give rise to strongly drug resistant flora in the Arabian Sea. As the bloom spreads across the entire Northern Arabian Sea basin - from coastal Oman to the shelf off Gujrat, such antibiotics-resistant microbes may also spread from fishing activities and be of human-concern.

4.3B Bacterial flora of *T erythraeum* bloom

Trichodesmium spp. have been difficult to maintain in axenic culture implying their essential dependence on their epibiotic bacteria while mucopolysaccharides surrounding *Trichodesmium* colonies forms an important nutritional source for bacterial proliferation (Sellner 1992). Fifty-five percent of both attached and free-living isolates grew anaerobically on thioglycollate media indicating their facultative nature. Culturable bacteria isolated from *Trichodesmium erythraeum* filaments were mostly gram-positive rods. Although uncharacteristic of

the normal marine flora, ability of most gram-positive bacteria to release extracellular enzymes more efficiently (Chrost 1991) can confer a selective advantage in the organic rich phycosphere of the *Trichodesmium* bloom. The dominance of rods in association with *Trichodesmium* however has been reported earlier (Nausch 1996) and was also observed in our epifluorescent image. Also, the higher occurrence of rods would provide a greater surface to volume ratios which can result in higher assimilation rates. Similar to the active phase bloom of *N miliaris*, the bacterial flora from *Trichodesmium* is also seen to be dominated by members of the *Bacillus* spp., whereas the γ-proteobacteria remained the least dominant. Further, several members of the phylum Actinobacteria belonging to *Corynebacterium* spp., *Microbacterium* spp. and *Leucobacter* sp., *Brachybacterium* sp. and *Salinibacterium* sp., constituting ~35% of the flora, appears to be important associates of the *Trichodesmium* colony. Since, the sample of bloom collected for isolation consisted of active/healthy filaments with high Chl *a* content as detected from HPLC and C-DOM signatures, they may play an important role in the bloom dynamics of *Trichodesmium* in the tropical waters of the Arabian Sea.

4.4 Salient results

Culturable bacterial counts from *Noctiluca miliaris* bloom in the Northern Arabian Sea during two consecutive cruises of Feb-Mar 2009, were ~2-3 fold higher in comparison to non-bloom waters and ranged from 3.20×10^5 - 6.84×10^5 CFU ml^{-1}. An analysis of the dominant bacteria associated with *Noctiluca* bloom resulted in retrieval of 70 phycospheric bacterial isolates from an overlapping active and declining bloom phase location near north-central Arabian Sea. The phenotypic charactersitics of the active phase flora were characterized by a higher percentage of gram positive forms (70.59%), highly motile (76.47%) and endospore forming rods (44.12%). In comparison, the declining phase flora was characterized by a significant reduction in gram positive forms (38.8%), motility (58.33%) and endspore forming rods (19.44%). Ability of isolates from the both the bloom phases to grow under anaerobic conditions remained similar and varied from 50 -47.2%. 16SrDNA phylogenetic and a detailed metabolic characterization helped assign isolates to their taxonomic levels of genera/species. 19 isolates from active phase were assigned to 15 different species constituting 55.8% of the active phase flora. During the declining phase 18 isolates were assigned to 14 different species constituting 50% of the flora. The remaining isolates were referred to the generic level / unassigned to genera based on 16SrDNA homologies with the nearest type strains. The active phase of the bloom was dominated by gram-positive forms of the genera *Bacillus* (35.29%) of *Firmicutes* and members of the fluorescent *Pseudomonas* group of the phylum *γ-proteobacteria* were the next dominant group, constituting 23.53% of the flora. During the declining phase Gram-negative forms (61.11%) were dominant and

they belonged predominantly to *γ-proteobacteria* represented by *Shewanella* (16.67%) and equal fractions of a *Cobetia-Pseudomonas-Psychrobacter-Halomonas* population (36.11%). The Shannon wiener index of generic diversity increased from 2.07 during active phase to 2.66 during the declining phase bloom of *N miliaris*. Principle coordinate analysis of 16SrDNA sequences using online Unifrac portal showed that active and declining bloom phase flora were significantly different which also differed from reported endocytic flora of *Noctiluca* (red). Antibiotic resistance patterns represented as a Non-parametric multidimensional (NMDS) scaling helped differentiation among closely related strains.

On the other hand, culturable counts from the *Trichodesmium erythraeum* bloom off Ratnagiri averaged 36±18.4×105 CFU mL−1 on Zobell's and 13.4±6.43×105 CFU mL−1 on Zobell's 1/10 strength media. The dominant flora from *Trichodesmium erythraeum* tuft colonies could be retrieved (21 isolates) along-with those isolated from the filtrate of colonies (6 isolates) and referred to as the phycospheric colonial forms. An overall predominance of gram-positive bacteria (85.7%) were observed among the colony associated/attached forms of which 57.14% were motile, 33.33% were endospore forming rods and 57.14% could grow anaerobically in thioglycollate broth. Of the free-living forms, 83.3% of the isolates were Gram positive, 66.67% were motile, 50% were endospore forming rods and could also grow in anaerobic conditions in the thioglycollate broth. 42.85% of the trichome associated isolates isolates could be assigned to 6 different species, whereas 33.33% isolates of the free-living forms were assigned

to two different species. Biochemical and 16SrDNA phylogenetic characterization showed that Firmicutes were the major phylum (47.62%) of the colony associated forms and were dominated by *Bacillus* spp. (28.57%), *Virgibacillus* (14.29%). Members of Actinobacteria constituted 38.09% of the flora and major representative genera were *Corynebacterium* (14.29%) and *Microbacterium* (9.52%). Members of *γ-proteobacteria* were the least dominant (14.28%) with *Halomonas* constituting 4.76% of the flora. The free-living forms were dominated in the order of *Bacillus* spp. (33.3%) and equal numbers of *Corynebacterium, Leucobacter and Shewanella* constituting 16.67% each of the population.

Chapter V

Phytoplankton Bloom –Microbe Relationship

The phytoplankton bloom-microbe relationship can be envisaged in light of the bloom ecosystem components. Such an approach takes into account relationship of retreived bacteria with its bloom source i.e. *N miliaris* and *T erythraeum,* in terms of bacterial enzymatic potentials to degrade/remineralize bloom organic matter, relationship with water-column nutrients and also the 'food-chain' as bacteria may bring back dissolved organics to support higher trophic levels (Microbial-loop). Further, as nearest phylogenetic neighbor of a large number of bacterial strains indicated Iron (III) binding siderophore producing capability (Chapter 4), it calls for examination of Iron acquisition via siderophores and their bioavailability during the bloom. Iron is an essential trace nutrient requirement for both bloom forming phytoplankton and bacteria, since it is required as an electron carrier and a catalyst during phytoplankton photosynthesis, to carry out carbon-metabolism, nucleic acid biosynthesis and as co-factors in enzymes, vitamin synthesis and for Nitrogen metabolism (Martin 1990, Morrisey and Bowler 2012). For the vast majority of oceanic provinces, it is now well known that Iron remains a limiting nutrient and affects bloom formation (Martin 1990, Morel et al. 1991, Rueter 1992, Boyd et al. 2007). Hence, the present chapter examines these metabolic/nutritional features of the retreived bacteria to decipher relationships of individual members as well as dominant phylogenetic clusters to the individual bloom particularly in regard to: (i) Nutrient cycle (ii) Food-chain and (iii) Acquisition of Iron under limiting conditions.

5.1 Materials and Methods

5.1.1 Enzymatic potential and nutrients

The enzymatic/metabolic potentials of bacterial flora (Chapter 4) with respect to water-column physico-chemical charactersitics (Chapter 2 and 3) was examined during bloom of *N miliaris* and *T erythraeum* to decipher relationships of individual members as well as dominant phylogenetic clusters to the individual bloom particularly in regard to Nutrient cycle. Available literature on nature of bloom organic-matter was taken into consideration and discussed in context of remineralizing potentials of the bacterial flora.

5.1.2 Utilization of dissolved carbohydrate

Utilization of dissolved carbohydrates from the <0.22 μm fraction of *Trichodesmium erythraeum* bloom by bacterial isolates was studied by the Anthrone-sulfuric acid method (Herbert, 1971). Fixed volumes of bacterial suspension were inoculated in 10 ml of the bacteria free *Trichodesmium* filtrate in duplicates and incubated upto 48 hours to measure the decrease in the total carbohydrate concentration.

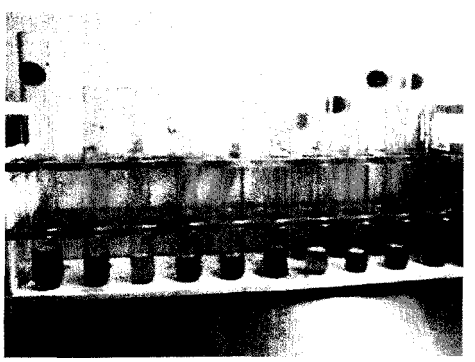

Plate 5.1 Anthrone-sulfuric acid test to measure dissolved carbohydrates utilization.

5.1.3 Evaluation of Food-chain

The trophic level relationship of bacteria, Nanoflagellate and *Noctiluca miliaris* in the food-chain were revisited from results projected in Chapter-2 and scrutinized in light of photomicrographic evidence, physiology of *N miliaris* and physico-chemical characteristics of the bloom.

5.1.4 Growth of bacteria in Iron-free media

A total of 97 bacterial isolates from blooms of the dinoflagellate green *Noctiluca miliaris* and the cyanobacteria *Trichodesmium erythraeum* were used to study their siderophore producing potentials.

A minimal composition of Iron-free succinate mineral salts (SMM) broth known to support high siderophore production was employed (Meyer and Abdallah, 1978). Since, most of the strains are marine halophiles, the SMM media was modified by adding 3.5% (w/v) NaCl. In addition, a nutrient rich deferrated composition of Nutrient-broth (Hi media, India) was prepared with 50% sea-water (D-NBS) was employed for 17 strains. Slants from refrigerated stock cultures were freshly streaked in Zobell's 2216E marine agar. A loop-touch from single colony was inoculated in 20 ml quantity of SMM medium or D-NBS and left shaking at 220 rpm at 25°C in a temperature controlled shaker. 1.5 ml of the culture was removed at 5 hr, 10 hr and 30 hr interval in the screening phase. 500µl ml of the culture broth was used for recording absorbance at 600 nm and 540 nm to record growth. 500µl of the cultures broth was centrifuged in acid-cleaned eppendorfs and supernatant was also stored at 4°c separately for checking presence of siderophore for positive cultures.

5.1.5 Quantitative Assay for Iron binding Siderophores

The modified Chrome Azurol S (CAS) assay was performed (Alexander and Zuberer 1991). Before assay, 5-sulfosalicylic acid was added as a shuttle solution to facilitate exchange of Iron between the CAS and the supernatant. Following growth of 60 hours, 1.5 ml of the culture broth was centrifuged and the supernatant was added to 1.5 ml of the CAS reagent. The mixture was incubated for an hour for probable siderophores to chelate Fe (III) from the CAS (containing 1 mM Iron) with a change in colour of the mixture from blue to orange. Absorbance was measured at 630 nm and the decrease in absorbance of the supernatant from the CAS reagent blank at 630 nm indicated chelation of Iron by siderophore and selected as positive strains.

This was expressed as the Percent Siderophore Production, defined as:

Percent Siderophore Unit = [(Ar - As)/Ar] x 100

Where, A_r is the absorbance at 630nm of reference (CAS assay solution+ SMM media) and A_s is the absorbance at 630nm of the sample. Supernatant from 0 - 30 hours interval, previously stored in the refrigerator were further selected for those culture broths showing a final time positive CAS reading. The siderophore standard Deferoxamine mesylate (DFOM) was also used. 1.5 mM stock of DFOM was diluted from 0.1 - 150 µM with ultra-pure MiliQ water. Prior to samples assay, the standard was run by adding 1.5 ml of CAS reagent containing shuttle solution, left to equilibrate for 1 hour and measured exactly as the sample. The concentration of siderophores from DFOM was calculated from a standard graph and expressed in units of µM DFOM equivalents.

Further, UV/Vis absorbance (200 – 800 nm) was noted for culture broths showing pigmentation and a positive CAS assay.

5.1.6 Growth of *P gessardii*, ^{GUSK256}-N6 under Iron limitation

5.1.6.1 Effect of Temperature and pH on Siderophore production

The most efficient isolate *Pseudomonas gessardii*, ^{GUFB}SK256-N6 (Accession No. JX429834), marked during the screening was selected for further studying the effect of temperature and pH on siderophore production in SMM media. Keeping in sea-surface temperature changes of NEAS from February to April, the strain was grown at 25°C and 29°C at pH 7.0 and 8.2, respectively. A loop-touch of inoculum was initially acclimatized in 5 ml broth of SMM to pH7, 7.6 and 8.2 for 6-hours at 25°C by shaking at 180 rpm. 1 ml (~OD = 0.1) was inoculated in 100 ml SMM broth. Growth was monitored upto 72 hours and every 6 hours OD was noted at 600 nm, 540 nm and 400 nm from 1.5 ml of culture diluted in 1:1 proportion with MiliQ water. The concentration of siderophore was calculated as given by Gupta et al. 2008 using extinction coefficient of 16,500 and expressed as:

Siderophore Concentration ($\mu g\ L^{-1}$) = (OD x 1500 x 1000) / 16500.

5.1.6.2 Growth in Noctiluca bloom filtrate (CFNB)

To check the possible ability of bacteria to grow on slime produced during bloom by *Noctiluca miliaris*, a refrigerated(2°C) crude filrate of the bloom containing *N miliaris* cells (~150 ml quantity), collected during the

active phase bloom period of February 2009 at station O-1 (Chapter 2.1a) was used for this purpose. The colloidal slime was decanted and passed repeatedly through syringe to homogenize. This resulted in a straw coloured liquid, which was centrifuged in acid-washed 50 ml sterile tubes (Tarsons). The pH was adjusted to 7 using 50% KOH and the entire volume was filter sterilized using 0.22 μm capsule filters in 100 ml quantities in sterile flasks. A scan of this crude-filtrate (CFNB) was taken immediately as control. The *P gessardii*, ^{GUFB}SK256-N6 was inoculated after acclimatizing to a 5 ml quantity of the CFNB containing 0.001%v/v succinate as initial boost for 2 hours, and then grown by shaking at 180rpm for 6 hours and 1 ml was inoculated in the CFNB broth at 25°C. Growth was monitored as described earlier.

5.2 Results and Discussion

5.2.1 Relationship of enzymic potential of flora with bloom nutrients

5.2.1A Ecosystem of dinoflagellate N miliaris bloom

The biochemical nature of the bloom organic matter can play an important role in selection of its bacterial associates (Azam and Malfatti 2007, Sapp et al. 2007). The green variant of *Noctiluca* are hosting *Pedinomonas noctilucae* as symbionts, which are Chl *a* and Chl *b* bearing prasinophytes and this makes green *Noctiluca* mixotrophic. The organic matter produced by this symbiont will be similar to the labile photosynthetic products rich in carbohydrates, amino-acids and fatty-acids. The high photosynthetic carbon fixation rates and production of dissolved organic matter containing mycosporine like amino acids as seen from the C-DOM estimates, indicates the high organic turnover of the bloom (Chapter 2). Few studies show that *Noctiluca miliaris* basically consists of starchy substrates (Sweeny 1971), sterols, free-fatty acids, triglycerides and ~26% phospho-lipids (Dikarev et al. 1982), and proteins/ amino-acids and produce mucus (Kirchner 1996). A detailed biochemical analysis of the mucilage of the green variant of *Noctiluca* has neither been performed by us nor at present available elsewhere. Further, *Noctiluca miliaris* is reported to have a CN content varying from 123-627 ngC $cell^{-1}$ and 36-232 ngN $cell^{-1}$ with a C: N ratio of 2.3- 4.4. These wide variations are attributed to their avaialable phagotrophic feeding habitat (Tada et al. 2000, Hansen et al. 2004). The possible functional role of these diverse bacteria

retreived from the major overlapping location (station O-1) of the two -bloom phases of *N miliaris* of Feb-Mar 2009 was indicated from their metabolic characteristics to utilize a host of carbohydrates, proteins and amino-acids, lipids, urea, solubilize phosphates, produce H_2S from organic-matter and reduce nitrate/denitrify. The contribution of bacterial genera to degrade complex organic substrates was over-whelming as several of these bacteria expressed multiple hydrolytic enzymes (Table 5.1, Fig. 5.4)

5.2.1.1 Hydrolysis of complex substrates

Carbohydrate degradation

Amylase producers were frequent and decreased from 50% during the active to 38.89% during the declining phase of the bloom (Table 5.1). Most frequent amylase producers belonged to the phylum *Actinobacteria*. All Actinobacterial members except *Dietzia schimae* (SS263-19) produced amylase during both-phases of the bloom. It was interesting to note that all members belonging to *Bacillus cereus* (SK256-17; SK256-22; SK256-20 and SS263-34) failed to produce amylase. Several of *γ-proteobacterial* amylase producers in the declining bloom phase were more strongly amylolytic and belonged to *Cobetia marina* (SS263-N5), *Halomonas axialensis* (SS263-24) and *Vibrio campbelii* (SS263-31) which also exhibited the highest zone (4.1cm) on starch plates.

Frequencies of cellulose degraders were low and varied from 20.59% during active phase to 13.89% during the declining phase. Dominant cellulose

producers in the active phase were *Firmicutes* members belonging to *Bacillus* spp. In the declining phase cellulose was hydrolyzed by *Pseudomonas* sp. (SS263-6), *Shewanella* sp. (SS263-9) and *Ochrobactrum* sp. (SS263-38A) of the α-Proteobacteria.

Protein degradation

Proteolytic bacteria were frequently detected during both bloom phases. Isolates expressing caseinase were equally dominant (55.88% - 58.34%) during both phases of bloom. Species belonging to *Bacillus* including all isolates of the *Bacillus cereus* group, *Virgibacillus, Oceanobacillus* and *Brevibacillus* were strongly proteolytic in the active phase. As the bloom declined, members of the genus *Pseudomonas, Cobetia, Psychrobacter* and *Halomonas* were important protease producers along with *Bacillus* spp. (Table 5.1).

In comparison, gelatin liquefiers decreased from 61.76% in active to 38.89% during the declining phase. Ability to degrade gelatin remained dominant among members of *Firmicutes* during both the active (36%) and declining (20%) phases of the bloom (Table 5.1)

Lipids degradation

Frequency of Tributyrin degraders were low (26.47%-30.56%) in comparison to Tween-80 degraders (52.94%-61.11%) during the bloom phases. γ *-proteobacterial* forms were strong lipase producers and majority of them belonged to the Fluorescent *Pseudomonas* spp. group (Table 5.1)

Table 5.1 Remineralization potentials of bacterial genera indicated from substrate utilization by isolates as percentage contribution to bacterial flora from *Noctiluca miliaris* active (declining) bloom.

Bacterial Genera	Hydrolysis of polymeric carbon substrates						Nitrogen transformations			Phosphate Solubilization	Sulfide Production
	Carbohydrates		Proteins		Lipids		Urea Hydrolysis	Nitrate reduction	Denitrification (Aerobic)		
	Starch	CM-Cellulose	Casein	Gelatin	Tributyrin	Tween-80					
Ochrobactrum		(2.7)	(2.7)			(2.7)	(2.7)	(2.7)	(2.7)		
Shewanella		(2.7)	(5.5)	(13.8)	(11.1)	(13.8)	(11.1)	(16.6)	(11.1)	(13.8)	(16.6)
Halomonas	2.9 (5.5)		(5.5)			2.9 (2.7)	(2.7)	(2.7)		2.9 (5.5)	2.9 (5.5)
Providencia			2.9			2.9		2.9			
Cobetia	(2.7)		(11.1)					(11.1)		(11.1)	
Psychrobacter			(8.3)			(8.3)		(8.3)	(8.3)	(8.3)	
Pseudoalteromonas	(2.7)		(2.7)	(2.7)		(2.7)					
Vibrio	(2.7)			(2.7)	(2.7)	(2.7)		(2.7)		(2.7)	
Pseudomonas	5.9 (2.7)	2.9 (2.7)	8.8 (2.7)	2.9	17.6 (8.3)	14.7(8.3)	11.76 (5.5)	23.5 (8.3)	23.5 (8.3)	17.6 (8.3)	2.9
Leucobacter				(2.7)	(2.7)	(2.7)	(2.7)				
Kocuria	(2.7)	(2.7)	(2.7)					(2.7)		(2.7)	
Brachybacterium	2.9 (2.7)							2.9 (2.7)		2.9 (2.7)	2.9 (2.7)
Dietzia	(2.7)					(2.7)	(2.7)	(2.7)			
Microbacterium	2.9 (2.7)		(2.7)	2.9				(2.7)		2.9 (2.7)	2.9 (2.7)
Micrococcus	5.9			5.8		5.8		2.9		5.8	
*Micrococcaceae**	2.9		2.9	2.9							
*Intrasporangiaceae**	2.9			2.9	2.9	2.9	2.94	2.9	2.9	2.9	
Brevibacillus			(2.7)	(2.7)				(2.7)	(2.7)		
Staphylococcus	(2.7)			2.9 (2.7)	(2.7)	2.9		(2.7)			
Virgibacillus	(2.7)		5.9	5.8 (2.7)				5.8 (2.7)	5.8 (2.7)		
Exiguobacterium	2.9	2.9	2.9	2.9				2.9		2.9	
Oceanobacillus			2.9	2.9	2.9	2.9		2.9			
Bacillus	17.6 (5.5)	14.7 (2.7)	26.4 (8.3)	26.4 (5.5)	2.9 (2.7)	14.7 (8.3)	14.7 (5.5)	26.4 (5.5)	17.6 (5.5)	14.7 (5.5)	
*Planococcaceae**	2.9		2.9 (2.7)	2.9 (2.7)		2.9 (5.5)	(2.7)	(5.5)			
Active (Declining)	**50 (38.8)**	**20.5 (13.8)**	**55.8 (58.3)**	**61.7 (38.8)**	**26.4 (30.5)**	**52.9 (61.1)**	**35.2 (52.7)**	**73.5 (83.3)**	**50 (41.67)**	**52.9 (63.8)**	**11.7 (27.7)**

*Unassigned genera

5.2.1.2 Phosphate solubilization

A large fraction of the flora (52.94%-63.89%) could solubilize Tricalcium-phosphate during both the bloom phases and dominant phosphate solubilizers belonged to *γ-proteobacterial* forms (Table 5.1). Members of *Cobetia marina* along with the Fluorescent *Pseuodomonas* group were detected as strong phosphatase producers. However, as many as 8 out of 12 Actinobacterial isolates also produced phosphatase during both bloom phases and were also important (Table 5.1).

As seen in Table 5.2, high dissolved inorganic phosphate is recorded from surface waters of active bloom in comparison to the water-column, with phosphate depletion during the latter stages of bloom (Fig. 5.2). The relationship between bacterial and phosphate solubilization is refelected in an excellent correlation between total bacterial counts and dissolved inorganic phosphate (R^2 = 0.829) during the active bloom of February 2009 (Fig. 5.1). This indicates the impact of the large fraction of phosphate solubilizing bacteria to release inorganic phosphates as they utilize/grow on the active bloom originated organics. Such trends in phosphate regeneration have also been noticed during red *Noctiluca* blooms (Montani et al. 1998). These bacteria predominantly belonged to the genera *Pseudomonas, Kocuria, Halomonas, Micrococcus, Microbacterium, Brachybacterium, Bacillus* and unclassified members of the family Intrasporangiaceae and Micrococcaceae (Table 5.1).

Table 5.2 Water-column characteristics at the overlapping 'active' and 'declining' *Noctiluca miliaris* bloom station in Northeastern Arabian Sea

Hydrological characteristics	**Active phase Feb-09 Surface (Mean±SD)***	**Declining phase Mar-09 Surface (Mean±SD)***
Wind-speed (m sec^{-1})	4.1	3.7
Temperature (^{o}C)	25.12 (24.91±0.13)	27.62(25.57±0.69)
Salinity (psu)	36.48 (36.51±0.01)	36.58(36.55±0.03)
pH	8.3 (8.35±0.2)	8.11 (8.17±0.16)
Dissolved Oxygen (ml L^{-1})	3.06(2.95±0.07)	2.71(2.94±0.28)
Dissolved Inorganic Nutrients:		
Nitrate (μM)	0.54 (0.79±0.27)	0.02 (6.86±7.78)
Nitrite (μM)	0.65 (0.77±0.13)	0.08 (0.12±0.05)
Phosphate (μM)	5.23 (1.82±1.64)	0.64 (1.29±0.86)
Silicate (μM)	19.79 (14.8±3.58)	1.77 (5.56±5.09)
Primary-Productivity (mgC m^{-3} day^{-1})	1426.93 (798.32±1112.96)	469.53 (160.24±179.75)
C-DOM (Ac 300 m^{-1})	1.14 (2.48±1.45)	0.61 (0.81±0.32)
Chlorophyll *a* (mg m^{-3})	27.7 (7.46±9.36)	0.99 (0.65±0.28)
Noctiluca counts (cells L^{-1})	9600 (2459±3588)	80 (45±41)

*(Mean±SD) is euphotic zone average.

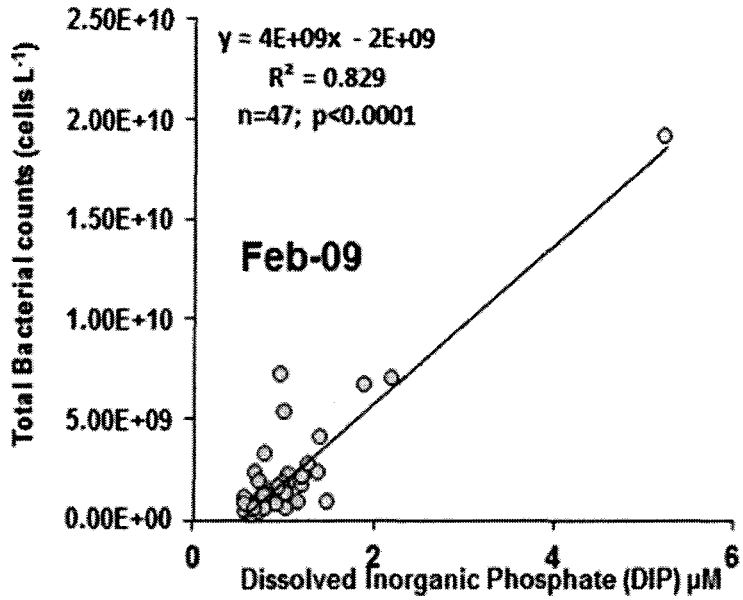

Fig. 5.1 Relationship between total bacterial counts and dissolved inorganic phosphate during active blooms of *N miliaris*, Feb-2009.

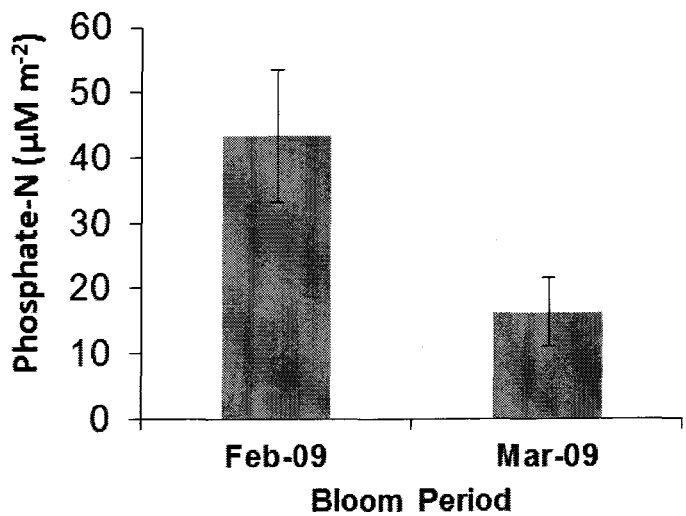

Fig. 5.2 Depletion of euphotic column phopshate from active to declining bloom phase of Feb-Mar 2009.

5.2.1.3 Nitrogen metabolism and Denitrification

Percentage of isolates able to break-down urea to produce ammonium in organic medium increased from 35.29% during active phase to 52.78% during the bloom declining phase. Dominant urea degrading bacteria of the active phase were *Bacillus* and *Pseudomonas*. In the declining phase, urea hydrolysis was exhibited by several other genera of *Pseudomonas*, *Shewanella, Halomonas and Psychrobacter* of γ-proteobacteria, *Dietzia* of the Actinobacteria and also *Bacillus* (Table 5.1, Fig. 5.4).

Ability to reduce nitrate (73.53%-83.33%) was wide spread and more significantly a large fraction (50% - 41.67%) of both the active and declining phase strains were denitrifying under aerobic conditions as well (Table 5.1).

A large number of strains showed denitrifying potentials under aerobic conditions which varied from 50% during the 'active' bloom to 49.67% during the declining bloom. These strains belonged to members of genera *Bacillus, Pseudomonas, Exiguobacterium, Virgibacillus* and unclassified members of intrasporangiaceae during the 'active' phase of February 2009. During the declining phase of March 2009, the members of *Pseudomonas, Bacillus, Shewanella, Halomonas* and *Virgibacillus* showed ability to denitrify under aerobic conditions. The ability to aerobically denitrify nitrate (Varbaendert et al. 2011), a trait which is coming to light only in recent times (Xiao et al. 2011, Zhang et al. 2011) is also indicated from the removal of nitrite from the active to the declining phase (Fig. 5.3) and hence, they can play an important role in nitrogen removal during the high-organic bloom of *Noctiluca miliaris*.

Desulfurase activity

H_2S production from organic matter increased from 11.76% during active to 27.78% during declining phase as all members of *Shewanella* produced H_2S (Fig. 5.4).

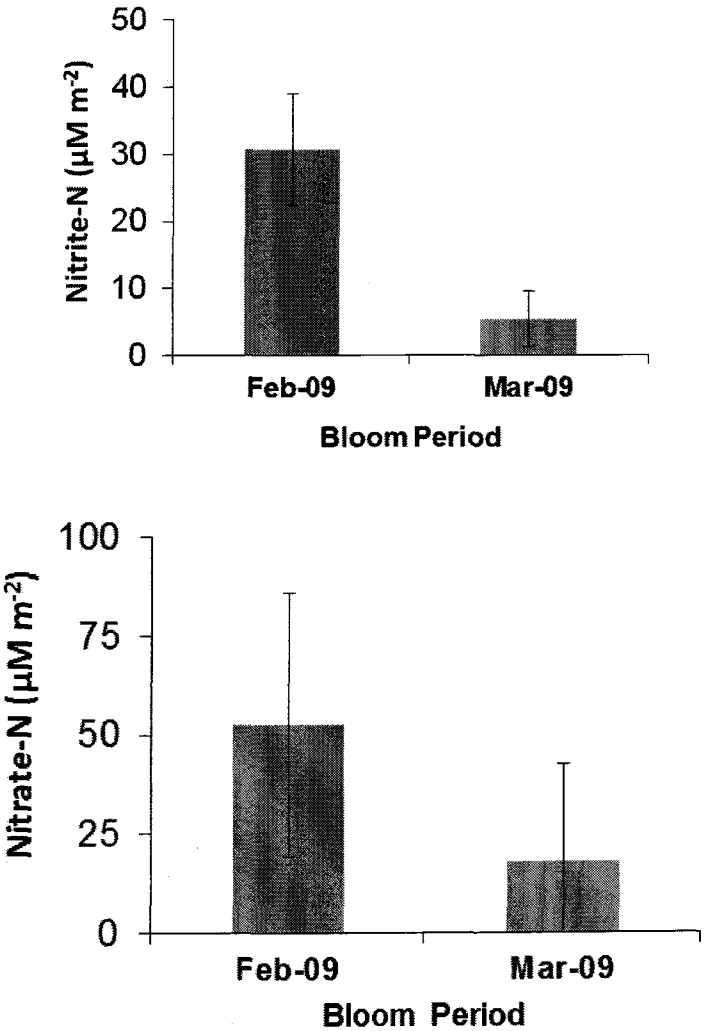

Fig. 5.3 Nitrate-N and Nitrite-N depletion in euphotic column from 'active' to 'declining' phase of March.

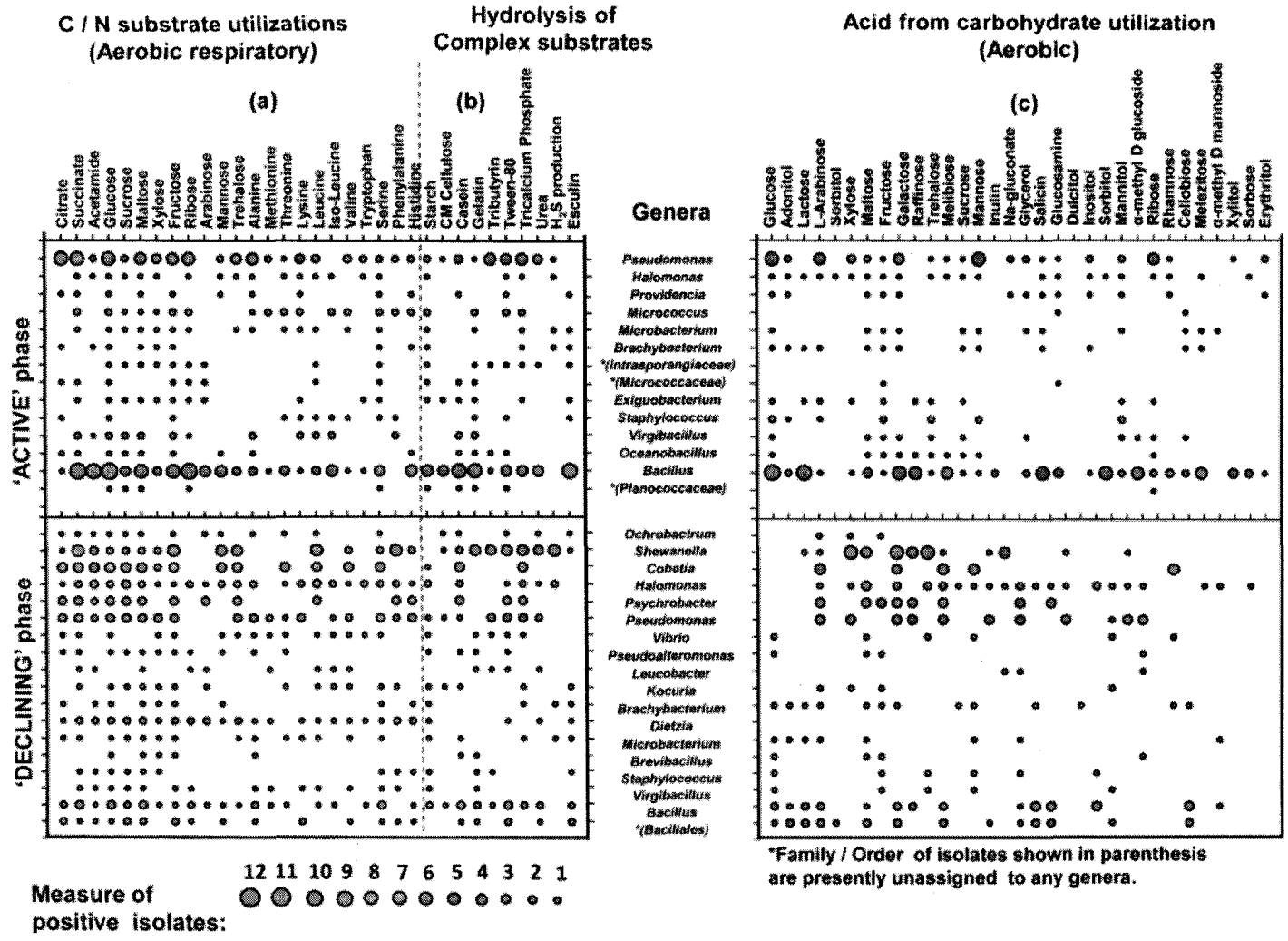

Fig. 5.4 Metabolic potentials of active and declining phase bacterial flora: (a) Utilization of carbon/nitrogen as sole sources (b) Hydrolysis of extracellular compounds and H_2S production on organic-matter breakdown (c) Utilization of carbohydrates with acid production under aerobic conditions.

5.2.1B Ecosystem of Trichodesmium erythraeum bloom

5.2.1B.1 Hydrolysis of complex substrates

In comparison, to the genesis of *N miliaris* bloom following nutrient enrichment of winter cooling, blooms of Nitrogen-fixing cyanobacteria *Trichodesmium* are favored in the warmer (>27°C) nitrate depleted and shallow stratified conditions in the Arabian Sea. Blooms of *Trichodesmium* do not attract grazers or fisheries (Sellner 1992), and hence the high bacterial aggregation in colonial space of *Trichodesmium* spp. as demonstrated in this study will be solely responsible for its remineralization and subsequent enrichment of the water-column (Table 5.3).

On considering the total flora of free-living and colony associated forms, the enzyme activity of the bacterial isolates showed a very high frequency of amylolytic activity (60%). The starch hydrolysis zones were not always clear and had reddish to pinkish tinge which indicates the different types of amylases that these isolates may produce as they breakdown starch polymers to dextrins. The starch hydrolysis zones for the *Trichodesmium* associated bacteria varied between 3-0.5 cm compared to that of 2-0.8 cm for the free-living bacteria The genera wise enzymatic potentials of the colony associated and free-living forms shows that members of *Bacillus* and *Corynebacterium* were the dominant metabolic groups associated with *Trichodesmium erythraeum* (Table 5.3). Percentages of only the colony associated flora to enzymatically degrade and utilize polymeric carbon substrates varied from: 57.14% exhibiting starch hydrolysis, 47.61% degrading casein, 23.8% hydrolysing gelatin and 33.3% degrading tributyrin. Measurements of enzymatic activities of

associated bacteria with *Trichodesmium* had led to an earlier conclusion that the free-living forms are more important than the colony associated forms (Nausch 1996). Our results indicates that, the attached / colony associated forms play an important role in processing polymeric carbon substrates during the bloom. The metabolic potentials of the flora also showed their importance in the nitrogen transformations as 76.19% of the isolates reduced Nitrate out of which 28.57% showed ability to denitrify under aerobic conditions. Further, 25.57% of the flora belonging to members of *Bacillus, Halomonas* and *Pseudomonas* also showed ability to solubilize inorganic phosphate and this may of importance in the availability of phosphate which has been seen to be an essential requirement for the growth of Trichodesmium to bloom proportions. However, it remains to be further studies, whether these isolates from both *N miliaris* and *T erythraeum* have the ability to release phosphate from the possibly phosphate rich bloom organics in the phycospheric environment of the bloom and can make P-Phosphorous readily available. Decomposition of *Trichodesmium* blooms at surface are commonly known to be associated with H_2S production in the Arabian Sea (Devassy et al. 1979). The retrieval of the well-known H_2S producing species *Shewanella algae* from the phycospheric space suggests their involvement and probable dominance during such decomposition processes.

Table 5.3 Remineralization potentials of bacterial genera indicated from substrate utilization by *Trichodesmium erythraeum* colony associated (free-living) isolates as percentage contribution to bacterial flora.

Bacterial Genera	Hydrolysis of polymeric carbon substrates				Nitrogen transformations			Phosphate Solubilization	Sulfide Production
	Carbohydrates	Proteins		Lipids	Urea	Nitrate	Denitrification		
	Starch	Casein	Gelatin	Tributyrin	Hydrolysis	reduction	(Aerobic)		
Shewanella					(16.6)				(16.6)
Halomonas	4.76				4.76	4.76		4.76	
Pseudomonas						4.76		4.76	
Corynebacterium	14.29	9.52	9.52	4.76		4.76			
			(16.6)						
Leucobacter		4.76			4.76	4.76			
	(16.67)	(16.6)			(16.6)				
Salinibacterium	4.76			4.76					
Microbacterium	4.76				9.52	4.76			9.52
Bacillus	14.29	23.81	4.76	14.29	9.52	23.81	9.52	14.29	
	(33.3)								
Virgibacillus	4.76	4.76	9.52	4.76		14.29	9.52		
Staphylococcus	4.76			4.76	4.76	4.76	4.76		
Brachybacterium					4.76	4.76	4.76	4.76	4.76
*Bacillaceae**	(16.67)	(16.6)		(16.6)		(16.6)	(16.6)		
*Halomonadaceae**	4.76	4.76		(16.6)	4.76	4.76			
Colony (Free-living)	**57.14 (66.5)**	**47.61 (33.3)**	**23.8 (16.6)**	**33.3 (33.3)**	**42.84 (33.2)**	**76.19 (16.6)**	**28.57 (16.6)**	**25.57**	**14.28 (16.6)**

*Unassigned genera

5.2.1B.2 Utilization of dissolved carbohydrates

Ability of the cultured isolates to utilize dissolved carbohydrates varied from a maximum of 1.84μgC hr^{-1} to 0.18 μgC hr^{-1} (Fig. 5.5). Bacterial strains belonging to Bacillus sp., ^{GUFB}Sama06-19 and member of an unclassified *Bacillaceae*, ^{GUFB}Sama06-19 showed highest ability to utilize dissolved carbohydrates and expressed multiple hydrolytic enzymes. However, some of the strains showed ability to utilize carbohydrates from crude filtrates, amylolytic activity was not seen and suggests other forms of glucosidases expressed by these bacteria.

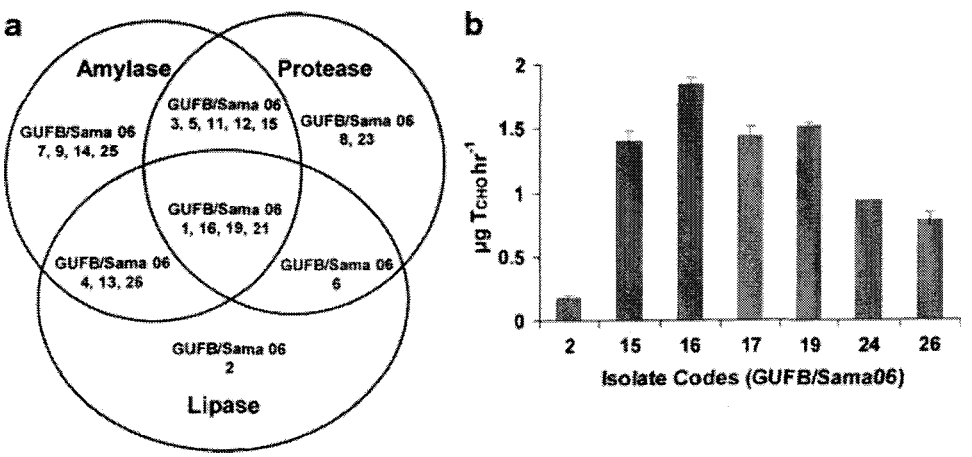

Fig. 5.5 *Trichodesmium erythraeum* associated bacterial isolates: (a) producing extracellular enzymes and utilizing dissolved carbohydrates from the bloom filtrate.

5.2.2 Clearance of bacteria from *N miliaris* food-chain

Total bacterial load estimated during blooms of *N miliaris* suggests that there is a decrease in counts as the bloom progressed into the declining phase from February-2009 to March-2009 of the consecutive sampling season (Chapter 2). On checking counts of the Heterotrophic nanoflagellates (HNF) during declining phase of March-2011 we further found that there is no significant inflation in the HNF population at latter stages of the bloom in comparison to the inflation in bacterial counts, which can result in quick clearance of bacterial cells from water-column. Instead, both bacteria and HNF tends to be negatively correlated/weakly correlated during the latter phases of the bloom (Fig. 5.6; Fig. 5.7). These results therefore do not suggest a strong 'microbial-loop' which can result in such quick clearance of bacterial population, known to be important in the Arabian Sea to sustain the biomass of the filter-feeding mesozooplankton Salps (siphonophores), following the winter diatom blooms from the Arabian Sea (Madhupratap et al. 1996). Swarms of Salps during this period have also been reported to exert strong grazing influence in restricting diatoms to bloom proportions during the month of February (Naqvi et al. 2004).

Examination of DAPI stained photomicrographs during our study suggests that there is particles formation colonized by bacteria as the bloom progresses, alongwith with a surprising reduction in total bacterial counts as clearly detected at the overlapping station O-1 (Fig. 5.7). Photomicrographic evidence further shows extensive phagotrophy by *Noctiluca miliaris* (Fig. 5.9).

Studies on the physiology and feeding habitat of *N miliaris* suggests that being a large sized dinoflagellate, *N miliaris* can feed on everything in its size range (Kiorbe and Titelman 1998, Kirchner 1996). The green form of *Noctiluca* with its photosynthetic symbiont is also highly mixotrophic (Sweeny 1979; Elbrachter and Qi 1998, Saito et al. 2006). *N miliaris* is well-known to be 'raptorial-feeder' of diatoms, dinoflagellates, bacteria, detrital particles, etc (Kirchner 1996, Kiorbe and Titlelman 1998).

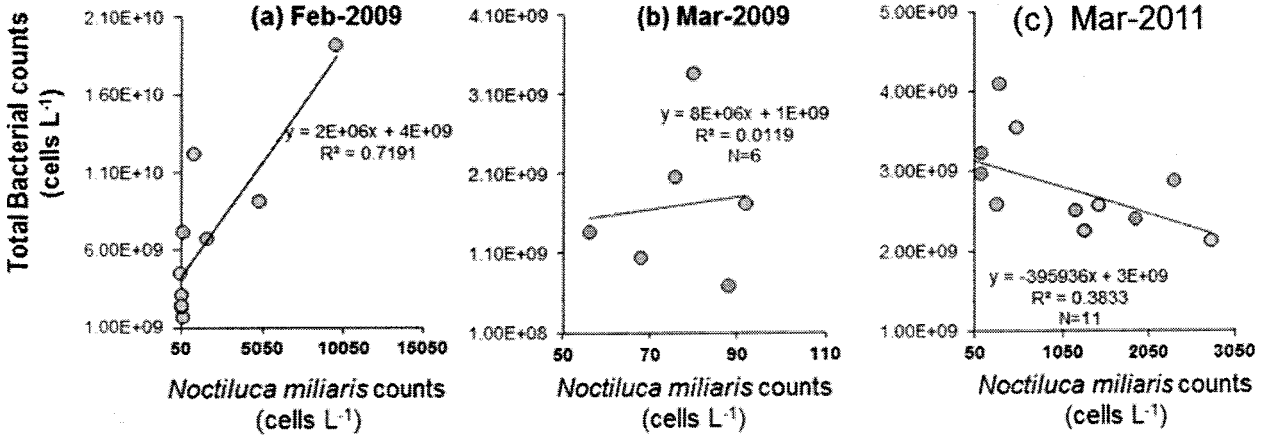

Fig. 5.6 Relationship between bacterial counts with > 50 cells L^{-1} of *N miliaris*.

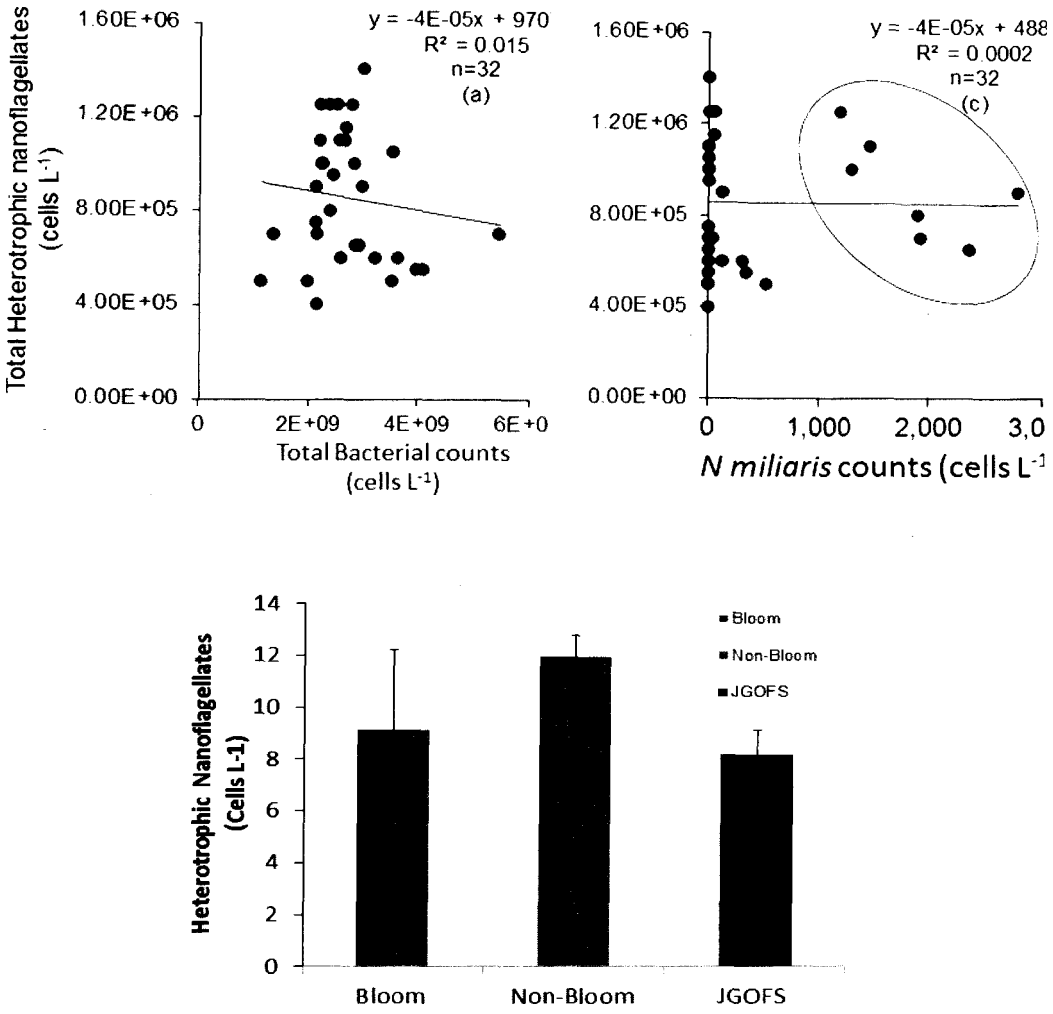

Fig. 5.6 Relationship of HNF population with: (a) total bacteria (b) *N miliaris* counts and (d) comparison of average counts with earlier data (JGOFS studies, 1990's) from bloom areas of the Northern Arabian Sea.

In this case of the mixotrophic green variety of *Noctiluca* blooms from the Arabian Sea, particles colonized by bacteria (Fig. 5.7) during March would be a rich nutritional source when warming of temperature and prey/nutrient limitations created unfavorable conditions. Such an additional pathway of the food-chain may probably explain the quick clearance in bacterial population

due to phagotrophic *Noctiluca,* and also help in further sustaining the bloom for a short-while during unfavorable conditions of March (Fig. 5.10).

On considering viral attack, and/or the rapid sinking of particles during the demise of the bloom as other possibilities for bacterial clearance, we found that use of sediment traps (personal communication to JI Goes) does not suggest that the organic material of the bloom is exported out of the euphotic zone even below <60-80 m. This is probably true, as the gelatinous/slimy nature of *N miliaris* aggregates may not counter the buoyancy required to sink as in cases of episodic sinking of aggregates formed from silicate shells of diatoms or that of the calciferous shells of the Coccolithophores, following their large scale blooms in the North-Atlantic and in the Southern Oceans (Smetacek 1985; Alldredge and Gotschalk 1989). With trapped particles inside the euphotic zone and fast nutrient depletion in the upper ocean (Fig. 5.2 and 5.3) due to shoaling of mixed layer during March, this additional pathway hijacking the 'microbial-loop', wherein: bacteria colonized particles are being fed by *N miliaris* as source of nutrition, appears to be the most feasible explanation for the sudden decrease in bacterial counts detected during the declining phases of Feb-Mar 2009 bloom.

Further, such clearance of colonized particles by bacteria would further constrain nutrient regneration through other mechanisms such as possible viral lysis (Balch et al. 2002) and probably helps in sustaining the bloom 'for a short while' during the unfavorable conditions as the bloom progresses into the declining phase.

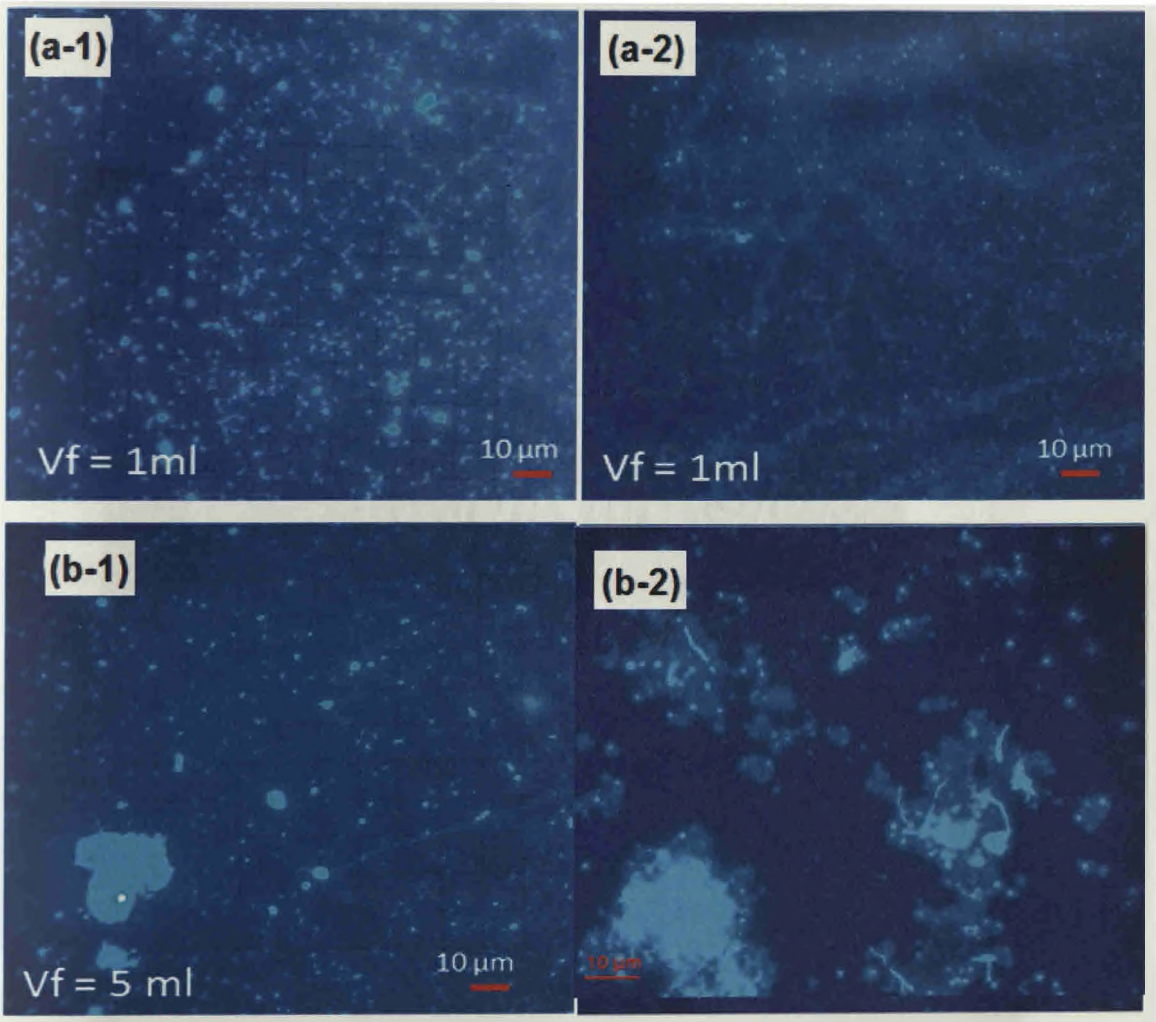

Fig. 5.8 DAPI stained photomicrographs showing bacteria at the major bloom station O-1: (a1-2) active phase of Feb-2009 and (b1-2) declining phase of Mar-2009 showing particles formations colonized by bacteria.

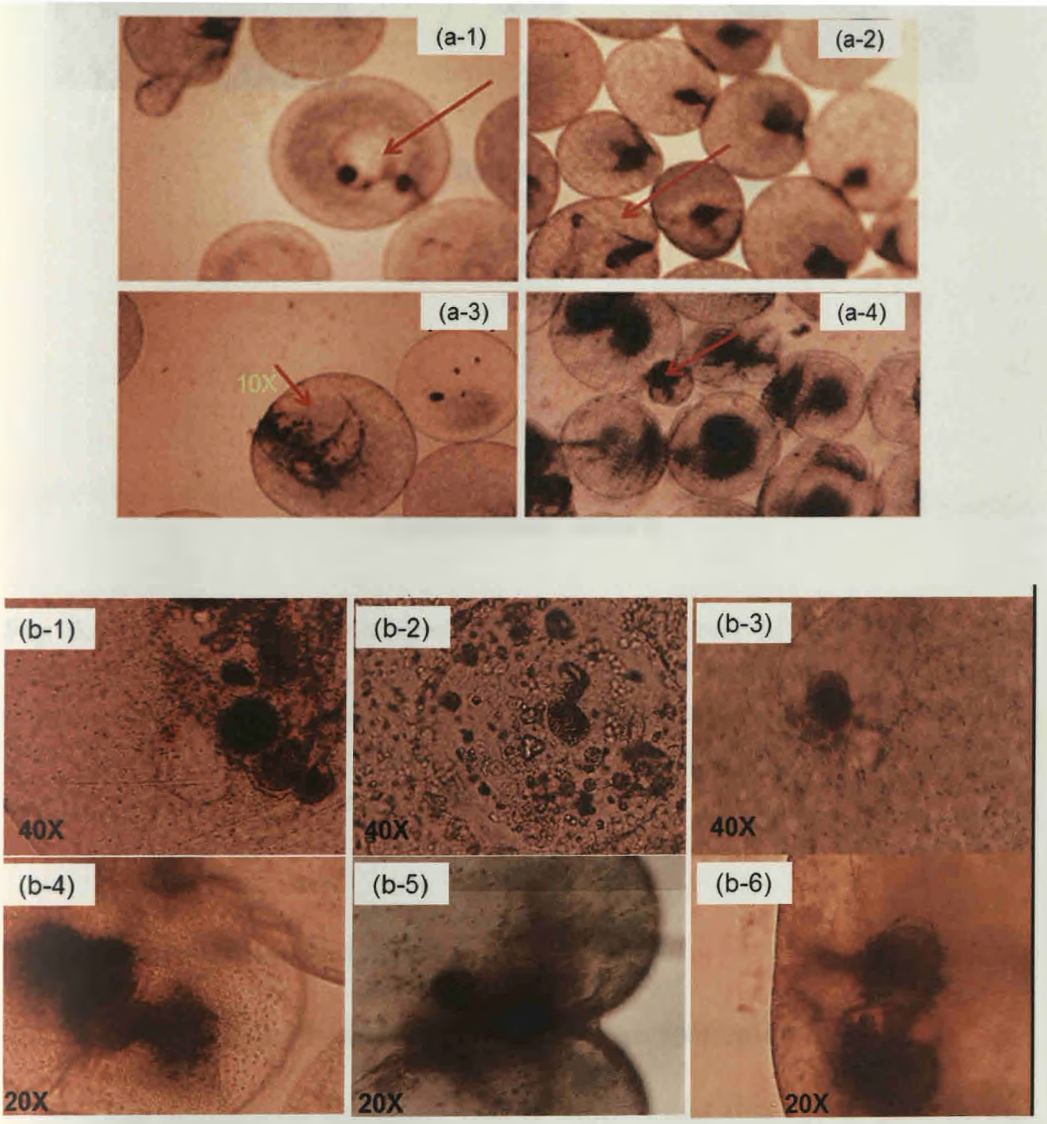

Fig. 5.9 (a1-a4) Phagotrophy by *N miliaris* and (b1-6) observations of food-vacuole during declining bloom phases of bloom.

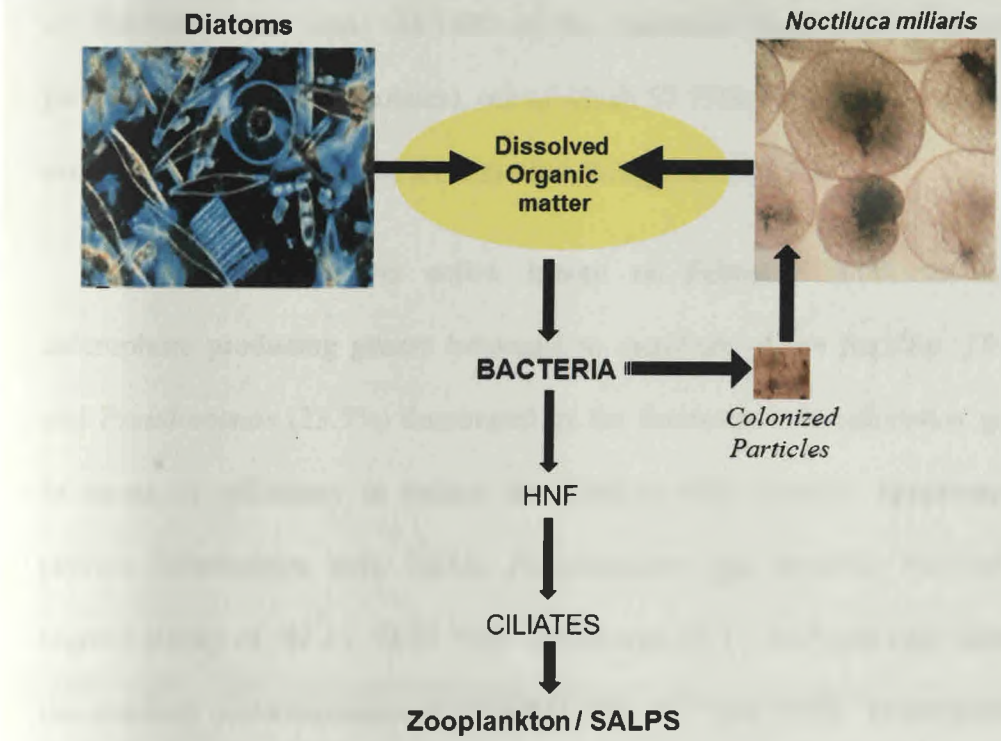

Fig. 5.10 Alterations depicting only the microbial part of food-chain during bloom of *N miliaris*. Phagotrophy on colonized particles by *N miliaris* strongly indicates hijacking / constraining the role of microbial-loop (DOM-Bacteria-HNF-Zooplanktons) to pass on nutrition from bloom DOM to support higher trophic levels during the declining phase bloom.

5.2.3 Iron acquisition by bacteria

5.2.3.1 Siderophorogenesis by micro-flora of phytoplankton blooms

The quantitative screening results showed that siderophorogenesis was highly frequent among bacteria associated with blooms of both *N miliaris* and *T erythaeum* (Fig. 5.11-5.12) on the iron-free succinate (SMM) and also for the strains grown on deferrated nutrient sea-water (DFNB) media. Fraction of siderophore producers varied from 76.47% during the active bloom (Feb-2009) to 69.89% during the declining bloom (Mar- 2009) of *N miliaris*. During bloom

of *Trichodesmium* spp., 48.14% of the bacterial flora were siderophore producers (13 out of 27 isolates), out of which 57.13% were colony / trichomes associated and only 16.67% were the free-living forms (Table 5.5).

During *N miliaris* active bloom of February 2009, the major siderophore producing genera belonged to members of the *Bacillus* (29.4%) and *Pseudomonas* (23.5%) dominated by the fluorescent *Pseudomonas* group. In terms of efficiency to reduce the CAS-Fe (III) complex (expressed as percent Siderophore unit, %SU), *Pseudomonas* spp. however showed the highest ability of 42.2 – 73.31 %SU which was 33.7 – 64.7 μM equivalent of the standard desferrioxamine B (DFOM) (Fig. 5.15 and 5.16). In comparison, the siderophorogenesis by members of the *Bacillus* were much lower and ranged from 18.32 - 40.26%SU (11.67 – 31.77 μM DFOM) (Table 5.5). The strain *Pseudomonas gessardii*, ^{GU}SK256-N6 showed the highest efficiency to produce siderophores with 73.31%SU on SMM and 66.81%SU on DFNB (Table 5.4). In terms of pigmentation, siderophores produced by the fluorescent *Pseudomonas* group of isolates were all parrot green, while siderophores from *Bacillus* and other isolates remained non-pigmented (Plate 5.3). Comparative siderophore production on DFNB and SMM suggested that in members of *M luteus* ^{GU}SK256-37 and *P stutzeri* ^{GU}SK256-33, siderophorogenesis increased significantly on nutrient rich DFNB media (Table 5.4).

On the other hand, during declining bloom of *N miliaris,* members of *γ-proteobacteria* were the dominant siderophore producers (38.86% of the flora). They belonged to *Psychrobacter* spp., *Pseudomonas* spp., *Halomonas* spp.,

Shewanella spp., *Pseudoalteromonas* sp. and *Cobetia marina*. The siderophore producing potentials of the major *γ-proteobacterial* genera varied from 50.55 – 69.55 %SU (42.04 – 61.04 μM DFOM) for the *Pseudomonas* spp., 37.34 – 52.12%SU (28.86 – 43.61 μM DFOM) for the *Halomonas* spp., 20.22 – 52.47%SU (11.77 – 43.9 μM DFOM) for *Shewanella* spp. and 28.5 -29.1 %SU (μM DFOM) for *Psychrobacter* spp. (Table 5.5, Fig. 5.16). The highest efficiency of siderophore production was exhibited by a red-pigmented *Actinobacteria* belonging to *Kocuria* sp.,^{GU}SS263-23 (Fig 5.14) which showed 81.26% reduction of CAS on SMM, (72.7 μM DFOM) (Table 5.4). Supernatant absorbance of this culture showed unknown absorbtion peak at 260 nm. Members of siderophore producing *Firmicutes* belonged to mostly *Bacillus* spp. (8.33%) and their siderophorogenesis of 26.2 – 28.9 %SU were much lower in comparison to *Virgibacillus* (56.01%SU) and the unclassified strain of Bacillales (55.9%SU) (Table 5.5).

Siderophores producers were also found to be frequent in association with *Trichodesmium* spp. colonies (Fig. 5.13). Dominant siderophore producing genera were the *Bacillus* (28.57%), followed by members of *Virgibacillus* and *Microbacterium* (9.52% each); and members of *Pseudomonas* and *Halomonas* (4.76% each). Ability to produce siderophore was highest in *Pseudomonas* (48.25%SU) (Table 5.5). Except siderophores from the florescent *Pseudomonas* group, which were always green pigmented, no visible pigmentation for siderophores from other genera were noticed.

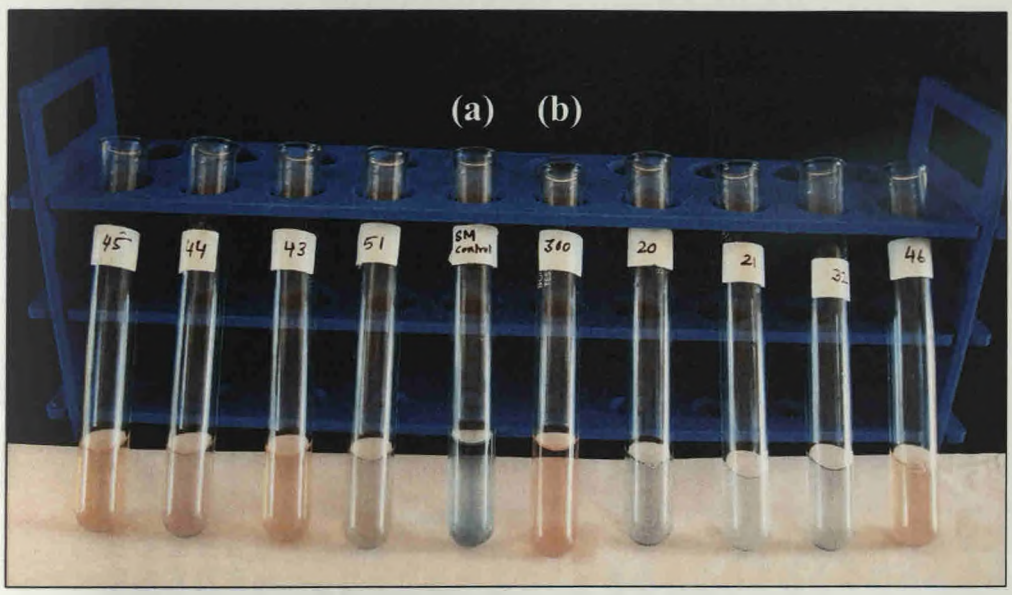

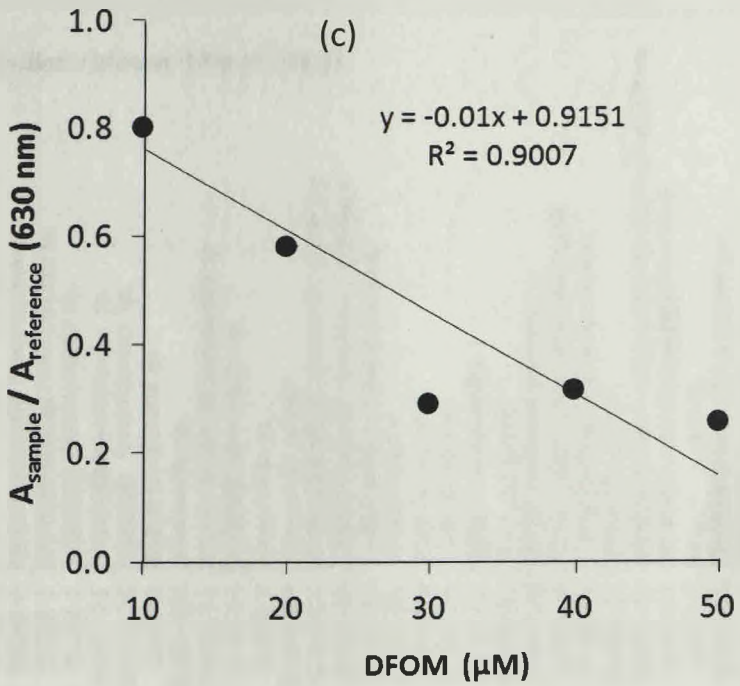

Fig 5.11 Quantitative Chrome Azurol S assay for screening of siderophore producing bacteria. Reduction of CAS dye against: (a) Reagent blank (Control); (b) Standard DFOM (Desferioxamine mesylate) 100µM; (c) Standard curve for estimating siderophore in terms of µM equivalents DFOM.

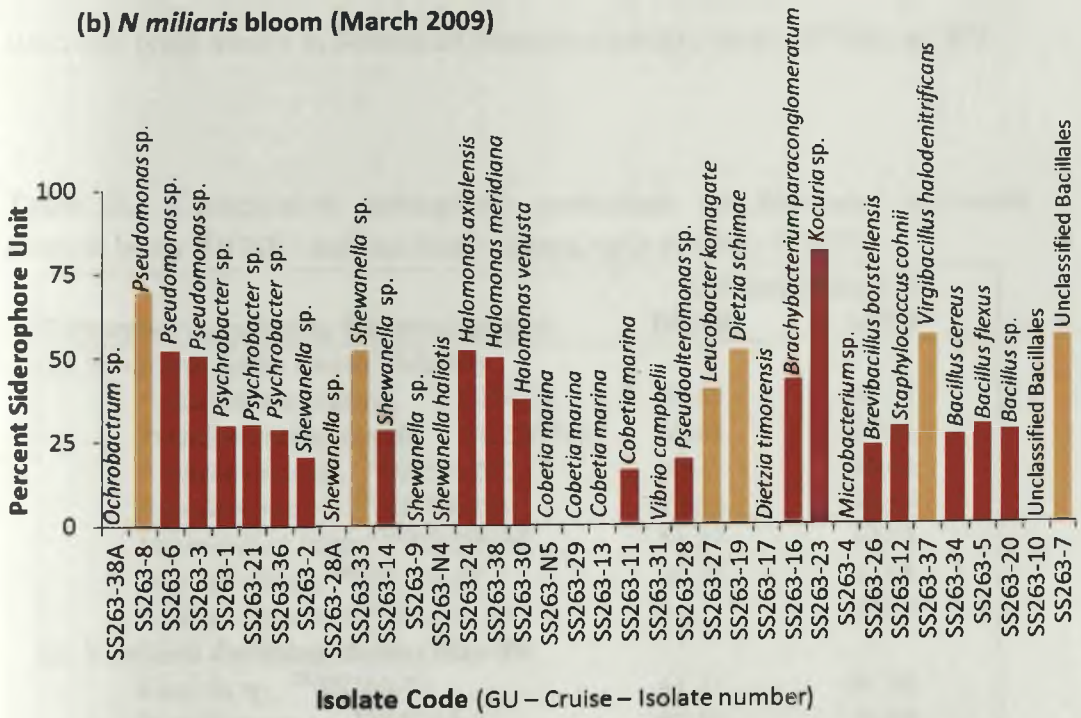

Fig. 5.12 Siderophore producing potentials of bacteria associated with *N miliaris* bloom of NEAS on the Iron-free succinate broth (SMM) and/or in deferrated Nutrient-seawater broth (DFNB) at 25°C: (a) Active phase (Feb-2009), and (b) Declining phase (Mar-2009).

(a) N miliaris bloom (February 2009)
Percent Siderophore Unit
0
25
50
75
100
Isolate Code (GU – Cruise – Isolate number)
SK256-N1 Pseudomonas sp.
SK256-N2 Pseudomonas sp.
SK256-N3 Pseudomonas sp.
SK256-N5 Pseudomonas sp.
SK256-N6 Pseudomonas gessardii
SK256-N7 Pseudomonas sp.
SK256-25A Pseudomonas xanthomarina
SK256-33 Pseudomonas stutzeri
SK256-29 Halomonas meridiana
SK256-16A Providencia rettgeri
SK256-35 Micrococcus luteus
SK256-37 Micrococcus luteus
SK256-N8 Microbacterium oxydans
SK256-N4 Brachybacterium paraconglomeratum
SK256-28 Unclassified Intrasporangiaceae
SK256-15 Unclassified Micrococcaceae
SK256-25B Exiguobacterium aurantiacum
SK256-30 Staphylococcus arlettae
SK256-21 Oceanobacillus sp.
SK256-19 Virgibacillus halodenitrficans
SK256-18 Virgibacillus halodenitrficans
SK256-20 Bacillus cereus
SK256-22 Bacillus cereus
SK256-17 Bacillus cereus
SK256-32 Bacillus subtilis
SK256-13 Bacillus mycoides
SK256-16 Bacillus flexus
SK256-S7 Bacillus sp.
SK256-5 Bacillus sp.
SK256-S9 Bacillus sp.
SK256-14 Bacillus sp.
SK256-12 Bacillus sp.
SK256-8 Bacillus sp.
SK256-38 Unclassified Planococcaceae

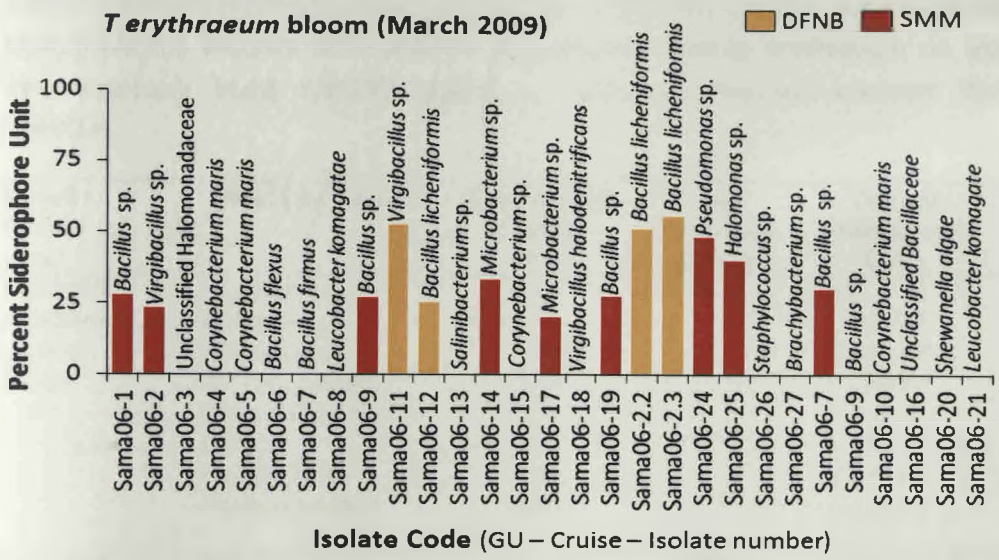

Fig. 5.13 Siderophore producing potentials of bacteria bacteria associated with *Trichodesmium erythraeum* bloom off Ratnagiri, April-08 on the Iron-free succinate broth and/or in deferrated Nutrient-seawater broth (DFNB) at 29°C.

Table 5.4 Comparative siderophore production on deferrated sea-water nutrient broth (DFNB) and succinate mineral salts medium (SMM).

Siderophore producing Bacterial species	% Siderophore Units DFNB	SMM
***(a) N miliaris* active bloom (Feb-09)**		
Pseudomonas stutzeri, ^{GU}SK256-33	55.65	27.37
Pseudomonas gessardii, ^{GU}SK256-N6	**66.81**	**73.31**
Pseudomonas sp., ^{GU}SK256-N2.	41.7	48.03
Pseudomonas sp., ^{GU}SK256-N3	44.08	46.11
Micrococcus luteus, ^{GU}SK256-37	51.87	19.86
Bacillus cereus, ^{GU}SK256-22	40.26	33.01
Bacillus mycoides, ^{GU}SK256-13	21.11	31.83
***(b) N miliaris* declining bloom (Mar-09)**		
Kocuria sp., ^{GU}SS263-23	41.21	81.26
Pseudomonas sp., ^{GU}SS263-8	69.58	38.08
Shewanella sp., ^{GU}SS263-33	52.47	25.15
***(c) T erythraeum* bloom (Apr-08)**		
Virgibacillus sp. ^{GUFB}Sama06-11	52.47	41.59
Bacillus licheniformis, ^{GUFB}Sama06-12	51.25	40.29
Pseudomonas sp., ^{GUFB}Sama06-24	36.99	48.25

Table 5.5 Siderophore producing potentials of bacterial genera associated with phytoplankton blooms of *N miliaris* and *Trichodesmium erythraeum* on Iron-free succinate broth (SMM) and/or in deferrated Nutrient-seawater broth (DFNB).

Period / Bloom / Area	**Bacterial Genera**	**Contribution of genera (%)**	**Total Percentage of flora**	**Percent Siderophore Units**	**DFOM Equivalent (μM)**
Feb-2009	*Pseudomonas*	23.5	**76.44**	42.2 – 73.31	33.7 – 64.77
N miliaris	*Halomonas*	2.94		16.07	7.62
(Active)	*Micrococcus*	5.94		23.4 – 51.8	15.02 - 43.36
NEAS[2]	*Microbacterium*	2.94		30.61	22.14
	Exiguobacterium	2.94		56.5	47.98
	Bacillus	29.4		18.32 -40.26	11.67 -31.77
	Virgibacillus	5.88		30.2 -31.12	21.75 - 22.65
	Planococcaceae*	5.88		30.21	21.74
Mar-2009	*Pseudomonas*	8.33	**69.4**	50.55 – 69.58	42.04 – 61.04
N miliaris	*Halomonas*	8.33		37.34 – 52.12	28.86 -43.61
	Shewanella	8.33		20.22 – 52.47	11.77 – 43.9
(Declining)	*Psychrobacter*	8.33		28.5 -29.91	20.03 – 21.44
NEAS[2]	*Pseudoalteromonas*	2.77		19.51	11.06
	Cobetia	2.77		16.21	7.76
	Dietzia	2.77		51.79	43.28
	Brachybacterium	2.77		43.09	34.60
	Staphylococcus	2.77		28.84	20.37
	Kocuria	2.77		81.26	72.70
	Leucobacter	2.77		40.1	31.61
	Brevibacillus	2.77		22.9	14.51
	Bacillus	8.33		26.2 – 28.9	17.76 – 20.48
	Virgibacillus	2.77		56.01	47.5
	Bacillales*	2.77		55.9	47.4
Apr-2008	**Colony associated**				
T erythraeum	*Pseudomonas*	4.76	**57.13**	48.25	39.75
EAS[2]	*Halomonas*	4.76		40.22	31.73
	Microbacterium	9.52		20.12-33.29	11.67 – 24.81
	Virgibacillus	9.52		23.11-52.47	14.65-43.96
	Bacillus	28.57		25.29-55.62	16.8 – 47.11
	Free-living				
	Bacillus	16.67	**16.67**	30.21	21.74

[2] NEAS – Northeastern Arabian Sea, station O-1; EAS – Eastern Arabian Sea (mid-west continental shelf off Ratnagiri).

*Unclassified strains presently placed under family/order

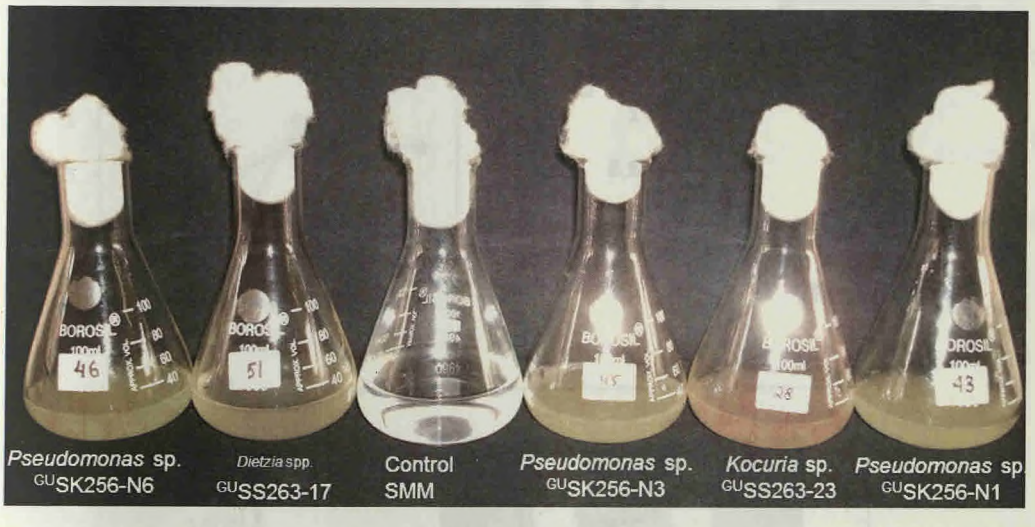

Plate 5.3 Growth of cultures in Iron free media producing siderophores.

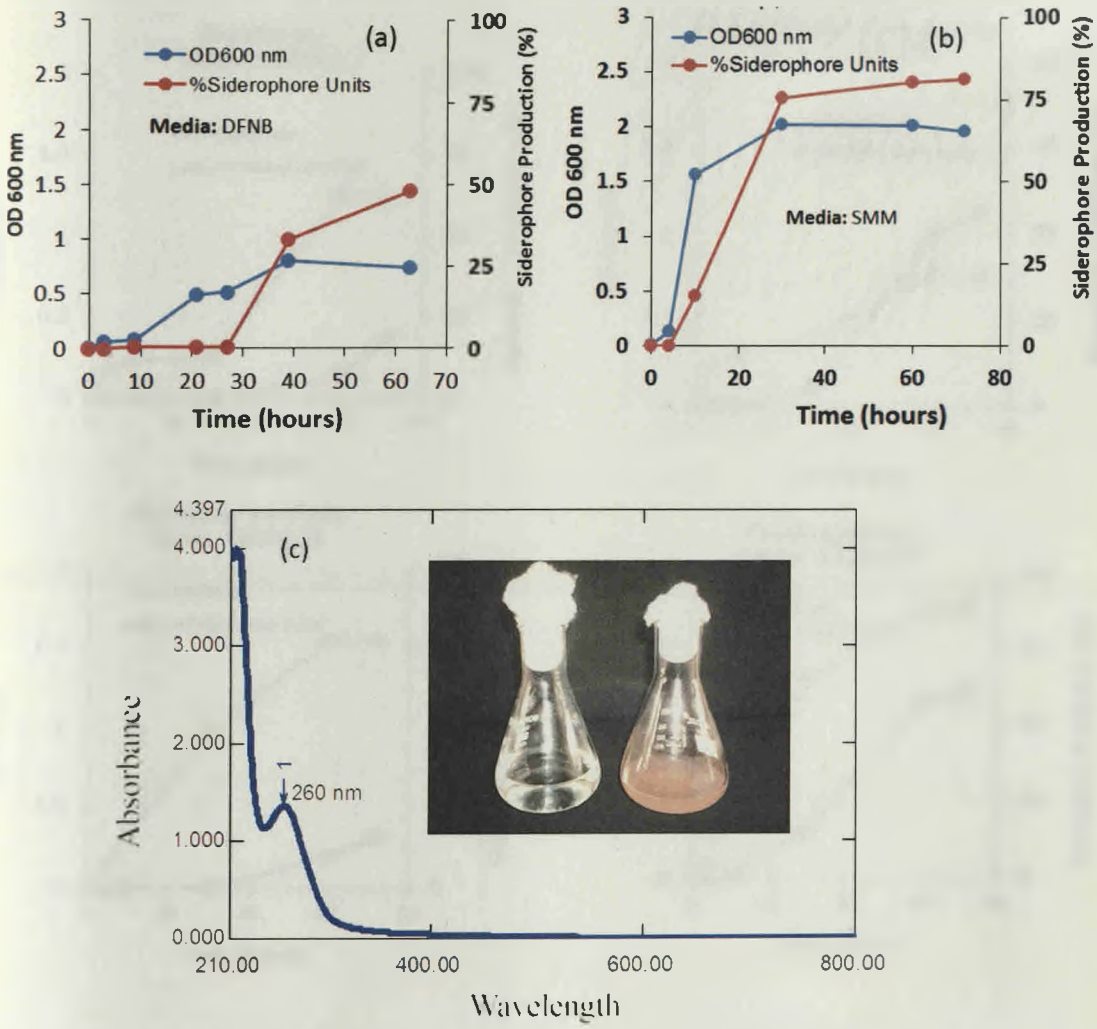

Fig. 5.14 Siderophore production by *Kocuria* sp., ^{GU}SS263-23: (a) Deferrated Nutrient broth in sea-water (DFNB) (b) Iron-free Succinate mineral salts media (SMM) and (c) UV/Vis scan showing peak absorbtion of culture supernatant in SMM at 260 nm.

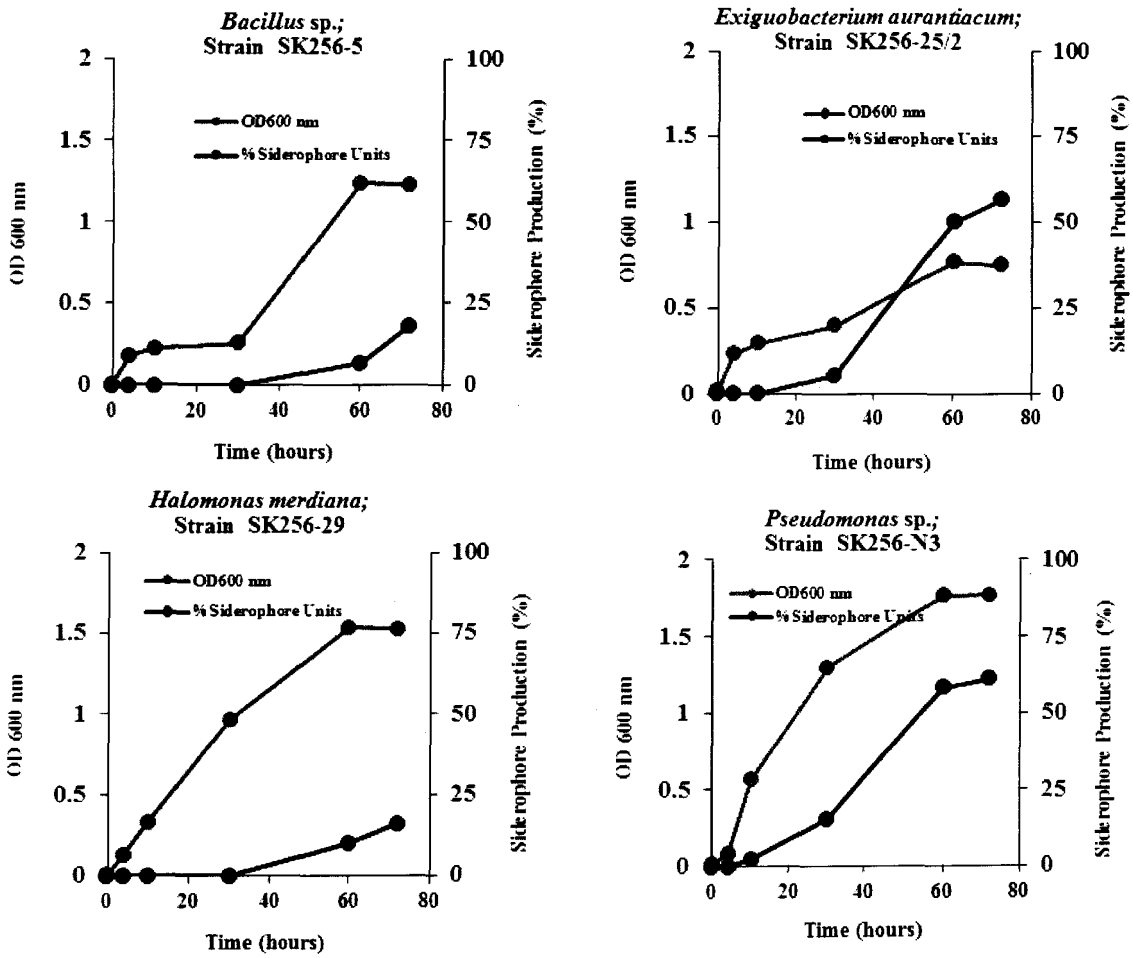

Fig. 5.15 Siderophore production on Iron-free succinate broth: (a) *Bacillus* sp. ^{GU}SK256-5; (b) *Exiguobacterium aurantiacum* ^{GU}SK256-25B; (c) Halomonas meridiana ^{GU}SK256-29 and (d) *Pseudomonas* sp. ^{GU}SK256-N3

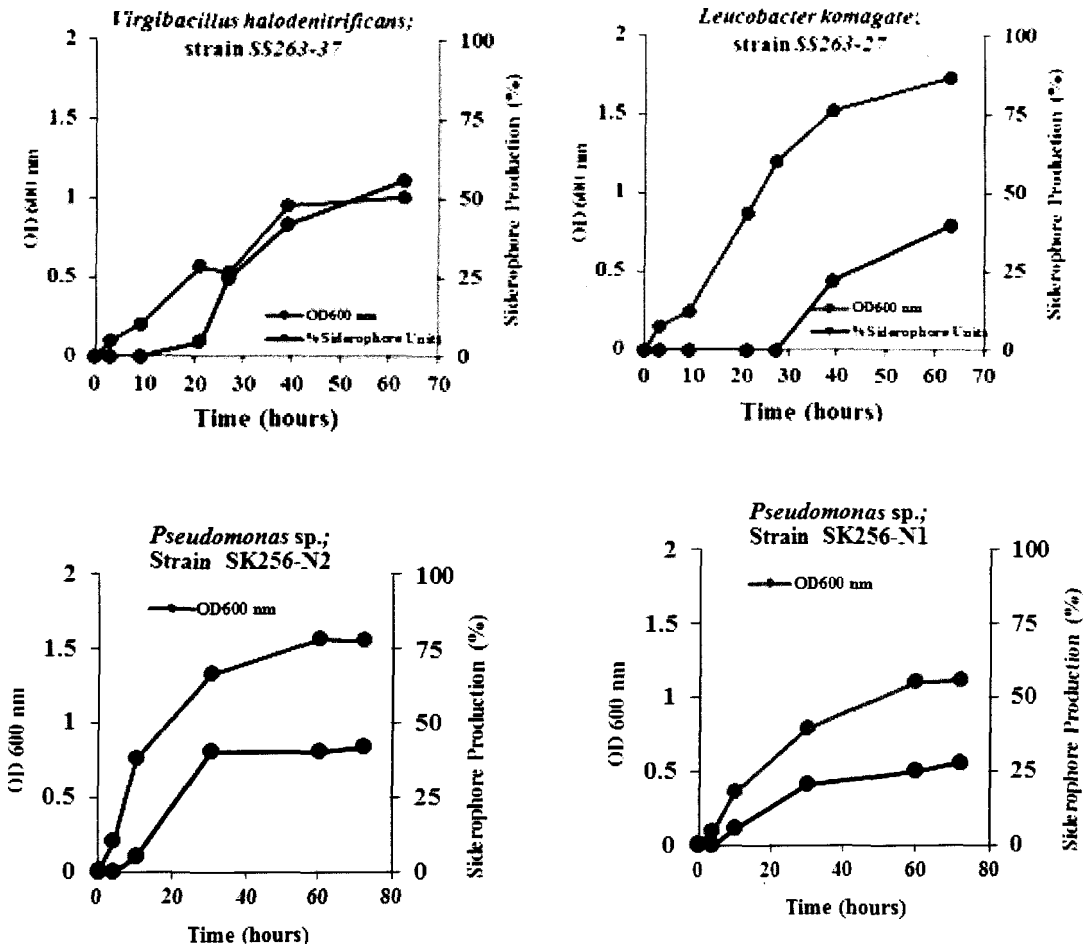

Fig. 5.16 Siderophore production on Iron-free succinate broth by: (a) *Virgibacillus halodenitrificans* ^{GU}SK256-37; (b) *Leucobacter komagatae* ^{GU}SS263-27; (c) *Pseudomonas* sp. ^{GU}SK256-N2 and (d) *Pseudomonas* sp. ^{GU}SK256-N1.

5.2.3.2 Siderophore production by *Pseudomonas gessardii*, ^{GU}SK256-N6

P gessardii, ^{GU}SK256-N6 produced a parrot green pigment and reduced the CAS dye to a maximum of 73.3% on Succinate mineral salts (SMM) and 66.8% on deferrated Nutrient-broth in sea-water (DFNB). Spectrophotometric scans of the pigment in SMM showed the charactersitic peak at 400 nm, identified as the Pyoverdine class of siderophores (Fig. 5.17). The strain was further grown in SMM medium at 25°C and 29°C with pH adjusted to 7 and 8.2 respectively.

Maximum siderophore production of 490.78μg ml^{-1} (98.9% siderophore unit) was obtained at 25°C, pH7 (Table 5.6), which decreased to 355.01 78μg ml^{-1} (78.13% siderophore unit) as the pH was increased to 8.2. The culture however grew at a faster pace at pH 8.2 with an average growth rate of 0.0940 hr^{-1}. At 25°C and pH7, growth rates were slightly retarded as 0.0881 hr^{-1} (Table 5.6).

Spectrophotometric scans and siderophore detected during growth at 25°C showed that siderophore production was initiated around 12 hours at 25°C at pH7, which was delayed to 18 hours at the higher pH 8.2 (Fig. 5.5 – 5.6). The higher growth at pH 8.2 was accompanied by prominent absorbtion shoulders between 295-298 nm and a much reduced 400 nm charactersitic peak of pyoverdine for the first 42 hours (Fig. 5.19). This resulted in the culture

broth at pH 8.2 remaining unpigmented during the first 42 hours and pigmentation in the broth was simultaneous with the increase in absorbtion at 400 nm (Fig. 5.19), during the latter half of the growth cycle.

In comparison, at 25°C, pH7, absorbtion at 400 nm (Fig. 5.18)was always exhibited as the primary feature during the early (12 hours) as well as later stages of the growth. The 295-298 nm shoulder, however appeared during 24 – 42 hours and later remained undetected in the scans. The culture broth started showing pigmentation after 20 hours, with sharp 400 nm peaks and the absorbance gradually increasing to greater than 0.5 (Fig. 5.18), alongwith fluorescent green pigmentation of the broth (Fig. 5.17).

Growth at 29°C was accompanied by a lower siderophore production of 295.11 $\mu g\ ml^{-1}$ at pH 7 and 266.25 $\mu g\ ml^{-1}$ at pH 8.2, in comparison to 25°C (Table 5.6). However, at this higher temperature, growth rates decreased to 0.0705 hr^{-1} at pH 7 and interstingly increased to 0.15 hr^{-1} at pH 8.2. The growth curves revealed that at 29°CpH 8.2, the log-phase was initiated after 6 hours which was delayed to ~12 hours at pH7 (Fig. 5.18). Further, at pH 8.2, a slight drop in the OD was noted during 30-36 hours (Fig. 5.18) and the nature of peaks remained similar to that obtained at 25°C.

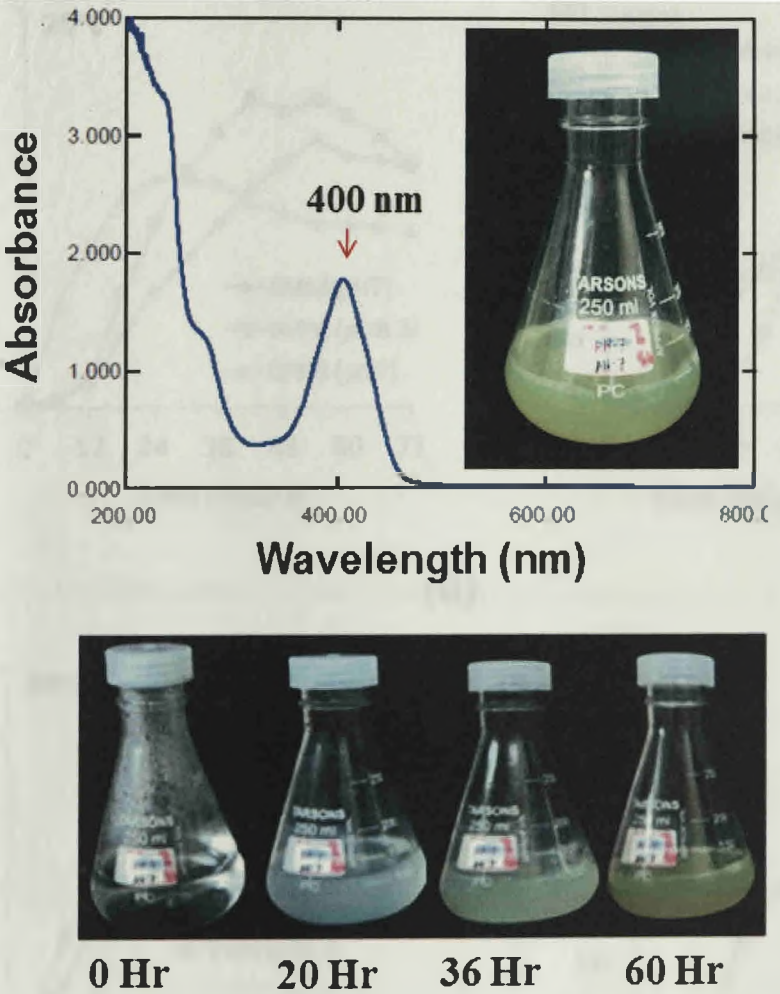

Fig. 5.17 Absorbance signature of siderophore (Pyoverdine) produced by *Pseudomonas gessardii*, ^{GU}SK256-N6 on SMM.at 25°C, pH7.

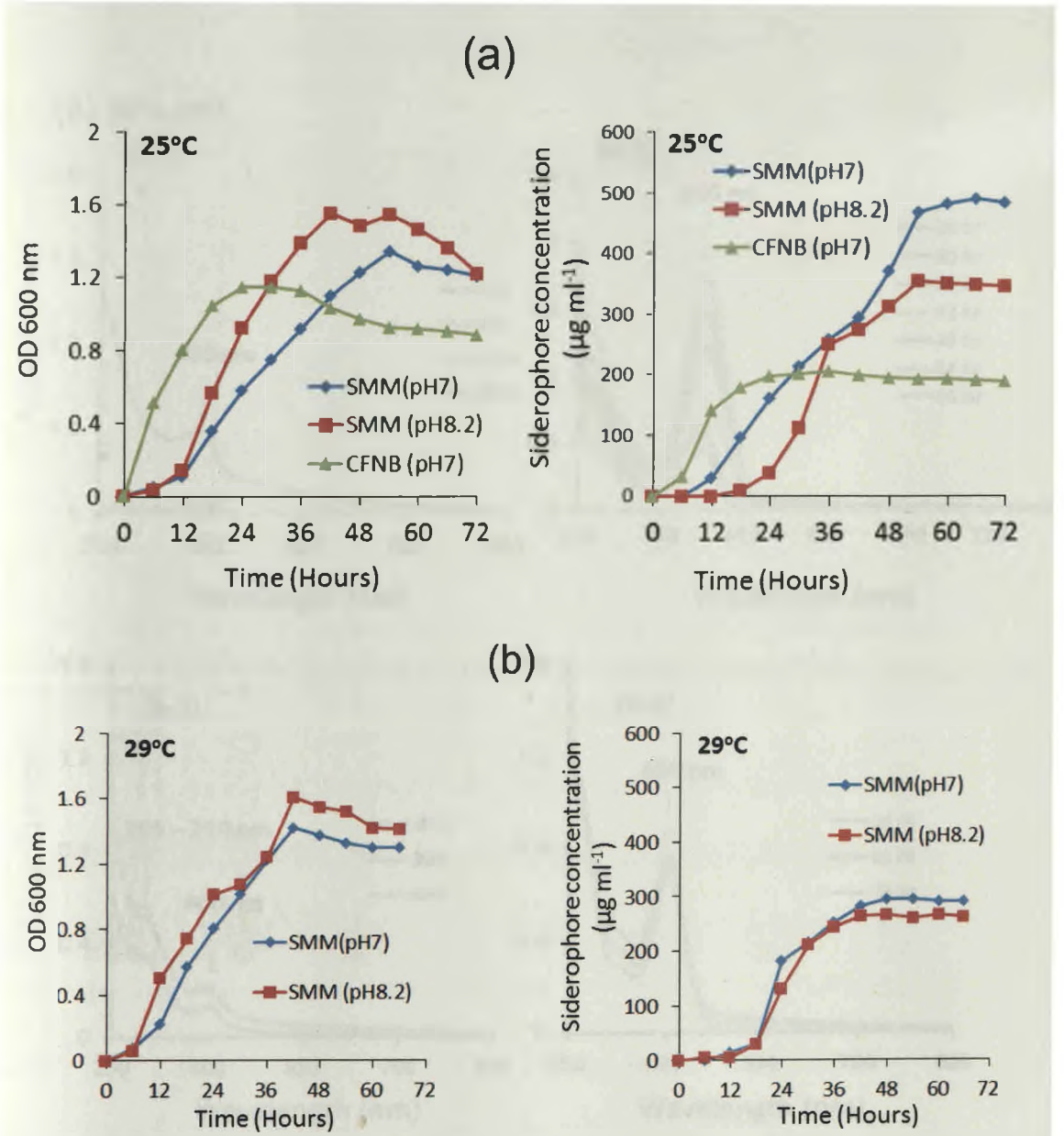

Fig. 5.18 Growth and siderophore production by *Pseudomonas gessardii*, ^{GU}SK256-N6 on SMM and CFNB at: (a) 25°C and (b) 29°C.

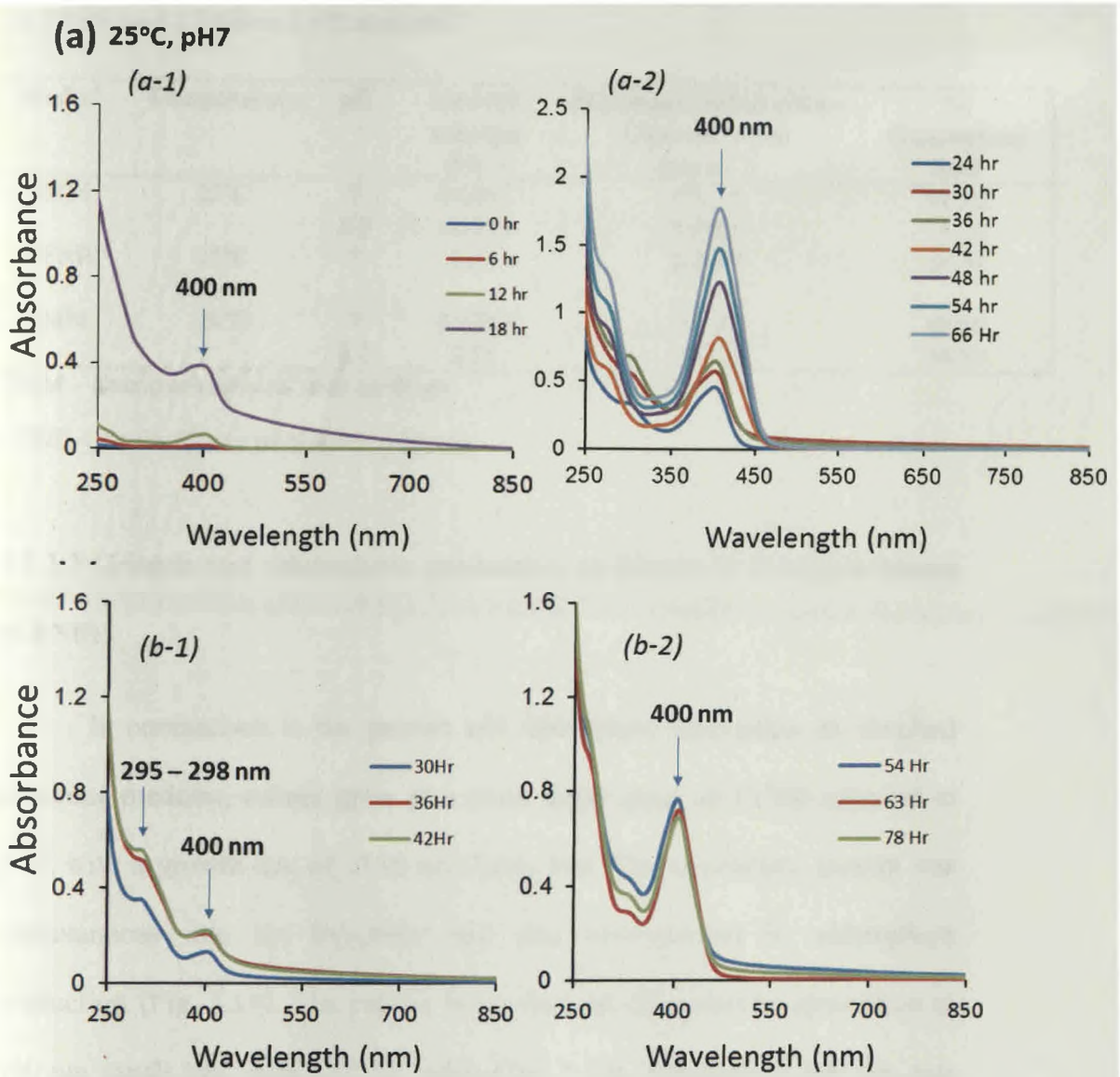

Fig. 5.19 Time-series absorbtion spectra of *P gessardii* supernatant at 25°C under varying conditions of: (a *1-2*) pH 7 and (*b1-2*) pH 8.2.

Table 5.6 Siderophore production by *Pseudomonas gessardii*, ^{GU}SK256-N6 on SMM and CFNB at 25°C and 29°C.

Media[1]	Temperature	pH	Growth rate (μ) (Hr^{-1})	Maximum Siderophore Concentration ($\mu g\ ml^{-1}$)	% Siderophore unit
SMM	25°C	7	0.0881	490.78	98.90
		8.2	0.0940	355.01	78.13
CFNB	25°C	7	0.16	205.93	55.32
SMM	29°C	7	0.0705	295.11	68.96
		8.2	0.15	266.25	64.54

SMM – Succinate mineral salts medium

CFNB – Cruse filtrate of *N miliaris* bloom

5.2.3.3 Growth and siderophore production on filtrate of *N miliaris* bloom (CFNB)

In comparison to the growth and siderophore production on standard succinate medium, culture grew at a much faster pace on CFNB adjusted to pH7, with a growth rate of 0.16 hr^{-1}(Table 5.6). On inoculation, growth was instantaneous into the log-phase and also accompanied by siderophore production (Fig. 5.18). The culture broth showed charactersitic absorbtion at 400 nm much late, during 63-72 hours (Fig. 5.20). The peak at 400 nm was adjacent to the characteristic peak at 337 nm of the CFNB mycosporine like amino acids (MAA). However, in comparison to the control CFNB, a similar shoulder to that earlier observed between 295-298 nm was detected, which was associated with high growth at pH 8.2, whereas the 400 nm peak remained

suppressed. The MAA peak during the course of the growth remained absolutely unchanged and showed no effect from the growth of the culture (Fig. 5.20).

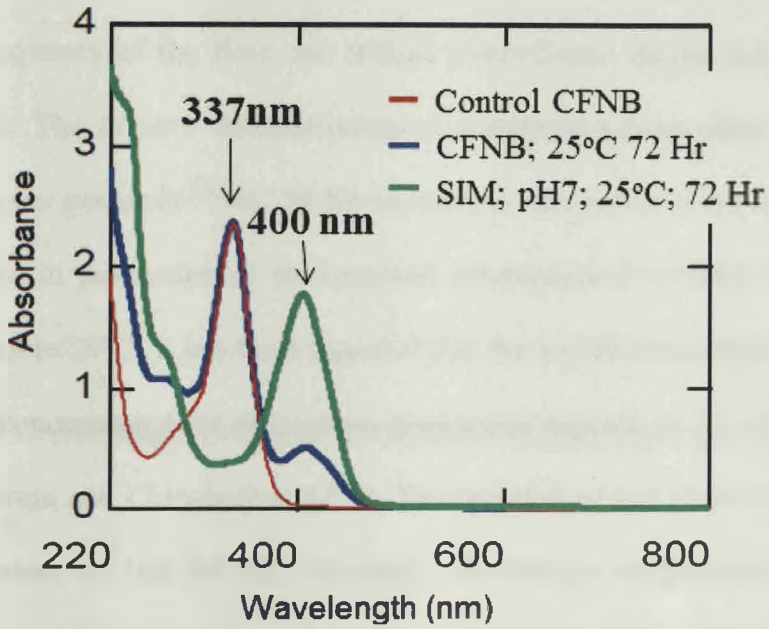

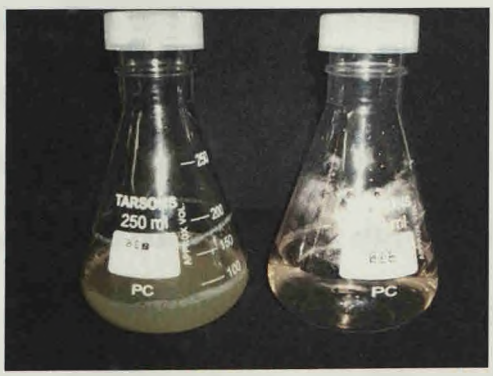

Fig. 5.20 Scans showing siderophore production on the crude filtrate of *Noctiluca* (CFNB) in comparison to the control CFNB and that produced at pH7 on succinate mineral salts medium at pH-7 (25°C) by *P gessardii*, ^{GUFB}SK256-N6. Peak at 400 nm is charactersitic of Pyoverdine type siderophores produced by the fluorescent Pseudomonads, whereas the 337 nm peak is characteristic signature of the *N miliaris* bloom.

The siderophore production was significant, although lower than that on succinate. Maximum siderophore detected was 205.93 $\mu g\ ml^{-1}$, corresponding to 65.32% siderophore units as detected during the CAS assay. Screening for siderophorogenesis among bacterial associates of the bloom clearly reveals that a high frequency of the flora can release siderophores during Iron deficient conditions. The *in vitro* demonstration of a dominant siderophore producer *Pseudomonas gessardii* ^{GU}SK256-N6 on mineral salts minimal medium, shows an increase in production of its dominant siderophore Pyoverdin at 25°C in comparison to 29°C. It has been regarded that the temperature requirement for optimum concentration for siderophore production depends on the origin of the strain (Varma and Chincholkar 2007). The retrieval of our strain from active bloom waters of the NEAS, recording an average temperature of 25°C strengthens this observation. Further, our results show that growth is accelerated with suppression of Pyoverdine production at a higher pH of 8.2 (sea-water pH) in comparison to neutral pH. Similar results have been echoed by Sayeed (2005) from *P fluorescens.* Although, the authors attributed this to an increase in Iron content of the media at the alkaline pH, the reasons are not clear. However, our results further shows that the higher growth rates at pH 8.2 are accompanied by a shoulder between 285-290 nm in the initial growth phases and then the concentration of the major siderophore Pyoverdine starts to increase. In these cases pigmentation of the broth is delayed to more than 36-48 hours.

The final attempt to inoculate a crude-filtrate of *N miliaris* bloom and examine whether the culture can grow / produce siderophores, returned the most promising results and a crucial evidence for this study. The strain *Pseudomonas gessardii,* ^{GU}SK256-N6 not only grew at a much faster growth rate on the CFNB at 25°C, but also was accompanied by production of pyoverdine, the charactersitic siderophore of the fluorescent Pseudomonads. These results imply 'foremost' the limiting Iron concentration of the '**amended extract and hence in the bloom enviroinment**', low enough to induce siderophores. Secondly, the high growth rates *in vitro* vindicates earlier field results of a massive inflation in bacterial biomass during the course of the bloom and the fact that bacterial growth is favored on the type of dissolved organics produced by the bloom.

On reviewing the literature on dissolved Iron concentrations from the Arabian Sea, few insightful findings throw significant light on our results. For example, the results from cruises of Jan-Mar 1995 (Witter et al. 2000), reveals that Iron binding ligand concentrations remained consistently higher than total iron concentrations at every site measured, with an average "excess" ligand concentration of 2.15±1.50 (n=10), and that measured total ligand concentrations in the Arabian Sea are much higher than the Pacific and Northwestern Atlantic. Based on these results, Witter et al. 2000 further suggested that in areas that receive high Fe inputs through upwelling and/or atmospheric deposition like that of the Arabian Sea, marine organisms may produce 'excess' ligands to keep Fe bioavailable in seawater for extended

intervals. In contrast, Naqvi et al. 2010 found depletion of Iron in the Southern Omani coast, following upwelling during the South-West monsoon of 2004. This lead to an unexpected 'High-nutrient-low chlorophyll' conditions, with Iron limiting primary-productivity. Although, the average Iron concentrations increase in the mid-depth anoxic zones of the Arabian Sea, wherein intense denitrification occurs, the Iron concentrations from the upper-ocean varies from sub-nanomolar to hardly 2-3 nM (Naqvi et al. 2010, Witter et al. 2000).

5.2.3.4 Hypothesis and future directions on Iron acquisition

Several studies have proposed the strong possibility of a siderophore mediated mechanism of Iron availability to Phytoplankton (Amin et al. 2009, Barbeau et al. 2001, Butler 2005, Deng and Horstmann 1995, Hopkinson and Morel 2009, Morel et al. 1991), and also an enhanced requirement of Iron for phytoplankton bloom formation (Martin 1990, Bertrand et al. 2011[a], Boyd et al. 2007, Morrisey and Bowler 2012). The Arabian Sea is an important ecosystem for seasonal genesis of phytoplankton blooms. In order to sustain such massive emerging blooms of *N miliaris* during Jan-March, bioavailability (through water-soluble ligands) of Iron and their supply in the euphotic zone should be a primary requirement. As blooms of *N miliaris* (green) coincides with that of the North-east monsoon, **dust-depositions via aerosols will probably be an important source of Iron in the bloom area**. The Iron inputs in the north-western Arabian Sea and Omani coasts during the cool-dry winter- monsoon (1995-1996) have been estimated to be higher in comparison to other seasons, varying around 0.15 -2.64 ($\mu g\ m^{-3}$) (Tindale

and Pease 1999). The transport and input of dust to the Arabian Sea is regarded to be complex as it is intimately linked to the influence of the monsoon winds (Tindale and Pease 1999), proximity to several desert dust sources from India, Iran, Pakistan and middle-east and in light of recent reports suggesting weakening of the northeast monsoon winds which can have larger biogeochemical ramifications on the genesis of phytoplankton blooms (Goes et al. 2005).

Recent decadal satellite trends (2002-2012) in the northeastern Arabian Sea compiled during the period of winter monsoon of December-February, (Fig. 5.21), further shows that: the month of active bloom of February remains the coolest, recording the highest Chl *a* alongwith highest aerosol optical thickness, consistent with recent observations of the *Noctiluca* bloom since the last. Hence, further studies of the links between Iron-binding siderophores and their relation to dust-deposits over the Arabian Sea will be important to gain insights into the favorable causes responsible for genesis/sustenance of these blooms. Role of siderophore producing bacteria appears to be important during blooms of *Trichodesmium* spp. as well, whose Iron requirements are known to ~10 fold higher than other blooming species (Rueter et al. 1992), owing to their need for fixing nitrogen during the nutrient limited and stratified conditions prior to upwelling.

Hence at this point, we suggest further investigations of the "**dust-bacteria-siderophore-phytoplankton**" links in the Arabian Sea which will be

crucial to unveil bacterial role in bloom dynamics of this unique tropical ocean basin, responsive to climatic forcings.

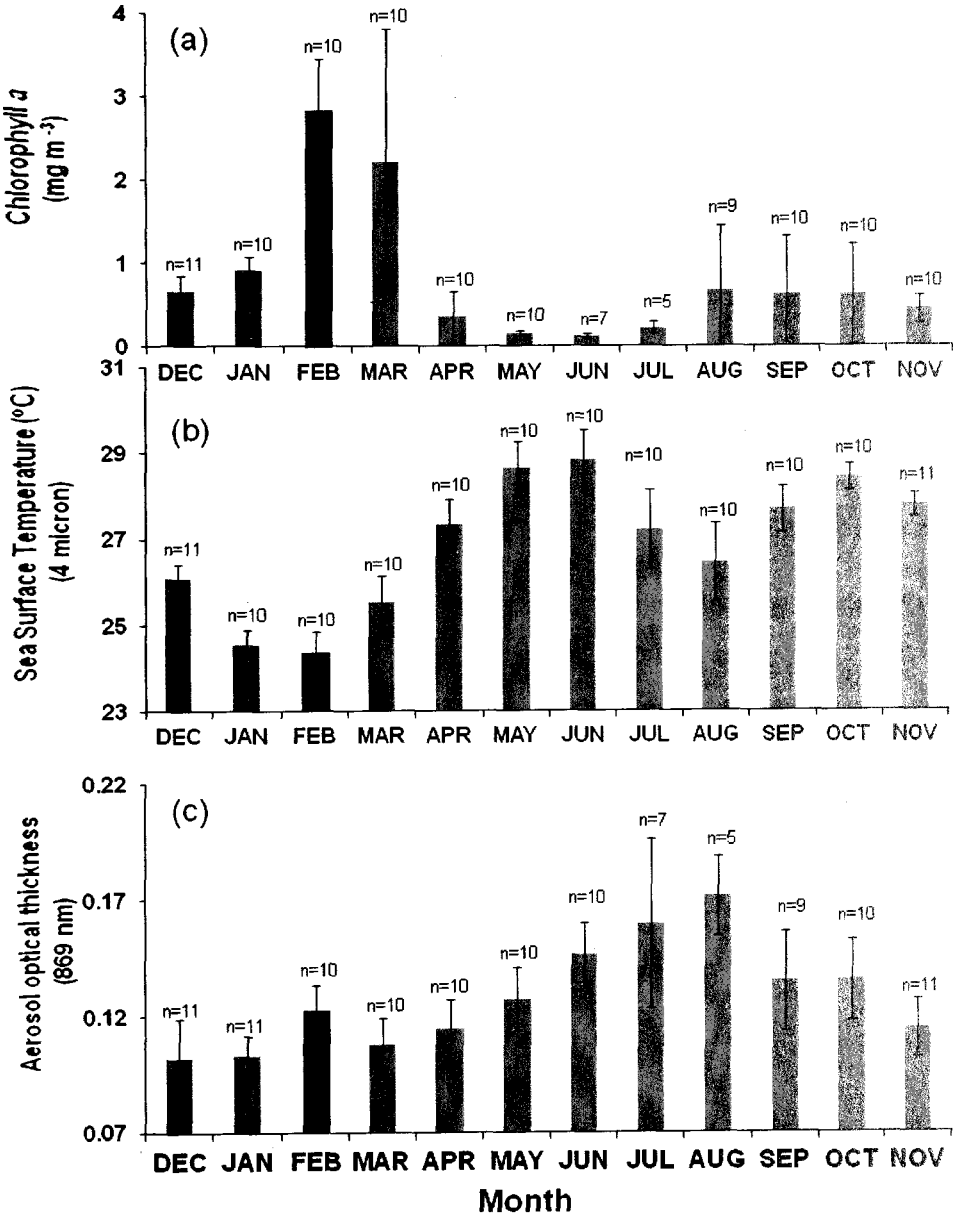

Fig. 5.21 Decadal trends (2002 -2012) in Chlorophyll a, Sea-surface temperature and Aerosol optical thickness in the Northeastern Arabian Sea (19.5°-23.5°N; 64°-67°E). Data extracted from NASA Giovanni DISC for MODIS Aqua-4km resolution satellite based measurements.

5.4 Salient Results

Relationship of retreived bacteria with its bloom source i.e. *N miliaris* and *T erythraeum*, were assessed in terms of their degradative enzymic potentials. These features of the retreived bacteria were analyzed to decipher relationships of individual members as well as dominant phylogenetic clusters in regard to: (i) Nutrient cycle (ii) Food-chain and (iii) Acquisition of Iron under limiting conditions.

The bloom biomass of *Noctiluca miliaris* basically consists of starchy substrates, lipids (free-fatty acids, triglycerides, phospho-lipids), proteins/ amino-acids and produce mucus. The high photosynthetic carbon fixation rates and production of dissolved organic matter containing mycosporine like amino acids as seen from the C-DOM estimates, indicated the high organic turnover of the bloom. Further, the ability of isolates to break-down/utilize complex substrates during active – declining phases of the bloom such as: (a) carbohydrates: starch (50 - 38.8 %), carboxy methyl cellulose (13.8 – 20.5%) (b) Proteins: casein (55.8 – 58.3%), gelatin (61.7 – 38.8%) (c) Lipids: Tributyrin (26.4 – 30.5%), tween-80 (52.9 – 61.1%) and a host of simple carbohydrates and amino-acids, clearly suggested that the organic matter synthesized by *Noctiluca miliaris* appears to be quickly utilized and remineralized.

Localized zones of high dissolved inorganic phosphate (DIP) detected in in the euphotic column of major *N miliaris* bloom areas of Feb-2009 suggested phosphate regeneration in the upper-ocean. DIP further showed a

strong correlation with total bacterial counts as R^2= 0.829, n=47. This is possibly the reason for almost half the strains (52.9%) during the active phase of bloom expressing phosphate solubilizing ability belonging to 8 different genera of *Pseudomonas, Halomonas, Micrococcus, Microbacterium, Brachybacterium, Bacillus* and unclassified members of the family Intrasporangiaceae and Micrococcaceae.

Significantly high water-column nitrite (nutrient) in the active bloom waters of Feb-09 (0.19 – 1.1 μM) was found to be suddenly depleted within 8-10 days during consecutive cruise of March-2009, suggesting nitrogen removal in the upper-ocean. As 50% strains from active and 49.67% strains from the declining phase bloom of Feb-Mar 2009 supported the unique possibility of nitrogen removal via denitrification under '*aerobic conditions*', these bacterial strains are implicated to carry out denitrification from the high-organic *N miliaris* bloom ecosystem of the Arabian Sea, also known for high denitrification process from the anoxic mid-depth oxygen-minimum zones. Denitrifying strains belonged to members of the genera *Pseudomonas, Bacillus, Virgibacillus, Shewanella, Psychrobacter, Ochrobactrum, Brevibacillus* and an unclassified strain of the Intrasporangiaceae.

In comparison, to the genesis of *N miliaris* bloom following nutrient enrichment of winter cooling, blooms of Nitrogen-fixing cyanobacteria *Trichodesmium* are favored by the warmer (>27°C) nitrate depleted and shallow stratified conditions in the Arabian Sea. Blooms of *Trichodesmium* do not attract grazers and hence the high bacterial aggregation in colonial space of

Trichodesmium erythraeum as demonstrated in this study will be solely responsible for its remineralization and subsequent enrichment of the water-column. Such a scenario is indicated as retreived bacteria from *Trichodesmium* colonies dominated by *Bacillus* spp., *Virgibacillus* spp., *Corynebacterium* spp. also showed high multiple extracellular enzymic abilities to degrade starch (60%), gelatin (21.7%), casein (44%), tributyrin (33%), phosphate solubilization (25.9%) and H_2S production from organic matter (13%) and cultured members also showing the ability to uptake dissolved carbohydrates from the bloom filtrate of *Trichodesmium* demonstrated by the anthrone-sulfuric acid method. The degrading *Trichodesmium* colonies are known to produce H_2S and the retrieval of the well-known H_2S producing species *Shewanella* algae from the phycosphere suggests their possible involvement and dominance during such decomposition processes. Further, the high bacterial load ($9.4x10^9$ cells L^{-1}) associated with *Trichodesmium* bloom, was seen as a factor in reducing oxygen content in the intra-colonial spaces.

During *N miliaris* bloom of Feb-Mar 2009, the decline of total bacterial counts from 'active' to 'declining' overlapping stations within 8-10 days raised questions on the sudden disappearance of water-column bacteria (Chapter 2). While particles with colonized bacteria were detected during March under epifluorescent microscope, the photomicrographic evidence of phagotrophy by *Noctiluca* was also documented during the cruises. *N miliaris* is well-known to be 'raptorial-feeder' of diatoms, dinoflagellates, bacteria, detrital particles, etc. In this case of the mixotrophic green variety of *Noctiluca* blooms from the

Arabian Sea, particles colonized by bacteria during March would be a rich nutritional source when warming of temperature and prey/nutrient limitations created unfavorable conditions. Such an additional pathway of the food-chain for a short period explains the clearance in bacterial population due to phagotrophic *Noctiluca* and further sustaining the bloom for a short-while during March.

The phylogenetic relatedness of bacteria associated with phytoplankton blooms showed their close homology with a variety of Iron binding siderophore producing strains. Bacterial ability to produce siderophores, detected using the Chrome Azurol-S quantitative assay in Iron limiting conditions, were positive for 76.4% and 69.89% of bacteria associated with 'active' and 'declining' bloom of *Noctiluca*, and 48.14% bacteria associated with *T erythraeum*. During bloom active bloom of *N miliaris,* percentages of siderophore producers *varied from* 29.4% of *Bacillus*, 23.5% of *Pseudomonas*, 5.88% each of *Virgibacillus* and Unclassified Planococcaceae, and 2.94% each of *Halomonas*, *Microbacterium* and *Exiguobacterium*. In terms of efficiency to reduce the CAS-Fe (III) complex (expressed as percent Siderophore unit, %SU), *Pseudomonas* spp. however showed the highest ability of 42.2 – 73.31 %SU which was 33.7 – 64.7 µM equivalent of the standard desferrioxamine B (DFOM) and the strain P *Pseudomonas gessardii*, ^{GU}SK256-N6 showed the highest efficiency to produce siderophores. Siderophores produced by the fluorescent *Pseudomonas* group of isolates were all parrot green, while

siderophores from *Bacillus* and other isolates remained non-pigmented, showing turbidity/growth in Iron stressed conditions and a positive CAS assay.

During *N miliaris* bloom of March-2009, percentages of siderophore producing bacteria varied from 8.33% each from *Pseudomonas, Halomonas, Shewanella, Psychrobacter and Bacillus*; and 2.77% of the genera *Pseudoalteromonas*, Cobetia, Dietzia, *Brachybacterium, Staphylococcus, Kocuria, Leucobacter, Brevibacillus, Virgibacillus* and Unclassified *Bacillaceae*. Siderophore units ranged 16.21 – 69.58% and 7.6- 61.04 µM equivalent of DFOM. The highest efficiency of siderophore production was exhibited by a red-pigmented *Actinobacteria* belonging to *Kocuria* sp.,^{GU}SS263-23 which showed 81.26% reduction of CAS, which was equivalent to 72.7 µM equivalent of DFOM. Supernatant scan of this culture showed unknown absorbtion peak at 260 nm.

Siderophores producers were also found to be frequent in association with *Trichodesmium* spp. bloom of April-2008 in the EAS. Overall, 47.8% of the flora was positive for siderophorogenesis. On considering only colony associated forms, percentages of siderophore producers varied from 28.57% of the genera Bacillus, followed by 9.52% each of *Virgibacillus* and *Microbacterium*, and 4.76% each of the genera *Pseudomonas* and *Halomonas*. Members of *Bacillus* constituting 16.6% were the only siderophore producers detected from the free-living fraction. Except siderophore from the florescent *Pseudomonas*, which were always green pigmented, no visible pigmentation for siderophores from other genera were noticed. In *Pseudomonas gessardii*,

GUSK256-N6 strain siderophore production was demonstrated to increase at a cooler temperature (25°C) and lower pH 7 in comparison to pH8.2. Further, the strain clearly exhibited high-growth on the crude-filtrate of *Noctiluca* bloom supplemented with basal-media and surprisingly accompanied by siderophore production (Pyoverdine). This suggested foremost the '*Iron limitation in the crude filtrate of bloom*' (and hence in the bloom environment), in triggering siderophorogenesis. The bloom of *Noctiluca* in the Northern Arabian Sea over an extended period of two months would deplete Iron and hence, as an essential trace-nutrient would be in continuous requirement by both algae and bacteria. Decadal satellite trends in the northeastern Arabian Sea suggests that the period of February (Active bloom period) remained the coolest month, having the highest Chlorophyll *a* and the highest Aerosol Optical Thickness (837 nm) within the period between December - April. Hence these results possibly implicate seasonal dust deposits during the winter-monsoon period as a probable factor. At this point, we strongly suspect a siderophore mediated process, wherein the closely associated bacteria of *N miliaris* can play an important role in keeping Iron bioavailable.

Summary

The present study carried out during 2007-2011 addressed the diversity of micro-flora and their relationship with ecosystem components of the two important bloom forming phytoplanktons of the Arabian Sea – the unique tropical open-ocean blooms of the dinoflagellate *Noctiluca miliaris* of the Northern Arabian Sea and those of the cyanobacteria *Trichodesmium erythraeum* from the coastal and shelf waters of the west coast.

Massive blooms of the dinoflagellate *Noctiluca miliaris* were tracked in the open-waters of the Northeastern Arabian Sea using Indian remote sensing satellite (IRSP4 - OCM) while on board the four different oceanographic cruises undertaken during February-March of 2009-2011. Based on the observations and experimental results, the occurrence of *N miliaris* bloom was established having an 'Active/peak' phase in February-2009 that was followed by 'Declining/Receeding' phase in March-2009. The declining phase of the bloom were observed to recur and studied during subsequent cruises undertaken in the year 2010 and 2011. The 'active' bloom of Feb-2009 was under influence of northeasterly winds, cooler temperature (24.96±0.49°C) and a nutrient rich deeper mixed layer (71.67 ± 24.5 m), showed that the active bloom promoted inflation in oceanic bacterial counts as high as 19.3×10^9 cells L^{-1} at the surface and averaged $11.73 \pm 7.55 \times 10^{13}$ cells m^{-2} in the euphotic column. Principle component analysis based on correlations showed that total bacterial counts remained significantly correlated ($p<0.05$) with chlorophyll *a*, *N miliaris* counts, C-DOM in terms of the absorbtion coefficient at 300 nm,

photosyntehtically fixed carbon and dissolved inorganic phosphate. High bacterial counts were supported by bacterial biomass production rates as high as 0.08±0.04 g C m^{-2} h^{-1} in the euphotic column.

The 'declining' bloom phase of March (2009-2011) was accompanied by withdrawal of the Northeast monsoon, increase in sea-surface temperature (25.15 – 26:07°C) and shallowing of average mixed layer (35.16 – 38m). At this time total bacterial counts at the surface decreased significantly from 5.71 ± 6.93x10^9 cells L^{-1} in Feb-2009 to 1.66 ± 1.26 x10^9 cells L^{-1} during consecutive cruise of Mar-2009, 1.35 x10^9 cells L^{-1} during Mar-2010 and 2.87±0.54 during Mar-2011. Concentration of nutrients (nitrate, nitrite and phosphate) depleted in the upper-ocean with rise in picocyanobacterial population dominated by phycoerythrin containing *Synechococcus* sp. Their importance to the system is further indicated from an average 47.9% contribution to the total surface carbon fixation rates by the <20µm plankton size fractions during declining bloom of Mar-2009. Heterotrophic Nanoflagellates estimated during March-2011 by epifluorescent microscopy remained uncorrelated with total-bacterial counts and showed negative relationships with *N miliaris* population.

Blooms of the cyanobacteria *Trichodesmium* spp. detected during the spring inter-monsoon month of April 2008, onboard CRV *Sagar Manjusha*-06 in the Eastern Arabian Sea (mid-west coast of India) were studied to examine the importance of associate bacteria. Based on observations and results, distinctively visible bloom of "saw-dust" color in the Ratnagiri shelf showed

presence of cyanobacteria *Trichodesmium erythraeum* and *T thieabautii* with trichome concentrations as high as $3.05x10^6$ trichomes L^{-1}. Total bacterial counts (TBC) varied between 94.09 x 10^8 cells L^{-1} in the bloom to 1.34 x 10^8 cells L^{-1} in the non-bloom area. C-DOM concentrations averaged 2.27± 3.02 m^{-1} in the bloom to 0.28 ± 0.07 m^{-1} in the non-bloom waters respectively. C-DOM composition varied from a higher molecular size in the bloom to lower molecular size and increased aromaticity in the non-bloom areas respectively. Strong positive relationship of TBC with Chlorophyll *a* (R^2=0.65, $p<0.01$) and C-DOM concentrations (R^2=0.8373, p=0.01) in the bloom area indicated hydrolysis and/or uptake of C-DOM by bacteria. The results demonstrated bloom specific flow of Carbon to bacteria via C-DOM from field measurements. Further, absorbtion by mycosporine like amino acid was recorded in the filtrate of the bloom. High bacterial aggregation in inter-colonial spaces of *Trichodesmium erythraeum* was seen as a factor to affect oxygen content of the bloom patches / slicks.

Culturable bacterial counts from *Noctiluca miliaris* bloom in the Northern Arabian Sea during two consecutive cruises of Feb-Mar 2009, were ~2-3 fold higher in comparison to non-bloom waters and ranged from 3.20×10^5 - 6.84×10^5 CFU ml^{-1}. An analysis of the dominant bacteria associated with *Noctiluca* bloom resulted in retrieval of 70 bacterial isolates from an overlapping active and declining bloom phase location near north-central Arabian Sea. 16SrDNA phylogenetic and a detailed metabolic characterization showed that the flora from active phase of the bloom was dominated by gram-

positive forms (70.59%) which were dominated by *Bacillus* (35.29%) of *Firmicutes*. During the declining phase Gram-negative forms (61.11%) were dominant and they belonged predominantly to *γ-proteobacteria* represented by *Shewanella (16.67%)* and equal fractions of a *Cobetia-Pseudomonas-Psychrobacter-Halomonas* population (36.11%). Principle coordinate analysis of 16SrDNA sequences using online Unifrac portal showed that active and declining bloom phase flora were significantly different which also differed from reported endocytic flora of *Noctiluca* (red). Antibiotic resistance patterns represented as a Non-parametric multidimensional (NMDS) scaling helped differentiation among closely related strains.

On the other hand, culturable counts from the *Trichodesmium erythraeum* bloom off Ratnagiri averaged $36\pm18.4\times10^5$ CFU mL^{-1} on Zobell's and $13.4\pm6.43\times10^5$ CFU mL^{-1} on Zobell's 1/10 strength media. The dominant flora from *Trichodesmium erythraeum* tuft colonies could be retrieved (21 isolates) along-with those isolated from the filtrate of colonies (6 isolates) and referred to as the phycospheric colonial forms. Biochemical and 16SrDNA phylogenetic characterization showed that Firmicutes were the major phylum (47.62%) of the colony associated forms and were dominated by *Bacillus* spp. (28.57%), *Virgibacillus* (14.29%). Members of Actinobacteria constituted 38.09% of the flora and major representative genera were *Corynebacterium* (14.29%) and *Microbacterium* (9.52%). Members of *γ-proteobacteria* were the least dominant (14.28%) with *Halomonas, Pseudomonas* and unclassified member of *Halomonadaceae* constituting equal percentages of 4.76% to the

flora. The free-living forms were dominated in the order of *Bacillus* spp. (33.3%) and equal percentages of *Corynebacterium, Leucobacter and Shewanella* of 16.67% each.

Relationship of retreived bacteria with its bloom source i.e. *N miliaris* and *T erythreaum*, were assessed for their degrdative enzymic potentials in order to unveil their metabolic potentials. These features of the retreived bacteria were analyzed to decipher relationships of individual members as well as dominant phylogenetic clusters to the individual bloom particularly in regard to: (i) Nutrient cycle (ii) Food-chain and (iii) Acquisition of Iron under limiting conditions.

The bloom biomass of *Noctiluca miliaris* basically consists of starchy substrates, lipids (free-fatty acids, triglycerides, phospho-lipids) and proteins/ amino-acids and produce mucus. The high photosynthetic carbon fixation rates and production of dissolved organic matter containing mycosporine like amino acids as seen from the C-DOM estimates, indicated the high organic turnover of the bloom. Further, the ability of isolates to break-down/utilize complex substrates during active – declining phases of the bloom such as: (a) carbohydrates: starch (50 - 38.8 %), carboxy methyl cellulose (13.8 – 20.5%) (b) Proteins: casein (55.8 – 58.3%), gelatin (61.7 – 38.8%) (c) Lipids: Tributyrin (26.4 – 30.5%), tween-80 (52.9 – 61.1%) and a host of simple carbohydrates and amino-acids, clearly suggested that the organic matter synthesized by *Noctiluca miliaris* appears to be quickly utilized and remineralized.

Localized zones of high dissolved inorganic phosphate (DIP) detected in in the euphotic column of major *N miliaris* bloom areas of Feb-2009 suggested phosphate regeneration in the upper-ocean. DIP further showed a strong correlation with total bacterial counts as R^2= 0.829, n=47. This is possibly the reason for almost half the strains (52.9%) during the active phase of bloom expressing phosphate solubilizing ability belonging to 8 different genera of *Pseudomonas, Halomonas, Micrococcus, Microbacterium, Brachybacterium, Bacillus* and unclassified members of the family Intrasporangiaceae and Micrococcaceae.

Significantly high water-column nitrite (nutrient) in the active bloom waters of Feb-09 (0.19 – 1.1 μM) was found to be suddenly depleted within 8-10 days during consecutive cruise of March-2009, suggesting nitrogen removal in the upper-ocean. As 50% strains from active and 49.67% strains from the declining phase bloom of Feb-Mar 2009 supported the unique possibility of nitrogen removal via denitrification under '*aerobic conditions*', these bacterial strains are implicated to carry out denitrification from the high-organic *N miliaris* bloom ecosystem of the Arabian Sea, also known for high denitrification process from the anoxic mid-depth oxygen-minimum zones. Denitrifying strains belonged to members of the genera *Pseudomonas, Bacillus, Virgibacillus, Shewanella, Psychrobacter, Ochrobactrum, Brevibacillus* and an unclassified strain of the Intrasporangiaceae.

In comparison, to the genesis of *N miliaris* bloom following nutrient enrichment of winter cooling, blooms of Nitrogen-fixing cyanobacteria

Trichodesmium are favored by the warmer (>27°C) nitrate depleted and shallow stratified conditions in the Arabian Sea. Blooms of *Trichodesmium* do not attract grazers and hence the high bacterial aggregation in colonial space of *Trichodesmium erythraeum* as demonstrated in this study will be solely responsible for its remineralization and subsequent enrichment of the water-column. Such a scenario is indicated as retreived bacteria from *Trichodesmium* colonies and the phycopsheric space, dominated by *Bacillus* spp., *Virgibacillus* spp., *Corynebacterium* spp. also showed high multiple extracellular enzymic abilities to degrade starch (60%), gelatin (21.7%), casein (44%), tributyrin (33%), phosphate solubilization (25.9%) and H_2S production from organic matter (13%). Cultured members also showed the ability to uptake dissolved carbohydrates from the bloom filtrate of *Trichodesmium* as demonstrated by the anthrone-sulfuric acid method. The degrading *Trichodesmium* colonies are known to produce H_2S and the retrieval of the well-known H_2S producing species *Shewanella* algae from the phycosphere suggests their possible involvement and dominance during such decomposition processes. Further, the high bacterial load ($9.4x10^9$ cells L^{-1}) associated with *Trichodesmium* bloom, was seen as a factor in reducing oxygen content in the intra-colonial spaces.

During *N miliaris* bloom of Feb-Mar 2009, the decline of total bacterial counts from 'active' to 'declining' overlapping stations within 8-10 days raised questions on the sudden disappearance of water-column bacteria (Chapter 2). While particles with colonized bacteria were detected during March under epifluorescent microscope, the photomicrographic evidence of phagotrophy by

Noctiluca was also documented during the cruises. *N miliaris* is well-known to be 'raptorial-feeder' of diatoms, dinoflagellates, bacteria, detrital particles, etc. In this case of the mixotrophic green variety of *Noctiluca* blooms from the Arabian Sea, particles colonized by bacteria during March would be a rich nutritional source when warming of temperature and prey/nutrient limitations created unfavorable conditions. Such an additional pathway of the food-chain for a short period explains the clearance in bacterial population due to phagotrophic *Noctiluca* and further sustaining the bloom for a short-while during March.

The phylogenetic relatedness of bacteria associated with phytoplankton blooms showed their close homology with a variety of Iron binding siderophore producing strains. Bacterial ability to produce siderophores, detected using the Chrome Azurol-S quantitative assay in Iron limiting conditions, were positive for 76.4% and 69.89% of bacteria associated with 'active' and 'declining' bloom of *Noctiluca*, and 48.14% bacteria associated with *T erythreaum*. The large fraction of these strains belonged to the genera *Pseudomonads* and *Bacillus* which represented the dominant flora as well. In *Pseudomonas gessardii*, ^{GU}SK256-N6 strain siderophore production was demonstrated to increase at a cooler temperature (25°C) and lower pH 7 in comparison to pH8.2. Further, the strain clearly exhibited high-growth on the crude-filtrate of *Noctiluca* bloom supplemented with basal-media and surprisingly accompanied by siderophore production (Pyoverdine). This suggested foremost the *'Iron limitation in the crude filtrate of bloom'* (and

hence in the bloom environment), in triggering siderophorogenesis. The bloom of *Noctiluca* in the Northern Arabian Sea over an extended period of two months would deplete Iron and hence, as an essential trace-nutrient would be in continuous requirement by both algae and bacteria. Decadal satellite trends in the northeastern Arabian Sea suggests that the period of February (Active bloom period) remained the coolest month, having the highest Chlorophyll *a* and the highest Aerosol Optical Thickness (837 nm) within the period between December - April. Hence these results possibly implicate seasonal dust deposits during the winter-monsoon period as a probable factor. At this point, we strongly suspect a siderophore mediated process, wherein the closely associated bacteria of *N miliaris* can play an important role in keeping Iron bioavailable.

Conclusions

The experimental findings recorded in Chapters 2-4 of this thesis with regard to the "**Microbial ecology of phytoplankton blooms of the Arabian Sea and their implications**" led to the following conclusions:

1. Alterations in the food-chain

Blooms of Noctiluca miliaris caused alterations in the food-chain of the Arabian Sea and hijacks 'microbial-loop' for a short while

- The inflation in counts of total bacteria supported by dissolved organic matter of *N miliaris* active phase bloom is quickly lost to *Noctiluca* itself during the declining phase as an additional pathway 'hijacking' the 'microbial-loop' as *N miliaris* voraciously feeds on particles colonized by heterotrophic bacteria, to meet their nutritional demands and thereby, leads to a reduction in the total bacterial counts. This helps in sustaining the bloom further for a short while during nutrient limited conditions of March.

Microbial succession in Noctiluca bloom:

- The progression of bloom into the declining phase of March is marked by depletion of upper-ocean nutrients which favors the succession of phycoerythrin containing picocyanobacteria and contributes a large fraction to the primary-productivity of the ecosystem.

2. Shift in Bacterial flora

Bloom phases as drivers of bacterial community

- The phycospheric flora of *N miliaris* bloom dominated by members of the phylum *Firmicutes* of the genera *Bacillus* during the active phase, shifts to a predominantly *γ-proteobacterial* population consisting of equal percentages of *Shewanella, Psychrobacter, Halomonas* and *Cobetia* during the declining bloom phase.
- The *Trichodesmium erythraeum* healthy trichomes and intra-colonial space were dominated by members of the phylum Firmicutes belonging to *Bacillus* spp., *Virgibacillus* and Actinobacterial forms of the genus *Corynebacterium* and *Microbacterium*, whereas, occurrence of H_2S producing *Shewanella algae* in free- living fractions can be important during the latter phases of the bloom.

3. Biogeochemical implications in:

- **Aerobic Denitrification:** The ability of a large fraction of N miliaris associated bacterial strains (50%- 41.67%) to '**aerobically denitrify**' indicates their potential for Nitrogen removal from these high-organic micro-niches of the *Noctiluca* bloom in the Arabian Sea, also known for high denitrification activity.

- **Iron acquisition and bioavailability:** Iron is a principal micro-nutrient for growth of both phytoplankton and bacteria. The high frequency of siderophore producing bacteria associated with blooms of both *Noctiluca miliaris* and *Trichodesmium* spp. would **increase bio-available Iron in the bloom environment**. Siderophore production is induced as bloom DOM supports high growth rates, increasing Iron demand for bacteria, pointing to a need of studying the "Aerosol-Siderophore-Bacteria" links to the blooms in the Arabian Sea, which possibly will throw light on bacterial role in bloom dynamics of this unique tropical ocean basin, responsive to climatic forcings.

Outcome of Research

a) 97 bacterial cultures associated with phytoplankton blooms of the Arabian Sea with potential/possible new taxonomically unassigned strains under further investigation.

b) 16SrDNA sequences of bloom associated bacterial strains deposited with GenBank accession numbers JX429827-JX429892.

c) **Research papers enlisted as below:**

1. Basu S, Matondkar SGP, Furtado I (2011) Enumeration of bacteria from a *Trichodesmium* spp. bloom of the eastern Arabian Sea: elucidation of their possible role in biogeochemistry. **J Applied Phycology**. 23(2): 309-319

2. Basu S, Matondkar SGP, Furtado I (2013) Retreived bacteria from Noctiluca miliaris (green) bloom of the Northeastern Arabian Sea. **Chinese J Oceanology and Limnology**. 31(1): 10-20
3. Basu S, Deobagkar DD, Matondkar SGP*, Furtado I (2013) Culturable bacterial associated with the dinoflagellate green *Noctiluca miliaris* during active and declining bloom phases in the Northern Arabian Sea. **Microbial Ecology**. 65(4): 934-954.

d) **Manuscripts under preparation/communication**

1. Basu S, Matondkar SGP, Furtado I. Charactersitics of three frequently retreived *Bacillus* and their anti-oxidant activity from *N miliaris* bloom of the Northern Arabian Sea. **Communicated.**
2. Basu S, Matondkar SGP, Furtado I. Relevance of the phycospheric bacterial associates in the dynamics of algal blooms of the Arabian Sea blooms. **Under Preparation.**
3. Basu S, Matondkar SGP, Furtado I. Siderophore producing bacteria associated with blooms of the Arabian Sea. **Under Preparation.**
4. Basu S, Matondkar SGP, Furtado I. Bacterial flora of *Trichodesmium* sp. bloom and their comparison with *N miliaris* bloom. **Under Preparation.**
5. Basu S, Matondkar SGP, Furtado I. Phytoplankton bloom-bacterial relationships: A review. **Under Preparation.**

e) **Papers presented in conferences:**

1. Basu S, Matondkar SGP, Furtado I (2009) Microbial aspects of the dinoflagellate *Noctilua miliaris* of the Arabian Sea. 2nd GEOHAB meeting, Scientific Committee of Oceanographic Reasearch, BEIJING, China.
2. Basu S, Furtado I, Matondkar SGP (2009) Bacterial enumeration from *Trichodesmium* spp. bloom of the eastern Sea and their role in biogeochemistry. 7th Asia-Pacific conference on biotechnology, New-Delhi.

Bibliography

Adachi M, Kanno T, Okamoto R, Itakura S, Yamaguchi M, Nishijima T (2003) Population Structure of Alexandrium (Dinophyceae) Cyst Formation-Promoting Bacteria in Hiroshima Bay, Japan. *Applied and Environmental Microbiology* 69(11): 6560-6568.

Adachi, M, Matsubara T, Okamoto R, Nishijima T, Itakura S, Yamaguchi M (2002) Inhibition of cyst formation in the toxic dinoflagellate Alexandrium (Dinophyceae) by bacteria from Hiroshima Bay, Japan. *Aquatic Microbial Ecology* 26:223–233.

Adachi M, Kanno T, Okamoto R, Shinozaki A, Fujikawa AK, Nishijima T (2004) *Jannaschia cystaugens* sp. nov., an Alexandrium (Dinophyceae) cyst formation-promoting bacterium from Hiroshima Bay, Japan. *International Journal of Systematic and Evolutionary Microbiology* 54(5): 1687-1692.

Alldredge AL, Gottschalk CC (1989) Direct observations of the mass flocculation of diatom blooms: characteristics, settling velocities and formation of diatom aggregates. *Deep Sea Research*-Part I 36(2): 159-171

Alexander DB, Zuberer (1991) Use of chrome azurol S reagents to evaluate siderophore production by rhizosphere bacteria. *Biology and Fertility of soils* 12(1): 39-45

Altayar M, Sutherland AD (2006) *Bacillus cereus* is common in the environment, but emetic toxin-producing isolates are rare. *Journal of Applied Microbiology* 100:7–14.

Amin AS, Green DH, Hart MC, Kupper FC, Sunda WG, Carrano CJ (2009) Photolysis of iron–siderophore chelates promotes bacterial–algal mutualism. *Proceedings of Natural Academy of Science USA* 106(40):17071-17076.

Amin SA, Parker MS, Armbrust VE (2012) Interactions between Diatoms and Bacteria. *Microbiology and Molecular Biology reviews* 76(3): 667-684.

Anderson DM, Alpermann TJ, Cembella AD, Collos Y, Masseret E, Montresor M (2012) The globally distributed genus *Alexandrium*: multifaceted roles in marine ecosystems and impacts on human health. *Harmful Algae* 14:10-35

Arrigo KR (2005) Marine microorganisms and global nutrient cycles. *Nature* 437:349–355

Azam F, Fenchel T, Field JG, Gray JS, Reil LAM, Thingstad F (1983) The ecological role of water-column microbes in the sea. *Marine Ecology Progress Series* 10:257-263.

Azam F, Malfatti F (2007) Microbial structuring of Marine ecosystems. *Nature Reviews Microbiology* 5:782-791

Azam F, Steward GF, Smith DC, Ducklow HW (1994) Significance of bacteria in the carbon fluxes of the Arabian Sea. *Journal of Earth System Science* 103(2):341-351

Babin SM, Carton JA, Dickey TD, Wiggert JD (2004) Satellite evidence of hurricane-induced phytoplankton blooms in an oceanic desert. *Journal of Geophysical Research* 109: C03043, doi: 10.1029/2003JC001938

Balch WM, Vaughn JM, Novotny JF, Drapeau DT, Goes JI, Lapierre JM, Scally E, Vining CL, Ashe A, Vaughn JMJ (2002) Fundamental changes in light scattering associated with infection of marine bacteria by bacteriophage. *Limnology and Oceanography* 47:1554-1561

Balcerak E (2012) Arabian Sea eddies promote seasonal phytoplankton blooms. *EOS Transactions American Geophysical Union* 93(2):28

Banse K (1987) Seasonality of phytoplankton chlorophyll in the central and northern Arabian Sea. *Deep Sea Research*-I 34:713–723.

Barbeau K, Rue EL, Bruland KW, Butler A (2001) Photochemical cycling of iron in the surface ocean mediated by microbial iron (III)-binding ligands. *Nature* 413:409–413.

Bell WH, Mitchell R (1972) Chemotactic and growth responses of marine bacteria to algal extracellular products. *Biological Bulletin* 143:265-77

Bertrand EM, Saito MA, Lee PA, Dunbar RB, Sedwick PN, DiTullio G (2011[a]) Iron Limitation of a Springtime Bacterial and Phytoplankton Community in the Ross Sea: Implications for Vitamin B_{12} Nutrition. *Frontiers in Microbiology* 2:160-187

Bertrand EM, Saito MA, Jeon YJ, Neilan BA (2011[b]) Vitamin B_{12} biosynthesis gene diversity in the Ross Sea: the identification of a new group of putative polar B_{12} biosynthesizers. *Environmental Microbiology* 13(5)1285-1298

Biddanda B and Benner R (1997) Carbon, nitrogen, and carbohydrate fluxes during the production of particulate and dissolved organic matter by marine phytoplankton. *Limnology and Oceanography* 42: 506–518

Boyd P, Jickells T, Law C et al. (2007) Mesoscale iron enrichment experiments 1993–2005: synthesis and future directions. *Science* 315, 612–617

Bratbak G, Egge JK, Heldal M (1993) Viral mortality of the marine alga *Emiliania huxleyi* (Haptophyceae) and termination of algal blooms. *Marine Ecology Progress Series 93*: 39-48

Brockmann UH, Eberlein K, Junge HD, Reimer-Maier E, Siebers D (1979) The development of a natural plankton population in an outdoor tank with nutrient poor sea-water-II. Changes in dissolved carbohydrates and amino acids. *Marine Ecology Progress Series* 1:283-291

Brussaard CPD (2004) Viral control of phytoplankton populations –a review. *Journal of Eukaryotic Microbiology* 51(2):125-138

Brophy JE, Carlson DJ (1989) Production of biologically refractory dissolved organic carbon by natural seawater microbial populations. *Deep Sea Research-II* 36:497–507

Buck DJ (1982) Non-staining (KOH) method for determination of Gram reactions of marine bacteria. *Applied and Environmental Microbiology* 44:992–993

Butler A (2005) Marine siderophores and microbial iron mobilization. *Biometals* 18:369–374.

Calbet A, Landry MR (2004) Phytoplankton growth, microzooplankton grazing, and carbon cycling in marine systems. *Limnology and Oceanography* 49(1): 51-57.

Capone DG, Zehr J, Paerl HW, Bergman B, Carpenter EJ (1997) *Trichodesmium*: a globally significant marine cyanobacterium. *Science* 276:1221–1229

Carreto JI, Carignan MO, Montoya NG (2005) A high-resolution reverse-phase liquid chromatography method for the analysis of mycosporine-like amino acids (MAAs) in marine organisms. *Marine Biology* 146: 237–252

Carder KL, Steward RG, Harvey GR, Ortner PB (1989) Marine humic and fulvic acids: their effects on remote sensing of ocean chlorophyll. *Limnology and Oceanography* 34:68–81

Carpenter JH (1965) The Chesapeake Bay Institute technique for the Winkler dissolved oxygen method. *Limnology and Oceanography* **10**: 141-143

Charlson RJ, Lovelock JE, Andreae MO, Warren SG (1987) Oceanic phytoplankton, atmospheric sulphur, cloud albedo and climate. *Nature* 326(6114): 655-661

Chin WC, Orellana MV, Verdugo P (1998) Spontaneous assembly of marine dissolved organic matter into polymer gels. *Nature* 391:581–572

Chin YP, Aiken GO, Loughlin E (1994) Molecular weight, polydispersity, and spectroscopic properties of aquatic humic substances. *Environmental Science Technology* 26:1853–1858

Chrost RJ (1991) Environmental control of the synthesis and activity of aquatic microbial ectoenzymes. In: Chrost RJ (ed.) *Microbial enzymes in aquatic environments*. Springer, New York, pp 29–59

Chen Y, Zhang Y, Jiao N (2011) Responses of aerobic anoxygenic phototrophic bacteria to algal blooms in the East China Sea. *Hydrobiologia* 661:435–443

Cole JJ (1982) Interactions between bacteria and algae in aquatic ecosystems. *Annual Review of Ecological Systematics* 13:291-314

Cole JR, Wang Q, Cardenas E et al. (2009) The Ribosomal Database Project: improved alignments and new tools for rRNA analysis. *Nucleic Acids Research* 37:D141–D145

Connon SA, Giovannoni SJ (2002) High-throughput methods for culturing microorganisms in very-low-nutrient media yield diverse new marine isolates. *Applied and Environmental Microbiology* 68: 3878–3885.

Croft MT, Lawrence AD, RauxDeery E, Warren MJ, Smith AG (2005) Algae acquire vitamin B_{12}through a symbiotic relationship with bacteria. *Nature* 438:90-93

Danger M, Oumarou C, Benest D, Lacroix G (2007) Bacteria can control stoichiometry and nutrient limitation of phytoplankton. *Functional ecology* 21(2): 202-210

Davis CO (1982) The importance of understanding phytoplankton life strategies in the design of enclosure experiments. *In*: Grice G D, Reeve M R, editors; Grice G D, Reeve M R, editors. Marine mesocosms: biological and chemical research in experimental ecosystems. Springer-Verlag, New York. pp 323–332.

De Haan H, De Boer T (1987) Applicability of light absorbance and fluorescence as measures of concentration and molecular size of dissolved organic carbon in humic Laken Tjeukemeer. *Water Research* 21: 731–734

Deng SS, Horstmann U (1995) Ferrioxamines B and E as iron sources for the marine diatom *Phaeodactylum tricornutum. Marine Ecology Progress Series* 127:269-277

DeLong EF (2009) The microbial ocean from genomes to biomes. *Nature* 459:200–206.

DeLong EF, Karl DM (2005) Genomic perspectives in microbial oceanography. *Nature* 437: 336–342

DeSousa SN, Kumar MD, Sardessai SV, Sarma VVSS, Shirodkar PV (1996) Seasonal variability in oxygen and nutrients in the central and eastern Arabian Sea. *Current Science* 71:857–862.

Devassy VP (1987) *Trichodesmium* red tides in the Arabian Sea. In: Rao TSS et al. (eds.) *Contributions in Marine Sciences*. Sastyabdapurti Felicitation Volume. National Institute of Oceanography, Dona Paula, Goa, India. pp 61–66

Devassy VP, Bhattathiri PMA, Qasim SZ (1979) Succession of organisms following *Trichodesmium* phenomenon. *Indian Journal of Marine Science* 8:89-93

Devassy VP, Nair SRS (1987) Discolouration of water and its effect on fisheries along the Goa coast. *Mahasagar* 20:121–128

Dikarev VP, Svetashev VI, Vaskovsky VE (1982) *Noctiluca miliaris* - one more protozoan with unusual lipid composition. *Comparative Biochemistry and Physiology* Part B 72(1): 137 – 140

Dwivedi RM, Raman M, Parab S, Matondkar SGP, Nayak S (2006) Influence of northeasterly trade winds on intensity of winter bloom in the Northern Arabian Sea. *Current Science* 90(10):1397-1406

Dwivedi RM, Raman M, Babu KN., Singh SK, Vyas NK, Matondkar SGP (2008) Formation of algal bloom in the northern Arabian Sea deep waters during January–March: a study using pooled *in situ* and satellite data. *International Journal of Remote Sensing* 29(15): 4537-4551

Doucette G, Kodama M, Franca S, Gallacher S (1998) Bacterial interactions with harmful algal bloom species: bloom ecology, toxigenesis, and cytology. In: Anderson DM, Cembella AD, Hallegraeff GM (Eds) *Physiological Ecology of Harmful Algal Blooms*. Springer-Verlag, Heidelberg, p 619-648

Doucette GJ, McGovern ER, Babinchak JA (1999) Algicidal bacteria active against *Gymnodinium breve* (Dinophyceae). I. Bacterial isolation and characterization of killing activity. *Journal of Phycology* 35:1447-1457

Droop MR (2007) Vitamins, phytoplankton and bacteria: symbiosis or scavenging? *Journal of Plankton Research* 29:107–113.

Druffel ERM, Williams PM, Bauer JE, Ertel JR (1992) Cycling of dissolved and particulate organic matter in the open ocean. *Journal of Geophysical Research* 97(15)639-659

Ducklow WH, Smith DC, Campbell L, Landry MR, Quinby HL, Steward GF, Azam F (2001[a]) Heterotrophic bacterioplankton in the Arabian Sea: Basinwide response to year-round high primary productivity. *Deep Sea Research-II* 48:1303-1323

Ducklow HW, Steinberg DK, Buesseler KO (2001[b]) Upper ocean carbon export and the biological pump. *Oceanography* 14 (4): 50-58

Ducklow HW (2000) Bacterial production and biomass in the oceans. In: Kirchman DL (ed.) Microbial ecology of the oceans. Wiley-Liss, New-York. pp 85–120

Elbrachter M, Qi Y (1998) Aspects of *Noctiluca* (Dinophyceae) population dynamics. In: Anderson DM, Cembella A, Hallegraeff G M (eds) *Physiological ecology of harmful algal blooms*. NATO ASI Series, 41, Berlin. pp 315-335

Eppley R W, Peterson B J (1979) Particulate organic matter flux and planktonic new production in the deep ocean. *Nature* 282: 677–680.

Ettoumi B, Raddadi N, Borin S, Daffonchio D, Boudabous A, Cherif A (2009) Diversity and phylogeny of culturable spore-forming *Bacilli* isolated from marine sediments. *Journal of Basic Microbiology* 49:S13-S23

Falkowski PG, Fenchel T, Delong EF (2008) The microbial engines that drive earth's biogeochemical cycles. *Science* 320: 1034 –1039

Falkowski PG, Raven J (2007) *Aquatic Photosynthesis*, 2nd Ed. Princeton. pp 476

Falkowski PG, Katz ME, Knoll AH, Quigg A, Raven JA, Schofield O, Taylor FJR (2004) The evolution of modern eukaryotic phytoplankton. *Science* 305: 354-360

Falkowski PG, Barber RT, Smetacek V (1998) Biogeochemical controls and feedbacks on ocean primary production. *Science* 281: 200–206.

Falkowski PG (1994) The role of phytoplankton photosynthesis in global biogeochemical cycles. *Photosynthesis Research* 39: 235-258

Fandino LB, Riemann L, Steward GF, Long RA, Azam F (2001) Variations in bacterial community structure during a dinoflagellate bloom analyzed by DGGE and 16SrDNA sequencing. *Aquatic Microbial Ecology* 23: 119–130

Ferreira JG, Andersen JH, Borja A et al. (2011) Overview of eutrophication indicators to assess environmental status within the European Marine Strategy Framework Directive. *Estuarine, Coastal and Shelf Science* 93(2):117-131

Fogg GE (1983) The ecological significance of extracellular products of phytoplankton photosynthesis. *Botanica marina* 26: 3-14

Fredrickson JK, Romine MF, Beliaev AS et al. (2008) Towards environmental systems biology of *Shewanella*. *Nature Reviews Microbiology* 6:592-603

Frost LS, Leplae R, Summers AO, Toussaint A (2005) Mobile genetic elements: the agents of open source evolution. *Nature Reviews Microbiology* 3:722-732

Fukami K, Nishijima T, Ishida Y (1997) Stimulative and inhibitory effects of bacteria on the growth of microalgae. *Hydrobiologia* 358: 185-191

Fukami K, Nishijima T, Murata H, Doi S, Hata Y (1991) Distribution of bacteria influential on the development and the decay of *Gymnodinium nagasakiense* red tide and their effect on algal growth. *Nippon Suisan Gakkaishi* 57:2321-2326

Furusawa G, Yoshikawa T, Yasuda A, Sakata T (2003) Algicidal activity and gliding motility of *Saprospira* sp. SS98-5. *Canadian Journal of Microbiology* 49:92-100

Gardes A, Iversen MH, Grossart HP, Passow U, Ullrich MS Diatom-associated bacteria are required for aggregation of *Thalassiosira weissflogii*. *The ISME Journal* (2011) 5, 436–445

Garrison LD, Gowing MM, Hughes MP, Campbell L, Caron AD, Dennett MR, Shalapyonok A, Olson RJ, Landry MR, Brown SL, Liu HB, Azam F, Steward GF, Ducklow HW, Smith DC (2000) Microbial Food web structure in the Arabian Sea: a US JGOFS study. *Deep Sea Research*-II 47: 1387-1322

Gerhardt P, Murray RGE, Costilow RW, Nester EW, Wood WA, Krieg NR, Phillips GB (1981) *Manual of methods for general bacteriology.* American Society of Microbiology, Washington DC. pp 524

Giovannoni S, Stingl U (2007) The importance of culturing bacterioplankton in the 'omics' age. *Nature Reviews Microbiology* 5(10): 820-826

Goecke F, Thiel V, Wiese J, Labes A, Imhoff JF (2013) Algae as an important environment for bacteria – phylogenetic relationships among new bacterial species isolated from algae. *Phycologia*: 52(1): 14-24.

Goes JI, Thoppil GP, Gomes HdoR, Fasullo JT (2005) Warming of the Eurasian Landmass Is Making the Arabian Sea More Productive. *Science* 308 (5721): 545 – 547

Goes JI, Gomes, HdoR, Kumar A, Gouveia A, Devassy VP, Parulekar AH, Rao, L.V.G (1992) Satellite and ship studies of phytoplankton along the west coast of India. In: Desai, B.N. (Ed.), *Oceanography of the Indian Ocean.* Oxford and IBH Publishing Co., New Delhi, pp. 67–80.

Gomes H doR, Goes JI, Matondkar SGP, Parab SG, Al-Azri ARN, Thoppil GP (2008) Blooms of *Noctiluca miliaris* in the Arabian Sea—An *in situ* and satellite study. *Deep-Sea Research*-I 55: 751– 765

Gonzalez JM, Simo R, Massana R, Covert JS, Casamayor EO, Pedros-Alio C, Moran MA (2000) Bacterial community structure associated with a Dimethylsulfoniopropionate-Producing North Atlantic Algal Bloom. *Applied Environmental Microbiology* 66(10): 4237-4246

Green DH, Llewellyn, Negri AP, Blackburn SI, Bolch CJS (2004) Phylogenetic and functional diversity of the cultivable bacterial community associated with the paralytic shellfish poisoning dinoflagellate *Gymnodinium catenatum. FEMS Microbiology Ecology* 47(3): 345-357

Grashoff K, Kremling K, Ehrhard M (1999) Methods of Seawater Analysis. Wiley VCH, Weinheim, New York. pp 419

Gribaldo S, Brochier-Armanet C (2006) The origin and evolution of Archaea: a state of the art. *Philosophical Transactions of the Royal Society B: Biological Sciences*. 361(1470): 1007 – 1022

Gupta V, Saharan K, Kumar L, Gupta R, Sahai V, Mitta A (2008) Spectrophotometric Ferric Ion Biosensor From *Pseudomonas fluorescens* Culture. *Biotechnology Bioengineering*. 100(2): 284-296

Guillard RRL, Kilham P (1977) The ecology of marine planktonic diatoms. In: D Werner (ed.) *The Biology of Diatoms*. Berkeley, University of California Press. pp 372-469

Guo C, Fuchao Li, Peng J, Zhaopu L, Song Q (2011) Bacterial diversity in surface water of the Yellow Sea during and after a green alga tide in 2008. *Chinese Journal of Oceanology and Limnology* 29(6): 1147-1154

Hagstrom A, Larsson U, Horstedt P, Normark S (1979) Frequency of dividing cells, a new approach to the determination of bacterial growth rates in aquatic environments. *Applied and Environmental Microbiology* 75(5)805-812

Haines KC, Guillard RRL (1974) Growth of vitamin B_{12}-requiring marine diatoms in mixed laboratory cultures with vitamin B_{12}-producing marine bacteria. *Journal of Phycology* 10:245–252

Hallegraeff GM (1993) A review of harmful algal blooms and their apparent global increase. *Phycologia* 32(2): 79–99

Hansen PJ, Miranda L, Azanza R (2004) Green *Noctiluca Scintillans*: a dinoflagellate with its own greenhouse. *Marine Ecology Progress Series* 275:79-87

Harrison P J, Furuya K, Gilbert PM, Xu J, Liu HB, Yin K, Lee JHW, Anderson DM, Gowen R, Al-Azri AR, Ho AYT (2011) Geographical distribution of red and green *Noctiluca scintillans*. *Chinese Journal of Oceanology and Limnology* 29(4): 807-831

Hau HH, Gralnick JA (2007) Ecology and biotechnology of the genus *Shewanella*. *Annual Review of Microbiology* 61:237-258

Haynes K, Hoffmann TA, Smith CJ, Ball AS, Underwood JC, Osborn AM (2007) Diatom-Derived Carbohydrates as factors affecting Bacterial Community Composition in Estuarine Sediments. *Applied and Environmental Microbiology* 73(19): 6112-6124

Heisler J, Gilbert PM, Burkholder JM, Anderson DM, Cochlane W, Dennison WC, Dortch Q, Gobler CJ, Heil CA, Humphries E, Lewitus A, Magnien R, Marshall HG, Sellner K, Stockwell DA, Stoecker DK, Suddleson M (2008) Eutrophication and harmful algal blooms: A scientific consensus. *Harmful Algae* 8: 3-13.

Helliwell KE, Wheeler GL, Leptos KC, Goldstein RE, Smith AG (2011) Insights into the Evolution of Vitamin B_{12} Auxotrophy from Sequenced Algal Genomes. *Molecular Biology and Evolution* 28(10):2921–2933

Helms RJ, Stubbins A, Ritchie DJ, Minor CE, Kieber JD, Mopper K (2008) Absorbtion spectral slopes and slope ratios as indicators of molecular weight, source and photobleaching of chromophoric dissolved organic matter. *Limnology and Oceanography* 53(3): 955-969

Hellebust JA (1965) Excretion of some organic compounds by marine phytoplankton. *Limnology and Oceanography*. 10:192-206

Herbert D, Phipps PJ, Strange RE (1971) Chemical analysis of microbial cells. In: Norris JR et al. (eds.) *Methods in microbiology*, volume 5B, Academic Press, London. pp 264 – 275

Holt J G, Krieg N R, Sneath P H A, Staley J T & Williams ST (1994) *Bergey's Manual of Determinative Bacteriology*. Williams and Wilkins, Baltimore. pp787

Hobbie JE, Daley RJ, Japer S (1977) Use of nucleopore filters for counting bacteria by fluorescence microscopy. *Applied and Environmental Microbiology* 33:1225-1228

Hopkinson BM, Morel FMM (2009) The role of siderophores in iron acquisition by photosynthetic marine microorganisms. *Biometals* 22:659–669

Hünken M, Harder J, Kirst GO (2008) Epiphytic bacteria on the Antarctic ice diatom Amphiprora kufferathii Manguin cleave hydrogen peroxide produced during algal photosynthesis. *Plant Biolology* 10:519 –526

ICES (2008) Report of the ICES special meeting on the causes, dynamics and effects of exceptional marine blooms and related events. *International Council Meeting Paper*, 4-5 October 1984/ E: 42, Copenhagen. pp 16

Imai I, Ishida Y, Sakaguchi K, Hata Y (1995) Algicidal marine bacteria isolated from northern Hiroshima Bay, Japan. *Fisheries Science* 61:624-632

Imai I, Sunahara T, Nishikawa T, Hori Y, Kondo R, Hiroishi S (2001) Fluctuation of the red tide flagellates *Chattonella* spp. (Raphidophyceae) and the algicidal bacterium *Cytophaga* sp. in the Seto Inland Sea, Japan. *Marine Biology* 138:1043-1049

Isnansetyo A, Kamei Y (2009) Bioactive substances produces by marine isolates of *Pseudomonas*. *Journal of Industrial Microbiology and Biotechnology* 36:1239-1248

Ivanova EP, Christen R, Sawabe T, Alexeeva YV, Lysenko AM, Chelomin VP, Mikhailov VV (2005) Presence of Ecophysiologically Diverse Populations

within *Cobetia marina* strains isolated from Marine Invertebrate, Algae and the Environments. *Microbes and Environment* 20(4):200-207

Jones KL, Mikulski CM, Barnhorst A, Doucette GJ (2010) Comparative analysis of bacterioplankton assemblages from Karenia brevis bloom and non-bloom water on the west Florida shelf (Gulf of Mexico, USA) using16S rRNA gene clone libraries. *FEMS Microbiology Ecology* 73:468–485

Jensen MM, Lam P, Revsbech NP, Nagel B, Gaye B, Jetten SMM, Kuypers MM (2011) Intensive nitrogen loss over the Omani Shelf due to annamox coupled with dissimilatory nitrite reduction to ammonium. *ISME J* 5:1660-1670

Jeswani H, Mukherji S (2012) Degradation of phenolics, nitrogen heterocyclics and polynuclear aromatic hydrocarbons in a rotating biological contactor. *Bioresource Technology* 111:12-20

Jeong H, Yim JH, Lee C, Choi SH, Park YK, Yoon SH, Hur CG, Kang HY, Kim D, Lee DH, Park KH, Park SH, Park HS, Lee KH, Oh KT, Kim JF (2005) Genomic blueprint of *Hahella chejuensis*, a marine microbe producing an algicidal agent. *Nucleic Acids Research* 33: 7066–7073.

Kannapiran E, Ravindran J (2012) Dynamics and diversity of phosphate mineralizing bacteria in the coral reefs of Gulf of Mannar. *Journal of Basic Microbiology* 52 91–98

Kaye JZ, Sylvan JB, Edwards KJ, Baross JA (2011) Halomonas and Marinobacter ecotypes from hydrothermal vent, sub seafloor and deep-sea environments. *FEMS Microbiology Ecology* 75 (2011) 123–133

Kemp PF, Sherr BF, Sherr EV, Cole. J.J. (1993) Handbook of Methods in Aquatic Microbial Ecology. Lewis Publishers, Boca Raton. pp 777

Keel C, Weller DM, Natsch, Defago G, Cook RJ, Thomashow LS (1996) Conservation of the 2, 4-diacaetlyphloroglucinol biosynthesis locus among fluorescent Pseudomonas strains from diverse geographic locations. *Applied and Environmental Microbiology* 62(2): 552-563

Keawtawee T, Fukami K, Songsangjinda P, Muangyao P (2011) Isolation and characterization of *Noctiluca*-killing bacteria from a shrimp aquaculture pond in Thailand. *Fisheries Science* 77:657–664

Keawtawee T, Fukami K, Songsangjinda P (2012) Use of a *Noctiluca*-killing bacterium Marinobacter salsuginis strain BS2 to reduce shrimp mortality caused by *Noctiluca scintillans*. *Fisheries Science* 78(3):641–646

Khandeparker R, Verma P, Meena RM, Deobagkar DD (2011) Phylogenetic diversity of carbohydrate degrading culturable bacteria from Mandovi and Zuari estuaries, Goa, west coast of India. *Estuarine, Coastal and Shelf Science* 95: 359-366

Kim OS, Cho YJ, Lee K, Yoon S H, Kim M, Na H, Park S C, Jeon Y S, Lee J H, Yi H, Won S, Chun J (2012) Introducing EzTaxon-e: A Prokaryotic 16S rRNA Gene Sequence Database with Phylotypes that Represent Uncultured Species. *International Journal of Systematic and Evolutionary Microbiology* 62:716-721

Kiorbe T, Titelman J (1998) Feeding, prey selection and prey encounter mechanisms in the heterotrophic dinoflagellate *Noctiluca scintillans*. Journal of Plankton Research 20(8): 1615-1636

Kirchman DL, Suzuki Y, Garside C, Ducklow HW (1991) High turnover rates of dissolved organic carbon during a spring phytoplankton bloom. *Nature* 352: 612-614

Kirchman DL (2008) Microbial Ecology of the Oceans, 2nd ED. John Wiley and Sons, Inc. pp 593

Kirchner M, Sahling G, Uhlig G, Gunkel W, Klings KW (1996) Does the red-ride forming dinoflagellate *Noctiluca scintillans* feed on bacteria? *Sarsia* 81:45-55

Kirchner M, Wichels A, Seibold A, Sahling G, Schutt C (2001) New and potentially toxic isolates from *Noctiluca scintillans* (Dinoflagellate). In: Hallegraff G (ed) Proceedings on Harmful Algae, 9th International conference on Harmful algae blooms, Tasmania 2000, pp 379-382

Kitaguchi H, Hiragushi N, Mitsutani A, Yamaguchi M, Ishida Y (2001) Isolation of an algicidal bacterium with activity against the harmful dinoflagellate Heterocapsa circularisquama (Dinophyceae). Phycologia 40:275-279

Knap A, Michaels A, Close A, Ducklow H, Dickson A (1996) Protocols for the Joint Global Ocean Flux Study (JGOFS) Core Measurements. *JGOFS Report No. 19*, Scientific Committee on Oceanic Research, International Council of Scientific Unions. Intergovernmental Oceanographic Commission, UNESCO 1994, Bergen, Norway. 170pp

Landry MR, Brown SL, Campbell L, Constaninou J, Liu H (1998) Estimating rates of growth and microzooplankton grazing in the Arabian Sea during monsoon forcing. *Deep Sea Research-Part II* 45:2353–2368.

Langdon C (2010) Determination of dissolved oxygen in sea water by winkler titration using the amperometric technique. The GO-SHIP Repeat Hydrography manual: A collection of expert reports and guidelines. IOCCP report 14, ICPO publication series 34, Ver-1. Pp 1-18

Lovejoy C, Bowman JP, Hallegraeff GM (1998) Algicidal effects of a novel marine *Pseudoalteromonas* isolate (class Proteobacteria, gamma subdivision) on harmful algal bloom species of the genera *Chattonella, Gymnodinium, and Heterosigma. Applied and Environmental Microbiology* 64:2806-2813

Lee SO, Kato J, Takiguchi N, Kuroda A, Ikeda T, et al. (2000) Involvement of an extracellular protease in algicidal activity of the marine bacterium *Pseudoalteromonas* sp strain A28. *Applied and Environmental Microbiology* 66(10): 4334–4339.

Lomas MW, Gilbert PM (1999) Temperature regulation of nitrate uptake: A novel hypothesis about nitrate uptake and reduction in cool-water diatoms. Limnology and Oceanography 44(3): 556–572

Long RA, Rowley DC, Zamora E, Liu J, Bartlett DH, Azam F (2005) Antagonistic interactions among Marine Bacteria Impede the Proliferation of *Vibrio cholerae. Applied and Environmental Microbiology* 71(12): 8531-8536

Lozupone C, Lladser ME, Knights D, Stombaugh J, Knight R (2011) UniFrac: an effective distance metric for microbial community comparison. ISME J 5:169-172

Mackey MD, Mackey DJ, Higgins HW, Wright SW (1996) CHEMTAX- A program for estimating class abundances from chemical markers: application to HPLC measurements of phytoplankton pigments. *Marine Ecology Progress Series* 144, 265-283

Madhupratap M, Prasanna Kumar S, Bhattathiri P M A, Dileep Kumar M, Raghukumar S, Nair K KC, Ramaiah N (1996) Mechanism of the biological response to winter cooling in the northeastern Arabian Sea. *Nature* 384: 549-552

Mague TH, Friberg E, Hughes DJ, Morris I (1980) Extracellular release of carbon by marine phytoplankton; a physiological approach. *Limnology and Oceanography* 25:262–279

Martin JH (1990) Glacial-Interglacial CO_2 change: The Iron Hypothesis. *Paleoceanography* 5(1): 1-13

Martin JD, Ito Yusai, Homann VV, Haygood MG, Butler A (2006) Structure and membrane affinity of new amphiphilic siderophores produced by *Ochrobactrum* sp. SP18. *Journal of Biological Inorganic Chemistry* 11:633-641

Martinez JL (2008) Antibiotics and antibiotics resistance genes in natural environments. *Science* 321:365-367

Matondkar SGP, Bhat SR, Dwivedi RM, Nayak SR (2004) Indian Satellite IRS-P4 (OCEANSAT) monitoring algal blooms in the Arabian Sea. *Harmful Algae News* 26:4-5,http://ioc.unesco.org/hab

Matondkar SGP, Parab SG, Desa E, Dwivedi RM (2006) Basin scale distribution of *Trichodesmium* spp. in the Arabian Sea using Oceansat I/ OCM. In: Robert JF et al. (eds.) *Remote Sensing of the Marine Environment.* Proc SPIE Vol. 6406 64060V, doi: 10.1117/12.693687

Matsuzaka E, Nomura N, Nakajima-Kambe T, Okada N, Nakahara T (2003) A simple screening procedure for heterotrophic nitrifying bacteria with oxygen-tolerant denitrification activity. *Journal of BioScience and BioEngineering* 95(4):409-411

Mayali X, Azam F (2004) Algicidal bacteria in the sea and their impact on algal blooms. *Journal of Eukaryotic Microbiology* 51:139-144

Mayali X, Franks PJS, Azam F (2007) Bacterial induction of temporary cyst-formation in the dinoflagellate *Lingulodinium polyedrum. Aquatic Microbial Ecology* 50:51-62

Mayali X, Doucette GJ (2002) Microbial community interactions and population dynamics of an algicidal bacterium active against Karenia brevis (Dinophyceae). *Harmful Algae* 1(3):277-293

Meyer JM, Abdallah MA (1978) The fluorescent pigment of *Pseudomonas fluorescens*. Biosynthesis, purification and physicochemical properties. *Journal of General Microbiology* 107:319–328

McGillicuddy DJ, Robinson AR (1997) Eddy-induced nutrient supply and new production in the Sargasso Sea. *Deep-sea Research-I* 44:1427-1450

Miller WL, Moran MA (1997) Interaction of photochemical and microbial processes in the degradation of refractory dissolved organic matter from a coastal marine environment. *Limnology and Oceanography* 42(6):1317-1324

Morel FMM, Rueter JG, Price NM (1991) Iron nutrition of phytoplankton and its possible importance in the ecology of ocean regions with high nutrient and low biomass. *Oceanography* 4(2): 56-61

Morrison JM, Codispoti LA, Smith SL et al. (1999) The oxygen minimum zone in the Arabian Sea during 1995. *Deep Sea Research*-II 46:1903-1931

Montani S, Pithakpol S, Tada K (1998) Nutrient regeneration in coastal seas by *Noctiluca scintillans*, a red tide-causing dinoflagellate. *Journal of Marine Biotechnology* 6:224–228

Morrisey J, Bowler C (2012) Iron Utilization in Marine Cyanobacteria and Eukaryotic Algae. *Frontiers in Microbiology* 3:43-75

Mouget JL, Dakhama A, Lavoie MC, De la Noüe J (1995) Algal growth enhancement by bacteria: is consumption of photosynthetic oxygen involved? *FEMS Microbiology Ecology* 18:35-44

Mulet M, Lalucat J, Valdes EG (2010) DNA sequence-based analysis of the *Pseudomonas* species. *Environmental Microbiology* 12(6):1513-1530

Myklestad S (1977) Production of carbohydrates by marine phytoplanktonic diatoms, Influence of N-P ratio in growth medium on assimilation ratio, growth rate and production of cellular and extracellular carbohydrates by *Chaetoceros affinis* var *willei* (Gran) husted and *Skeletonema costatum* (Grev) cleve. *Journal of Experimental Marine Biology and Ecology* 29: 161–17

Myklestad SM (1989) Release of extracellular products by phytoplankton with special emphasis on polysaccharides. *Science of the Total Environment* 165:155–164

Nausch M (1996) Microbial activities on *Trichodesmium* colonies. *Marine Ecology Progress Series* 141:173-181

Nawata T, Sibaoka T (1976) Ionic composition and pH of the vacuolar sap in marine dinoflagellate *Noctiluca*. *Plant Cell Physiology* 17(2):265-272

Nayak BB, Karunasagar I, Karunasagar I (2000) Bacteriological and physico-chemical factors associated with Noctiluca miliaris bloom along Mangalore south west coast of India. *Indian Journal of Marine Science* 29:139-143

Naqvi SWA, Jayakumar DA, Narvekar PV, Naik H, Sarma VVSS, D'Souza W, Joseph S, George MD (2000) Increased marine production of N_2O due to intensifying anoxia on the Indian continental shelf. Nature 408:334-346

Naqvi SWA, Mofett JW, Gauns MU, Narvekar PV, Pratihary AK, Naik H, Shenoy DM, Jayakumar DA, Goepert TJ, Patra PK, Al-Azri A, Ahmed SI (2010) The Arabian Sea as a high-nutrient, low-chlorophyll region during the late Southwest Monsoon. *Biogeosciences* 7: 2091-2100

Naqvi SWA, VVSS Sarma, Jayakumar DA (2002) Carbon cycling in the northern Arabian Sea during the northern monsoon: Significance of salps. *Marine Ecology Progress Series* 226:35-44

Nelson NB, Carlson CA, Steinberg DK (2004) Production of chromophoric dissolved organic matter by Sargasso Sea microbes. *Marine Chemistry* 89: 273–287.

Nelson NB, Siegel DA (2002) Chromophoric DOM in the open ocean. In: Hansell D and Carlson C (Eds.) Biogeochemistry of Marine Dissolved Organic Matter. Academic Press, San Diego. pp 547-578

Nelson DL, Lehninger AL, Cox MM (2013) Lehninger Principles of Biochemistry. W.H. Freeman, ISBN 1464109621. pp 1198

Ogawa H, Amagai Y, Koike I, Kaiser K, Benner R (2001) Production of refractory dissolved organic matter by bacteria. *Science* 292: 917– 920

Padmakumar KB, Menon NR, Sanjeevan VN (2012) Is Occurrence of Harmful Algal Blooms in the Exclusive Economic Zone of India on the rise. *International Journal of Oceanography*. Article ID 263946. pp 7 doi: http://dx.doi.org/10.1155/2012/263946

Parab SG, Matondkar SGP (2012) Primary productivity and nitrogen fixation by *Trichodesmium* spp. in the Arabian Sea. *Journal of Marine Systems* 105-108: 82-95

Parab SG, Matondkar SGP, Gomes HR, Goes JI (2006) Monsoon driven changes in phytoplankton populations in the eastern Arabian Sea as revealed by microscopy and HPLC pigment analysis. *Continental Shelf Research* 26: 2358-2558

Passow U (2002) Production of transparent exopolymer particles (TEP) by phyto- and bacterioplankton. *Marine Ecology Progress Series* 238: 1–12.

Park YT, Park JB, Chung SY, Song BC, Lim WA, Kim CH, Lee WJ (1998) Isolation of marine bacteria killing red tide microalgae I. Isolation and algicidal properties of *Micrococcus* sp. LG-1 possessing killing activity for harmful dinoflagellate, *Cochlodinium polykrikoides*. *Journal of Korean Fishery Society* 31:767-773

Parsons TR, Takahashi M and Hargrave B (1984) *Biological Oceanographic Processes* (3rd edn). Pergamon Press, Oxford. pp 330

Paul C, Pohnert G (2011) Interactions of the Algicidal Bacterium *Kordia algicida* with Diatoms: Regulated Protease Excretion for Specific Algal Lysis. *PLoS ONE* 6(6): e21032. doi:10.1371/journal.pone.0021032

Pednekar SM, Matondkar SGP, Kerkar V (2012) Spatiotemporal Distribution of Harmful Algal Flora in the Tropical Estuarine Complex of Goa, India. *The Scientific World Journal.* Article ID 596276, pp 11

Penna A, Berluti S, Penna N, Magnani M (1999) Influence of nutrient ratios on the in vitro extracellular polysaccharide production by marine diatoms from the Adriatic Sea. *Journal of Plankton Research* 21(9): 1681-1690

Porter KG, YS Feig (1980) The use of DAPI for identifying and counting aquatic microflora. *Limnology and Oceanography* 25:943-948

Ramaiah N , Raghukumar S, Mangesh G, Madhupratap M (2005) Seasonal variations in carbon biomass of bacteria, thraustochytrids and microzooplankton in the Northern Arabian Sea. *Deep-Sea Research*-II 52 (2005) 1910–1921

Reimann L, Steward GF, Fandino LB, Campbell L, Landry MR , Azam F (1999) Bacterial community composition during two consecutive NE Monsoon periods in the Arabian Sea studied by denaturing gradient gel electrophoresis (DGGE) of rRNA genes. *Deep-Sea Research*-II 46(8):1791-1811.

Rueter JG, Hutchins DA, Smith RW, Unsworth NL (1992) Iron nutrition of *Trichodesmium* In Marine Pelagic Cyanobacteria: *Trichodesmium* and other Diazotrophs, Carpenter EJ et al (eds) Kluwer Academic Publishers: 289-306

Renaud F, Pringault O, Rochelle-Newall E (2005) Effects of the colonial cyanobacterium *Trichodesmium* spp. on bacterial activity. *Aquatic Microbial Ecology* 41:261-270

Romera-Castillo C, Sarmento H, Alvarez-Salgado XA, Gasol JM, Marrase´ C (2010) Production of chromophoric dissolved organic matter by marine phytoplankton. *Limnology and Oceanography* 55(1): 446–454

Raux E, Schuber HL, Warren MJ (2000) Biosynthesis of cobalamin (vitamin B_{12}): a bacterial conundrum. *Cellular and Molecular Life Sciences* 57(13-14):1880-1893

Rodionov DA, Vitreschak AG, Mironov AA, Gelfand MS (2003) Comparative genomics of the vitamin B_{12} metabolism and regulation in prokaryotes. *Journal of Biological Chemistry* 278(42):41148-59

Sakata T, Yoshikawa T, Nishitarimizu S (2011) Algicidal activity and identification of an algicidal substance produced by marine *Pseudomonas* metabolism and regulation in prokaryotes. *Journal of Biological Chemistry* 278:41148

Sapp M, Schwaderer AS, Wiltshire KH, Hoppe HG, Gerdts G, Wichels A (2007) Species-specific bacterial communities in the phycosphere of microalgae? *Microbial Ecology* 53(4): 683-699

Sarmento H, Romera-Castillo C, Lindh M, Pinhassi J, Montserrat Sala M, Gasol JM, Marase C, Taylor G (2013) Phytoplankton species-specific release of dissolved free amino acids and their selective consumption by bacteria. *Limnology and Oceanography* 58(3): 1123-1135

Saito H, Furuya K, Lirdwityaprasit T (2006) Photoautotrophic growth of *Noctiluca scintillans* with the endosymbiont *Pedinomonas noctilucae*. *Plankton and benthos research* 1(2): 97-101

Sasser M (1990) Identification of Bacteria by Gas Chromatography of Cellular Fatty Acids. *Technical Note 101. MIDI Inc.* (www.midi-inc.com)

Sawant SS, Madhupratap M (1996) Seasonality and composition of phytoplankton in the Arabian Sea. *Current Science 71*, 869–873.

Sayeed RZ, Badgujar MD, Sonawane HM, Mhaske MM, Chincholkar SB (2005) Production of microbial iron chelators (siderophores) by fluorescent Pseudomonads. *Indian Journal of Biotechnology* 4:484-490

Schäfer H, Abbas B, Witte H, Muyzer G (2002) Genetic diversity of 'satellite' bacteria present in cultures of marine diatoms. *FEMS Microbiology Ecology* 42:25–35

Schlitzer R (2002) Interactive analysis and visualization of geoscience data with Ocean Data View. *Computers and Geosciences* 28(10): 1211-1218

Seibold A, Wichels A, Schutt C (2001) Diversity of endocytic bacteria in the dinoflagellate *Noctiluca scintillans*. *Aquatic Microbial Ecology* 25:229–235

Sellner KG (1992) Trophodynamics of marine cyanobacteria blooms. In: Carpenter EJ et al. (eds.) Marine Pelagic Cyanobacteria: *Trichodesmium* and other Diazotrophs. Kluwer Academic Publishers, Dordrecht, The Netherlands. pp. 75–94

Sheridan CC, Steinberg DK, Kling GW (2002) The microbial and metazoan community associated with colonies of *Trichodesmium* spp.: a quantitative survey. *Journal of Plankton Research* 24 (9): 913- 922

Sherr EB, Sherr BF (1993) Preservation and storage of samples for enumeration of heterotrophic protists. *In Kemp P et al. (eds.) Current Methods in Aquatic Microbial Ecology,* Lewis Publishers, New York. pp. 207–212

Shetye SR, Gouveia AD, Shenoi SSC, Sundar D, Michael GS, Almeida, Santanam K (1990) Hydrography and circulation off the west coast of India. *Journal of Marine Research* 48:359-378

Shetye SR, Gouveia AD, Shankar D, Shenoi SSC, Vinayachandran PN, Sundar D, Michael GS, Nampoothiri GN (1996) Hydrography and circulation in the western Bay of Bengal during the northeast monsoon. *Journal of Geophysical Research* 101 (C6): 14011- 14025

Simeon J, Roesler C, Pegau WS, Dupouy C (2003) Sources of spatial variability in light absorbing components along an equatorial transect from 165°E to 150°W. *Journal of Geophysical Research* 108(C10):3333.

Skerratt JH, Bowman JP, Hallegraeff GM, James S, Nichols PD (2002) Algicidal bacteria associated with blooms of a toxic dinoflagellate in a temperate Australian estuary. *Marine Ecology Progress Series* 244:1-15

Smayda TJ, White AW (1990) Has there been a global expansion of algal blooms? If so is there a connection with human activities? In: Granelli E (ed) Toxic Marine Phytoplankton p. 516, Elsevier.

Smayda TJ (1997) What is a bloom? A commentary. *Limnology and Oceanography.* 42(5):1132-1136

Smetacek VS (1985) Role of sinking in diatom life-history cycles: ecological, evolutionary and geological significance. *Marine Biology* 84(3): 239-251

Smibert R M, Krieg N R (1994) Phenotypic characterization. In: Gerhardt P (ed) Methods for General and Molecular Bacteriology. American Society for Microbiology, Washington DC, pp 607-654.

Steinberg KD, Nelson NB, Carlson AC, Prusak AC (2004) Production of chromophoric dissolved organic matter (CDOM) in the open ocean by zooplankton and the colonial cyanobacterium *Trichodesmium* spp. *Marine Ecology Progress Series* 267: 45-56

Subramaniam A, Carpenter EJ, Karentz D, Falkowski PG (1999) Optical properties of the marine diazotrophic cyanobacteria *Trichodesmium*; I - Absorption and spectral photosynthetic characteristics. *Limnology and Oceanography* 44(3): 618-627

Summers RS, Cornel PK, Roberts PV (1987) Molecular size distribution and spectroscopic characterization of humic substances. *Science of the Total Environment* 62:27-37

Sweeny BM (1971) Laboratory studies of a green Noctiluca from New-Guinea. *Journal of Phycology* 7(1): 53-58

Tada K, Pithakpol S, Yano R, Montani S (2000) Carbon and Nitrogen content of *Noctiluca scintillans* in the Seto Inland Sea, Japan. *Journal of Plankton Research* 22(6): 1203-1211

Tada Y, Taniguchi A, Nagao I, Miki T, Uematsu M, Tsuda A, Hamasaki K (2011) Differing Growth Responses of Major Phylogenetic Groups of Marine Bacteria to Natural Phytoplankton Blooms in the Western North Pacific Ocean. *Applied and Environmental Microbiology* 77(12): 4055-4065

Tamura K, Peterson D, Peterson N, Stecher G, Nei M, Kumar S (2011) MEGA5: Molecular Evolutionary Genetics Analysis using Maximum Likelihood, evolutionary Distance, and Maximum Parsimony Methods. Molecular Biology and Evolution 28:2731-2739

Tang YZ, Koch F, Gobler JC (2010) Most harmful algal bloom species are vitamin B_1 and B_{12} auxotrophs. *Proceedings of the Natural Academy of Sciences USA* 107(48): 20756-20761

Tindale NW, Pease PP (1999) Aerosols over the Arabian Sea: Atmospheric transport pathways and concentrations of dust and sea salt. *Deep-Sea Research -II* 46 (1999) 1577 -1595

Twardowski MS, Boss E, Sullivan JM, Donaghay PL (2004) Modeling spectral absorption by chromophoric dissolved organic matter (CDOM). *Marine Chemistry* 89: 69-88

Varma A, Chincholkar SB (2007) Microbial Siderophores. Springer-Verlag, Berlin. pp 243

Valiela I (1995) *Marine ecological processes*. 2nd Ed, Springer-Verlag, New-York. pp 686

Verbaendert I, Vos PD, Boon N, Heylen K (2011) Denitrification in Gram positive bacteria: an underexplored trait. *Biochemical Society Transactions* 39(1): 254-258

Wang XL, Gong LY, Liang SK, Han XR, Zhu CJ, et al. (2005) Algicidal activity of rhamnolipid biosurfactants produced by *Pseudomonas aeruginosa*. Harmful Algae 4: 433–443.

Wang Q, Garrity GM, Tiedje JM, Cole JR (2007) Naïve Bayesian Classifier for rapid Assignment of rRNA sequences into the new Bacterial Taxonomy. *Applied and Environmental Microbiology* 73(16):5261-5267

Ward BB, Devol AH, Rich JJ, Chang BX, Bulow SE, Naik H, Pratihary A, Jayakumar A (2009) Denitrification as the dominant nitrogen loss process in the Arabian Sea. *Nature* 461:78-81

Wassmann P (1997) Retention versus export food chains: processes controlling sinking loss from marine pelagic systems. *Hydrobiologia* 363(3): 29-57

Wiggert JD, Hood RR, Banse K, Kindle J C (2005) Monsoon-driven biogeochemical processes in the Arabian Sea. *Progress in Oceanography* 65:176-213

Witter AE, Lewis BL, Luther GW (2000) Iron speciation in the Arabian Sea. Deep-Sea Research Part II. 47: 1517–1539.

Woese CR, Kandler O, Wheelis ML (1990) Towards a natural system of organisms: proposal for the domains Archaea, Bacteria, and Eucarya. *Proceedings of the National Academy of Sciences of the United States of America.* 87(12): 4576-4579

Wright SW, Jeffrey SW, Mantoura RFC, Llewellyn CA, Bjornland T, repeat D, Welschmeyer N (1991) Improved HPLC method for the analysis of chlorophylls and carotenoids from marine phytoplankton. *Marine Ecology Progress Series,* 77: 183-196

Wyrtki K (1973) Physical oceanography of the Indian Ocean: *The Biology of the Indian Ocean*, B. Zeitzschel, Ed., Springer-Verlag, Berlin. 18-36

Xiao J, Zhu C, Sun D, Guo P, Yunlong T (2011) Removal of ammonium-N from ammonium-rich sewage using an immbolized *Bacillus subtilis* AYC biorecator system. *Journal of Environmental Science* 23(8): 1279-1285

Yoch CD (2002) Dimethylsulfoniopropionate: Its Sources, Role in the Marine Food Web, and Biological Degradation to Dimethylsulfide. *Applied and Environmental Microbiology* 68(12): 5804-5815

Yoshinaga I, Kim M-C, Katanozaka N, Imai I, Uchida A, Ishida Y (1998) Population structure of algicidal marine bacteria targeting the red tide forming alga Heterosigma akashiwo (Raphidophyceae), determined by restriction fragment length polymorphism analysis of the bacterial 16S ribosomal RNA genes. *Marine Ecology Progress Series* 170:33-44

Yoshinaga I, Kawai T, Ishida Y (1997) Analysis of algicidal ranges of the bacteria killing the marine dinoflagellate Gymnodinium mikimotoi isolated from Tanabe Bay, Wakayama Pref., Japan. *Fishery Science* 63:94-98

Zhang Y, Dijk VMA, Liu M, Zhu G, Qin B (2009) The contribution of phytoplankton degradation to chromophoric dissolved organic matter (CDOM) in eutrophic shallow lakes: Field and experimental evidence. *Water Research* 43: 4685-4697

Zhang J, Wu P, Yu Z (2011) Heterotrophic nitrification and aerobic denitrification by the bacterium *Pseudomonas stutzeri* YZN-001. *Bioresource Technology* 102(21):9866-9869

Zuo Y, Jones RD (1995) Formation of Carbon Monoxide by Photolysis of Dissolved Marine Organic Material and Its Significance in the Carbon Cycling of the Oceans. *Naturwissenschaften* 82: 472-474 [Abstract]

Zwirglmaier, Katrin, Jardillier, Ludwig, Ostrowski, Martin, Mazard, Sophie, Garczarek, Laurence, Vaulot, Daniel, Not, Fabrice, Massana, Ramon, Ulloa, Osvaldo, Scanlan, David J et al. (2008) Global phylogeography of marine Synechococcus and Prochlorococcus reveals a distinct partitioning of lineages among oceanic biomes. *Environmental Microbiology* 10 (1):147-161.

Appendix I: Reagents and Media

A. Reagents and Buffers

1. Chrome Azurol S assay dye solution

All reagents used were AR grade and all glasswares used for media preparation soaked with 6M HCl and washed with ultra-pure MiliQ water (18.2MΩ.cm^{-1}).

(i) Hexadecyl trimethyl ammonium bromide (HDTMA):
21.9 mg dissolved in 25 ml ultra-pure MiliQ water.

(ii) Ferric chloride hexahydrate: 1mM dissolved in 10mM HCl

(iii) Chrome Azurol S (CAS): 2mM CAS in 7.5 ml MiliQ water

(iv) 2-(N-morpholino) ethanesulfonic acid (MES): 9.76 g dissolved in 50 ml MiliQ water and pH adjusted to 5.6 using 50% KOH.

Preparation of CAS assay solution: Solution (ii) and (iii) are mixed and then added to solution (i) slowly with shaking in a 100 ml volumetric flask. The MES buffer is added and the volume is made upto 100 ml using MiliQ water. The solution is stored in 100 ml plastic bottles and prepared fresh.

2. SSC buffer (20X stock)

Sodium Chloride	175.3 g
Sodium citrate	88.2 g
Distilled water	1000 ml
Final pH	7.0

5. STE buffer (1X)

Tris-HCl	10mM, pH8
NaCl	0.1M
EDTA	1mM, pH8

Individual solutions prepared using distilled water and added in the above proportions to obtain final buffer solution. Sterilized by autoclaving for 15 mins at 120°C, 15lbs pressure and stored at 4°C.

3. TAE buffer (50X stock)

Tris-base	242 g
Glacial acetic acid	57.1 ml
EDTA (0.5M)	100 ml
Final volume	1000 ml (adjusted using distilled water)
Final pH	8 (adjusted using 1N NaOH / 1N HCl)

B. Media compositions

1. Succinate mineral salts media (SMM)

Ingredients	*Grams per 100 ml*
Dipotassium hydrogen phosphate	0.6
Potassium dihydrogen phosphate	0.3
Ammonium sulphate	0.1
Magnesium sulphate heptahydrate	0.02
MiliQ water 18.2MΩ.cm^{-1}	90 ml
pH	7 (Adjusted using 1N NaOH)
Succinate 10X stock (0.22µm filter sterilized)	10 ml

All glasswares used for media preparation soaked with 6M HCl and washed with ultra-pure MiliQ water. The basal media was distributed into 50 ml flasks and autoclaved at 15 lbs pressure (121°C) for 10 minutes. On cooling, the filtered sterilized succinate stocks were added aseptically prior to inoculation.

2. Deferrated Nutrient Sea-water broth

Ingredients	*Grams per L*
Peptic digest of animal tissue	5.0
Sodium chloride	35
Beef extract	1.5
Yeast extract	1.5
Sea-water	1000 ml

Final pH (at 25°C) 7.4±0.2

The nutrient broth prepared was deferrated by adding equal volumes of 3% 8-hydroxyquinoline in Chloroform and left in shaker for 24 hours. The top-aquous layer was taken out and re-extracted one more time to ensure complete removal of Iron. Media was dispensed into flasks and autoclaved at 15 lbs pressure (121°C) for 15 minutes.

3. Nitrite-Giltay's broth

Ingredients	*Grams per L*
Sodium nitrite	0.06
L-Asparagine	1
Sodium citrate	8.5
Potassium dihydrogen phosphate	1
Magnesium sulphate heptahydrate	1
Calcium chloride	0.2
Ferric Chloride hexahydrate	0.05
Bromothymol blue (1% in alcoholic)	5ml
Final pH	7

Media dispensed in tubes with durham's tubes and autoclaved at 15 lbs pressure (121°C) for 15 minutes. Cultures were inoculated for 3 days under aerobic conditions. Change in colour from green to blue and collection of gas in durham's tubes indicated denitrification.

4. Nitrate reduction broth

Ingredients	*Grams per L*
Peptic digest of animal tissue	5.0
Meats extract	3.0
Potassium nitrate	1.0
Sodium chloride	30.0

Final pH (at 25°C) 7.0±0.2

Test reagents: Sulfanilic Acid: 8 g in 1 litre 5 N acetic acid.
Alpha-Naphthylamine: 5 g in 1 litre 5 N acetic acid.

Media dispensed in test-tubes with durham's tubes and autoclaved at 15 lbs pressure (121°C) for 15 minutes. Cultures were inoculated for 48-72 hours under aerobic conditions. Development of red-colour on addition of 0.5 ml each of test reagents indicated positive test (reduction of nitrate to nitrite). On development of no colour, Zinc dust (pinch) was added. Development of red colour indicated a negative test (Zn converting unused Nitrate to Nitrite). No colour on addition of Zn, with collection of gas in durham's tubes indicated reduction of Nitrate beyond Nitrite (Denitrification).

5. Verstraete and Alexander media

Ingredients	*Grams per L*
Acetamide	2
Potassium dihydrogen phosphate	8.2
Sodium hydroxide	1.6
Magnesium sulphate heptahydrate	0.5
Potassium Chloride	0.5
Calcium sulphate dehydrate	0.005
Copper-sulphate pentahydrate	0.0005
Ferric Chloride hexahydrate	0.0005
Zinc Sulphate	0.0005
Distilled water	1000 ml
pH	7 (adjusted with 1N NaOH)

Media dispensed in tubes and autoclaved at 15 lbs pressure (121°C) for 15 minutes.

6. Sea-water Agar

Peptone	5.0
Beef extract	1.5
Yeast extract	1.5
Aged filtered (<0.22µm) Sea-water	1000 ml

Final pH (at 25°C) 8±0.2
Autoclaved at 15 lbs pressure (121°C) for 15 minutes.

7. Motility agar medium (Hi-media)

Ingredients	*Grams per L*
Tryptose	10.0
Sodium chloride	5.0
Agar	5.0

Final pH (at 25°C) 7.2±0.2

Suspended 20 grams in 1000 ml distilled water and heated to boiling to dissolve the medium completely. Dispensed 5 ml into tubes and sterilized by autoclaving at 10 lbs pressure (115°C) for 20 minutes. On cooling to <50°C aseptically added 0.1% tetrazolium chloride indicator and allowed to set. Cultures were stabbed and reddish zones of growth during incubation helped to differentiate motile / non-motile cultures.

8. Zobell's marine 2216E Agar (Hi media, India)

Ingredients	*Grams per L*
Peptic digest of animal tissue	5.0
Yeast extract	1.0
Ferric citrate	0.1
Sodium chloride	19.45
Magnesium chloride	8.8
Sodium sulphate	3.24
Calcium chloride	1.8
Potassium chloride	0.55
Sodium bicarbonate	0.16
Potassium bromide	0.08
Strontium chloride	0.03
Boric acid	0.02
Sodium silicate	0.004
Sodium fluorate	0.0024
Ammonium nitrate	0.0016
Disodium phosphate	0.008
Agar	15.00
Final pH (at 25°C)	7.6±0.2

Directions for Use

Dissolved 55.25 g per Liter, heated to boiling and autoclaved 15 lbs pressure (121°C) for 15 minutes.

9. Starch agar (Hi media, India)

Ingredients	*Grams per L*
Meat Extract	3.0
Peptic digest of animal tissue	5.0
Starch, soluble	2.0
Agar	15.0
Final pH (at 25°C) 7.2±0.1	

Suspended 25 grams in 1000 ml distilled water and amended with 3.5% w/v NaCl, heated to boiling to dissolve the medium completely and sterilized by autoclaving at 15 lbs pressure (121°C) for 10 minutes. Zones of hydrolysis were observed on addition of gram's Iodine.

10. Standard methods Caseinate Agar (Hi media, India)

Ingredients	*Grams per L*
Casein enzymic hydrolysate	5.00
Yeast extract	2.5
Dextrose	1.0
Sodium caseinate	10.0
Trisodium citrate	4.41
Calcium chloride	2.22
Agar	15.0
Final pH (at 25°C) 7.0±0.2	

Suspended 40.13 grams in 1000 ml distilled water and amended with 3.5% w/v NaCl, heated to boiling to dissolve the medium completely and sterilized by autoclaving at 15 lbs pressure (121°C) for 10 minutes. Zones of hydrolysis were observed on addition of 0.5% Trichloro acetic acid (TCA).

11. Gelatin agar (Hi media, India)

Ingredients	*Grams per L*
Peptic digest of animal tissue	25.00
Meat-extract	7.50
Sodium chloride	5.0
Gelatin	120.0
Ferrous chloride	0.5
Final pH (at 25°C) 7.0±0.2	

Suspended 15.9 grams in 100 ml distilled water, heated to boiling to dissolve the medium completely, dispensed in test-tubes and sterilized by autoclaving. Liquefaction observed after placing test-tubes in 4°C.

12. Pikovskaya's agar medium

Ingredients	*Grams per L*
Yeast Extract	0.50
Dextrose	10.0
Calcium Phosphate	5.0
Ammonium Sulphate	0.5
Potassium Chloride	0.2
Magnesium Sulphate	0.1
Manganese Sulphate	0.0001
Ferrous Sulphate	0.0001

Agar	15.0
Final pH (at 25°C) 7.0±0.2	

All ingredients dissolved in distilled water and volume made upto 1L, dissolved completely by boiling and sterilized by autoclaving at 15 lbs pressure (121°C) for 10 minutes. Zones of hydrolysis indicated as zones of clearance.

13. Cellulose Agar

Ingredients	*Grams per L*
Ammonium phosphate	1.0
Potassium Chloride	0.2
Magnesium sulphate heptahydrate	1.0
Yeast extract	1.0
Carboxymethyl cellulose	26.0
Agar	15.0
Final pH (at 25°C) 7.0±0.2	

All ingredients dissolved in distilled water and volume made upto 1L, dissolved completely by boiling and sterilized by autoclaving at 15 lbs pressure (121°C) for 10 minutes. Zones of hydrolysis indicated on staining plates with congo-red (1 mg ml^{-1}) for 3 hours, destained with 1M NaCl, to indicate zones of hydrolysis.

14. Tributyrin agar (Hi media, India)

Ingredients	*Grams per L*
Peptic digest of animal tissue	5.0
Yeast extract	3.0
Agar	15.0
Final pH (at 25°C) 7.5±0.2	

Suspended 23 grams and added 3.5% NaCl in 990 ml distilled water and added 10 ml of Tributyrin (FD081). Mixed and heated to boiling to dissolve the medium completely, sterilized by autoclaving at 15 lbs pressure (121°C) for 15 minutes. Zones indicated as clearance around colonies.

15. Urea agar (Hi media, India)

Ingredients	*Grams per L*
Peptic digest of animal tissue	1.0
Dextrose	1.0
Sodium chloride	5.0
Disodium phosphate	1.2
Monopotassium phosphate	0.8
Phenol red	0.012
Agar	15.0
Final pH (at 25°C) 6.8±0.2	

Suspended 24.01 grams in 950 ml distilled water and heated to boiling to dissolve the medium completely. Sterilized by autoclaving at 10 lbs pressure (115°C) for 20 minutes. On cooling to <50°C aseptically added 50 ml of sterile 40% Urea Solution (FD048) and mixed well. Dispensed into sterile tubes as slants. Urea hydrolysis indiacted as color-change from orange to pink.

C. Water-column Chemistry

1. Dissolved Oxygen (Amperometric method)

Winkler's A: 600 g of $MnCl_2 \cdot 4H_2O$ was dissolved in 500-700 ml of distilled water in a graduated beaker and the volume made upto 1 Liter.

Winkler's B: 320 g of NaOH was dissolved in 500 ml distilled water by placing the beaker in a tub of cold water. Slowly added 600 g of NaI and after cooling the solution made upto 1 L.

Sulfuric acid (5 M): 280 ml of concentrated reagent grade H_2SO_4 was slowly to added to 500 ml distilled water in a beaker placed on cold-water tub. The volume was made upto 1 L in a graduated glass beaker.

Sodium thiosulfate (0.11M): 27.4 g of $Na_2S_2O_3 \cdot 5H_2O$ was dissolved in dissolved water, made upto 1.0 L in a volumetric flask.

Potassium iodate (0.00167 M or 0.0100 N): 0.3567 g of oven dried (170 °C for 2 hours) KIO_3 was dissolved in distilled water and made up to exactly 1 L in a volumetric flask.

Dissolved Oxygen was calculated as below:

O_2 in ml L^{-1} =

[{(Vx –Vb)×VIO3×NIO3×5598} ÷ {(Vstd-Vb) -1000×DOreg}] ÷ [Vbot-Vreg]

Where,

Vx=endpoint of sample titration in µL

Vb=reagent blank in µL

VIO3=volume of Iodate standard in µL

NIO3=normality of iodate standard

Vstd=endpoint of the standard in µL

DOreg=0.0017 ml O2 in volume of reagents added to samples

Vbot= volume of bottle in ml

Vreg=volume of reagents added (2 ml)

D. Enumeration of Total Bacterial Counts

Total Bacterial Counts (cells per liter) = [(Sc-Bc) x CF x F]/V

Sc = Mean of sample counts per quadrat (100x100µm^2 counting Grid);

Bc = Mean of background counts per quadrat;

CF = Effective filter Area / Quadrat Area;

F = (Volume of preservative/Volume of sample preserved) +1;

V= Volume of sample filtered in liters.

Appendix II

A. 16SrDNA sequences of *N miliaris* active bloom associated bacterial flora:

[>Gen Bank Accession; Identity, strain designation (Length of sequence: 5 - 3)]

>JX429861; *Bacillus* sp., ^{GU}SK256-8 (1497nt)

TGCAAGTCGAGCGGACGGATGGGAGCTTGCTCCCAGACCGTCAGCGGCGGACGGGTGAGTAAC
ACGTGGGCAACCTGCCTGTAAGACTGGGATAACTCCGGGAAACCGGGGCTAATACCGGATAAN
TCTTTNCCTCACATGAGGNAAAGCTGAAAGATGGCATCTCGCTATCACTTACAGATGGGCCCG
CGGCGCATTAGCTAGTTGGTGAGGTAACGGCTCACCAAGGCNACGATGCGTAGCCGACCTGAG
AGGGTGATCGGCCACACTGGGACTGAGACACGGCCCAGACTCCTACGGGAGGCAGCAGTAGGG
AATCTTCCGCAATGGACGAAAGTCTGACGGAGCAACGCCGCGTGAGTGATGAAGGTTTTCGGA
TCGTAAAACTCTGTTGTCAGGGAAGAACAAGTACCGGAGTAACTGCCGGTACCTTGACGGTAC
CTGACCAGAAAGCCACGGCTAACTACGTGCCAGCAGCCGCGGTAATACGTAGGTGGCAAGCGT
TGTCCGGAATTATTGGGCGTAAAGCGCGCGCAGGCGGTTCCTTAAGTCTGATGTGAAAGCCCC
CGGCTCAACCGGGGAGGGTCATTGGAAACTGGGGAACTTGAGTGCAGAAGAGAAGAGTGGAAT
TCCACGTGTAGCGGTGAAATGCGTAGAGATGTGGAGGAACACCAGTGGCGAAGGCGACTCTTT
GGTCTGTAACTGACGCTGAGGCGCGAAAGCGTGGGGAGCAAACAGGATTAGATACCCTGGTAG
TCCACGCCGTAAACGATGAGTGCTAAGTGTTAGAGGGTTTCCGCCCTTTAGTGCTGCAGCAAA
CGCATTAAGCACTCCGCCTGGGGAGTACGGCCGCAAGGCTGAAACTCAAAGGAATTGACGGGG
GCCCGCACAAGCGGTGGAGCATGTGGTTTAATTCGAAGCAACGCGAAGAACCTTACCAGGTCT
TGACATCTCCTGACAACCCTAGAGATAGGGCGTTCCCCTTCGGGGGACAGGATGACAGGTGGT
GCATGGTTGTCGTCAGCTCGTGTCGTGAGATGTTGGGTTAAGTCCCGCAACGAGCGCAACCCT
TGATCTTAGTTGCCAGCATTCAGTTGGGCACTCTAAGGTGACTGCCGGTGACAAACCGGAGGA
AGGTGGGGATGACGTCAAATCATCATGCCCCTTATGACCTGGGCTACACACGTGCTACAATGG
ATGGTACAAAGGGCTGCAAGACCGCGAGGTTAAGCGAATCCCATAAAACCATTCTCAGTTCGG
ATTGCAGGCTGCAACTCGCCTGCATGAAGCCGGAATCGCTAGTAATCGCGGATCAGCATGCCG
CGGTGAATACGTTCCCGGGCCTTGTACACACCGCCCGTCACACCACGAGAGTTTGTAACACCC
GAAGTCGGTGGGGTAACCTTTTGGAGCCAGCCGCCTAAGGTGGGACAGATGATTGGGGTGAAG
TCGTAACAAGGTAGCCGTATCGGAAGGTGCGGCTGGATCACCTCCTTA

>JX429860; *Bacillus* sp., ^{GU}SK256-12 (822nt)

TTGGGCGTAAAGCGCGCGCAGGCGGTCCTTTAAGTCTGATGTGAAAGCCCACGGCTCAACCGT
GGAGGGTCATTGGAAACTGGGGGACTTGAGTGCAGAAGAGGAGAGCGGAATTCCACGTGTAGC
GGTGAAATGCGTAGAGATGTGGAGGAACACCAGTGGCGAAGGCGGCTCTCTGGTCTGTAACTG
ACGCTGAGGCGCGAAAGCGTGGGGAGCGAACAGGATTAGATACCCTGGTAGTCCACGCCGTAA
ACGATGAGTGCTAAGTGTTAGAGGGTTTCCGCCCTTTAGTGCTGCAGCAAACGCATTAAGCAC
TCCGCCTGGGGAGTACGGTCGCAAGACTGAAACTCAAAGGAATTGACGGGGGCCCGCACAAGC
GGTGGAGCATGTGGTTTAATTCGAAGCAACGCGAAGAACCTTACCAGGTCTTGACATCCTCTG
ACACTCCTAGAGATAGGATTTTCCCTTCGGGGACAGAGTGACAGGTGGTGCATGGTTGTCGTC
AGCTCGTGTCGTGAGATGTTGGGTTAAGTCCCGCAACGAGCGCAACCCTTGATCTTAGTTGCC
AGCATTTAGTTGGGCACTCTAAGGTGACTGCCGGTGACAAACCGGAGGAAGGTGGGGATGACG
TCAAATCATCATGCCCCTTATGACCTGGGCTACACACGTGCTACAATGGATGGTACAAAGGGC
AGCGAAACCGCGAGGTTAAGCCAATCCCATAAAACCATTCTCAGTTCGGATTGCAGGCTGCAA
CTCGCCTGCATGAAGCCGGAATCGCTAGTAATCGCGGGATCAGCATGCCGCGGTGAATACGTT
CCC

>JX429859; *Bacillus mycoides*, ^{GU}SK256-13 (793nt)

TCGAGCGAATGGATTAAGAGCTTGCTCTTATGAAGTTAGCGGCGGACGGGTGAGTAACACGTG
GGTAACCTGCCCATAAGACTGGGATAACTCCGGGAAACCGGGGCTAATACCGGATAACATTTT

GCGCTGCATGGCGCGAAATTGAAAGGCGGCTTCGGCTGTCACTTATGGATGGACCCGCGTCGC
ATTAGCTAGTTGGTGAGGTAACGGCTCACCAAGGCAACGATGCGTAGCCGACCTGAGAGGGTG
ATCGGCCACACTGGGACTGAGACACGGCCCAGACTCCTACGGGAGGCAGCAGTAGGGAATCTT
CCGCAATGGACGAAAGTCTGACGGAGCAACGCCGCGTGAGTGATGAAGGCTTTCGGGTCGTAA
AACTCTGTTGTTAGGGAAGAACAAGTGCTAGTTGAATAAGCTGGCACCTTGACGGTACCTAAC
CAGAAAGCCACGGCTAACTACGTGCCAGCAGCCGCGGTAATACGTAGGTGGCAAGCGTTATCC
GGAATTATTGGGCGTAAAGCGCGCGCAGGTGGTTTCTTAAGTCTGATGTGAAAGCCCACGGCT
CAACCGTGGAGGGTCATTGGAAACTGGGAGACTTGAGTGCAGAAGAGGAAAGTGGAATTCCAT
GTGTAGCGGTGAAATGCGTAGAGATATGGAGGAACACCAGTGGCGAAGGCGACTTTCTGGTCT
GTAACTGACACTGAGGCGCGAAAGCGTGGGGAGCAAACAGGATTAGATACCCTGGTAGTCCAC
GCCGTAAACGATGAGTGCTAAGTGTTAGAGGGTTTCC

>JX429858; *Bacillus* sp., ^{GU}SK256-14 (284nt)

ATGGGAGCTTGCTCCCTGAAGTCAGCGGCGGACGGGTGAGTAACACGTGGGCAACCTGCCTGT
AAGACTGGGATAACTCCGGGAAACCGGGGCTAATACCGGATAACTCTTTTCCTCACATGAGGA
AAAGCTGAAAGATGGTTTCGGCTATCACTTACAGATGGGCCCGCGGCGCATTAGCTAGTTGGT
GAGGTAACGGCTCACCAAGGCCACGATGCGTACCCGACCTGAGAGGGTGATCGGCCACACTGG
GACTGAGACACGGCCCAGACTCCTACGGGAGG

>JX429857; *Bacillus* sp., ^{GU}SK256-S9 (474nt)

GCTGGCGGCGTGCCTATTACATGCAAGTCGAGCGGACAGATGGGAGCTTGCTCCCTGAAGTCA
GCGGCGGACGGGTGAGTAACACGTGGGCAACCTGCCTGTAAGACTGGGATAACTCCGGGAAAC
CGGGGCTAATACCGGATAATTCTTTCCCTCACATGAGGGAAAGCTGAAAGATGGTTTCGGCTA
TCACTTACAGATGGGCCCGCGGCGCATTAGCTAGTTGGTGAGGTAACGGCTCACCAAGGCAAC
GATGCGTAGCCGACCTGAGAGGGTGATCGGCCACACTGGGACTGAGACACGGCCCAGACTCCT
ACGGGAGGCAGCAGTAGGGAATCTTCCGCAATGGACGAAAGTCTGACGGAGCAACGCCGCGTG
AGTGATGAAGGTTTTCGGATCGTAAAACTCTGTTGTTAGGGAAGAACAAGTACCGGAGTAACT
GCCGGTACCTTGACGGTACCTAACCAGAAAGCC

>JX429856; *Bacillus flexus,* ^{GU}SK256-16 (423nt)

CGCTGGCGGCGTGCCTATTACATGCAGTCGAGCGAACTGATTAGAAGCTTGCTTCTATGACGT
TAGCGGCGGACGGGTGAGTAACACGTGGGCAACCTGCCTGTAAGACTGGGATAACTCCGGGAA
ACCGGAGCTAATACCGGATAACATTTTTTCTTGCATAAGAGAAAATTGAAAGATGGTTTCGGC
TATCACTTACAGATGGGCCCGCGGTGCATTAGCTAGTTGGTGAGGTAACGGCTCACCAAGGCA
ACGATGCATAGCCGACCTGAGAGGGTGATCGGCCACACTGGGACTGAGACACGGCCCAGACTC
CTACGGGAGGCAGCAGTAGGGAATCTTCCGCAATGGACGAAAGTCTGACGGAGCAACGCCGCG
TGAGTGATGAAGGCTTTCGGGTCGTAAAACTCTGTTGTTAGGGAAAAACAA

>JX429855; *Bacillus cereus,* ^{GU}SK256-17 (833nt)

CCTAATACATGCAAGTCGAGCGAATGGATTAAGAGCTTGCTCTTATGAAGTTAGCGGCGGACG
GGTGAGTAACACGTGGGTAACCTGCCCATAAGACTGGGATAACTCCGGGAAACCGGGGCTAAT
ACCGGATAACATTTTGAACCGCATGGTTCGAAATTGAAAGGCGGCTTCGGCTGTCACTTATGG
ATGGACCCGCGTCGCATTAGCTAGTTGGTGAGGTAACGGCTCACCAAGGCAACGATGCGTAGC
CGACCTGAGAGGGTGATCGGCCACACTGGGACTGAGACACGGCCCAGACTCCTACGGGAGGCA
GCAGTAGGGAATCTTCCGCAATGGACGAAAGTCTGACGGAGCAACGCCGCGTGAGTGATGAAG
GCTTTCGGGTCGTAAAACTCTGTTGTTAGGGAAGAACAAGTGCTAGTTGAATAAGCTGGCACC
TTGACGGTACCTAACCAGAAAGCCACGGCTAACTACGTGCCAGCAGCCGCGGTAATACGTAGG
TGGCAAGCGTTATCCGGAATTATTGGGCGTAAAGCGCGCGCAGGTGGTTTCTTAAGTCTGATG
TGAAAGCCCACGGCTCAACCGTGGAGGGTCATTGGAAACTGGGAGACTTGAGTGCAGAAGAGG
AAAGTGGAATTCCATGTGTAGCGGTGAAATGCGTAGAGATATGGAGGAACACCAGTGGCGAAG
GCGACTTTCTGGTCTGTAACTGACACTGAGGCGCGAAAGCGTGGGGAGCAAACAGGATTAGAT
ACCCTGGTAGTCCACGCCGTAAACGATGAGTGCTAAGTGTTAGAGGGTTTCCGCCCTTTAGTG
CTGAAGTTAACGCA

>JX429854; *Oceanobacillus* sp., ^{GU}SK256-21 (819nt)

ACGCTGGCGGCGTGCCTAATACATGCAAGTCGAGCGCAGGAAGTTATCTGATCCTCTTTTAGA
GGTGACGATAATGGAATGAGCGGCGGACGGGTGAGTAACACGTAGGCAACCTGCCTGTAAGAC
TGGGATAACTCGTGGAAACGCGAGCTAATACCGGATAACACTTTTCATCTCCTGATGAGAAGT
TGAAAGGCGGCTTTTGCTGTCACTTACAGATGGGCCTGCGGCGCATTAGCTAGTTGGTAAGGT
AATGGCTTACCAAGGCGACGATGCGTAGCCGACCTGAGAGGGTGATCGGCCACACTGGGACTG
AGACACGGCCCAGACTCCTACGGGAGGCAGCAGTAGGGAATCTTCCGCAATGGACGAAAGTCT
GACGGAGCAACGCCGCGTGAGTGATGAAGGTTTTCGGATCGTAAAACTCTGTTGTTAGGGAAG
AACAAGTGCCATAGTAACTGATGGCACCTTGACGGTACCTAACCAGAAAAGCCACGGCTAACT
ACGTGCCAGCAGCCGCGGTAATACGTAGGTGGCAAGCGTTGTCCGGAATTATTGGGCGTAAAG
CGCTCGCAGGCGGTTCTTTAAGTCTGATGTGAAATCTTACGGCTCAACCGTAAACGTGCATTG
GAAACTGGGGAACTTGAGTGCAGAAGAGGAGAGTGGAATTCCACGTGTAGCGGTGAAATGCGT
AGAGATGTGGAGGAACACCAGTGGCGAAGGCGACTCTCTGGTCTGTAACTGACGCTGAGGAGC
GAAAGCGTGGGGAGCGAACAGGATTAGATACCCTGGTAGTCCACGCCGTAAACGATGAGTGCT

>JX429853; *Virgibacillus halodenitrificans*, ^{GU}SK256-18 (535nt)

GCTGGCGGCGTGCCTATTACATGCAAGTCGAGCGCGGGAAGCAAGCTGATCCTCTTCGGAGGT
GACGCTTGTGGAACGAGCGGCGGACGGGTGAGTAACACGTGGGCAACCTGCCTGTAAGACTGG
GATAACCCCGGGAAACCGGGGCTAATACCGGATAATACTTTTCATCACCTGATGAGAAGTTGA
AAGGTGGCTTTTAGCTACCACTTACAGATGGGCCCGCGGCGCATTAGCTAGTTGGTGAGGTAA
CGGCTCACCAAGGCAACGATGCGTAGCCGACCTGAGAGGGTGATCGGCCACACTGGGACTGAG
ACACGGCCCAGACTCCTACGGGAGGCAGCAGTAGGGAATCTTCCGCAATGGACGAAAGTCTGA
CGGAGCAACGCCGCGTGAGTGATGAAGGTTTTCGGATCGTAAAGCTCTGTTGTTAGGGAAGAA
CAAGTGCCGTTCGAATAGGGCGGCACCTTGACGGTACCTAACCAGAAAGCCCCGGCTAACTAC
GTGCCAGCAGCCGCGGTAATACGTAGGGGGC

>JX429852; *Virgibacillus halodenitrificans*, ^{GU}SK256-19 (701nt)

GCTGGCGGCGTGCCTAATACATGCAAGTCGAGCGCGGGAAGCAAGCTGATCCTCTTCGGAGGT
GACGCTTGTGGAACGAGCGGCGGACGGGTGAGTAACACGTGGGCAACCTGCCTGTAAGACTGG
GATAACCCCGGGAAACCGGGGCTAATACCGGATAATACTTTTCATCACCTGATGAGAAGTTGA
AAGGTGGCTTTTAGCTACCACTTACAGATGGGCCCGCGGCGCATTAGCTAGTTGGTGAGGTAA
CGGCTCACCAAGGCAACGATGCGTAGCCGACCTGAGAGGGTGATCGGCCACACTGGGACTGAG
ACACGGCCCAGACTCCTACGGGAGGCAGCAGTAGGGAATCTTCCGCAATGGACGAAAGTCTGA
CGGAGCAACGCCGCGTGAGTGATGAAGGTTTTCGGATCGTAAAGCTCTGTTGTTAGGGAAGAA
CAAGTGCCGTTCGAATAGGGCGGCACCTTGACGGTACCTAACCAGAAAGCCCCGGCTAACTAC
GTGCCAGCAGCCGCGGTAATACGTAGGGGGCAAGCGTTGTCCGGAATTATTGGGCGTAAAGCG
CGCGCAGGCGGTCCTTTAAGTCTGATGTGAAAGCCCACGGCTCAGCCGTGGAGGGTCATTGGA
AACTGGAGGACTTGAGTACAGAAGAGGAGAGTGGAATTCCACGTGTAGCGGTGAAATGCGTAT
AGATGTGT

>JX429851; *Staphylococcus arlettae* ^{GU}SK256-30 (765nt)

ACGCTGGCGGCGTGCCTATTACATGCAAGTCGAGCGAACAGATAAGGAGCTTGCTCCTTTGAC
GTTAGCGGCGGACGGGTGAGTAACACGTGGGTAACCTACCTATAAGACTGGAATAACTCCGGG
AAACCGGGGCTAATGCCGGATAACATTTAGAACCGCATGGTTCTAAAGTGAAAGATGGTTTTG
CTATCACTTATAGATGGACCCGCGCCGTATTAGCTAGTTGGTAAGGTAATGGCTTACCAAGGC
AACGATACGTAGCCGACCTGAGAGGGTGATCGGCCACACTGGAACTGAGACACGGTCCAGACT
CCTACGGGAGGCAGCAGTAGGGAATCTTCCGCAATGGGCGAAAGCCTGACGGAGCAACGCCGC
GTGAGTGATGAAGGGTTTCGGCTCGTAAAACTCTGTTATTAGGGAAGAACAAACGTGTAAGTA
ACTGTGCACGTCTTGACGGTACCTAATCAGAAAGCCACGGCTAACTACGTGCCAGCAGCCGCG
GTAATACGTAGGTGGCAAGCGTTATCCGGAATTATTGGGCGTAAAGCGCGCGTAGGCGGTTTC
TTAAGTCTGATGTGAAAGCCCACGGCTCAACCGTGGAGGGTCATTGGAAACTGGGAGACTTGA
GTGCAGAAGAGGAAAGTGGAATTCCATGTGTAGCGGTGAAATGCGCAGAGATATGGAGGAACA
CCAGTGGCGAAGGCGACTTTCTGGTCTGTAACTGACGCTGATGTGCGAAAGCGTGGGGATCAA
ACAGGATTA

>JX429850; Unclassified Planococcaceae, ^{GU}SK256-38 (925nt)

GCGCGCGCAGGTGGTCCTTTAAGTCTGATGTGAAAGCCCACGGCTCAACCGTGGAGGGTCATT
GGAAACTGGGGGACTTGAGTGCAGAAGAGGAAAGTGGAATTCCAAGTGTAGCGGTGAAATGCG
TAGAGATTTGGAGGAACACCAGTGGCGAAGGCGACTTTCTGGTCTGTAACTGACACTGAGGCG
CGAAAGCGTGGGGAGCAAACAGGATTAGATACCCTGGTAGTCCACGCCGTAAACGATGAGTGC
TAAGTGTTAGGGGGTTTCCGCCCCTTAGTGCTGCAGCTAACGCATTAAGCACTCCGCCTGGGG
AGTACGGTCGCAAGACTGAAACTCAAAGGAATTGACGGGGGCCCGCACAAGCGGTGGAGCATG
TGGTTTAATTCGAAGCAACGCGAAGAACCTTACCAGGTCTTGACATCCCATTGACCACTATGG
AGACATAGTTTTCCCTTCGGGGACAGTGGTGACAGGTGGTGCATGGTTGTCGTCAGCTCGTGT
CGTGAGATGTTGGGTTAAGTCCCGCAACGAGCGCAACCCTTGTTCTTAGTTGCCATCATTTAG
TTGGGCACTCTAAGGAGACTGCCGGTGACAAACCGGAGGAAGGTGGGGATGACGTCAAATCAT
CATGCCCCTTATGACCTGGGCTACACACGTGCTACAATGGACGGTACAAACGGTTGCCAACCC
GCGAGGGGGAGCTAATCCGATAAAACCGTTCTCAGTTCGGATTGTAGGCTGCAACTCGCCTAC
ATGAAGCCGGAATCGCTAGTAATCGCGGATCAGCATGCCGCGGTGAATACGTTCCCGGGCCTT
GTACACACCGCCCGTCACACCACGAGAGTTTGTAACACCCGAAGCCGGTGGGGTAACCCTTTG
GGAGCCAGCCGTCGAAGGTGGGACAGATGATTGGGGTGAAGTC

>JX429849; *Bacillus* sp., ^{GU}SK256-5 (1420nt)

TGCAAGTCGAGCGGATTGATGGGAGCTTGCTCCCTGATATCAGCGGCGGACGGGTGAGTAACA
CGTGGGTAACCTGCCTGTAAGACTGGGATAACTCCGGGAAACCGGGGCTAATACCGGATAACT
CATTTCCTCGCATGAGGAAATGTTGAAAGGTGGCTTNTAGCTACCACTTACAGATGGACCCGC
GGCGCATTAGCTAGTTGGTGAGGTAACGGCTCACCAAGGCGACGATGCGTAGCCGACCTGAGA
GGGTGATCGGCCACACTGGGACTGAGACACGGCCCAGACTCCTACGGGAGGCAGCAGTAGGGA
ATCTTCCGCAATGGACGAAAGTCTGACGGAGCAACGCCGCGTGAGTGATGAAGGTTTTCGGAT
CGTAAAGCTCNGTTGTTAGGGAAGAACAAGTGCCGTTCGAATAGGGCGGCACCTTGACGGTAC
CTAACCAGAAAGCCACGGCTAANTACTTGCCANCAGCCGCGGTATTACNTAGNTGGCAAGCGT
NGTCCGGAATTATTGGGCGTAAAGCGCGCGCAGGTGGTTCCTTAAGTCTGATGTGAAAGCCCA
CGGCTCAACCGTGGAGGGTCATTGGAAACTGGGGAACTTGAGTGCAGAAGAGGAAAGTGGAAT
TCCAAGTGTAGCGGTGAAATGCGTAGATATTTGGAGGAACACCAGTGGCGAAGGCGACTTTCT
GGTCTGTAACTGACACTGAGGCGCGAAAGCGTGGGGAGCAAACAGGATTAGATACCCTGGTAG
TCCACGCCGTAAACGATGAGTGCTAAGTGTTAGGGGGTTTCCGCCCCTTAGTGCTGCAGCTAA
CGCATTAAGCACTCCGCCTGGGGAGTACGGTCGCAAGACTGAAACTCAAAGGAATTGACGGGG
GCCCGCACAAGCGGTGGAGCATGTGGTTTAATTCGAAGCAACGCGAAGAACCTTACCAGGTCT
TGACATCCTCTGACAACCCTAGAGATAGGGCTTTCCCCTTCGGGGGACAGAGTGACAGGTGGT
GCATGGTTGTCGTCAGCTCGTGTCGTGAGATGTTGGGTTAAGTCCCGCAACGAGCGCAACCCT
TGATCTTAGTTGCCAGCATTCAGTTGGGCACTCTAAGATGACTGCCGGTGACAAACCGGAGGA
AGGTGGGGATGACGTCAAATCATCATGCCCCTTATGACCTGGGCTACACACGTGCTACAATGG
ACGGTACAAAGGGCAGCGAGACCGCGAGGTTTAGCCAATCCCATAAAACCGTTCTCAGTTCGG
ATTGTAGGCTGCAACTCGCCTACATGAAGCTGGAATCGCTAGTAATCGCGGATCAGCATGCCG
CGGTGAATACGTTCCCGGGCCTTGTACACACCGCCCGTCACACCACGAGAGTTTGTAACACCC
GAAGTCGGTGAGGTAACCTTTTGGAGCCAGCCGC

>JX429848; *Bacillus cereus*, ^{GU}SK256-22 (420nt)

GCTGGCGGCGTGCCTATTACATGCGAGTCGAGCGAATGGATTAAGAGCTTGCTCTTATGAAGT
TAGCGGCGGACGGGTGAGTAACACGTGGGTAACCTGCCCATAAGACTGGGATAACTCCGGGAA
ACCGGGGCTAATACCGGATAACATTTTGAACCGCATGGTTCGAAATTGAAAGGCGGCTTCGGC
TGTCACTTATGGATGGACCCGCGTCGCATTAGCTAGTTGGTGAGGTAACGGCTCACCAAGGCA
ACGATGCGTAGCCGACCTGAGAGGGTGATCGGCCACACTGGGACTGAGACACGGCCCAGACTC
CTACGGGAGGCAGCAGTAGGGAATCTTCCGCAATGGACGAAAGTCTGACGGAGCAACGCCGCG
TGAGTGATGAAGGCTTTCGGGTCGTAAAACTCTGTTGTTAGG

>JX429847; *Bacillus subtilis* subsp *subtilis*, ^{GU}SK256-32 (418nt)

GCTGGCGGCGTGCCTATACATGCAAGTCGAGCGGACAGATGGGAGCTTGCTCCCTGATGTTAG
CGGCGGACGGGTGAGTAACACGTGGGTAACCTGCCTGTAAGACTGGGATAACTCCGGGAAACC
GGGGCTAATACCGGATGGTTGTTTGAACCGCATGGTTCAAACATAAAAGGTGGCTTCGGCTAC

CACTTACAGATGGACCCGCGGCGCATTAGCTAGTTGGTGAGGTAACGGCTCACCAAGGCAACG
ATGCGTACCCGACCTGAGAGGGTGATCGGCCACACTGGGACTGAGACACGGCCCAGACTCCTA
CGGGAGGCAGCAGTAGGGAATCTTCCGCAATGGACGAAAGTCTGACGGAGCAACGCCGCGTGA
GTGATGAAGGTTTTCGGATCGTATTGCTCTGTTGTTAGGG

>JX429846; *Bacillus* sp., ^{GU}SK256-S7 (388nt)

ACGCTGGCGGCGTGCCTAATACATGCAAGTCGAGCGGACTTTGAAAGCTTGCTTTTAAAGTTA
GCGGCGGACGGGTGAGTAACACGTGGGCAACCTGCCTGTAAGACTGGGATAACTTCGGGAAAC
CGGAGCTAATACCGGATAATCCTTTTCCTCTCATGAGGAAAAGCTGAAAGACGGCATCTCGCT
GTCACTTACAGATGGGCCCGCGGCGCATTAGCTAGTTGGTGAGGTAACGGCTCACCAAGGCAA
CGATGCGTACCCGACCTGAAAGGGTGATCGGCCACACTGGGACTGAAACACGGCCCAAACTCC
TACGGGAGGCAGCAGTAGGGAATCTTCCGCAAGGGACAAAAGTCTGACGGAGCAACGCCGCGT
GAGTGATGAA

>JX429845; *Bacillus cereus*, ^{GU}SK256-20 (1014nt)

GATCCTGGCTCAGGATGAACGCTGGCGGCGTGCCTAATACATGCAAGTCGAGCGAATGGATTA
AGAGCTTGCTCTTATGAAGTTAGCGGCGGACGGGTGAGTAACACGTGGGTAACCTGCCCATAA
GACTGGGATAACTCCGGGAAACCGGGGCTAATACCGGATAACATTTTGAACCGCATGGTTCGA
AATTGAAAGGCGGCTTCGGCTGTCACTTATGGATGGACCCGCGTCGCATTAGCTAGTTGGTGA
GGTAACGGCTCACCAAGGCAACGATGCGTAGCCGACCTGAGAGGGTGATCGGCCACACTGGGA
CTGAGACACGGCCCAGACTCCTACGGGAGGCAGCAGTAGGGAATCTTCCGCAATGGACGAAAG
TCTGACGGAGCAACGCCGCGTGAGTGATGAAGGCTTTCGGGTCGTAAAACTCTGTTGTTAGGG
AAGAACAAGTGCTAGTTGAATAAGCTGGCACCTTGACGGTACCTAACCAGAAAGCCACGGCTA
ACTACGTGCCAGCAGCCGCGGTAATACGTAGGTGGCAAGCGTTATCCGGAATTATTGGGCGTA
AAGCGCGCGCAGGTGGTTTCTTAAGTCTGATGTGAAAGCCCACGGCTCAACCGTGGAGGGTCA
TTGGAAACTGGGAGACTTGAGTGCAGAAGAGGAAAGTGGAATTCCATGTGTAGCGGTGAAATG
CGTAGAGATATGGAGGAACACCAGTGGCGAAGGCGACTTTCTGGTCTGTAACTGACACTGAGG
CGCGAAAGCGTGGGGAGCAAACAGGATTAGATACCCTGGTAGTCCACGCCGTAAACGATGAGT
GCTAAGTGTTAGAGGGTTTCCGCCCTTTAGTGCTGAAGTTAACGCATTAAGCACTCCGCCTGG
GGAGTACGGCCGCAAGGCTGAAACTCAAAGGAATTGACGGGGGCCCGCACAAGCGGTGGAGCA
TGTGGTTTAATTCGAAGCAACGCGAAGAACCTTACCAGGTCTTGACATCCTCTGAAAACCCTA
GAGATA

>JX429844; *Exiguobacterium aurantiacum*, ^{GU}SK256-25B (844nt)

TGCAAGTCGAGCGCAGGAAGCCATCTGAACCCTTCGGGGGGACGTTGGCGGAATGAGCGGCGG
ACGGGTGAGTAACACGTAAAGAACCTGCCCTCAGGTCTGGGATAACCACGAGAAATCGGGGCT
AATACCGGATGGGTCATCGGACCGCATGGTCCGAGGATGAAAGGCGCTTCGGCGTCGCCTGGG
GATGGCTTTGCGGTGCATTAGCTAGTTGGTGGGGTAATGGCCCACCAAGGCGACGATGCATAG
CCGACCTGAGAGGGTGATCGGCCACACTGGGACTGAGACACGGCCCAGACTCCTACGGGAGGC
AGCAGTAGGGAATCTTCCACAATGGACGAAAGTCTGATGGAGCAACGCCGCGTGAACGATGAA
GGCCCTCGGGTCGTAAAGTTCTGTTGTAAGGGAAGAACAAGTGCCGCAGGCAATGGCGGCACC
TTGACGGTACCTTGCGAGAAAGCCACGGCTAACTACGTGCCAGCAGCCGCGGTAATACGTAGG
TGGCAAGCGTTGTCCGGAATTATTGGGCGTAAAGCGCGCGCAGGCGGCCTCTTAAGTCTGATG
TGAAAGCCCCCGGCTCAACCGGGGAGGGCCATTGGAAACTGGGAGGCTTGAGTATAGGAGAGA
AGAGTGGAATTCCACGTGTAGCGGTGAAATGCGTAGAGATGTGGAGGAACACCAGTGGCGAAG
GCGACTCTTTGGCCTATAACTGACGCTGAGGCGCGAAAGCGTGGGGAGCAAACAGGATTAGAT
ACCCTGGTAGTCCACGCCGTAAACGATGAGTGCTAGGTGTTGGAGGGTTTCCGCCCTTCAGTG
CTGAAGCTAACGCATTAAGCACTCC

>JX429843; Unclassified Micrococcaceae, ^{GU}SK256-15 (1428nt)

TGGCAAGTCGAACGCTGAAGCTCCCAGCTTGCTGGGGGTGGATGAGTGGCGAAGGGAGAATAG
CACGTGAGTAACCTGCCCTTGACTTCAGGATACGTTCGGGAAACTGGGTCTAATACTGGATAC
GACCGATCCTCGCATGGGGTGTTGGTGGAAAGATTTTATCGGTCTTGGATGGACTCGCGGCCT
ATCAGCTTGACGGTGGGGTAATGGCTCACCGTGGCGATGACGGGTAGCCGGCCTGAGAGGGTG
ACCGGTCACACTGGGACTGAGACACGGCCCAGACTCCTACGGGAGGCAGCAGTGGGGAATATT

GCACAATGGGCGCAAGCCTGATGCAGCGACGCCGCGTGCGGGATGACGGCCTTCGGGTTGTAA
ACCGCTTTCAGTACAGAAGAAGCCCCTTGTGGGTGACGTTATGTGCAGAAGAAGCGCCGGCTA
ACTACTTGCCAGCAGCCGCGGTAATACGTAGGGCGCGAGCGTTATCCGGAATTATTGGGCGTA
AAGGGCTCGTAGGCGGTTTGCCGCGTCTGCTGTGAAAGCCCGGGGCTTAAACCCGGGTCTGCA
GTGGGTACGGGCAGACTAGAGTGCAGTACGGGAGACTGGAATTCCTGGTGTAGCGGTGAAATG
CGCAGATATCAGGAGGAACACCGATGGCGAAGGCAGGTCTCTGTCTCTGTTACTGACGCTGAG
GAGCGAAAGCATGGGGAGCGAACAGGATTAGATACCCTGGTAGTCCATGCCGTAAACGATGGG
CACTAGGTGTGGGGGACATTCCACGTTCTCCGCGCCGTAGCTAACGCATTAAGTGCCCCGCCT
GGGGAGTACGGCCGCAATGCTAAAACTCAAAGGAATTGACGGGGGCCCGCACAAGCGGCGGAG
CATGCGGATTAATTCGATGCAACGCGAAGAACCTTACCAAGGCTTGACATGGACCGGATCGCC
GCAGAAATGTGGTTTCCGGGCGGGGCTGGTTCACAGGTGAAAGCATGGTTGTCGTCAGCTCGT
GTCAAAAAAAAAATTGGGTTAAGTCCCGCAACGAGCGCAACCCTTGTCCTATGTTGCCAGCAC
GTAGTGGTGGGGACTCATGGGAGACTGCCGGGGTCAACTCGGAGGAAGGTGGGGATGACGTCA
AATCATCATGCCCCTTATGTCTTGGGCTTCACGCATGCTACAATGGCCGGTACAGTGGGTTGC
GATACTGTGAGGTGGAGCTAATCCCTAAAAGCCGGTCTCAGTTCGGATCGAATTTTTTATGAT
AGAAATCGTGAAGTTGGAGTCGCTAGTAATCGCAGATCAGCAACGCTGCGGTGAATACGTTCC
CGGGCCTTGTACTCCCGCCCGTCAAGTCACGAAAGTTGGTAACACCCGACTCCTTTTCCTAAC
CCTTGTGGGGGGAGCCGTCGAAGGTGGGACTAGCGATTGGGA

>JX429842; Unclassified Intrasporangiaceae, ^{GU}SK256-28 (641nt)

TGGCGGCGTGCTTAACACATGCAAGTCNAACGGTGATCTCGAGAGCTTGCTCTCGAGTGATCA
GTGGCGAACGGGTGAGTAACACGTGAGTAACCTGCCCCAGACTCTGGAATAACCCCGGGAAAC
CGGAGCTAATACCGGATACGAGACGGAGAGGCATCTCTACCGTCTGGAAAGTTTTTCGGTCTG
GGATGGACTCGCGGCCTATCAGCTTGTTGGTGAGGTAATGGCTCACCAAGGCGACGACGGGTA
GCCGGCCTGAGAGGGCGACCGGCCACACTGGGACTGAGACACGGCCCAGACTCCTACGGGAGG
CAGCAGTGGGGAATATTGCACAATGGGCGAAAGCCTGATGCAGCGACGCCGCGTGAGGGATGA
CGGCCTTCGGGTTGTAAACCTCTTTCAGCAGGGAAGAAGCGAAAGTGACGGTACCTGCAGAAG
AAGCACCGGCTAACTACGTGCCAGCAGCCGCGGTAATACGTAGGGTGCGAGCGTTGTCCGGAA
TTATTGGGCGTAAAGAGCTTGTAGGCGGTTTGTCGCGTCTGCCGTGAAAATTCGAGGCTCAAC
CTCGAACTTGCGGTGGGTACGGGCAGACTAGAGTGTGGTAGGGGAGACTGGAATTCCTGGTGT
AGCGGTGAAAT

>JX429841; *Micrococcus luteus*, ^{GU}SK256-35 (1323nt)

GCTGGCGGCGTGCTTATCACATGCAAGTCGAACGATGAAGCCCAGCTTGCTGGGTGGATTAGT
GGCGAACGGGTGAGTAACACGTGAGTAACCTGCCCTTAACTCTGGGATAAGCCTGGGAAACTG
GGTCTAATACCGGATAGGAGCGTCCACCGCATGGTGGGTGTTGGAAAGATTTATCGGTTTTGG
ATGGACTCGCGGCCTATCAGCTTGTTGGTGAGGTAATGGCTCACCAAGGCGACGACGGGTAGC
CGGCCTGAGAGGGTGACCGGCCACACTGGGACTGAGACACGGCCCAGACTCCTACGGGAGGCA
GCAGTGGGGAATATTGCACAATGGGCGCAAGCCTGATGCAGCGACGCCGCGTGAGGGATGACG
GCCTTCGGGTTGTAAACCTCTTTCAGTAGGGAAGAAGCGAAAGTGACGGTACCTGCAGAAGAA
GCACCGGCTAACTACGTGCCAGCAGCCGCGGTAATACGTAGGGTGCGAGCGTTATCCGGAATT
ATTGGGCGTAAAGAGCTCGTAGGCGGTTTGTCGCGTCTGTCGTGAAAGTCCGGGGCTTAACCC
CGGATCTGCGGTGGGTACGGGCAGACTAGAGTGCAGTAGGGGAGACTGGAATTCCTGGTGTAG
CGGTGGAATGCGCAGATATCAGGAGGAACACCGATGGCGAAGGCAGGTCTCTGGGCTGTAACT
GACGCTGAGGAGCGAAAGCATGGGGAGCGAACAGGATTAGATACCCTGGTAGTCCATGCCGTA
AACGTTGGGCACTAGGTGTGGGGACCATTCCACGGTTTCCGCGCCGCAGCTAACGCATTAAGT
GCCCCGCCTGGGGAGTACGGCCGCAAGGCTAAAACTCAAAGGAATTGACGGGGGCCCGCACAA
GCGGCGGAGCATGCGGATTAATTCGATGCAACGCGAAGAACCTTACCAAGGCTTGACATGTTC
TCGATCGCCGTAGAGATACGGTTTCCCCTTTGGGGCGGGTTCACAGGTGGTGCATGGTTGTCG
TCAGCTCGTGTCGTGAGATGTTGGGTTAAGTCCCGCAACGAGCGCAACCCTCGTTCCATGTTG
CCAGCACGTAATGGTGGGGACTCATGGGAGACTGCCGGGGTCAACTCGGAGGAAGGTGAGGAC
GACGTCAAATCATCATGCCCCTTATGTCTTGGGCTTCACGCATGCTACAATGGCCGGTACAAT
GGGTTGCGATACTGTGAGGTGGAGCTAATCCCAAAAAGCCGGTCTCAGTTCGGATTGGGGTCT
GCAACTCGACCCCATGAAGTCGGAGTCGCTAGTAATCGCAGATCAGCAACGCTGCGGTGAATA

>**JX429840; *Micrococcus luteus*, ^{GU}SK256-37** (696nt)

ATCCTGGCTCAGGATGAACGCTGGCGGCGTGCTTAACACATGCAAGTCGAACGATGAAGCCCA
GCTTGCTGGGTGGATTAGTGGCGAACGGGTGAGTAACACGTGAGTAACCTGCCCTTAACTCTG
GGATAAGCCTGGGAAACTGGGTCTAATACCGGATAGGAGCGCCTACCGCATGGTGGGTGTTGG
AAAGATTTATCGGTTTTGGATGGACTCGCGGCCTATCAGCTTGTTGGTGAGGTAATGGCTCAC
CAAGGCGACGACGGGTAGCCGGCCTGAGAGGGTGACCGGCCACACTGGGACTGAGACACGGCC
CAGACTCCTACGGGAGGCAGCAGTGGGGAATATTGCACAATGGGCGCAAGCCTGATGCAGCGA
CGCCGCGTGAGGGATGACGGCCTTCGGGTTGTAAACCTCTTTCAGTAGGGAAGAAGCGAAAGT
GACGGTACCTGCAGAAGAAGCACCGGCTAACTACGTGCCAGCAGCCGCGGTAATACGTAGGGT
GCGAGCGTTATCCGGAATTATTGGGCGTAAAGAGCTCGTAGGCGGTTTGTCGCGTCTGTCGTG
AAAGTCCGGGGCTTAACCCCGGATCTGCGGTGGGTACGGGCAGACTAGAGTGCAGTAGGGGAG
ACTGGAATTCCTGGTGTAGCGGTGGAATGCGCAGATATCAGGAGGAACACCGATGGCGAAGGC
AGG

>**JX429839; *Microbacterium oxydans*, ^{GU}SK256-N8** (476nt)

AACACGGAGCTTGCTCTGTGGGATCAGTGGCGAACGGGTGAGTAACACGTGAGCAACCTGCCC
CTGACTCTGGGATAAGCGCTGGAAACGGCGTCTAATACTGGATATGTGACGTGACCGCATGGT
CTGCGTCTGGAAAGAATTTCGGTTGGGGATGGGCTCGCGGCCTATCAGCTTGTTGGTGAGGTA
ATGGCTCACCAAGGCGTCGACGGGTAGCCGGCCTGAGAGGGTGACCGGCCACACTGGGACTGA
GACACGGCCCAGACTCCTACGGGAGGCAGCAGTGGGGAATATTGCACAATGGGCGCAAGCCTG
ATGCAGCAACGCCGCGTGAGGGACGACGGCCTTCGGGTTGTAAACCTCTTTTAGCAGGGAAGA
AGCGAAAGTGACGGTACCTGCAGAAAAAGCGCCGGCTAACTACGTGCCAGCAGCCGCGGTAAT
ACGTAGGGCGCAAGCGTTATCCGGAATTATTGGGC

>**JX429838; *Brachybacterium paraconglomeratum*, ^{GU}SK256-N4** (417nt)

CGCTGGCGGCGTGCTTAACACATGCAAGTCGAACGATGACGGTGGTGCTTGCACCGCCTGATT
AGTGGCGAACGGGTGAGTAACACGTGAGTAACCTGCCCTCCACTTCGGGATAACCTCGGGAAA
TCGTGGCTAATACCGGATATGAGCACTCATCGCATGGTGAGTGCTGGAAAGATTTATCGGTGG
GGGATGGACTCGCGGCCTATCAGTTTGTTGGTGAGGTGATGGCTCACCAAGACGATGACGGGT
AGCCGGCCTGAGAGGGCGACCGGCCACACTGGGACTGAGACACGGCCCAGACTCCTACGGGAG
GCAGCAGTGGGGAATATTGCACAATGGGCGAAAGCCTGATGCAGCGACGCCGCGTGGGGGATG
ACGGCCTTCGGGTTGTAAACCCCTTTCAGTAGGGAAAGC

>**JX429837; *Pseudomonas stutzeri*, ^{GU}SK256-33** (409nt)

GGCGGCAGGCCTATCACATGCATGTCGAGCGGATGAGTGGAGCTTGCTCCATGATTCAGCGGC
GGACGGGTGAGTAATGCCTAGGAATCTGCCTGGTAGTGGGGGACAACGTTTCGAAAGGAACGC
TAATACCGCATACGTCCTACGGGAGAAAGTGGGGGATCTTCGGACCTCACGCTATCAGATGAG
CCTAGGTCGGATTAGCTAGTTGGTGAGGTAAAGGCTCACCAAGGCGACGATCCGTAACTGGTC
TGAGAGGATGATCAGTCACACTGGAACTGAGACACGGTCCAGACTCCTACGGGAGGCAGCAGT
GGGGAATATTGGACAATGGGCGAAAGCCTGATCCAGCCATGCCGCGTGTGTGAAGAAGGTCTT
CGGATTGTAAAGCACGTTAAGGTGGGAGGAA

>**JX429836; *Pseudomonas* sp., ^{GU}SK256-N1** (394nt)

ACGCTGGCGGCAGGCCTATCACATGCAAGTCGAGCGGTAGAGAGAAGCTTGCTTCTCTTGAGA
GCGGCGGACGGGTGAGTAATGCCTAGGAATCTGCCTGGTAGTGGGGGATAACGTTCGGAAACG
GACGCTAATACCGCATACGTCCTACGGGAGAAAGCAGGGGACCTTCGGGCCTTGCGCTATCAG
ATGAGCCTAGGTCGGATTAGCTAGTTGGTGAGGTAATGGCTCACCAAGGCGACGATCCGTAAC
TGGTCTGAGAGGATGATCAGTCACACTGGAACTGAGACACGGTCCAGACTCCTACGGGAGGCA
GCAGTGGGGAATATTGGACAATGGGCGAAAGCCTGATCCAGCCATGCCGCGTGTGTGAAGAAG
GTCTTCGGATTGTAAA

>**JX429835; *Pseudomonas* sp., ^{GU}SK256-N2** (366nt)

GTCGAGCGGTAGAGAGAAGCTTGCTTCTCTTGAGAGCGGCGGACGGGTGAGTAATGCCTAGGA
ATCTGCCTGGTAGTGGGGGATAACGTTCGGAAACGGACGCTAATACCGCATACGTCCTACGGG

AGAAAGCAGGGGACCTTCGGGCCTTGCGCTATCAGATGAGCCTAGGTCGGATTAGCTAGTTGG
TGAGGTAATGGCTCACCAAGGCGACGATCCGTAACTGGTCTGAGAGGATGATCAGTCACACTG
GAACTGAGACACGGTCCAGACTCCTACGGGAGGCAGCAGTGGGGAATATTGGACAATGGGCGA
AAGCCTGATCCAGCCATGCCGCGTGTGTGAAGAAGGTCTTCGGATTGTAAA

>JX429834; *Pseudomonas gessardii*, ^{GU}SK256-N6 (1406nt)

ACATGCAAGTCGAGCGGTAGAGAGAAGCTTGCTTCTCTTGAGAGCGGCGGACGGGTGAGTAAT
GCCTAGGAATCTGCCTGGTAGTGGGGGATAACGTTCGGAAACGGACGCTAATACCGCATACGT
CCTACGGGAGAAAGCAGGGGACCTTCGGGCCTTGCGCTATCAGATGAGCCTAGGTCGGATTAG
CTAGTTGGTGAGGTAATGGCTCACCAAGGCGACGATCCGTAACTGGTCTGAGAGGATGATCAG
TCACACTGGAACTGAGACACGGTCCAGACTCCTACGGGAGGCAGCAGTGGGGAATATTGGACA
ATGGGCGAAAGCCTGATCCAGCCATGCCGCGTGTGTGAAGAAGGTCTTCGGATTGTAAAGCAC
TTTAAGTTGGGAGGAAGGGTTGTAGATTAATACTCTGCAATTTTGACGTTACCGACAGAATAA
GCACCGGCTAACTCTGTGCCAGCAGCCGCGGTAATACAGAGGGTGCAAGCGTTAATCGGAATT
ACTGGGCGTAAAGCGCGCGTAGGTGGTTTGTTAAGTTGGATGTGAAATCCCCGGGCTCAACCT
GGGAACTGCATTCAAAACTGACTGACTAGAGTATGGTAGAGGGTGGTGGAATTTCCTGTGTAG
CGGTGAAATGCGTAGATATAGGAAGGAACACCAGTGGCGAAGGCGACCACCTGGACTAATACT
GACACTGAGGTGCGAAAGCGTGGGGAGCAAACAGGATTAGATACCCTGGTAGTCCACGCCGTA
AACGATGTCAACTAGCCGTTGGAAGCCTTGAGCTTTTAGTGGCGCAGCTAACGCATTAAGTTG
ACCGCCTGGGGAGTACGGCCGCAAGGTTAAAACTCAAATGAATTGACGGGGGCCCGCACAAGC
GGTGGAGCATGTGGTTTAATTCGAAGCAACGCGAAGAACCTTACCAGGCCTTGACATCCAATG
AACTTTCTAGAGATAGATTGGTGCCTTCGGGAACATTGAGACAGGTGCTGCATGGCTGTCGTC
AGCTCGTGTCGTGAGATGTTGGGTTAAGTCCCGTAACGAGCGCAACCCTTGTCCTTAGTTACC
AGCACGTTATGGTGGGCACTCTAAGGAGACTGCCGGTGACAAACCGGAGGAAGGTGGGGATGA
CGTCAAGTCATCATGGCCCTTACGGCCTGGGCTACACACGTGCTACAATGGTCGGTACAGAGG
GTTGCCAAGCCGCGAGGTGGAGCTAATCCCATAAAACCGATCGTAGTCCGGATCGCAGTCTGC
AACTCGACTGCGTGAAGTCGGAATCGCTAGTAATCGCGAATCAGAATGTCGCGGTGAATACGT
TCCCGGGCCTTGTACACACCGCCCGTCACACCATGGGAGTGGGTTGCACCAGAAGTAGCTAGT
CTAACCTTCGGGAGGACGGT

> JX429833; *Pseudomonas* sp., ^{GU}SK256-N7 (335nt)

TGCGTGCGGGTCGAGCGGTAGAGAGAAGCTTGCTTCTCTTGAGAGCGGCGGACGGGTGAGTAA
TGCCTAGGAATCTGCCTGGTAGTGGGGGATAACGTTCGGAAACGGACGCTAATACCGCATACG
TCCTACGGGAGAAAGCAGGGGACCTTCGGGCCTTGCGCTATCAGATGAGCCTAGGTCGGATTA
GCTAGTTGGTGAGGTAATGGCTCACCAAGGCGACGATCCGTAACTGGTCTGAGAGGATGATCA
GTCACACTGGAACTGAGACACGGTCCAGACTCCTACGGGAGGCAGCAGTGGGGAATATTGGAC
AATGGGCGAAAGCCTGATCC

> JX429832; *Halomonas meridiana*, ^{GU}SK256-29 (826nt)

GCCTACCATGCAAGTCGAGCGGTAACAGATCCAGCTTGCTGGATGCTGACGAGCGGCGGACGG
GTGAGTAATGCATAGGAATCTGCCCGATAGTGGGGGATAACCTGGGGAAACCCAGGCTAATAC
CGCATACGTCCTACGGGAGAAAGGGGGCTCCGGCTCCCGCTATGGGATGAGCCTATGTCGGAT
TAGCTAGTTGGTGAGGTAACGGCTCACCAAGGCCACGATCCGTAGCTGGTCTGAGAGGATGAT
CAGCCACATCGGGACTGAGACACGGCCCGAACTCCTACGGGAGGCAGCAGTGGGGAATATTGG
ACAATGGGGGCAACCCTGATCCAGCCATGCCGCGTGTGTGAAGAAGGCCCTCGGGTTGTAAAG
CACTTTCAGCGAGGAAGAACGCCTAGCGGTTAATACCCGCTAGGAAAGACATCACTCGCAGAA
GAAGCACCGGCTAACTCCGTGCCAGCAGCCGCGGTAATACGGAGGGTGCAAGCGTTAATCGGA
ATTACTGGGCGTAAAGCGCGCGTAGGTGGCTTGATAAGCCGGTTGTGAAAGCCCCGGGCTCAA
CCTGGGAACGGCATCCGGAACTGTCAAGCTAGAGTGCAGGAGAGGAAGGTAGAATTCCCGGTG
TAGCGGTGAAATGCGTAGAGATCGGGAGGAATACCAGTGGCGAAGGCGGCCTTCTGGACTGAC
ACTGACACTGAGGTGCGAAAGCGTGGGTAGCAAACAGGATTAGATACCCTGGTAGTCCACGCC
GTAAACGATGTCGACCAGCCGTTGGGTGCCTAGCGCACTTTGTGGCGAAGTTAACGCGATAAG
TCGACCG

> **JX429831; *Providencia rettgeri*, ^{GU}SK256-16A** (867nt)

TGCAAGTCGAGCGGTAACAGGGGAAGCTTGCTTCTCGCTGACGAGCGGCGGACGGGTGAGTAA
TGTATGGGGATCTGCCCGATAGAGGGGGATAACTACTGGAAACGGTAGCTAATACCGCATAAT
CTCTCAGGAGCAAAGCAGGGGAACTTCGGTCCTTGCGCTATCGGATGAACCCATATGGGATTA
GCTAGTAGGTGAGGTAATGGCTCACCTAGGCGACGATCCCTAGCTGGTCTGAGAGGATGATCA
GCCACACTGGGACTGAGACACGGCCCAGACTCCTACGGGAGGCAGCAGTGGGGAATATTGCAC
AATGGGCGCAAGCCTGATGCAGCCATGCCGCGTGTATGAAGAAGGCCCTAGGGTTGTAAAGTA
CTTTCAGTCGGGAGGAAGGCGTTGATGCTAATATCATCAACGATTGACGTTACCGACAGAAGA
AGCACCGGCTAACTCCGTGCCAGCAGCCGCGGTAATACGGAGGGTGCAAGCGTTAATCGGAAT
TACTGGGCGTAAAGCGCACGCAGGCGGTTGATTAAGTTAGATGTGAAATCCCCGGGCTTAACC
TGGGAATGGCATCTAAGACTGGTCAGCTAGAGTCTTGTAGAGGGGGGTAGAATTCCATGTGTA
GCGGTGAAATGCGTAGAGATGTGGAGGAATACCGGTGGCGAAGGCGGCCCCCTGGACAAAGAC
TGACGCTCAGGTGCGAAAGCGTGGGGAGCAAACAGGATTAGATACCCTGGTAGTCCACGCTGT
AAACGATGTCGATTTGAAGGTTGTTCCCTAGAGGAGTGGCTTTCGGAGCTAACGCGTTAAATC
GACCGCCTGGGGAGTACGGCCGCAAGGTTAAAACTCAAATGAATTGAC

> **JX429830; *Pseudomonas* sp., ^{GU}SK256-N5** (385nt)

GCTGGCGGCAGGCCTGTCATGCAGGTCGAGCGGTAGAGAGAAGCTTGCTTCTCTTGAGAGCGG
CGGACGGGTGAGTAATGCCTAGGAATCTGCCTGGTAGTGGGGGATAACGTTCGGAAACGGACG
CTAATACCGCATACGTCCTACGGGAGAAAGCAGGGGACCTTCGGGCCTTGCGCTATCAGATGA
GCCTAGGTCGGATTAGCTAGTTGGTGAGGTAATGGCTCACCAAGGCTACTATCCTTAACTGGT
CTGAGAGGATGATCAGTCACACTGGAACTGAGACACGGTCCAGACTCCTACGGGAGGCAGCAG
TGGGGAATATTGGACAATGGGCGAAAGCCTGATCCAGCCATGCCGCGTGTGTGAAGAAGGTCT
TCGGATT

> **JX429829; *Pseudomonas* sp., ^{GU}SK256-N3** (227nt)

GCTGGCGGCAGGCCTAACACATGCAAGTCCGAGCGGTAGAGAGAAGCTTGCTTCTCTTGAGAG
CGGCGGACGGGTGAGTAATGCCTAGGAATCTGCCTGGTAGTGGGGGATAACGTTCGGAAACGG
ACGCTAATACCGCATACGTCCTACGGGAGAAAGCAGGGGACCTTCGGGCCTTGCGCTATCAGA
TGAGCCTAGGTCGGATTAGCTAGTTGGTGAGGTAATGG

> **JX429828; *Pseudomonas xanthomarina*, ^{GU}SK256-25A** (513nt)

ATGAACGCTGGCGGCAGGCCTACACATGCAAGTCGAGCGGATGAAGAGAGCTTGCTCTCTGAT
TCAGCGGCGGACGGGTGAGTAATGCCTAGGAATCTGCCTGGTAGTGGGGGACAACGTTTCGAA
AGGAACGCTAATACCGCATACGTCCTACGGGAGAAAGGCAGGGGACCTTCGGGCCTTGCGCTA
TCAGATGAGCCTAGCTCGGATTAGCTAGTTGGTGAGGTAATGGCTCACCAAGGCGACGATCCG
TAACTAGTCTGAGAGGATGATCAGTCACACTGGAACTGAGACACGGTCCAGACTCCTACGGGA
GGCAGCAGTGGGGAATATTGGACAATGGGCGAAAGCCTGATCCAGCCATGCCGCGTGTGTGAA
GAAGGTCTTCGGATTGTAAAGCACTTTAAGTTGGGAGGAAGGGCATTAACCTAATACGTTAGT
GTTTTGACGTTACCGACAGAATAAGCACCGGCTAACTTCGTGCCAGCAGCCGCGGTAATACGA
AGGGTGCAA

B. 16SrDNA sequences of *N miliaris* declining bloom associated bacterial flora:

[>Gen Bank Accession; Identity, strain designation (Length of sequence: 5 - 3)]

>JX429827; Unclassified Bacillales, ^{GU}SS263-7 (269nt)

GCGGATGACGGAGGAGCTTGCTCCTCTAGATTCAGCGGCGGACGGGTGAGTAACACGTGGGCA
ACCTGCCCTGTAGATTGGGATAACTCCGGGAAACCGGGGCTAATACCGAATAATCCTTCGGAC
CTCATGGTCCGATGTTGAAAGGCGGCTTCGGCTGTCCCTACCGGATGGGCCCGCGGCGCATTA
ACTAGTTGGTGAGGTAACGGCTCCCCCAGGGCACGATGCGTAACCCAACTGAAAGGGTGATCG
GCCCCACTGGGACTGAA

>JX429826; *Bacillus* sp., ^{GU}SS263-20 (726nt)

GCGGACCGATGGGAGCTTGCTCCCTGAAGTCAGCGGCGGACGGGTGAGTAACACGTGGGCAAC
CTGCCTGTAAGACTGGGATAACTCCGGGAAACCGGGGCTAATACCGGATAATTCTTTCCCTCA
CATGAGGGAAAGCTGAAAGATGGTTTCGGCTATCACTTACAGATGGGCCCGCGGCGCATTAGC
TAGTTGGTGAGGTAACGGCTCACCAAGGCAGCGATGCGTAGCCGACCTGATAGGGTGATCGGC
CACACTGGGACTGAGACACGGCCCAGACTCCTACGGGAGGCAGCAGTAGGGAATCTTCCGCAA
TGGACGAAAGTCTGACGGAGCAACGCCGCGTGAGTGATGAAGGTTTTCGGATCGTAAAACTCT
GTTGTTAGGGAAGAACAAGTACCGGAGTAACTGCCGGTACCTTGACGGTACCTAACCAGAAAG
CCACGGCTAACTACGTGCCAGCAGCCGCGGTAATACGTAGGTGGCAAGCGTTGTCCGGAATTA
TTGGGCGTAAAGCGCGCGCAGGCGGTTCCTTAAGTCTGATGTGAAAGCCCCCGGCTCAACCGG
GGAGGGTCATTGGAAACTGGGGAACTTGAGTGCAGAAGAGAAGAGTGGAATTCCACGTGTAGC
GGTGAAATGCGTAGAGATGTGGAGGAACACCAGTGGCGAAGGCGACTCTTTGGTCTGTAACTG
ACGCTGAGGCGCGAAAGCGTGGGGAGCAAACAG

>JX429825; *Bacillus flexus*, ^{GU}SS263-5 (1461nt)

TACATGCAAGTCGAGCGAACTGATTAGAAGCTTGCTTCTATGACGTTAGCGGCGGACGGGTGA
GTAACACGTGGGCAACCTGCCTGTAAGACTGGGATAACTCCGGGAAACCGGAGCTAATACCGG
ATAACATTTTCTCTTGCATAAGAGAAAATTGAAAGATGGTTTCGGCTATCACTTACAGATGGG
CCCGCGGTGCATTAGCTAGTTGGTGAGGTAACGGCTCACCAAGGCAACGATGCATAGCCGACC
TGAGAGGGTGATCGCCACACTGGGACTGAGACACGGCCCCAGACTCCTACGGGA

> JX429824; *Bacillus cereus*, ^{GU}SS263-34 (1503nt)

GATCCTGGCTCAGGATGAACGCTGGCGGCGTGCCTAATACATGCAAGTCGAGCGAATGGATTA
AGAGCTTGCTCTTATGAAGTTAGCGGCGGACGGGTGAGTAACACGTGGGTAACCTGCCCATAA
GACTGGGATAACTCCGGGAAACCGGGGCTAATACCGGATAACATTTTGAACCGCATGGTTCGA
AATTGAAAGGCGGCTTCGGCTGTCACTTATGGATGGACCCGCGTCGCATTAGCTAGTTGGTGA
GGTAACGGCTCACCAAGGCAACGATGCGTAGCCGACCTGAGAGGGTGATCGGCCACACTGGGA
CTGAGACACGGCCCAGACTCCTACGGGAGGCAGCAGTAGGGAATCTTCCGCAATGGACGAAAG
TCTGACGGAGCAACGCCGCGTGAGTGATGAAGGCTTTCGGGTCGTAAAACTCTGTTGTTAGGG
AAGAACAAGTGCTAGTTGAATAAGCTGGCACCTTGACGGTACCTAACCAGAAAGCCACGGCTA
ACTACGTGCCAGCAGCCGCGGTAATACGTAGGTGGCAAGCGTTATCCGGAATTATTGGGCGTA
AAGCGCGCGCAGGTGGTTTCTTAAGTCTGATGTGAAAGCCCACGGCTCAACCGTGGAGGGTCA
TTGGAAACTGGGAGACTTGAGTGCAGAAGAGGAAAGTGGAATTCCATGTGTAGCGGTGAAATG
CGTAGAGATATGGAGGAACACCAGTGGCGAAGGCGACTTTCTGGTCTGTAACTGACACTGAGG
CGCGAAAGCGTGGGGAGCAAACAGGATTAGATACCCTGGTAGTCCACGCCGTAAACGATGAGT
GCTAAGTGTTAGAGGGTTTCCGCCCTTTAGTGCTGAAGTTAACGCATTAAGCACTCCGCCTGG
GGAGTACGGCCGCAAGGCTGAAACTCAAAGGAATTGACGGGGGCCCGCACAAGCGGTGGAGCA
TGTGGTTTAATTCGAAGCAACGCGAAGAACCTTACCAGGTCTTGACATCCTCTGAAAACCCTA
GAGATAGGGCTTCTCCTTCGGGAGCAGAGTGACAGGTGGTGCATGGTTGTCGTCAGCTCGTGT
CGTGAGATGTTGGGTTAAGTCCCGCAACGAGCGCAACCCTTGATCTTAGTTGCCATCATTAAG
TTGGGCACTCTAAGGTGACTGCCGGTGACAAACCGGAGGAAGGTGGGGATGACGTCAAATCAT
CATGCCCCTTATGACCTGGGCTACACACGTGCTACAATGGACGGTACAAAGAGCTGCAAGACC

GCGAGGTGGAGCTAATCTCATAAAACCGTTCTCAGTTCGGATTGTAGGCTGCAACTCGCCTAC
ATGAAGCTGGAATCGCTAGTAATCGCGGATCAGCATGCCGCGGTGAATACGTTCCCGGGCCTT
GTACACACCGCCCGTCACACCACGAGAGTTTGTAACACCCGAAGTCGGTGGGGTAACCTTTTT
GGAGCCAGCCGCCTAAGGTGGGACAGATGATTGGGGTGAAGTCGTAACAAGGTA

> **JX429823; Unclassified Bacillales, ^{GU}SS263-10** (215nt)

GCTGGCGGCGTGCCTATTACATGCAAGTCGAGCGAACTGATTAGAAGCTTGCTTCTATGACGT
TAGCGGCGGACGGGTGAGTAACACGTGGGCAACCTGCCTGTAAGACTGGGATAACTCCGGGAA
ACCGGAGCTAATACCGGATAACATTTTTTCTTGCATAAGAGAAAATTGAAAGATGCTGTCGGC
TATCACATACAAATGGGTCTGCGGTG

> **JX429822; *Virgibacillus halodenitrificans*, ^{GU}SS263-37** (663nt)

GCTGGCGGCGTGCCTAATACATGCAAGTCGAGCGCGGGAAGCAAGCTGATCCTCTTCGGAGGTGACGCTT
GTGGAACGAGCGGCGGACGGGTGAGTAACACGTGGGCAACCTGCCTGTAAGACTGGGATAACCCCGGGAA
ACCGGGGCTAATACCGGATAATACTTTTCATCACCTGATGAGAAGTTGAAAGGTGGCTTTTAGCTACCAC
TTACAGATGGGCCCGCGGCGCATTAGCTAGTTGGTGAGGTAACGGCTCACCAAGGCAACGATGCGTAGCC
GACCTGAGAGGGTGATCGGCCACACTGGGACTGAGACACGGCCCAGACTCCTACGGGAGGCAGCAGTAGG
GAATCTTCCGCAATGGACGAAAGTCTGACGGAGCAACGCCGCGTGAGTGATGAAGGTTTTCGGATCGTAA
AGCTCTGTTGTTAGGGAAGAACAAGTGCCGTTCGAATAGGGCGGCACCTTGACGGTACCTAACCAGAAAG
CCCCGGCTAACTACGTGCCAGCAGCCGCGGTAATACGTAGGGGGCAAGCGTTGTCCGGAATTATTGGGCG
TAAAGCGCGCGCAGGCGGTCCTTTAAGTCTGATGTGAAAGCCCACGGCTCAGCCGTGGAGGGTCATTGGA
AACTGGAGGACTTGAGTACAGAAGAGGAGAGTG

>**JX429821; *Staphylococcus cohnii*, ^{GU}SS263-12** (440nt)

GCTGGCGGCGTGCCTATTACATGCAAGTCGAGCGAACAGATAAGGAGCTTGCTCCTTTGACGT
TAGCGGCGGACGGGTGAGTAACACGTGGGTAACCTACCTATAAGACTGGAATAACTCCGGGAA
ACCGGGGCTAATGCCGGATAACATTTAGAACCGCATGGTTCTAAAGTGAAAGATGGTTTTGCT
ATCACTTATAGATGGACCCGCGCCGTATTAGCTAGTTGGTAAGGTAACGGCTTACCAAGGCAA
CGATACGTAGCCGACCTGAGAGGGTGATCGGCCACACTGGAACTGAGACACGGTCCAGACTCC
TACGGGAGGCAGCAGTAGGGAATCTTCCGCAATGGGCGAAAGCCTGACGGAGCAACGCCGCGT
GAGTGATGAAGGTCTTCGGATCGTAAAACTCTGTTATTAGGGAAGAACAAATGTGTAAGTAA

>**JX429820; *Brevibacillus borstellensis*, ^{GU}SS263-26** (776nt)

GCCTTATACATGCAAGTCGAGCGAGTCCCTTCGGGGGCTAGCGGCGGACGGGTGAGTAACACG
TAGGCAACCTGCCCGTAAGCTCGGGATAACATGGGGAAACTCATGCTAATACCGGATAGGGTC
TTCTCTCGCATGAGAGGAGACGGAAAGGTGGCGCAAGCTACCACTTACGGATGGGCCTGCGGC
GCATTAGCTAGTTGGTGGGGTAACGGCCTACCAAGGCGACGATGCGTAGCCGACCTGAGAGGG
TGACCGGCCACACTGGGACTGAGACACGGCCCAGACTCCTACGGGAGGCAGCAGTAGGGAATT
TTCCACAATGGACGAAAGTCTGATGGAGCAACGCCGCGTGAACGATGAAGGTCTTCGGATTGT
AAAGTTCTGTTGTCAGAGACGAACAAGTACCGTTCGAACAGGGCGGTACCTTGACGGTACCTG
ACGAGAAAGCCACGGCTAACTACGTGCCAGCAGCCGCGGTAATACGTAGGTGGCAAGCGTTGT
CCGGAATTATTGGGCGTAAAGCGCGCGCAGGCGGCTATGTAAGTCTGGTGTTAAAGCCCGGGG
CTCAACCCCGGTTCGCATCGGAAACTGTGTAGCTTGAGTGCAGAAGAGGAAAGCGGTATTCCA
CGTGTAGCGGTGAAATGCGTAGAGATGTGGAGGAACACCAGTGGCGAAGGCGGCTTTCTGGTC
TGTAACTGACGCTGAGGCGCGAAAGCGTGGGGAGCAAACAGGATTAGATACCCTGGTAGTCCA
CGCCGTAAACGATGAGTGCT

> **JX429819; *Microbacterium* sp., ^{GU}SS263-4** (316nt)

GCTGGCGGCGTGCTTATCACATGCAAGTCGAACGGTGAACACGGAGCTTGCTCTGTGGGATCA
GTGGCGAACGGGTGAGTAACACGTGAGCAACCTGCCCCTGACTCTGGGATAAGCGCTGGAAAC
GGCGTCTAATACTGGATATGTGACGTGACCGCATGGTCTGCGTCTGGAAAGAATTTCGGTTGG
GGATGGGCTCGCGGCCTATCAGCTTGTTGGTGAGGTAATGGCTCACCAAGGCGTCGACGGGTA
GCCGGCCTGAGAGGGTGACCGGCCACACTGGGACTGAGACACGGCCCAGACTCCTACGGGAGG
C

> **JX429818; *Dietzia timorensis*, ^{GU}SS263-17** (513nt)

ACGCTGGCGGCGTGCTTAACACATGCAAGTCGAACGGTAAGGCCCTTCGGGGTACACGAGTGG
CGAACGGGTGAGTAACACGTGGGTAATCTGCCCTGCACTTCGGGATAAGCCTGGGAAACTGGG
TCTAATACCGGATATTCAGCTTCTGCCGCATGGTGGTTGTTGGAAAGTTTTTCGGTGCAGGAT
GTGCCCGCGGCCTATCAGCTTGTTGGTGGGGTAATGGCCTACCAAGGCGACGACGGGTAGCCG
GCCTGAGAGGGTGATCGGCCACATTGGGACTGAGACACGGCCCAGACTCCTACGGGAGGCAGC
AGTGGGGAATATTGCACAATGGGCGCAAGCCTGATGCAGCGACGCCGCGTGAGGGATGACGGT
CTTCGGATTGTAAACCTCTTTCGGCAGGGACGAAGCGCAAGTGACGGTACCTGCAGAAGAAGC
ACCGGCCAACTACGTGCCAGCAGCCGCGGTAATACGTAGGGTGCGAGCGTTGTCCGGAATTAC
TGGGCGTAA

> **JX429817; *Dietzia schimae*, ^{GU}SS263-19** (433nt)

CGCTGGCGGCGTGCTTAACACATGCAAGTCGAACGGTAAGGCCCCTTCGGGGGTACACGAGTG
GCGAACGGGTGAGTAACACGTGGGTAATCTGCCCTGCACTTCGGGATAAGCCTGGGAAACTGG
GTCTAATACCGGATATGAACTCCTGCCGCATGGTGGGGGTTGGAAAGTTTTTCGGTGCAGGAT
GAGCCCGCGGCCTATCAGCTTGTTGGTGGGGTAATGGCCTACCAAGGCGACGACGGGTAGCCG
GCCTGAGAGGGTGATCGGCCACACTGGGACTGAGACACGGCCCAGACTCCTACGGGAGGCAGC
AGTGGGGAATATTGCACAATGGGCGAAAGCCTGATGCAGCGACGCCGCGTGGGGGATGACGGT
CTTCGGATTGTAAACCCCTTTCAGTAGGGACGAAGCGCAAGTGACGGTACCTGCA

> **JX429816; *Brachybacterium paraconglomeratum*, ^{GU}SS263-16** (798nt)

GCTGGCGGCGTGCTTATCACATGCAAGTCGAACGATGACGGTGGTGCTTGCACCGCCTGATTA
GTGGCGAACGGGTGAGTAACACGTGAGTAACCTGCCCTCCACTTCGGGATAACCTCGGGAAAT
CGTGGCTAATACCGGATATGAGCACTCATCGCATGGTGAGTGCTGGAAAGATTTATCGGTGGG
GGATGGACTCGCGGCCTATCAGTTTGTTGGTGAGGTGATGGCTCACCAAGACGATGACGGGTA
GCCGGCCTGAGAGGGCGACCGGCCACACTGGGACTGAGACACGGCCCAGACTCCTACGGGAGG
CAGCAGTGGGGAATATTGCACAATGGGCGAAAGCCTGATGCAGCGACGCCGCGTGGGGGATGA
CGGCCTTCGGGTTGTAAACCCCTTTCAGTAGGGAAGAAGCGAGAGTGACGGTACCTGCAGAAG
AAGCGCCGGCTAACTACGTGCCAGCAGCCGCGGTAATACGTAGGGCGCAAGCGTTGTCCGGAA
TTATTGGGCGTAAAGAGCTTGTAGGTGGCTTGTCGCGTCTGCCGTGAAAACCCGAGGCTCAAC
CTCGGGCGTGCGGTGGGTACGGGCAGGCTAGAGTGTGGTAGGGGAGACTGGAACTCCTGGTGT
AGCGGTGAAATGCGCAGATATCACGAAGAACACCGATGGCGAAGGCAGGTCTCTGGGCCATTA
CTGACACTGAGAAGCGAAAGCATGGGTAGCGAACAGGATTAGATACCCTGGTAGTCCATGCCG
TAAACGTTGGGCACTAGGTGTGGGGGACATTCCACGTTTTCC

> **JX429815; *Kocuria* sp., ^{GU}SS263-23** (1420nt)

TGCAAGTCGAACGATGATCTCCCGCTTGCGGGGGTGATTAGTGGCGAACGGGTGAGTAATACG
TGAGTAACCTGCCCTTGACTCTGGGATAAGCCTGGGAAACCGGGTCTAATACTGGATACTACT
TCCTGCCGCATGGTGGGGGGTGGAAAGGGTTCTACTGGTTTTGGATGGGCTCACGGCCTATCA
GCTTGTTGGTGGGGTAATGGCTCACCAAGGCGACGACGGGTAGCCGGCCTGAGAGGGTGACCG
GCCACACTGGGACTGAGACACGGCCCAGACTCCTACGGGAGGCAGCAGTGGGGAATATTGCAC
AATGGGCGGAAGCCTGATGCAGCGACGCCGCGTGAGGGATGACGGCCTTCGGGTTGTAAACCT
CTTTCAGCAGGGAAGAAGCCACAAGTGACGGTACCTGCAGAAGAAGCGCCGGCTAACTACGTG
CCAGCAGCCGCGGTAATACGTAGGGCGCAAGCGTTGTCCGGAATTATTGGGCGTAAAGAGCTC
GTAGGCGGTTTGTCGCGTCTGCTGTGAAAGCCCGGGGCTCAACCCCGGGTCTGCAGTGGGTAC
GGGCAGACTAGAGTGCAGTAGGGGAGACTGGAATTCCTGGTGTAGCGGTGAAATGCGCAGATA
TCAGGAGGAACACCGATGGCGAAGGCAGGTCTCTGGGCTGTTACTGACGCTGAGGAGCGAAAG
CATGGGGAGCGAACAGGATTAGATACCCTGGTAGTCCATGCCGTAAACGTTGGGCACTAGGTG
TGGGGGACATTCCACGTTCTCCGCGCCGTAGCTAACGCATTAAGTGCCCCGCCTGGGGAGTAC
GGCCGCAAGGCTAAAACTCAAAGGAATTGACGGGGGCCCGCACAAGCGGCGGAGCATGCGGAT
TAATTCGATGCAACGCGAAGAACCTTACCAAGGCTTGACATTCACCGGACCGCACTGGAGACA
GTGCTTCCCTTCGGGGTCGGTGGACAGGTGGTGCATGGTTGTCGTCAGCTCGTGTCGTGAGAT
GTTGGGTTAAGTCCCGCAACGAGCGCAACCCTCGTTCTATGTTGCCAGCACGTGATGGTGGGG
ACTCATAGGAGACTGCCGGGGTCAACTCGGAGGAAGGTGGGGATGACGTCAAATCATCATGCC
CCTTATGTCTTGGGCTTCACGCATGCTACAATGGCCGGTACAAAGGGTTGCGATACTGTGAGG

TGGAGCTAATCCCAAAAAGCCGGTCTCAGTTCGGATTGAGGTCTGCAACTCGACCTCATGAAG
TCGGAGTCGCTAGTAATCGCAGATCAGCAACGCTGCGGTGAATACGTTCCCGGGCCTTGTACA
CACCGCCCGTCAAGTCACGAAAGTTGGTAACACCCGAAGCCGGTGGCCTAACCCCTTTGTGGG
AGGGAGCCGTCGAAGGTGGGACTGGCGATTGGGA

> **JX429814; *Leucobacter komagate*, ^{GU}SS263-27** (631nt)

CGCTGGCGGCGTGCTTAACACATGCAAGTCGAACGATGAAGCCCAGCTTGCTGGGTGGAAGAG
TGGCGAACGGGTGAGTAACACGTGAGTAACCTGCCCTGAACTCTGGGATAAGCACTGGAAACG
GTGTCTAATACTGGATACGACCTATCACCGCATGGTGTGTGGGTGGAAAGATTTATCGGTTCT
GGATGGACTCGCGGCCTATCAGCTAGATGGTGAGGTAATGGCTCACCATGGCGACGACGGGTA
GCCGGCCTGAGAGGGTGACCGGCCACACTGGGACTGAGACACGGCCCAGACTCCTACGGGAGG
CAGCAGTGGGGAATATTGCACAATGGGCGCAAGCCTGATGCAGCAACGCCGCGTGAGGGATGA
CGGCCTTCGGGTTGTAAACCTCTTTTAGTAGGGAAGAAGCGAAAGTGACGGTACCTGCAGAAA
AAGCACCGGCTAACTACGTGCCAGCAGCCGCGGTAATACGTAGGGTGCAAGCGTTGTCCGGAA
TTATTGGGCGTAAAGAGCTCGTAGGCGGCTTGTCGCGTCTGCTGTGAAAACCCGGGGCTCAAC
CCCGGGCCTGCAGTGGGTACGGGCAGGCTAGAGTGCGGTAGGGGAGATTGGAATTCCTGGTGT
A

> **JX429813; *Psychrobacter* sp., ^{GU}SS263-1** (402nt)

GCTGGCGGCAGGCTTATCACATGCAAGTCGAGCGGAAACGATGGGAGCTTGCTCCCAGGCGTC
GAGCGGCGGACGGGTGAGTAACACTTAGGAATCTACCTAGTAGTGGGGGATAGCTCGGGGAAA
CTCGAATTAATACCGCATACGTCCTACGGGAGAAAGGGGGCAGTTTACTGCTCTCGCTATTAG
ATGAGCCTAAGTCGGATTAGCTAGTTGGTGGGGTAAAGGCCTACCAAGGCGACGATCTGTAGC
TGGTCTGAGAGGATGATCAGCCACACCGGGACTGAGACACGGCCCGGACTCCTACGGGAGGCA
GCAGTGGGGAATATTGGACAATGGGGGAAACCCTGATCCAGCCATGCCGCGTGTGTGAAGAAG
GCCTTTTGGTTGTAAAGCACTTTA

> **JX429812; *Pseudomonas* sp., ^{GU}SS263-3** (392nt)

ACGCTGGCGGCAGGCCTATCACATGCAAGTCGAGCGGTAGAGAGAAGCTTGCTTCTCTTGAGA
GCGGCGGACGGGTGAGTAATGCCTAGGAATCTGCCTGGTAGTGGGGGATAACGTTCGGAAACG
GACGCTAATACCGCATACGTCCTACGGGAGAAAGCAGGGGACCTTCGGGCCTTGCGCTATCAG
ATGAGCCTAGGTCGGATTAGCTAGTTGGTGAGGTAATGGCTCACCAAGGCGACGATCCGTAAC
TGGTCTGAGAGGATGATCAGTCACACTGGAACTGAGACACGGTCCAGACTCCTACGGGAGGCA
GCAGTGGGGAATATTGGACAATGGGCGAAAGCCTGATCCAGCCATGCCGCGTGTGTGAAGAAG
GTCTTCGGATTGTA

> **JX429811; *Pseudomonas* sp., ^{GU}SS263-6** (389nt)

GTGGCGGCAGGCCTATCACATGCAAGTCGAGCGGTAGAGAGAAGCTTGCTTCTCTTGAGAGCG
GCGGACGGGTGAGTAATGCCTAGGAATCTGCCTGGTAGTGGGGGATAACGTTCGGAAACGGAC
GCTAATACCGCATACGTCCTACGGGAGAAAGCAGGGGACCTTCGGGCCTTGCGCTATCAGATG
AGCCTAGGTCGGATTAGCTAGTTGGTGAGGTAATGGCTCACCAAGGCGACGATCCGTAACTGG
TCTGAGAGGATGATCAGTCACACTGGAACTGAGACACGGTCCAGACTCCTACGGGAGGCAGCA
GTGGGGAATATTGGACAATGGGCGAAAGCCTGATCCAGCCATGCCGCGTGTGTGAAGAAGGTC
TTCGGATTGTA

> **JX429810; *Pseudomonas* sp., ^{GU}SS263-8** (619nt)

ACATGCAAGTCGAGCGGTAGAGAGAAGCTTGCTTCTCTTGAGAGCGGCGGACGGGTGAGTAAT
GCCTAGGAATCTGCCTGGTAGTGGGGGATAACGTTCGGAAACGGACGCTAATACCGCATACGT
CCTACGGGAGAAAGCAGGGGACCTTCGGGCCTTGCGCTATCAGATGAGCCTAGGTCGGATTAG
CTAGTTGGTGAGGTAATGGCTCACCAAGGCGACGATCCGTAACTGGTCTGAGAGGATGATCAG
TCACACTGGAACTGAGACACGGTCCAGACTCCTACGGGAGGCAGCAGTGGGGAATATTGGACA
ATGGGCGAAAGCCTGATCCAGCCATGCCGCGTGTGTGAAGAAGGTCTTCGGATTGTAAAGCAC
TTTAAGTTGGGAGGAAGGGTTGTAGATTAATACTCTGCAATTTTGACGTTACCGACAGAATAA
GCACCGGCTAACTCTGTGCCAGCAGCCGCGGTAATACAGAGGGTGCAAGCGTTAATCGGAATT

ACTGGGCGTAAAGCGCGCGTAGGTGGTTTGTTAAGTTGGATGTGAAATCCCCGGGCTCAACCT
GGGAACTGCATTCAAAACTGACTGACTAGAGTATGGTAGAGGGTGGTGGAAT

> **JX429809; *Shewanella* sp., ^{GU}SS263-9** (1452nt)

TGCAAGTCGAGCGGTAACATTTCAAAAGCTTGCTTTTGAAGATGACGAGCGGCGGACGGGTGA
GTAATGCCTGGGAATTTGCCCATTTGTGGGGGATAACAGTTGGAAACGACTGCTAATACCGCA
TACGCCCTACGGGGGAAAGCAGGGGACCTTCGGGCCTTGCGCTGATGGATAAGCCCAGGTGGG
ATTAGCTAGTAGGTGAGGTAAAGGCTCACCTAGGCGACGATCCCTAGCTGGTCTGAGAGGATG
ATCAGCCACACTGGGACTGAGACACGGCCCAGACTCCTACGGGAGGCAGCAGTGGGGAATATT
GCACAATGGGGGAAACCCTGATGCAGCCATGCCGCGTGTGTGAAGAAGGCCTTCGGGTTGTAA
AGCACTTTCAGCGAGGAGGAAAGGGTGTAAGTTAATACCTTACATCTGTGACGTTACTCGCAG
AAGAAGCACCGGCTAACTCCGTGCCAGCAGCCGCGGTAATACGGAGGGTGCGAGCGTTAATCG
GAATTACTGGGCGTAAAGCGTGCGCAGGCGGTTTGTTAAGCGAGATGTGAAAGCCCCGGGCTC
AACCTGGGAACCGCATTTCGAACTGGCAAACTAGAGTCTTGTAGAGGGGGGTAGAATTCCAGG
TGTAGCGGTGAAATGCGTAGAGATCTGGAGGAATACCGGTGGCGAAGGCGGCCCCCTGGACAA
AGACTGACGCTCAGGCACGAAAGCGTGGGGAGCAAACAGGATTAGATACCCTGGTAGTCCACG
CCGTAAACGATGTCTACTCGGAGTTTGGTGTCTTGAACACTGGGCTCTCAAGCTAACGCATTA
AGTAGACCGCCTGGGGAGTACGGCCGCAAGGTTAAAACTCAAATGAATTGACGGGGGCCCGCA
CAAGCGGTGGAGCATGTGGTTTAATTCGATGCAACGCGAAGAACCTTACCTACTCTTGACATC
CACAGAATCTGGTAGAGATACCTCAGTGCCTTCGGGAACTGTGAGACAGGTGCTGCATGGCTG
TCGTCAGCTCGTGTTGTGAAATGTTGGGTTAAGTCCCGCAACGAGCGCAACCCCTATCCTTAC
TTGCCAGCGGGTAATGCCGGGAACTTTAGGGAGACTGCCGGTGATAAACCGGAGGAAGGTGGG
GACGACGTCAAGTCATCATGGCCCTTACGAGTAGGGCTACACACGTGCTACAATGGTCAGTAC
AGAGGGTTGCGAAGCCGCGAGGTGGAGCTAATCCCATAAAGCTGGTCGTAGTCCGGATTGGAG
TCTGCAACTCGACTCCATGAAGTCGGAATCGCTAGTAATCGTGGATCAGAATGCCACGGTGAA
TACGTTCCCGGGCCTTGTACACACCGCCCGTCACACCATGGGAGTGGGCTGCACCAGAAGTAG
ATAGCTTAACCTTCGGGAGGGCGTTTACCACGGTGTGGTTCATGACTGGGGTGAAGTCGTAAC
AAG

> **JX429808; *Cobetia marina*, ^{GU}SS263-11** (648nt)

GCTGGCGGCAGGCTTATCACATGCAAGTCGAGCGGAAACGATTCTAGCTTGCTAGAAGGCGTC
GAGCGGCGGACGGGTGAGTAATGCATGGGAATCTGCCCGATAGTGGGGGACAACCTGGGGAAA
CTCAGGCTAATACCGCATACGTCCTACGGGAGAAAGCAGGGGATCTTCGGACCTTGCGCTATC
GGATGAGCCCATGTCGGATTAGCTTGTTGGTGAGGTAACGGCTCACCAAGGCGACGATCCGTA
GCTGGTCTGAGAGGATGATCAGCCACACTGGGACTGAGACACGGCCCAGACTCCTACGGGAGG
CAGCAGTGGGGAATATTGGACAATGGGCGAAAGCCTGATCCAGCCATGCCGCGTGTGTGAAGA
AGGCCTTCGGGTTGTAAAGCACTTTCAGCGAGGAGGAACGCCTCGGGATTAATACTTCCGAGG
AAAGACATCACTCGCAGAAGAAGCACCGGCTAACTCCGTGCCAGCAGCCGCGGTAATACGGAG
GGTGCAAGCGTTAATCGGAATTACTGGGCGTAAAGCGCGCGTAGGTGGCTAAGTCAGCCAGGT
GTGAAAGCCCCGGGCTCAACCTGGGAACGGCATCTGGAACTGCTTGGCTAGAGTGCAGGAGAG
GAAGGTAGAATTCCCGGT

> **JX429807; *Cobetia marina*, ^{GU}SS263-13** (633nt)

CATGCAAGTCGAGCGGAAACGATTCTAGCTTGCTAGAAGGCGTCGAGCGGCGGACGGGTGAGT
AATGCATGGGAATCTGCCCGATAGTGGGGGACAACCTGGGGAAACTCAGGCTAATACCGCATA
CGTCCTACGGGAGAAAGCAGGGGATCTTCGGACCTTGCGCTATCGGATGAGCCCATGTCGGAT
TAGCTTGTTGGTGAGGTAACGGCTCACCAAGGCGACGATCCGTAGCTGGTCTGAGAGGATGAT
CAGCCACACTGGGACTGAGACACGGCCCAGACTCCTACGGGAGGCAGCAGTGGGGAATATTGG
ACAATGGGCGAAAGCCTGATCCAGCCATGCCGCGTGTGTGAAGAAGGCCTTCGGGTTGTAAAG
CACTTTCAGCGAGGAAGAACGCCTCGGGATTAATACTTCCGAGGAAAGACATCACTCGCAGAA
GAAGCACCGGCTAACTCCGTGCCAGCAGCCGCGGTAATACGGAGGGTGCAAGCGTTAATCGGA
ATTACTGGGCGTAAAGCGCGCGTAGGTGGCTAAGTCAGCCAGGTGTGAAAGCCCCGGGCTCAA
CCTGGGAACGGCATCTGGAACTGCTTGGCTAGAGTGCAGGAGAGGAAGGTAGAATTCCCGGTG
TAG

> **JX429806; *Shewanella* sp., ^{GU}SS263-14** (296nt)

GCTGGCGGCAGGCCTATCACATGCAGGTCGAGCGGTACCTTTTCAAAGCTTGCTTTTGAAGAT
GACGAGCGGCGGACGGGTGAGTAATGCCTGGGAATTTGCCCATTTGTGGGGGATAACAGTTGG
AAACGACTGCTAATACCGCATACGCCCTACGGGGGAAAGCAGGGGACCTTCGGGCCTTGCGCT
GATGGATAAGCCCAGGTGGGATTAGCTAGTAGGTGAGGTAAAGGCTCGCCTAGGCGACGATCC
CTAGCTGGTCTGAGAGGATGATCACCCGCACTGGGACTGAGACA

> **JX429805; *Psychrobacter* sp., ^{GU}SS263-21** (629nt)

GCGGCAGGCTTATCACATGCAAGTCGAGCGGAAACGATGGGAGCTTGCTCCCAGGCGTCGAGC
GGCGGACGGGTGAGTAACACTTAGGAATCTACCTAGTAGTGGGGGATAGCTCGGGGAAACTCG
AATTAATACCGCATACGTCCTACGGGAGAAAGGGGGCAGTTTACTGCTCTCGCTATTAGATGA
GCCTAAGTCGGATTAGCTAGATGGTGGGGTAAAGGCCTACCATGGCGACGATCTGTAGCTGGT
CTGAGAGGATGATCAGCCACACCGGGACTGAGACACGGCCCGGACTCCTACGGGAGGCAGCAG
TGGGGAATATTGGACAATGGGGGGAACCCTGATCCAGCCATGCCGCGTGTGTGAAGAAGGCCT
TTTGGTTGTAAAGCACTTTAAGCAGTGAAGAAGACCTAACGGTTAATACCCGTTAGCGATGAC
ATTAGCTGCAGAATAAGCACCGGCTAACTCTGTGCCAGCAGCCGCGGTAATACAGAGGGTGCA
AGCGTTAATCGGAATTACTGGGCGTAAAGCGAGCGTAGGTGGCTTGATAAGTCAGATGTGAGA
TCCCCGGGCTTAACCTGGGAACTGCATCTGATACTGTTAAGCTAGAGTAGGTGAGAGGGGAA

> **JX429804; *Pseudoalteromonas* sp., ^{GU}SS263-28** (1438nt)

AGTCGAGCGGAAACGAAGAGTAGCTTGCTACTCTGGCGTCGAGCGGCGGACGGGTGAGTAATG
CTTGGGAACATGCCTTGAGGTGGGGGACAACAGTTGGAAACGACTGCTAATACCGCATAATGT
CTACGGACCAAAGGGGGCTTCGGCTCTCGCCTTTAGATTGGCCCAAGTGGGATTAGCTAGTTG
GTGAGGTAATGGCTCACCAAGGCGACGATCCCTAGCTGGTTTGAGAGGATGATCAGCCACACT
GGGACTGAGACACGGCCCAGACTCCTACGGGAGGCAGCAGTGGGGAATATTGCACAATGGGCG
CAAGCCTGATGCAGCCATGCCGCGTGTGTGAAGAAGGCCTTCGGGTTGTAAAGCACTTTCAGT
CAGGAGGAAAGGTTAGTAGTTAATACCTGCTAGCTGTGACGTTACTGACAGAAGAAGCACCGG
CTAACTCCGTGCCAGCAGCCGCGGTAATACGGAGGGTGCGAGCGTTAATCGGAATTACTGGGC
GTAAAGCGTACGCAGGCGGTTTGTTAAGCGAGATGTGAAAGCCCCGGGCTCAACCTGGGAACT
GCATTTCGAACTGGCAAACTAGAGTGTGATAGAGGGTGGTAGAATTTCAGGTGTAGCGGTGAA
ATGCGTAGAGATCTGAAGGAATACCGATGGCGAACGCAGCCACCTGGGTCAACACTGACGCTC
ATGTACGAAAGCGTGGGGAGCAAACAGGATTAGATACCCTGGTAGTCCACGCCGTACACGATG
TCTACTAGAAGCTCAGAACCTCGGTTCTGTTTTTCAAGCTAACGCATTAAGTAGACCGCCTGG
GGAGTACGGCCGCAAGGTTAAAACTCAAATGAATTGACGGGGGCCCGCACAAGCGGTGGAGCA
TGTGGTTTAATTCGATGCAACGCGAAGAACCTTACCTACACTTGACATACAGAGAACTTACCA
GAGATGGTTTGGTGCCTTCGGGAACTCTGATACAGGTGCTGCATGGCTGTCGTCAGCTCGTGT
TGTGAGATGTTGGGTTAAGTCCCGCAACGAGCGCAACCCCTATCCTTAGTTGCTAGCAGGTAA
TGCTGAGAACTCTAAGGAGACTGCCGGTGATAAACCGGAGGAAGGTGGGGACGACGTCAAGTC
ATCATGGCCCTTACGTGTAGGGCTACACACGTGCTACAATGGCGCATACAGAGTGCTGCGAAC
TCGCGAGAGTAAGCGAATCACTTAAAGTGCGTCGTAGTCCGGATTGGAGTCTGCAACTCGACT
CCATGAAGTCGGAATCGCTAGTAATCGCGTATCAGAATGACGCGGTGAATACGTTCCCGGGCC
TTGTACACACCGCCCGTCACACCATGGGAGTGGGTTGCTCCAGAAGTAGATAGTCTAACCCTC
GGGAGGACGTTTACCACGGAGTGATTCATGACTGGGGTGAAGTCGAACAAGG

> **JX429803; *Cobetia marina*, ^{GU}SS263-29** (1305nt)

GCTTACCATGCAAGTCGAGCGGAAACGATTCTAGCTTGCTAGAAGGCGTCGAGCGGCGGACGG
GTGAGTAATGCATGGGAATCTGCCCGATAGTGGGGGACAACCTGGGGAAACTCAGGCTAATAC
CGCATACGTCCTACGGGAGAAAGCAGGGGATCTTCGGACCTTGCGCTATCGGATGAGCCCATG
TCGGATTAGCTTGTTGGTGAGGTAACGGCTCACCAAAGCGACGATCCGTAGCTGGTCTGAGAG
GATGATCAGCCACACTGGGACTGAGACACGGCCCAGACTCCTACGGGAGGCAGCAGTGGGGAA
TATTGGACAATGGGCGAAAGCCTGATCCAGCCATGCCGCGTGTGTGAAGAAGGCCTTCGGGTT
GTAAAGCACTTTCAGCGAGGAAGAACGCCTCGGGATTAATACTCCCGAGGAAAGACATCACTC
GCAGAAGAAGCACCGGCTAACTCCGTGCCAGCAGCCGCGGTAATACGGAGGGTGCAAGCGTTA
ATCGGAATTACTGGGCGTAAAGCGCGCGTAGGTGGCTAAGTCAGCCAGGTGTGAAAGCCCCGG
GCTCAACCTGGGAACGGCATCTGGAACTGCTTGGCTAGAGTGCAGGAGAGGAAGGTAGAATTC

CCGGTGTAGCGGTGAAATGCGTAGAGATCGGGAGGAATACCAGTGGCGAAGGCGGCCTTCTGG
ACTGACACTGACACTGAGGTGCGAAAGCGTGGGTAGCAAACAGGATTAGATACCCTGGTAGTC
CACGCCGTAAACGATGTCAACTAGCCGTTGGGTCCCTTGAGGACTTAGTGGCGCAGCTAACGC
AATAAGTTGACCGCCTGGGGAGTACGGCCGCAAGGTTAAAACTCAAATGAATTGACGGGGGCC
CGCACAAGCGGTGGAGCATGTGGTTTAATTCGATGCAACGCGAAGAACCTTACCTACCCTTGA
CATCCAGAGGACTTTCCAGAGATGGATTGGTGCCTTCGGGAACTCTGAGACAGGTGCTGCATG
GCTGTCGTCAGCTCGTGTTGTGAAATGTTGGGTTAAGTCCCGTAACGAGCGCAACCCCTATCC
TTATTTGCCAGCGAGTAATGTCGGGAACTCTAAGGAGACTGCCGGTGACAAACCGGAGGAAGG
TGGGGACGACGTCAAGTCATCATGGCCCTTACGGGTAGGGCTACACACGTGCTACAATGGCAA
GTACAAAGGGTTGCAATACGGCGACGTGGAGCCAATCCCATAAAGCTTGCCTCAGTCCGGATT
GGAGTCTGCAACTCGACTCCATGAAGTCGGAATCGCTAGTAATCG

> JX429802; *Halomonas venusta*, GUSS263-30 (1430nt)

TGCAAGTCGAGCGGTAACAGGGGTAGCTTGCTACCCGCTGACGAGCGGCGGACGGGTGAGTAA
TGCATAGGAATCTGCCCGATAGTGGGGGATAACCTGGGGAAACCCAGGCTAATACCGCATACG
TCCTACGGGAGAAAGGGGGCTCCGGCTCCCGCTATTGGATGAGCCTATGTCGGATTAACTAGT
TGGTGAGGTAAAGGCTCACCAAGGCGACGATCCGTAGCTGGTCTGAGAGGATGATCAGCCACA
TCGGGACTGAGACACGGCCCGAACTCCTACGGGAGGCAGCAGTGGGGAATATTGGACAATGGG
CGAAAGCCTGATCCAGCCATGCCGCGTGTGTGAAGAAGGCCCTCGGGTTGTAAAGCACTTTCA
GCGAGGAAGAACGCCTAGTGGTTAATACCCATTAGGAAAGACATCACTCGCAGAAGAAGCACC
GGCTAACTCCGTGCCAGCAGCCGCGGTAATACGGAGGGTGCAAGCGTTAATCGGAATTACTGG
GCGTAAAGCGCGCGTAGGTGGCTTGATAAGCCGGTTGTGAAAGCCCCGGGCTCAACCTGGGAA
CGGCATCCGGAACTGTCAAGCTAGAGTGCAGGAGAGGAAGGTAGAATTCCCGGTGTAGCGGTG
AAATGCGTAGAGATCGGGAGGAATACCAGTGGCGAAGGCGGCCTTCTGGACTGACACTGACAC
TGAGGTGCGAAAGCGTGGGTAGCAAACAGGATTAGATACCCTGGTAGTCCACGCCGTAAACGA
TGTCGACCAGCCGTTGGGTGCCTAGCGCACTTTGTGGCGAAGTTAACGCGATAAGTCGACCGC
CTGGGGAGTACGGCCGCAAGGTTAAAACTCAAATGAATTGACGGGGGCCCGCACAAGCGGTGG
AGCATGTGGTTTAATTCGATGCAACGCGAAGAACCTTACCTACTCTTGACATCCTGCGAACTT
GGTGCCTTCGGGAACGCAGAGACAGGTGCTGCATGGCTGTCGTCAGCTCGTGTTGTGAAATGT
TGGGTTAAGTCCCGTAACGAGCGCAACCCTTGTCCTTATTTGCCAGCGCGTAATGGCGGGAAC
TCTAAGGAGACTGCCGGTGACAAACCGGAGGAAGGTGGGGACGACGTCAAGTCATCATGGCCC
TTACGAGTAGGGCTACACACGTGCTACAATGGCCGGTACAAAGGGTTGCGAGCTCGCGAGAGT
CAGCTAATCCCGAAAAGCCGGTCTCAGTCCGGATCGGAGTCTGCAACTCGACTCCGTGAAGTC
GGAATCGCTAGTAATCGTGAATCAGAATGTCACGGTGAATACGTTCCCGGGCCTTGTACACAC
CGCCCGTCACACCATGGGAGTGGACTGCACCAGAAGTGGTTAGCTTAACCTTCGGGAAAGCGA
TCACCACGGTGTGGTTCATGACTGGGGTGAAGTCGTAACAAGGT

> JX429801; *Shewanella* sp., GUSS263-33 (630nt)

AGGCCTATCACATGCAAGTCGAGCGGTAACATTTCAAAAGCTTGCTTTTGAAGATGACGAGCG
GCGGACGGGTGAGTAATGCCTGGGAATTTGCCCATTTGTGGGGGATAACAGTTGGAAACGACT
GCTAATACCGCATACGCCCTACGGGGGAAAGCAGGGGACCTTCGGGCCTTGCGCTGATGGATA
AGCCCAGGTGGGATTAGCTAGTAGGTGAGGTAAAGGCTCACCTAGGCGACGATCCCTAGCTGG
TCTGAGAGGATGATCAGCCACACTGGGACTGAGACACGGCCCAGACTCCTACGGGAGGCAGCA
GTGGGGAATATTGCACAATGGGGGAAACCCTGATGCAGCCATGCCGCGTGTGTGAAGAAGGCC
TTCGGGTTGTAAAGCACTTTCAGCGAGGAGGAAAGGGTGTAAGTTAATACCTTACATCTGTGA
CGTTACTCGCAGAAGAAGCACCGGCTAACTCCGTGCCAGCAGCCGCGGTAATACGGAGGGTGC
GAGCGTTAATCGGAATTACTGGGCGTAAAGCGTGCGCAGGCGGTTTGTTAAGCGAGATGTGAA
AGCCCCGGGCTCAACCTGGGAACCGCATTTCGAACTGGCAAACTAGAGTCTTGTAGAGGGGGG

> JX429800; *Psychrobacter* sp., GUSS263-36 (613nt)

AGGCCTATCACGTGCAAGTCGAGCGGAAACGATGGGAGCTTGCTCCCAGGCGTCGAGCGGCGG
ACGGGTGAGTAACACTTAGGAATCTACCTAGTAGTGGGGGATAGCTCGGGGAAACTCGAATTA
ATACCGCATACGTCCTACGGGAGAAAGGGGGCAGTTTACTGCTCTCGCTATTAGATGAGCCTA
AGTCGGATTAGCTAGATGGTGGGGTAAAGGCCTACCATGGCGACGATCTGTAGCTGGTCTGAG
AGGATGATCAGCCACACCGGGACTGAGACACGGCCCGGACTCCTACGGGAGGCAGCAGTGGGG
AATATTGGACAATGGGGGGAACCCTGATCCAGCCATGCCGCGTGTGTGAAGAAGGCCTTTTGG

TTGTAAAGCACTTTAAGCAGTGAAGAAGACCTAACGGTTAATACCCGTTAGCGATGACATTAG
CTGCAGAATAAGCACCGGCTAACTCTGTGCCAGCAGCCGCGGTAATACAGAGGGTGCAAGCGT
TAATCGGAATTACTGGGCGTAAAGCGAGCGTAGGGGGCTTGATAAGTCAGATGTGAAATCCCC
GGGCGTAACCTGGGAACTGCATCTGATACTGTTAAGCTAGAGTAGG

> **JX429799; *Vibrio campbelli*, ^{GU}SS263-31** (430nt)

ACGCTGGCGGCAGGCCTAACACATGCAAGTCGAGCGGAAACGAGTTATCTGAACCTTCGGGGA
ACGATAACGGCGTCGAGCGGCGGACGGGTGAGTAATGCCTAGGAAATTGCCCTGATGTGGGGG
ATAACCATTGGAAACGATGGCTAATACCGCATGATGCCTACGGGCCAAAGAGGGGGACCTTCG
GGCCTCTCGCGTCAGGATATGCCTAGGTGGGATTAGCTAGTTGGTGAGGTAAGGGCTCACCAA
GGCGACGATCCCTAGCTGGTCTGAGAGGATGATCAGCCACACTGGAACTGAGACACGGTCCAG
ACTCCTACGGGAGGCAGCAGTGGGGAATATTGCACAATGGGCGCAAGCCTGATGCAGCCATGC
CGCGTGTGTGAAGAAGGCCTTCGGGTTGTAAAGCACTTTCAGTCGTGAGGAA

> **JX429798; *Halomonas meridiana*, ^{GU}SS263-38** (1374nt)

ACCATGCAAGTCGAGCGGTAACAGATCCAGCTTGCTGGATGCTGACGAGCGGCGGACGGGTGA
GTAATGCATAGGAATCTGCCCGATAGTGGGGGATAACCTGGGGAAACCCAGGCTAATACCGCA
TACGTCCTACGGGAGAAAGGGGGCTCCGGCTCCCGCTATGGGATGAGCCTATGTCGGATTAGC
TAGTTGGTGAGGTAACGGCTCACCAAGGCCACGATCCGTAGCTGGTCTGAGAGGATGATCAGC
CACATCGGGACTGAGACACGGCCCGAACTCCTACGGGAGGCAGCAGTGGGGAATATTGGACAA
TGGGGGCAACCCTGATCCAGCCATGCCGCGTGTGTGAAGAAGGCCCTCGGGTTGTAAAGCACT
TTCAGCGAGGAAGAACGCCTAGCGGTTAATACCCGCTAGGAAAGACATCACTCGCAGAAGAAG
CACCGGCTAACTCCGTGCCAGCAGCCGCGGTAATACGGAGGGTGCAAGCGTTAATCGGAATTA
CTGGGCGTAAAGCGCGCGTAGGTGGCTTGATAAGCCGGTTGTGAAAGCCCCGGGCTCAACCTG
GGAACGGCATCCGGAACTGTCAAGCTAGAGTGCAGGAGAGGAAGGTAGAATTCCCGGTGTAGC
GGTGAAATGCGTAGAGATCGGGAGGAATACCAGTGGCGAAGGCGGCCTTCTGGACTGACACTG
ACACTGAGGTGCGAAAGCGTGGGTAGCAAACAGGATTAGATACCCTGGTAGTACACGCCGTAA
ACGATGTCGACCAGCCGTTGGGTGCCTAGCGCACTTTGTGGCGAAGTTAACGCGATAAGTCGA
CCGCCTGGGGAGTACGGCCGCAAGGTTAAAACTCAAATGAATTGACGGGGGCCCGCACAAGCG
GTGGAGCATGTGGTTTAATTCGATGCAACGCGAAGAACCTTACCTACTCTTGACATCCTGCGA
ATTTGGTAGAGATACCTTAGTGCCTTCGGGAACGCAGAGACAGGTGCTGCATGGCTGTCGTCA
GCTCGTGTTGTGAAATGTTGGGTTAAGTCCCGTAACGAGCGCAACCCTTGTCCTTATTTGCCA
GCGTGTAATGGCGGGAACTCTAAGGAGACTGCCGGTGACAAACCGGAGGAAGGTGGGGACGAC
GTCAAGTCATCATGGCCCTTACGAGTAGGGCTACACACGTGCTACAATGGTCGGTACAAAGGG
TTGCCAACTCGCGAGAGTGAGCCAATCCCGAAAAGCCGATCTCAGTCCGGATCGGAGTCTGCA
ACTCGACTCCGTGAAGTCGGAATCGCTAGTAATCGTGGATCAGAATGCCACGGTGAATACGTT
CCCGGGCCTTGTACACACCGCCCGTCACACCATGGGAGTGGACTGCACCAG

> **JX429797; *Shewanella haliotis*, ^{GU}SS263-N4** (1456nt)

ACATGCAAGTCGAGCGGTAACATTTCAAAAGCTTGCTTTTGAAGATGACGAGCGGCGGACGGG
TGAGTAATGCCTGGGAATTTGCCCATTTGTGGGGGATAACAGTTGGAAACGACTGCTAATACC
GCATACGCCCTACGGGGGAAAGCAGGGGACCTTCGGGCCTTGCGCTGATGGATAAGCCCAGGT
GGGATTAGCTAGTAGGTGAGGTAAAGGCTCACCTAGGCGACGATCCCTAGCTGGTCTGAGAGG
ATGATCAGCCACACTGGGACTGAGACACGGCCCAGACTCCTACGGGAGGCAGCAGTGGGGAAT
ATTGCACAATGGGGGAAACCCTGATGCAGCCATGCCGCGTGTGTGAAGAAGGCCTTCGGGTTG
TAAAGCACTTTCAGCGAGGAGGAAAGGGTGTAAGTTAATACCTTACATCTGTGACGTTACTCG
CAGAAGAAGCACCGGCTAACTCCGTGCCAGCAGCCGCGGTAATACGGAGGGTGCGAGCGTTAA
TCGGAATTACTGGGCGTAAAGCGTGCGCAGGCGGTTTGTTAAGCGAGATGTGAAAGCCCCGGG
CTCAACCTGGGAACCGCATTTCGAACTGGCAAACTAGAGTCTTGTAGAGGGGGGTAGAATTCC
AGGTGTAGCGGTGAAATGCGTAGAGATCTGGAGGAATACCGGTGGCGAAGGCGGCCCCCTGGA
CAAAGACTGACGCTCAGGCACGAAAGCGTGGGGAGCAAACAGGATTAGATACCCTGGTAGTCC
ACGCCGTAAACGATGTCTACTCGGAGTTTGGTGTCTTGAACACTGGGCTCTCAAGCTAACGCA
TTAAGTAGACCGCCTGGGGAGTACGGCCGCAAGGTTAAAACTCAAATGAATTGACGGGGGCCC
GCACAAGCGGTGGAGCATGTGGTTTAATTCGATGCAACGCGAAGAACCTTACCTACTCTTGAC
ATCCACAGAATCTGGTAGAGATACCTCAGTGCCTTCGGGAACTGTGAGACAGGTGCTGCATGG
CTGTCGTCAGCTCGTGTTGTGAAATGTTGGGTTAAGTCCCGCAACGAGCGCAACCCCTATCCT

TACTTGCCAGCGGGTAATGCCGGGAACTTTAGGGAGACTGCCGGTGATAAACCGGAGGAAGGT
GGGGACGACGTCAAGTCATCATGGCCCTTACGAGTAGGGCTACACACGTGCTACAATGGTCAG
TACAGAGGGTTGCGAAGCCGCGAGGTGGAGCTAATCCCATAAAGCTGGTCGTAGTCCGGATTG
GAGTCTGCAACTCGACTCCATGAAGTCGGAATCGCTAGTAATCGTGGATCAGAATGCCACGGT
GAATACGTTCCCGGGCCTTGTACACACCGCCCGTCACACCATGGGAGTGGGCTGCACCAGAAG
TAGATAGCTTAACCTTCGGGAGGGCGTTTACCACGGTGTGGTTCATGACTGGGGTGAAGTCGT
AACAAGG

> **JX429796; *Cobetia marina*, ^{GU}SS263-N5** (1413nt)

ACACATGCAAGTCGAGCGGAACGATTCTAGCTTGCTAGAAGGCGTCGAGCGGCGGACGGGTGA
GTAATGCATGGGAATCTGCCCGATAGTGGGGGACAACCTGGGGAAACTCAGGCTAATACCGCA
TACGTCCTACGGGAGAAAGCAGGGGATCTTCGGACCTTGCGCTATCGGATGAGCCCATGTCGG
ATTAGCTTGTTGGTGAGGTAACGGCTCACCAAGGCGACGATCCGTAGCTGGTCTGAGAGGATG
ATCAGCCACACTGGGACTGAGACACGGCCCAGACTCCTACGGGAGGCAGCAGTGGGGAATATT
GGACAATGGGCGAAAGCCTGATCCAGCCATGCCGCGTGTGTGAAGAAGGCCTTCGGGTTGTAA
AGCACTTTCAGCGAGGAAGAACGCCTCGGGATTAATACTTCCGAGGAAAGACATCACTCGCAG
AAGAAGCACCGGCTAACTCCGTGCCAGCAGCCGCGGTAATACGGAGGGTGCAAGCGTTAATCG
GAATTACTGGGCGTAAAGCGCGCGTAGGTGGCTAAGTCAGCCAGGTGTGAAAGCCCCGGGCTC
AACCTGGGAACGGCATCTGGAACTGCTTGGCTAGAGTGCAGGAGAGGAAGGTAGAATTCCCGG
TGTAGCGGTGAAATGCGTAGAGATCGGGAGGAATACCAGTGGCGAAGGCGGCCTTCTGGACTG
ACACTGACACTGAGGTGCGAAAGCGTGGGTAGCAAACAGGATTAGATACCCTGGTAGTCCACG
CCGTAAACGATGTCAACTAGCCGTTGGGTCCCTTGAGGACTTAGTGGCGCAGCTAACGCAATA
AGTTGACCGCCTGGGGAGTACGGCCGCAAGGTTAAAACTCAAATGAATTGACGGGGGCCCGCA
CAAGCGGTGGAGCATGTGGTTTAATTCGATGCAACGCGAAGAACCTTACCTACCCTTGACATC
CAGAGGACTTTCCAGAGATGGATTGGTGCCTTCGGGAACTCTGAGACAGGTGCTGCATGGCTG
TCGTCAGCTCGTGTTGTGAAATGTTGGGTTAAGTCCCGTAACGAGCGCAACCCCTATCCTTAT
TTGCCAGCGAGTAATGTCGGGAACTCTAAGGAGACTGCCGGTGACAAACCGGAGGAAGGTGGG
GACGACGTCAAGTCATCATGGCCCTTACGGGTAGGGCTACACACGTGCTACAATGGCAAGTAC
AAAGGGTTGCAATACGGCGACGTGGAGCCAATCCCATAAAGCTTGCCTCAGTCCGGATTGGAG
TCTGCAACTCGACTCCATGAAGTCGGAATCGCTAGTAATCGTGGATCAGAATGCCACGGTGAA
TACGTTCCCGGGCCTTGTACACACCGCCCGTCACACCATGGGAGTGGACTGCACCAGAAGTGG
TTAGCCTAACCTTCGGGAGGGCGATCA

> **JX429795; *Shewanella* sp., ^{GU}SS263-28A** (692nt)

ACATGCTGGTCGAGCGGTAACATTTCAAAAGCTTGCTTTTGAAGATGACGAGCGGCGGACGGG
TGAGTAATGCCTGGGAATTTGCCCATTTGTGGGGGATAACAGTTGGAAACGACTGCTAATACC
GCATACGCCCTACGGGGGAAAGCAGGGGACCTTCGGGCCTTGCGCTGATGGATAAGCCCAGGT
GGGATTAGCTAGTAGGTGAGGTAAAGGCTCACCTAGGCGACGATCCCTAGCTGGTCTGAGAGG
ATGATCAGCCACACTGGGACTGAGACACGGCCCAGACTCCTACGGGAGGCAGCAGTGGGGAAT
ATTGCACAATGGGGGAAACCCTGATGCAGCCATGCCGCGTGTGTGAAGAAGGCCTTCGGGTTG
TAAAGCACTTTCAGCGAGGAGGAAAGGGTGTAAGTTAATACCTTACATCTGTGACGTTACTCG
CAGAAGAAGCACCGGCTAACTCCGTGCCAGCAGCCGCGGTAATACGGAGGGTGCGAGCGTTAA
TCGGAATTACTGGGCGTAAAGCGTGCGCAGGCGGTTTGTTAAGCGAGATGTGAAAGCCCCGGG
CTCAACCTGGGAACCGCATTTCGAACTGGCAAACTAGAGTCTTGTAGAGGGGGGTAGAATTCC
AGGTGTAGCGGTGAAATGCGTAGAGATCTGGAGGAATACCGGTGGCGAACGCGGCCCCCTGG

> **JX429794; *Halomonas axialensis*, ^{GU}SS263-24** (409nt)

GCAGGCCTAACACATGCAAGTCGAGCCGTAACAGATCCAGCTTGCTGGATGCTGACGAGCGGC
GGACGGGTGAGTAATGCATAGGAATCTGCCCGATAGTGGGGGATAACCTGGGGAAACCCAGGC
TAATACCGCATACGTCCTACGGGAGAAAGGGGGCTCCGGCTCCCGCTATGGGATGAGCCTATG
TCGGATTAGCTAGTTGGTGAGGTAACGGCTCACCAAGGCGACGATCCGTAGCTGGACTGAGAG
GATGATCAGCCACATCGGGACTGAGACACGGCCCGAACTCCTACGGGAGGCAGCAGTGGGGAA
TATTGGACAATGGGGGAAACCCTGATCCAGCCATGCCGCGTGTGTGAAGAAGGCCCTCGGGTT
GTAAAGCACTTTCAGCGAGGAAGAACGCCTA

> **JX429793; *Shewanella* sp., ^{GU}SS263-2** (645nt)

GGCGGCAGGCCTATCACATGCAGGTCGAGCGGTAACATTTCAAAAGCTTGCTTTTGAAGATGA
CGAGCGGCGGACGGGTGAGTAATGCCTGGGAATTTGCCCATTTGTGGGGGATAACAGTTGGAA
ACGACTGCTAATACCGCATACGCCCTACGGGGGAAAGCAGGGGACCTTCGGGCCTTGCGCTGA
TGGATAAGCCCAGGTGGGATTAGCTAGTAGGTGAGGTAAAGGCTCACCTAGGCGACGATCCCT
AGCTGGTCTGAGAGGATGATCAGCCACACTGGGACTGAGACACGGCCCAGACTCCTACGGGAG
GCAGCAGTGGGGAATATTGCACAATGGGGGAAACCCTGATGCAGCCATGCCGCGTGTGTGAAG
AAGGCCTTCGGGTTGTAAAGCACTTTCAGCGAGGAGGAAAGGGTGTAAGTTAATACCTTACAT
CTGTGACGTTACTCGCAGAAGAAGCACCGGCTAACTCCGTGCCAGCAGCCGCGGTAATACGGA
GGGTGCGAGCGTTAATCGGAATTACTGGGCGTAAAGCGTGCGCAGGCGGTTTGTTAAGCGAGA
TGTGAAAGCCCCGGGCTCAACCTGGGAACCGCATTTCGAACTGGCAAACTAGAGTCTTGTAGA
GGGGGGTAGAATTCC

> **JX429792; *Ochrobactrum* sp., ^{GU}SS263-38A** (305nt)

CGACGCTGGCGGCAGGCTTAACACATGCAAGTCGAGCGCCCCGCAAGGGGAGCGGCAGACGGG
TGAGTAACGCGTGGGAACGTACCTTTTGCTACGGAATAACTCAGGGAAACTTGTGCTAATACC
GTATGTGCCCTTCGGGGGAAAGATTTATCGGCAAAGGATCGGCCCGCGTTGGATTAGCTAGTT
GGTGAGGTAAAGGCTCACCAAGGCGACGATCCATAGCTGGTCTGAGAGGATGATCAGCCACAC
TGGGACTGAGACACGGCCCAGACTCCTACGGGAGGCAGCAGTGGGGAATATTG

C. List of 16SrDNA sequences of *T eryathraeum* bloom associated bacterial flora:

[>Gen Bank Accession; Identity, strain designation (Length of sequence: 5 - 3)]

>KF495537; *Bacillus* sp., ^{GUFB}Sama06-1 (466nt)

CATGCAAGTCGAGCGAATGGATTAAGAGCTTGCTCTTATGAAGTTAGCGGCGGACGGGTGAGT
AACACGTGGGTAACCTGCCCATAAGACTGGGATAACTCCGGGAAACCGGGGCTAATACCGGAT
AACATTTTGAACCGCATGGTTCGAAATTGAAAGGCGGCTTCGGCTGTCACTTATGGATGGACC
CGCGTCGCATTAGCTAGTTGGTGAGGTAACGGCTCACCAAGGCAACGATGCGTAGCCGACCTG
AGAGGGTGATCGGCCACACTGGGACTGAGACACGGCCCAGACTCCTACGGGAGGCAGCAGTAG
GGAATCTTCCGCAATGGACGAAAGTCTGACGGAGCAACGCCGCGTGAGTGATGAAGGCTTTCG
GGTCGTAAAACTCTGTTGTTAGGGAAGAACAAGTGCTAGTTGAATAAGCTGGCACCTTGACGG
TACCTAACCAGAAAGCCACGGCTAA

> KF495538; *Virgibacillus* sp., ^{GUFB}Sama06-2 (442nt)

TGTGCGGCGTGCCTATTACATGCAAGTCGAGCGCGGGAAGCAAGCAGATCTCCTTCGGGAGTG
ACGCTTGTGGAACGAGCGGCGGACGGGTGAGTAACACGTGGGCAACCTACCTGTAAGACTGGG
ATAACTCCGGGAAACCGGGGCTAATACCGGATGAAACAAAGCGTCGCATGACGCAATGTTAAA
AGGCGGCATATGCTGTCACTTACAGATGGGCCCGCGGCGCATTAGCTAGTTGGTGAGGTAAAG
GCTCACCAAGGCAACGATGCGTAGCCGACCTGAGAGGGTGATCGGCCACACTGGGACTGAGAC
ACGGCCCAGACTCCTACGGGAGGCAGCAGTAGGGAATCTTCCGCAATGGACGAAAGTCTGACG
GAGCAACGCCGCGTGAGTGATGAAGGTTTTCGGATCGTAAAACTCTGTTGTTAGGGAAGAACA
G

> KF495539; Unclassified Halomonadaceae, ^{GUFB}Sama06-3 (481nt)

GGCCTACCTTTGCAGTCGAGCGGTAACAGGTCCGGCTTGCTGGATGCTGACGAGCGGCGGACG
GGTGAGTAATGCATAGGAATCTGCCCGATAGTGGGGGATAACCTGGGGAAACCCAGGCTAATA
CCGCAGACGTCCTACGGGAGAAAGGGGGCTCCGGCTCCCGCTATGGGATGAGCCTATGTCGGA
TTAACTATTTGGGGAGGCAACGGCTCTTCTCGGCCACGATCCGTATCTGGTCTGATAGGATGA
TCAGCCACATCGGGACTGACACACGGCCCGAACTCCTACGGCAGGTTACAGTGGGGAATATTG
GACAATGGGGGAAACCCTGATCCAGCCATGCCGCGTGTGTGAAGAAGGCCCTCGGGTTGTAAA
GCACTTTCAGCGAGGGAGAACGCCTAGCGGTTAATACCCGCTAGGAAAGACATCACTCGCAAA
AGAAGCACGGGCTAACTCCGTGGCAGCAGCCGAGGTAATA

> KF495540; *Corynebacterium maris*, ^{GUFB}Sama06-4 (512nt)

TGAACGCTGGCGGCGTGCTTAACACATGCAAGTCGAACGGAAAGGCCCCTGCTTGCAGGGGTA
CTCGAGTGGCGAACGGGTGAGTAACACGTGGGTGATCTACCCCGCACTTCGGGGTAACCCCGG
GAAACTGGGTCTAATACCGGATATTCACGCCCCTTTTGTGTGGGGTGTGGAAAGATTTATCGG
TGTGGGATGAGCTTGCGGCCTATCAGCTTGTTGGTGGGGTAATGGCCTACCAAGGCGTCGACG
GGTAGCCGGCCTGAGAGGGTGTACGGCCACATTGGGACTGAGATACGGCCCAGACTCCTACGG
GAGGCAGCAGTGGGGAATATTGCACAATGGGCGCAAGCCTGATGCAGCGACGCCGCGTGGGGG
ATGACGGCCTTCGGGTTGTAAACTCCTTTCGCCCACGACGAAGCCCTTCGGGGTGACGGTAGT
GGGATAAGAAGCACCGGCTAACTACGTGCCAGCAGCCGCGGTAATACGTAGGGTGCGAGCGTT
GTCCGGAA

> KF495541; *Corynebacterium maris*, ^{GUFB}Sama06-5 (504nt)

GATGAACGCTGGCGGCGTGCTTAACACATGCAAGTCGAACGGAAAGGCCCCTGCTTGCAGGGG
TACTCGAGTGGCGAACGGGTGAGTAACACGTGGGTGATCTACCCCGCACTTCGGGGTAACCCC
GGGAAACTGGGTCTAATACCGGATATTCACGCCCCTTTTGTGTGGGGTGTGGAAAGATTTATC
GGTGTGGGATGAGCTTGCGGCCTATCAGCTTGTTGGTGGGGTAATGGCCTACCAAGGCGTCGA
CGGGTAGCCGGCCTGAGAGGGTGTACGGCCACATTGGGACTGAGATACGGCCCAGACTCCTAC
GGGAGGCAGCAGTGGGGAATATTGCACAATGGGCGCAAGCCTGATGCAGCGACGCCGCGTGGG

GGATGACGGCCTTCGGGTTGTAAACTCCTTTCGCCCACGACGAAGCCCTTCGGGGTGACGGTA
GTGGGATAAGAAGCACCGGCTAACTACGTGCCAGCAGCCGCGGTAATACGTAGGGTGCGAGCG

>KF495542; *Bacillus flexus,* ^{GUFB}Sama06-6 (524nt)

TGGCGGCGTGCCTATTACATGCAAGTCGAGCGAACTGATTAGAAGCTTGCTTCTATGACGTTA
GCGGCGGACGGGTGAGTAACACGTGGGCAACCTGCCTGTAAGACTGGGATAACTCCGGGAAAC
CGGAGCTAATACCGGATAACATTTTTTCTTGCATAAGAGAAAATTGAAAGATGGTTTCGGCTA
TCACTTACAGATGGGCCCGCGGTGCATTAGCTAGTTGGTGAGGTAACGGCTCACCAAGGCAAC
GATGCATAGCCGACCTGAGAGGGTGATCGGCCACACTGGGACTGAGACACGGCCCAGACTCCT
ACGGGAGGCAGCAGTAGGGAATCTTCCGCAATGGACGAAAGTCTGACGGAGCAACGCCGCGTG
AGTGATGAAGGCTTTCGGGTCGTAAAACTCTGTTGTTAGGGAAGAACAAGTACAAGAGTAACT
GCTTGTACCTTGACGGTACCTAACCAGAAAGCCACGGCTAACTACGTGCCAGCAGCCGCGGTA
ATACGTAGGTGGCAAGCGTT

>KF495543; *Bacillus* sp., ^{GUFB}Sama06-7 (616nt)

GAGTTTGATCCTGGCTCAGGACGAACGCTGGCGGCGTGCCTAATACATGCAAGTCGAGCGGAC
AGACGGGAGCTTGCTCCCTGAAGTCAGCGGCGGGCGGGTGAGTAACACGTGGGCAACCTGCCT
GTAAGACTGGGATAACTCCGGGAAACCGGGGCTAATACCGGATAATTCTTTCCCTCACATGAG
GGAAAGCTGAAAGATGGTTTCGGCTATCACTTACAGATGGGCCCGCGGCGCATTAGCTAGTTG
GTGAGGTAACGGCTCACCAAGGCAACGATGCGTAGCCGACCTGAGAGGGTGATCGGCCACACT
GGGACTGAGACACGGCCCAGACTCCTACGGGAGGCAGCAGTAGGGAATCTTCCGCAATGGACG
AAAGTCTGACGGAGCAACGCCGCGTGAGTGATGAAGGTTTCCGGATCGTAAAACTCTGTTGTT
AGGGAAGAACAAGTACCGGAGTAACTGCCGGTACCTTGACGGTACCTAACCAGAAAGCCACGG
CTACTACGTGCCAGCAGCCGCGGTAATACGTAGGTGGCAAGCGTTGTCCGGAATTATTGGGCG
TAAAGCGCGCGCAGGCGGTTCCTTAAGTCTGATGTGAAAGCCCCCGGCT

>KF495544; *Leucobacter komagatae,* ^{GUFB}Sama06-8 (459nt)

TGGCGGCGTGCTTAACACATGCAAGTCGAACGATGAAGCCCAGCTTGCTGGGTGGAAGAGTGG
CGAACGGGTGAGTAACACGTGAGTAACCTGCCCTGAACTCTGGGATAAGCACTGGAAACGGTG
TCTAATACTGGATACGACCTATCACCGCATGGTGTGTGGGTGGAAAGATTTATCGGTTCTGGA
TGGACTCGCGGCCTATCAGCTAGATGGTGAGGTAATGGCTCACCATGGCGACGACGGGTAGCC
GGCCTGAGAGGGTGACCGGCCACACTGGGACTGAGACACGGCCCAGACTCCTACGGGAGGCAG
CAGTGGGGAATATTGCACAATGGGCGCAAGCCTGATGCAGCAACGCCGCGTGAGGGATGACGG
CCTTCGGGTTGTAAACCTCTTTTAGTAGGGAAGAAGCGAAAGTGACGGTACCTGCAGAAAAAG
CACCGGCTAACTACGTGC

>KF495545; *Bacillus* sp., ^{GUFB}Sama06-9 (409nt)

CGGCGTGCCTATTACATGCAAGTCGAGCGAATGGATTAAGAGCTTGCTCTTATGAAGTTAGCG
GCGGACGGGTGAGTAACACGTGGGTAACCTGCCCATAAGACTGGGATAACTCCGGGAAACCGG
GGCTAATACCGGATAACATTTTGAACCGCATGGTTCGAAATTGAAAGGCGGCTTCGGCTGTCA
CTTATGGATGGACCCGCGTCGCATTAGCTAGTTGGTGAGGTAACGGCTCACCAAGGCAACGAT
GCGTAGCCGACCTGAGAGGGTGATCGGCCACACTGGGACTGAGACACGGCCCAGACTCCTACG
GGAGGCAGCAGTAGGGAATCTTCCGCAATGGACAGAAGTCTGACGGAGCAACGCCGCGTGAGT
GATGAAGGCTTTCGGGGCGGAAAAGTCTGTT

>KF495546; *Corynebacterium* sp., ^{GUFB}Sama06-10 (496nt)

TGAACGCTGGCGGCGTGCTTAACACATGCAAGTCGAACGGAAAGGCCCCTGCTTGCAGGGGTA
CTCGAGTGGCGAACGGGTGAGTAACACGTGGGTGATCTACCCCGCACTTCGGGGTAACCCCGG
GAAACTGGGTCTAATACCGGATATTCACGCCCCTTTTGTGTGGGGTGTGGAAAGATTTATCGG
TGTGGGATGAGCTTGCGGCCTATCAGCTTGTTGGTGGGGTAATGGCCTACCAAGGCGTCGACG
GGTAGCCGGCCTGAGAGGGTGTACGGCCACATTGGGACTGAGATACGGCCCAGACTCCTACGG
GAGGCAGCAGTGGGGAATATTGCACAATGGGCGCAAGCCTGATGCAGCGACGCCGCGTGGGGG
ATGACGGCCTTCGGGTTGTAAACTCCTTTCGCCCACGACGAAGCCCTTCGGGGTGACGGTAGT
GGGATAAGAAGCACCGGCTAACTACGTGCCAGCAGCCGCGGGAATACGTAGGGTG

> KF495547; *Virgibacillus* sp., ^{GUFB}Sama06-11 (395nt)

ACGCTGTGCGGCGTGCCTATTACATGCAAGTCGAGCGCGGGAAGCAAGCAGATCTCCTTCGGG
AGTGACGCTTGTGGAACGAGCGGCGGACGGGTGAGTAACACGTGGGCAACCTACCTGTAAGAC
TGGGATAACTCCGGGAAACCGGGGCTAATACCGGATGAAACAAAGCGTCGCATGACGCAATGT
TAAAAGGCGGCATATGCTGTCACTTACAGATGGGCCCGCGGCGCATTAGCTAGTTGGTGAGGT
AAAGGCTCACCAAGGCAACGATGCGTAGCCGACCTGAGAGGGTGATCGGCAGGCACTGGGACT
GAAACACGGCCCATACTCCTACGGGAGGCAGCAGTAGGGAATCTTCCGCAATGGACGAAGGTC
TGACGGAGCAACGCCGC

> KF495548; *Bacillus licheniformis*, ^{GUFB}Sama06-12 (507nt)

TGGAAGCTGGGGAACTTGAGTGCAGAAGAGGAGAGTGGAATTCCACGTGTAGCGGTGAAATGC
GTAGAGATGTGGAGGAACACCAGTGGCGAAGGCGACTCTCTGGTCTGTAACTGACGCTGAGGC
GCGAAAGCGTGGGGAGCGAACAGGATTAGATACCCTGGTAGTCCACGCCGTAAACGATGAGTG
CTAAGTGTTAGAGGGTTTCCGCCCTTTAGTGCTGCAGCAAACGCATTAAGCACTCCGCCTGGG
GAGTACGGTCGCAAGACTGAAACTCAAAGGAATTGACGGGGGCCCGCACAAGCGGTGGAGCAT
GTGGTTTAATTCGAAGCAACGCGAAGAACCTTACCAGGTCTTGACATCCTCTGACAACCCTAG
AGATAGGGCTTCCCCTTCGGGGGCAGAGTGACAGGTGGTGCATGGTTGTCGTCAGCTCGTGTC
GTGAGATGTTGGGTTAAGTCCCGCAACGAGCGCAACCCTTGATCTTAGTTGCCAGCATTCAGT
TAA

> KF495549; *Salinibacterium* sp., ^{GUFB}Sama06-13 (497nt)

AACACATGCAGGTCGAACGATGAAGCCGGAGCTTGCTCTGGTGGATTAGTGGCGAACGGGTGA
GTAACACGTGAGTAACCTGCCCTTGACTCTGGAATAAGCGTTGGAAACGACGTCTAATACCGG
ATACGAGCTTCCGCCGCATGGTGAGGAGCTGGAAAGAATTTCGGTCAAGGATGGACTCGCGGC
CTATCAGGTAGTTGGTGAGGTAATGGCTCACCAAGCCTACGACGGGTAGCCGGCCTGAGAGGG
TGACCGGCCACACTGGAACTGAGACACGGTCCAGACTCCTACGGGAGGCAGCAGTGGGGAATA
TTGCACAATGGGCGCAAGCCTGATGCAGCAACGCCGCGTGAGGGACGACGGCCTTCGGGTTGT
AAACCTCTTTTAGTAGGGAAGAAGCGAAAGTGACGGTACCTGCAGAAAAAGCACCGGCTAACT
ACGTGCCAGCAGCCGCGGTAATACGTAGGGTGCAAGCGTTATCCGGAATTATTGGG

> KF495550; *Microbacterium* sp., ^{GUFB}Sama06-14 (460nt)

CACGGAGCTTGCTCTGTGGGATCAGTGGCGAACGGGTGAGTAACACGTGAGCAACCTGCCCCT
GACTCTGGGATAAGCGCTGGAAACGGCGTCTAATACTGGATATGTGACGTGACCGCATGGTCT
GCGTCTGGAAAGAATTTCGGTTGGGGATGGGCTCGCGGCCTATCAGCTTGTTGGTGAGGTAAT
GGCTCACCAAGGCGTCGACGGGTAGCCGGCCTGAGAGGGTGACCGGCCACCCTGGGACTGAGA
CACGGCCCAGACTCCTACGGGAGGCAGCAGTGGGGAATATTGCACAATGGGCGCAAGCCTGAT
GCAGCAACGCCGCGTGAGGGACGACGGCCTTCGGGTTGTAAACCTCTTTTAGCAGGGAAGAAG
CGAAAGTGACGGTACCTGCAGAAAAAGCGCCGGCTAACTACGTGCCAGCAGCCGCGGTAATAC
GTAGGGCGCAAGCGTTATC

> KF495551; *Corynebacterium* sp., ^{GUFB}Sama06-15 (314nt)

GCTGGCGGCGTGCTTAACACATGCAAGTCGAACGGAAAGGCCTGCTTGCAGGGTACTCGAGTG
GCGAACGGGTGAGTAACACGTGGGTGATCTGCCCTGTACTTCGGGATAAGCTTGGGAAACTGG
GTCTAATACCGGATATTCAACTTTGTGTTGGAAAGCCTTTGGGGGGTATGGGATGAGCTTGCG
GCCTATCAGCTTGTTGGTGGGGTAATGCCCTACCAAGGCGTCGACGGGTAGCCGGCCTGAGAG
GGTGTACGGCCACATTGGGACTGAGATACGGCCCAGACTCCTACGGGAGGCAGCAGTGGGGA

> KF495552; Unclassified Bacillaceae, ^{GUFB}Sama06-16 (500nt)

ATGTTTTCTTGCGGACCGATGGTAGCTTGCTCCCTGTATTCAGCGGCGGACGGGTGAGTGCTC
GTGGGCAACCTGCCTGTCGACTGGGATAACTCCGGGAAACCGGCCTTAATACCGGAAAATTCT
TTCCCTCACATGAGGGACCCCGTTTGATGGTTTCGGCTATCACTTACAGATGGGCCCGCGGCG
CATTAGTTTTTTGGTGAGGTAACGGCTCACCAAGGTTGCGATGCTCCCCCGACCTGATAGGGT
GATCGGCCACACTGGGACTGAGACACGGCCCATACTCCTACGGGAGGCAGCAGTAGGGAATCT
TCCGCAATGGACGAAAGTCTGACGGAGCAACGCCGCGTGAGTGATGAAGGTTTTCGGATCGTA

AAACTCTGTTGTTAGGGAAGAACACGTACCGGAGTAACTGCCGGTACCTTGACGCTACCTACT
CCCAATTCCTGGGCTAACTACTCGCCAGCACCAGCGGTATGACGTAGGTGGCAATTCGT

>KF495553; *Microbacterium* sp., ^{GUFB}Sama06-17 (385nt)

AACACGGAGCTTGCTCTGTGGGATCAGTGGCGAACGGGTGAGTAACACGTGAGCAACCTGCCC
CTGACTCTGGGATAAGCGCTGGAAACGGCGTCTAATACTGGATATGTGACGTGACCGCATGGT
CTGCGTCTGGAAAGAATTTCGGTTGGGGATGGGCTCGCGGCCTATCAGCTTGTTGGTGAGGTA
ATGGCTCACCAAGGCGTCGACGGGTAGCCGGCCTGAGAGGGTGACCGGCCACACTGGGACTGA
GACACGGCCCAGACTCCTACGGGAGGCAGCAGTGGGGAATATTGCACAATGGGCGCAAGCCTG
ATGCAGCAACGCCGCGTGAGGGACGACGGCCTTCGGGTTGTAAACCTCTTTTAGCAGGGAAGA
AGCGAAA

>KF495554; *Virgibacillus halodenitrificans*, ^{GUFB}Sama06-18 (536nt)

GCTGGCGGCGTGCCTATTACATGCAAGTCGAGCGCGGGAAGCAAGCTGATCCTCTTCGGAGGT
GACGCTTGTGGAACGAGCGGCGGACGGGTGAGTAACACGTGGGCAACCTGCCTGTAAGACTGG
GATAACCCCGGGAAACCGGGGCTAATACCGGATAATACTTTTCATCACCTGATGAGAAGTTGA
AAGGTGGCTTTTAGCTACCACTTACAGATGGGCCCGCGGCGCATTAGCTACCTTGGTGAGGTA
ACGGCTCACCAAGGCAACGATGCGTAGCCGACCTGAGAGGGTGATCGGCCACACTGGGACTGA
GACACGGCCCAGACTCCTACGGGAGGCAGCAGTAGGGAATCTTCCGCAATGGACGAAAGTCTG
ACGGAGCAACGCCGCGTGAGTGATGAAGGTTTTCGGATCGTAAAGCTCTGTTGTTAGGGAAGA
ACAAGTGCCGTTCGAATAGGGCGGCACCTTGACGGTACCTAACCAGAAAGCCCCGGCTAACTA
CGTGCCAGCAGCCGCGGTAATACGTAGGGGGC

>KF495555; *Bacillus* sp., ^{GUFB}Sama06-19 (422nt)

GCGGCGTGCCTATTACATGCAAGTCGAGCGAATGGATTAAGAGCTTGCTCTTATGAAGTTAGC
GGCGGACGGGTGAGTAACACGTGGGTAACCTGCCCATAAGACTGGGATAACTCCGGGAAACCG
GGGCTAATACCGGATAACATTTTGAACCGCATGGTTCGAAATTGAAAGGCGGCTTCGGCTGTC
ACTTATGGATGGACCCGCGTCGCATTAGCTAGTTGGTGAGGTAACGGCTCACCAAGGCAACGA
TGCGTAGCCGACCTGAGAGGGTGATCGGCCACACTGGGACTGAGACACGGCCCAGACTCCTAC
GGGAGGCAGCAGTAGGGAATCTTCCGCAATGGACAGAAGTCTGACGGAGCAACGCCGCGTGAG
TGATGAAGGCTTTCGGGGCGGAAAAGTCTGTTGTTAGGGAAAAA

>KF495556; *Shewanella algae*, ^{GUFB}Sama06-20 (737nt)

GTTTGATCCTGGCTCAGATTGAACGCTGGCGGCAGGCCTAACACATGCAAGTCGAGCGGTAAC
ATTTCAAAAGCTTGCTTTTGAAGATGACGAGCGGCGGACGGGTGAGTAATGCCTGGGAATTTG
CCCATTTGTGGGGGATAACAGTTGGAAACGACTGCTAATACCGCATACGCCCTACGGGGGAAA
GCAGGGGACCTTCGGGCCTTGCGCTGATGGATAAGCCCAGGTGGGATTAGCTAGTAGGTGAGG
TAAAGGCTCACCTAGGCGACGATCCCTAGCTGGTCTGAGAGGATGATCAGCCACACTGGGACT
GAGACACGGCCCAGACTCCTACGGGAGGCAGCAGTGGGGAATATTGCACAATGGGGGAAACCC
TGATGCAGCCATGCCGCGTGTGTGAAGAAGGCCTTCGGGTTGTAAAGCACTTTCAGCGAGGAG
GAAAGGGTGTAAGTTAATACCTTACATCTGTGACGTTACTCGCAGAAGAAGCACCGGCTAACT
CCGTGCCAGCAGCCGCGGTAATACGGAGGGTGCGAGCGTTAATCGGAATTACTGGGCGTAAAG
CGTGGGCAGGCGGTTTGTTAAGCGAGATGTGAAAGCCCCGGGCTCAACCTGGGAACCGCATTT
CGAACTGGCAAACTAGAGTCTTGTAGAGGGGGGTAGAATTCCAGGTGTAGCGGTGAAATGCGT
AGAGATCTGGAGGAATACCGGTGGCGAAGGCGGCCCCCTGGACA

>KF495557; *Leucobacter komagatae*, ^{GUFB}Sama06-21 (616nt)

TGGCGGCGTGCTTAACACATGCAAGTCGAACGATGAAGCCCAGCTTGCTGGGTGGAAGAGTGG
CGAACGGGTGAGTAACACGTGAGTAACCTGCCCTGAACTCTGGGATAAGCACTGGAAACGGTG
TCTAATACTGGATACGACCTATCACCGCATGGTGTGTGGGTGGAAAGATTTATCGGTTCTGGA
TGGACTCGCGGCCTATCAGCTAGATGGTGAGGTAATGGCTCACCATGGCGACGACGGGTAGCC
GGCCTGAGAGGGTGACCGGCCACACGGGACTGAGACACGGCCCAGACTCCTACGGGAGGCAGC
AGTGGGGAATATTGCACAATGGGCGCAAGCCTGATGCAGCAACGCCGCGTGAGGGATGACGGC
CTTCGGGTTGTAAACCTCTTTTAGAGGGAAGAAGCGAAAGTGACGGTACCTGCAGAAAAAGCA
CCGGCTAACTACGTGCCAGCAGCCGCGGTAATACGTAGGGTGCAAGCGTTGTCCGGAATTATT

GGGCGTAAAGAGCTCGTAGGCGGCTTGTCGCGTCTGCTGTGAAAACCCGGGGCTCAACCCCGG
GCCTGCAGTGGGTACGGGCAGGCTAGAGTGCGGTAGGGGAGATTGGAAT

> KF495558; *Bacillus licheniformis,* ^{GUFB}SAMA06-2.2 (469nt)

GGCGAACTTGAGTGCAGAAGAGGAGAGTGGAATTCCACGTGTAGCGGTGAAATGCGTAGAGAT
GTGGAGGAACACCAGTGGCGAAGGCGACTCTCTGGTCTGTAACTGACGCTGAGGCGCGAAAGC
GTGGGGAGCGAACAGGATTAGATACCCTGGTAGTCCACGCCGTAAACGATGAGTGCTAAGTGT
TAGAGGGTTTCCGCCCTTTAGTGCTGAAGCAAACGCATTAAGCACTCCGCCTGGGGAGTACGG
TCGCAAGACTGAAACTCAAAGGAATTGACGGGGGCCCGCACAAGCGGTGGAGCATGTGGTTTA
ATTCGAAGCAACGCGAAGAACCTTACCAGGTCTTGACATCCTCTGACAACCCTAGAGATAGGG
CTTCCCCTTCGGGGGCAGAGTGACAGGTGGTGCATGGTTGTCGTCAGCTCGTGTCGTGAGATG
TTGGGTTAAGTCCCGCAACGAGCGCAAG

> KF495559; *Bacillus licheniformis,* ^{GUFB}Sama06-2.3 (495nt)

GGGAATTGAGTGCAGAAGAGGAGAGTGGAATTCCACGTGTAGCGGTGAAATGCGTAGAGATGT
GGAGGAACACCAGTGGCGAAGGCGACTCTCTGGTCTGTAACTGACGCTGAGGCGCGAAAGCGT
GGGGAGCGAACAGGATTAGATACCCTGGTAGTCCACGCCGTAAACGATGAGTGCTAAGTGTTA
GAGGGTTTCCGCCCTTTAGTGCTGCAGCAAACGCATTAAGCACTCCGCCTGGGGAGTACGGTC
GCAAGACTGAAACTCAAAGGAATTGACGGGGGCCCGCACAAGCGGTGGAGCATGTGGTTTAAT
TCGAAGCAACGCGAAGAACCTTACCAGGTCTTGACATCCTCTGACAACCCTAGAGATAGGGCT
TCCCCTTCGGGGGCAGAGTGACAGGTGGTGCATGGTTGTCGTCAGCTCGTGTCGTGAGATGTT
GGGTTAAGTCCCGCAACGAGCGCAACCCTTGATCTTAGTTGCCAGCATTCAGTT

> KF495560; *Pseudomonas* sp., ^{GUFB}Sama06-24 (582nt)

GCAAGTCGAGCGGTAGAGAGAAGCTTGCTTCTCTTGAGAGCGGCGGACGGGTGAGTAATGCCT
AGGAATCTGCCTGGTAGTGGGGGATAACGTTCGGAAACGGACGCTAATACCGCATACGTCCTA
CGGGAGAAAGCAGGGGACCTTCGGGCCTTGCGCTATCAGATGAGCCTAGGTCGGATTAGCTAG
TTGGTGAGGTAATGGCTCACCAAGGCGACGATCCGTAACTGGTCTGAGAGGATGATCAGTCAC
ACTGGAACTGAGACACGGTCCAGACTCCTACGGGAGGCAGCAGTGGGGAATATTGGACAATGG
GCGAAAGCCTGATCCAGCCATGCCGCGTGTGTGAAGAAGGTCTTCGGATTGTAAAGCACTTTA
AGTTGGGAGGAAGGGTTGTAGATTAATACTCTGCAATTTTGACGTTACCGACAGAATAAGCAC
CGGCTAACTCTGTGCCAGCAGCCGCGGTAATACAGAGGGTGCAAGCGTTAATCGGAATTACTG
GGCGTAAAGCGCGCGTAGGTGGTTTGTTAAGTTGGATGTGAAATCCCCGGGCTCAACCTGGGA
ACTGCATTCAAAACT

> KF495561; *Halomonas* sp., ^{GUFB}Sama06-25 (560nt)

CGCTGGCGGCAGGCCTATCACATGCAAGTCGAGCGGTAACAGATCCAGCTTGCTGGATGCTGA
CGAGCGGCGGACGGGTGAGTAATGCATAGGAATCTGCCCGATAGTGGGGGATAACCTGGGGAA
ACCCAGGCTAATACCGCATACGTCCTACGGGAGAAAGGGGGCTCCGGCTCCCGCTATGGGATG
AGCCTATGTCGGATTAGCTAGTTGGTGAGGTAGCGGTTCACCAAGGCCACGATCCGAACCTGG
TCTGAAAGGATGATCAGCCACATCGGGACTGAGACACGGCCCGAACTCCTACGGGAGGCAGCA
GTGGGGAATATTGGACAATGGGGGCAACCCTGATCCAGCCATGCCGCGTGTGTGAAGAAGGCC
CTCGGGTTGTAAAGCACTTTCAGCGAGGAAGAACGCCTAGCGGTTAATACCCGCTAGGAAAGA
CATCACTCGCAGAAGAAGCACCGGCTAACTCCGTGCCAGCAGCCGCGGTAATACGGAGGGTGC
AAGCGTTAATCGGAATTACTGGGCGTAAAGCGCGCGTAGGTGGCTTGATAAGCCGG

> KF495562; *Staphylococcus* sp., ^{GUFB}Sama06-26 (502nt)

GCGTGCCTATTACATGCAAGTCGAGCGAACAGATAAGGAGCTTGCTCCTTTGACGTTAGCGGC
GGACGGGTGAGTAACACGTGGATAACCTACCTATAAGACTGGGATAACTTCGGGAAACCGGAG
CTAATACCGGATAACATATTGAACCGCATGGTTCAATAGTGAAAGGCGGCTTTGCTGTCACTT
ATAGATGGATCCGCGCCGTATTAGCTAGTTGGTAAGGTAACGGCTTACCAAGGCAACGATACG
TAGCCGACCTGAGAGGGTGATCGGCCACACTGGAACTGAGACACGGTCCAGACTCCTACGGGA
GGCAGCAGTAGGGAATCTTCCGCAATGGGCGAAAGCCTGACGGAGCAACGCCGCGTGAGTGAT
GAAGGTCTTCGGATCGTAAAACTCTGTTATCAGGGAAGAACAAATGTGTAAGTAACTGTGCAC
ATCTTGACGGTACCTGATCAGAAAGCCACGGCTAACTACGTGCCAGCAGCCGCGGTAATAC

> KF495563; *Brachybacterium* sp., ^{GUFB}Sama06-27 (870nt)

GATCCTGGCTCAGGACGAACGCTGGCGGCGTGCTTAACACATGCAAGTCGAACGATGACGGTG
GTGCTTGCACCGCCTGATTAGTGGCGAACGGGTGAGTAACACGTGAGTAACCTGCCCTCCACT
TCGGGATAACCTCGGGAAATCGTGGCTAATACCGGATATGAGCACTCATCGCATGGTGAGTGC
TGGAAAGATTTATCGGTGGGGGATGGACTCGCGGCCTATCAGTTTGTTGGTGAGGTGATGGCT
CACCAAGACGATGACGGGTAGCCGGCCTGAGAGGGCGACCGGCCACACTGGGACTGAGACACG
GCCCAGACTCCTACGGGAGGCAGCAGTGGGGAATATTGCACAATGGGCGAAAGCCTGATGCAG
CGACGCCGCGTGGGGGATGACGGCCTTCGGGTTGTAAACCCCTTTCAGTAGGGAAGAAGCGAG
AGTGACGGTACCTGCAGAAGAAGCGCCGGCTAACTACGTGCCGGCAGCCGCGGTAATACGTAG
GGCGCAAGCGTTGTCCGGAATTATTGGGCGTAAAGAGCTTGTAGGTGGCTTGTCGCGTCTGCC
GTGAAAACCCGAGGCTCAACCTCGGGCGTGCGGTGGGTACGGGCAGGCTAGAGTGTGGTAGGG
GAGACTGGAACTCCTGGTGTAGCGGTGAAATGCGCAGATATCAGGAAGAACACCGATGGCGAA
GGCAGGTCTCTGGGCCATTACTGACACTGAGAAGCGAAAGCATGGGTAGCGAACAGGATTAGA
TACCCTGGTAGTCCATGCCGTAAACGTTGGGCACTAGGTGTGGGGGACATTCCACGTTTTCCG
CGTCGTAGCTAACGGATTAAGTGCCCCGCCTGGGGAGTACGGCCGCAAGGG

T-631